UNIVERSITY OF
Southampton
School of Medicine

Interactions between human embryonic stem cell and foetal femur derived cell populations – development of strategies for tissue regeneration.

Ayshe Ismail,
Bone and Joint Research Group.

Doctor of Philosophy,
August 2010.

UNIVERSITY OF SOUTHAMPTON
FACULTY OF MEDICINE, HEALTH AND LIFE SCIENCES
SCHOOL OF MEDICINE

Abstract

Doctor of Philosophy

Interactions between human embryonic stem cell and foetal femur derived cell populations – development of strategies for tissue regeneration.

By Ayshe Ismail

Research into skeletal stem cell biology offers significant therapeutic opportunities in the development of bone tissue engineering strategies. The pluripotency of human embryonic stem (ES) cells as well as their potentially unlimited supply makes these cells highly desirable for differentiation to produce functional bone cells (osteoblasts). Equally, cells derived from foetal tissue offer enormous potential for cell based tissue regeneration, however to date there has been little research into the interactions between the two cell types for differentiation purposes.

Initial studies characterised the cell populations to be utilised. Foetal cells were expanded in basal conditions from explant cultures of human foetal femurs at 8–12 weeks post conception. Foetal-derived cells expressed type I collagen, alkaline phosphatase and two unique progenitor markers, STRO-1 and 7D4. Expression of STRO-1 in foetal samples ranged from 0.6–12.6% and 7D4 ranged from 0.1-5.1%, and was seen in basal conditions for up to 21 days in culture. Molecular characterisation of the cell fractions showed the STRO-1 positive fraction to express early bone markers, SOX-9 and RUNX-2 and to lack markers of more mature osteogenic cells. Characterisation of the foetal femur derived cells indicated that the cells were suitable for use as a halfway model between embryonic and adult cells in bone development and that the STRO-1 positive cell population found within displayed osteogenic propensity.

Human embryonic stem cells were characterised and differentiation studies performed in monolayer culture using single ES cells or by the formation of embryoid bodies (ES cell aggregates). Molecular characterisation showed an increase in BMP-4 expression in both monolayer and 3-D cultures, indicative of mesoderm differentiation. Additionally, foetal cells were co-cultured with human ES cells in both monolayer and 3-D pellets to investigate their potential for differentiation. These studies demonstrated a spatial organisation of the cells as well as a potential inhibition of the foetal cell differentiation by the presence of the ES cells, which was observed in both monolayer and 3-D culture conditions.

The use of dielectrophoresis (DEP) as a cell characterisation technique that does not require the use of biochemical markers or tags was utilised. Differences in specific membrane capacitance in MG-63, SAOS-2 and STRO-1 positive cells (from human bone marrow) were observed, a parameter that could be exploited at a later stage to separate the cells from mixed populations in a DEP based sorting device.

These studies demonstrate the potential of human ES cells and foetal cells as an alternative cell source in the development of bone tissue engineering strategies.

99% perspiration, 1% inspiration.

This thesis is dedicated to my mother and father, Pelin and Ismail, without whom I would not be where I am today. To my grandmother Hatige Tossoun, I miss you everyday. Also to my sister, Hatige and my younger cousins and friends who gave me the strength to continue. I will never be able to express enough my gratitude for all the love and support I received by all those closest to me.

For you, with all my love.

Table of Contents

Table of Figures

Table of Tables

Declaration of Authorship

I, Ayshe Ismail, declare that the thesis entitled:

Interactions between human embryonic stem cell and foetal femur derived cell populations – development of strategies for tissue regeneration.
and the work presented in it are my own. I confirm that:

- this work was done wholly or mainly while in candidature for a research degree at this University;
- where any part of this thesis has previously been submitted for a degree or any other qualification at this University or any other institution, this has been clearly stated;
- where I have consulted the published work of others, this is always clearly attributed;
- where I have quoted from the work of others, the source is always given. With the exception of such quotations, this thesis is entirely my own work;
- I have acknowledged all main sources of help;
- where the thesis is based on work done by myself jointly with others, I have made clear exactly what was done by others and what I have contributed myself;
- none of this work has been published before submission

Signed: ……..

Date:…….

Acknowledgements

This work was carried out in the Bone and Joint Research Group, Institute of Developmental Sciences, Southampton General Hospital, University of Southampton, United Kingdom.

First and foremost, I wish to thank my supervisors, Prof Richard OC Oreffo and Dr Franchesca Houghton. Special thanks to all in the Bone & Joint Research Group at the University of Southampton, in particular Ms Kate Murawski, Ms Stephanie Inglis, Dr Rahul Tare, Dr Jodie Pound and Dr Sayed-Hadi Mirmalek-Sani for their advice and support. Also to the members of the Human Genetics research groups in particular Prof David Wilson for providing the human foetal tissue and Ms Kate Wright and Ms Kelly Wilkinson.

Thanks must go also to the collaborators at the University of Surrey, Michael Hughes and Fatima Labeed, as well as the post-doctoral staff, Kai Hoettges and the PhD students for all their help. I would also like to thank the collaborators at the University of Cardiff, Prof. Bruce Caterson, and Dr Anthony Hayes.

Finally, I would like to thank the Gerald Kerkut Charitable Trust their financial support, as without, none of this would have been possible.

Abbreviations

A/S	Alcian blue/Sirius red
AEC	3-Amino-9-ethyl-carbazol
ALP	Alkaline phosphatase
ANOVA	Analysis of variance
α-MEM	Alpha modification of eagles medium
BMP-2	Bone morphogenetic protein 2
BRY	Brachyury
BSA	Bovine serum albumin
cDNA	Complementary DNA
CFU-F	Colony forming unit-fibroblast
CM	Clausius-Mossotti (factor)
CT	Computed tomography
CTG	Cell tracker green
CTO	Cell tracker orange
DAPI	4',6-diamidino-2-phenylindole
dH_20	Distilled water
DEP	Dielectrophoresis
DMEM	Dulbeco's modified Eagles media
DNA	Deoxyribonucleic acid
dNTPs	Deoxynucleotide triphosphates
DPX	Distyreme plasticiser xylene
ECM	Extracellular matrix
EDTA	Ethylenediaminetetraacetic acid
EG	Embryonic germ (cell)
EH-1	Ethidium homodimer 1
ES	Embryonic stem (cell)
FACS	Fluorescent activated cell sorting
FCS	Foetal calf serum
FDA	Food and Drug Administration (USA)
FGF	Fibroblastic growth factor
FITC	Fluorescein isothiocynate
GAPDH	Glyceraldehyde-3-phosphate dehydrogenase

GAG	Glycosaminoglycans
HBMC	Human bone marrow stromal cell
HFEA	Human Fertilisation and Embryology Authority (UK)
HTA	Human Tissue Authority (UK)
HUES-7	Human Embryonic Stem cell line-7
ICM	Inner cell mass
IHC	Immunohistochemistry
ITS	Insulin, transferrin, selenium
LASER	Light amplification by stimulated emission of radiation
MACS	Magnetically activated cell sorting
MEF	Mouse Embryonic Fibroblast
MSC	Marrow stromal cell
OA	Osteoarthritis
OB	Osteoblast
OC	Osteoclast
OCT-4	Octomer binding transcription factor-4
PBS	Phosphate buffered saline
PCR	Polymerase chain reaction
PFA	Paraformaldehyde
PS	Primitive streak
pNNP	Para-nitrophenolphosphate
qPCR	Quantitative PCR
RNA	Ribonucleic acid
Runx2	Runt-related transcription factor 2
SOX-1	SRY (sex determining region Y)-box 1
SOX-2	SRY (sex determining region Y)-box 2
SOX-9	SRY (sex determining region Y)-box 9
SOX-17	SRY (sex determining region Y)-box 17
SSC	Skeletal stem cell
SSEA-3/4	Stage specific embryonic antigen 3/4
TE	Tris EDTA
TGF-β3	Transforming growth factor-β3
TRA-1-60	Tumour rejection antigen 1-60
TRA-1-81	Tumour rejection antigen 1-81

TRIT-C	Tetramethyl Rhodamine Iso-Thiocyanate
THR	Total hip replacement
UPW	Ultra pure water
WPC	Weeks post conception

Chapter 1 Introduction

1.1 Overview

As the standard mortality age of the population continues to rise, the clinical requirement to replace degenerated musculoskeletal tissue also increases and has become a major socio-economic problem (Tare et al., 2008). Key to resolving this issue is an understanding of the developmental physiology of skeletal cells and the process of skeletal cell differentiation. Skeletal stem cell based medicine offers applications for osteodegenerative medicine, including an understanding of stem cell differentiation, the repair of traumatic bone damage and the treatment of genetic skeletal deficiencies. However, the understanding of this process is dependent, in part, on deriving information on the presence, activity, and plasticity of bone marrow stromal cells (BMSCs), which can be derived from adult, foetal or embryonic sources and the differences and similarities between the three cell types.

1.2 Skeletal Stem Cells

Skeletal stem cells (SSCs) (Bianco and Robey, 2001b), are multipotent stem cells that can give rise to cells found in the skeletal connective tissue, osteoblasts, chondrocytes, tenocytes and bone marrow adipocytes. SSCs have the potential to self replicate to produce more SSCs (Bianco et al., 2006). It is this property of self-renewal, which makes the SSCs attractive for use in regenerative medicine. SSCs can be isolated and harvested from human bone marrow and expanded using culture expansion of adherent cells. Cultured SSCs are also referred to as colony-forming unit-fibroblasts (CFU-F) (Owen and Friedenstein, 1988, Bianco et al., 2001a). Bone marrow aspirates and trabecular bone have also been recognised as sources of SSCs (Pountos et al., 2006). There is a large degree of variation in the literature as to the appropriate naming of this cell fraction, also commonly referred to as mesenchymal stem cells (Goshima et al., 1991), marrow stromal fibroblastic cells, osteogenic stem cells (Triffitt, 2002) and bone marrow stromal cells (Bianco et al., 2001a).

To date, protocols for the isolation of a homogenous population of SSCs have proved elusive. Currently, morphological and functional criteria are used to identify SSCs, these include; i) adherent growth on plastic, ii) resistance to trypsin, iii) presence of various (albeit non-specific) cell surface antigens and, iv) differentiation potential into cells of the osteogenic, adipogenic and chondrogenic lineages. The SSCs are

characterised further by both positive and negative phenotypic staining using various techniques. Examples of phenotypic markers are surface antigens, extracellular matrix (ECM) components and secreted proteins (see Table 1:3 in section 1.8).

1.3 Embryonic Stem Cells

Following fertilisation of the oocyte by spermatozoa, a zygote is formed. The zygote then undergoes a series of mitotic divisions called cleavage. The first cleavage division generates a 2-cell embryo, the cells of which are called the blastomeres. Each blastomere then undergoes subsequent divisions yielding the 4, 8 and 16 daughter cells. It takes approximately 24 hours from fertilisation to reach the two-cell stage, with the four-cell stage being reached at approximately 2 days; the 16-cell stage (morula) is reached at approximately 4 days; and the blastocyst at approximately 5-6 days (Senger, 2003). Embryonic development is shown in Figure 1:1.

Embryonic stem cells (ES cells) are derived from the inner cell mass (ICM) of a blastocyst and are described as pluripotent, that is they have the potential to generate all the cells and tissues which make up the embryo and have unlimited growth potential. The inner cells of the morula constitute the ICM, and surrounding cells the trophectoderm. It is the ICM that goes on to form the embryo proper and the outer cell layer that forms the trophectoderm, which later contributes to the placenta (Sadler, 2003). At approximately the third week of gestation, gastrulation occurs; this is the process of establishing the three germ layers (ectoderm, mesoderm and endoderm) in the embryo. Gastrulation begins with the formation of the primitive streak (PS) on the surface of the epiblast (one of the tissue types derived from the ICM). It is the epiblast, through the process of gastrulation that establishes the germ layers. At day 15/16 the PS is clearly visible and is described as a narrow groove with a slightly bulging region on either side. A marker for PS and the early mesoderm is Brachyury. Other mesoderm and mesenchyme marker genes are Mox-1, Pax-1 and Runx-2 (the expression of which suggests bone-forming potential). Cells of the epiblast migrate toward the PS and become flask shaped before detaching from the epiblast and slipping beneath it. This inward movement is known as invagination. Once the cells have invaginated, some displace the hypoblast (cell layer between the ICM and the blastocyst cavity), creating the embryonic endoderm. Other cells come to lie between the epiblast and the newly created endoderm to form the mesoderm, with the cells that remain in the epiblast

forming the ectoderm. It is the mesoderm layer, which consists of the mesenchyme cells that later develop into cells of the stromal lineage including skeletal, cardiac and muscle tissues (Sadler, 2003).

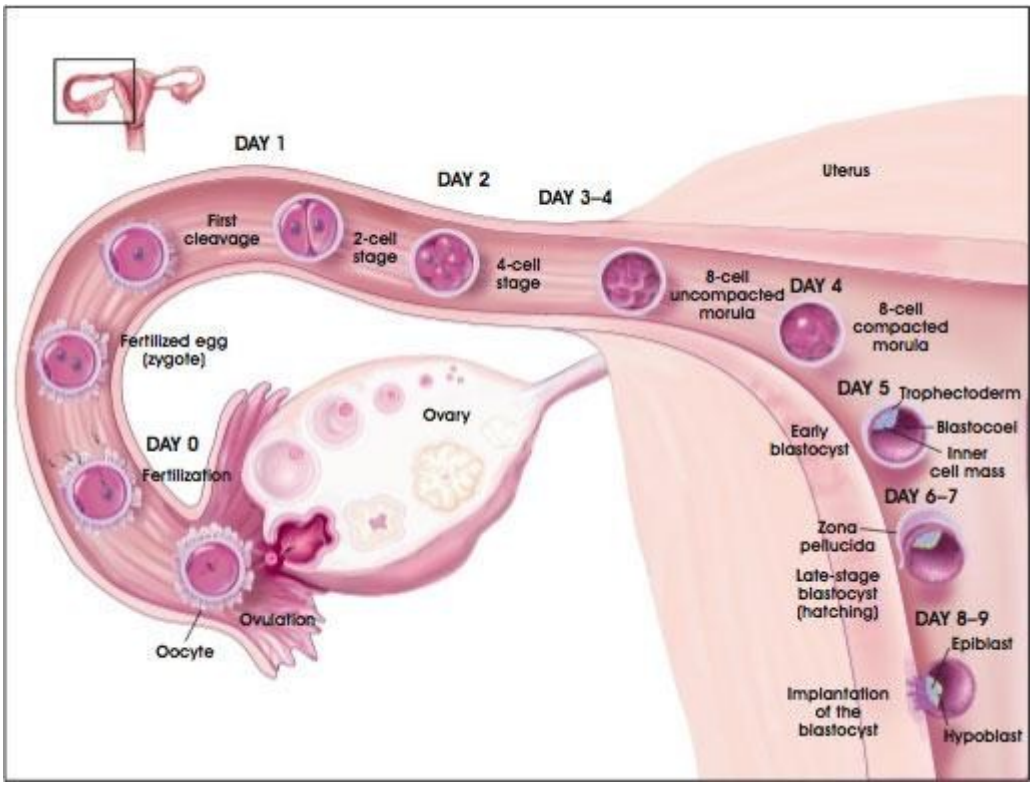

Figure 1:1 Development of the preimplantation blastocyst in humans. Following fertilisation, a series of cell divisions occur in the zygote. By day 4 of development, a compacted morula is formed which then divides again to produce an outer rim of cells, the trophectoderm and an inner core of cells, the inner cell mass. By day 5, the morula has developed to become the blastocyst. The blastocyst reaches the uterus between days 5-7 by on or about day 8-9, the blastocyst implants in the uterine wall. From www.stemcells.nih.gov.

1.3.1 Isolation and Culture of Embryonic Stem Cells

Pluripotent mouse ES cells were first isolated in 1981 (Evans and Kaufman) by immunosurgically digesting the outer trophectoderm layer of the mouse blastocyst to isolate the ICM. The cells were initially grown on mitotically inactivated mouse embryonic fibroblast (MEF) feeder cells, which provided nutrients critical for the maintenance of the undifferentiated stem cell state. The establishment of ES cell culture is shown in Figure 1:2. The feeder cell layer is thought to act to remove deleterious components from the media or to be involved in cell-contact mediated mechanisms to

prevent ES cell differentiation. It was later discovered that leukaemia inhibitory factor (LIF), a product produced by the feeder cells, could replace the feeder cells along with foetal calf serum (FCS) in order to maintain the undifferentiated state of mouse ES cells (Gadue et al., 2005). Ying and colleagues (2003) also showed that bone morphogenetic proteins (BMPs) could be used as a replacement for serum, therefore enabling the growth of cells in the absence of feeders in serum free conditions whilst sustaining self renewal and preserving multilineage differentiation. Specifically, BMP-4 has been shown to contribute to maintaining the self-renewal of ES cells (observed in the mouse) in the presence of leukaemia inhibitory factor (LIF) or serum (Duplomb et al., 2006).

Upon removal from the natural environment, ES cells can remain undifferentiated under specific culture conditions. For human cells these conditions include the presence of a mouse embryonic fibroblast (MEF) feeder layer, in serum replacement media supplemented with basic fibroblastic growth factor (bFGF) (Carpenter et al., 2003). However, it has been observed that when grown to confluence and allowed to accumulate within the culture dish, the ES cell can differentiate spontaneously (Draper et al., 2004, Olivier et al., 2006, Thomson et al., 1998). When ES cells are allowed to differentiate in a single cell suspension culture or from aggregates of cells (following LIF and bFGF removal from the media), they form spherical multicellular aggregates called embryoid bodies (EBs). EBs have been shown to contain a variety of cell populations and have been used as the ES cell source in a number of differentiation experiments (Kawaguchi, 2006, Kawaguchi et al., 2005, Khoo et al., 2005). EBs growth mimics many of the stages involved in developing embryo differentiation.

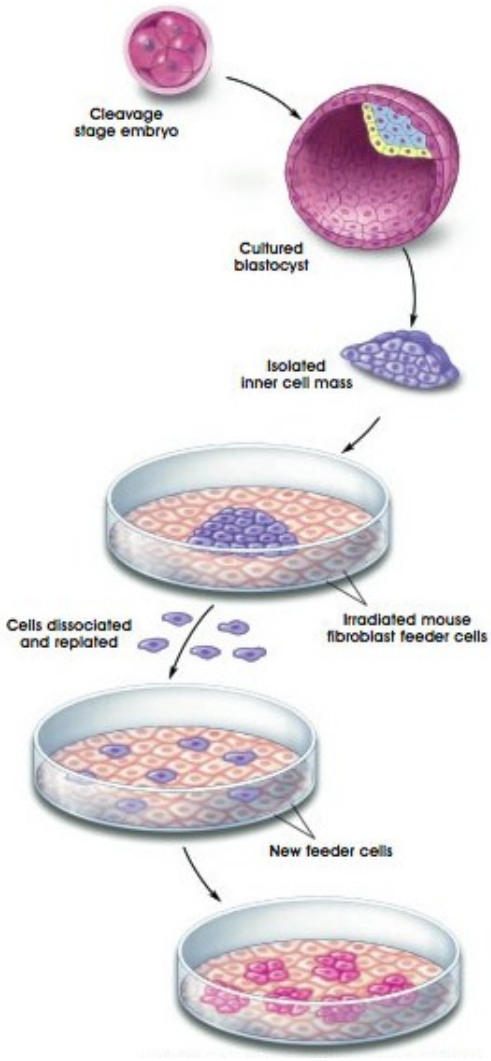

Figure 1:2 Establishment of embryonic stem cell cultures. To generate human ES cell cultures, cells from the inner cell mass of a human blastocyst are cultured in a multi-step process. The pluripotent cells of the inner cell mass are separated from the surrounding trophectoderm by immunosurgery. The inner cell masses were plated in culture dishes containing growth medium supplemented with foetal bovine serum on feeder layers of gamma-irradiated mouse embryonic fibroblasts to prevent their replication. After 9 to 15 days, when the inner cell masses had divided and formed clumps of cells, cells from the periphery of the clumps were chemically or mechanically dissociated and replated in the same culture conditions. Colonies of homogeneous cells were selectively removed, mechanically dissociated, and replated. These were expanded and passaged, thus creating a cell line. Image modified from www.stemcells.nih

The origin of human ES cells from the pre-implantation embryo is the defining feature that distinguishes ES cell lines from other pluripotent stem cell lines such as human embryonal carcinoma (EC) cell and human embryonic germ cell (EGC) lines. EC cells

are derived from the undifferentiated stem cell components of spontaneously arising germ cell tumours, whereas EGC lines are derived from human and mouse primordial germ cells from the genital ridge of the foetus (Odorico et al., 2001). Germ cells are the sole means of transmitting genetic information to the next generation as haploid gametes (either spermatozoa or ova). Before meiosis, these cells exist as diploid primordial germ cells (PGCs) that share similarities to the cells of the ICM and when placed into in vitro culture can generate germ cells (GCs). GCs possess the ability to differentiate into the three germ layers with associated loss of pluripotency markers (Turnpenny et al., 2003, Turnpenny et al., 2006) thus providing a parallel to the ES system. Human germ cells have been more difficult to study partly due to their difficulty in isolating from human foetal material as well as difficulty in culture (Turnpenny et al., 2006). EC cells typically express many of the same markers as ES cells, in contrast though, they often have a limited capacity for differentiation, with some EC cell lines defined as 'nullipotent' having completely lost their differentiation capacity (Andrews et al., 2005).

Morphologically, human ES cells form relatively flat compact colonies making them distinct from human EG cells which more closely resemble mouse ES cells (more tight and spherical) (Odorico et al., 2001). Studies suggest mouse ES cells grow at a faster rate than human ES cells, although the rate of growth of the cells is also dependent on the cell line (Odorico et al., 2001). Human ES cells also contain a high ratio of nucleus to cytoplasm and prominent nuclei (Thomson et al., 1998). It has been observed that the media components used in culture can result in differences in the morphology of the cells. When cultured in DMEM:12, knock-out serum and fibroblastic growth factor-2 (FGF-2), the ES cells are thinner, flatter and more angular, with the cells contained in the colonies smaller and more tightly packed in comparison to growth in serum (Laslett et al., 2003).

Laminin is the first extracellular matrix protein expressed in the two- and four- cell stage mouse embryo (Xu et al., 2001). This knowledge along with the finding that human ES cells require matrix for the maintenance of the undifferentiated state, led to the evaluation of integrin expression for human ES cells maintained on feeder or feeder-free conditions. Cells in both conditions expressed the same levels of various integrins, consistent with the finding that the cells grow appropriately on laminin or matrigel.

Matrigel is composed of a complex mixture of extracellular matrix proteins obtained from an animal basement membrane extracted from Engelbreth-Holm-Swarm mouse sarcoma cells, a tumour rich in extracellular matrix (ECM) proteins, laminin, collagen IV, heparin sulphate proteoglycans, and entactin, but also matrix-degrading enzymes, their inhibitors and a broad variety of other proteins (Kleinman and Martin, 2005). Undifferentiated ES cells within colonies also express connexin 43 indicating the presence of gap junctions (Hoffman and Carpenter, 2005). The application of matrigel and MEF conditioned media is not ideal for the potential medical application of human ES cells at a later stage, as xenogeneic pathogens can be transmitted through culture conditions (Stojkovic et al., 2005). The concern over xenogeneic contaminants from mouse feeder cells may restrict transplantation to humans. Furthermore, the variability in MEFs from batch-to-batch and laboratory-to-laboratory may contribute to some of the variability in experimental results observed. Additionally, use of any feeder layer increases the work load and subsequently limits the large-scale culture of human ES cells (Mallon et al., 2006). To eliminate this difficulty, human ES cells have been successfully cultured on human embryonic fibroblasts, with the cells shown to retain the same pattern of characteristic marker expression as those cells cultured on mouse feeder layers (Richards and Bongso, 2006, Draper et al., 2004). Serum replacements remain an area of ongoing research in embryonic stem cell culture, although the exact chemical composition is often complicated due to intellectual property rights associated with such work.

Stojkovic and his group (2005) demonstrated that human ES cells cultured using human serum as a matrix and medium conditioned by differentiated human ES cells retained all pluripotent features. This method reduced the exposure of the cells to animal components, providing a safer direction towards completely animal-free conditions for the handling and therapeutic application of the cells. Cultures maintained in basic fibroblastic growth factor (bFGF) alone or in combination with other factors showed characteristics similar to MEF conditioned medium cultures (Xu et al., 2005).

1.3.2 Signalling Pathways of Embryonic Stem Cells

Stem cells can undergo either differentiation or self-renewal. These processes are highly regulated by intrinsic signals and the external microenvironment, suggesting that the cells function within specialised niches (Avery et al., 2006). Self-renewal of cells

occurs naturally by the proliferation/replication of the cells, in culture however, the cells, as detailed in section 1.3.1 need to be maintained, typically on a feeder cell layer in media containing serum. The maintenance of self renewal and the pluripotent state of embryonic stem cells is vital in successful culture of the cells as well as for differentiation studies which rely on the initial pluripotent state of the cells in order to interpret the observations made. Some of the pathways implicated in stem cell renewal are shown in Figure 1:3.

Human embryonic stem cells are currently recognised by the expression of various select surface markers, antigens and transcription factors which are associated with the undifferentiated state and were originally identified on human embryonal carcinoma cells or in human pre-implantation embryos (Hoffman and Carpenter, 2005). Undifferentiated human ES cells express the globoseries glycolipid antigens, stage specific embryonic antigen, SSEA-3 and SSEA-4, the keratan sulfate-related antigens Tra-1-60 and Tra-1-81 and alkaline phosphatase (Thomson et al., 1998, Andrews et al., 1984). Recently, it has been shown that SSEA-4 also identifies adult SSC populations and can act as a marker for the isolation of the SSC from whole human bone marrow aspirates (Gang et al., 2007). In addition, human ES cells also express integrins, which play a role in attachment to the ECM. The expression of markers is dependent on the stage of differentiation, and can be specific to a particular lineage. Another characteristic of human ES cell lines is high levels of telomerase activity. Telomerase is a ribonucleoprotein which adds telomere repeats onto chromosome ends and acts to maintain the telomere length, this plays an important role in replicative lifespan (and it is likely that reduced telomerase activity in adult cell lines will explain decreased lifespan of ES cells) (Thomson et al., 1998).

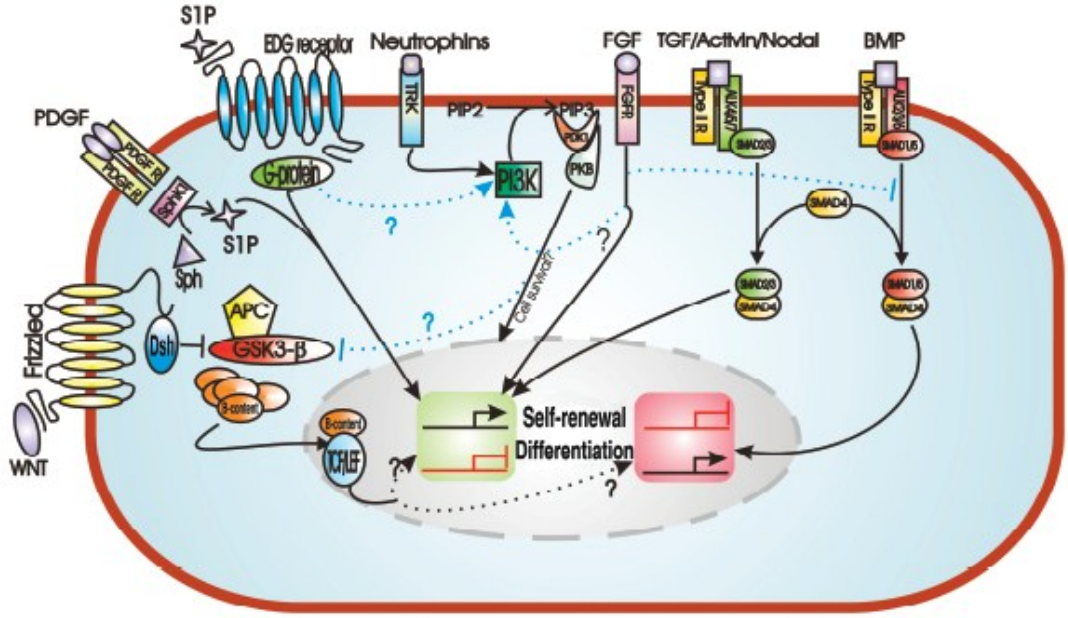

Figure 1:3 Signalling pathways implicated in human ES cell self renewal and differentiation (Avery et al., 2006). The intracellular signalling pathways activated by BMP, and TGF/Activin/Nodal binding to the TGF-β receptors induces the phosphorylation of SMADS. These form complexes with co-SMADS and accumulate in the nucleus where they regulate gene transcription. In human ES cells, BMP4 is reported to induce differentiation. Wnt binds to its receptor Frizzled, the downstream effect is the activation of dishevelled which inactivates the APC/Axin/GSK3β complex. This complex is responsible for the degradation of β-catenin. Its inactivation in the presence of Wnt results in the stabilisation and accumulation of β-catenin in the nucleus and activates LEF/TCF transcription factors. The Wnt/β-catenin pathway is thought to promote self-renewal. The S1P pathway also supports ES cell self-renewal, binding to the EDG receptors coupled to G-proteins. PDGF promotes the intracellular signalling of S1P by activating SphK, which in turn converts Sphingosine to S1P. Crosstalk between the signalling pathways is thought to occur although this is unconfirmed. Equally, the signalling pathways for some receptors are not completely understood.

Both extrinsic and transcription factors have been identified as key factors in self-renewal, however the mechanisms by which this is controlled are relatively unknown. However, it is likely that these pathways are interdependent of one another and that there are cross talk mechanisms. As the culture media of ES cells become more defined, the identification of essential pathways will undoubtedly be systematically approached.

1.3.2.1 Extrinsic Factors

ES cells can maintain their pluripotent state for extended periods when maintained in specific culture conditions and can be influenced to differentiate down a specific lineage pathway upon manipulation of culture conditions. There are a number of specific factors linked to regulation of ES cell differentiation i) LIF. As mentioned previously, LIF signalling plays a major role in maintenance of the pluripotent state, particularly for mouse ES cells. LIF is a member of the interleukin-6 (IL-6) family and signals via a heterodimeric complex composed of specific low-affinity LIFR-β receptor chain and the gp130 chain, common to all receptors of the IL-6 family. However, it is important to note that mouse ES cells compared to human ES cells require different signals to maintain pluripotency. In human ES cells, LIF alone does not support the undifferentiated state, requiring that the human cells are cultured on MEF feeder cell layers containing serum or with MEF conditioned medium. To date the factors from mouse fibroblast conditioned medium that maintains pluripotency remain undefined (Laslett et al., 2003, Draper et al., 2004). LIF provided by the MEF feeder layer is unlikely to contribute to maintaining the undifferentiated state, as the human LIF receptor complex is unresponsive to murine LIF. ii) Nodal. Nodal, is essential for gastrulation and germ layer formation, the absence of which causes the PS not to form. Studies in the human ES cell system have used Activin A as a substitute for Nodal, as both factors bind and signal through the same receptor (Gadue et al., 2005). It is also worth noting that a mutation in the receptor for Activin A (ACVR1), which is included in the BMP receptor family, is responsible for the disorder Fibrodysplasia Ossificans Progressiva (FOP) a rare autosomal dominant disorder of extra skeletal ossification in humans (Shore et al., 2006). iii) WNT proteins. The WNT family of growth factors are involved in many embryonic inductive and patterning processes and are also thought to play a role in osteoblasts differentiation as well as maintenance and differentiation of adult mesenchymal progenitor cells, reviewed in (Etheridge et al., 2004, Gadue et al., 2005). Canonical WNT signalling involves the binding of WNT ligands to Frizzled receptors. Components of the WNT signalling pathway are present in human ES cells with the levels of various receptors differing in the undifferentiated and the differentiated cell populations.

1.3.2.2 Transcription Factors

Oct-4 (an abbreviation of Octamer-4) is a commonly used synonym for POU5F1 (POU class 5 homeobox 1). It is a homeodomain transcription factor of the POU family involved with the self-renewal of undifferentiated cells and is used as a marker for undifferentiated cells and typically serves as a control in differentiation experiments. Oct-4 encodes a class V POU transcription factor initially identified in EC cells. Most ES cell lines appear to express high levels of Oct-4, with the precise level determining cell fate, therefore Oct-4 expression must be closely regulated as a deficiency or excess will lead to the differentiation of the cells (Niwa, 2001, Niwa et al., 2000). Other transcriptional regulators such as Sox-2 (Hoffman and Carpenter, 2005) and Nanog (Chambers, 2004) act co-operatively with Oct-4. Oct-4 is highly expressed in the human ICM, however, during gastrulation the expression of Oct 4 is down regulated allowing the 3 germ layers to begin to form (Laslett et al., 2003). It was shown that a sub-population of SSCs incubated in serum free medium for 2-4 weeks began to proliferate once placed in medium containing serum. Once characterised using RT-PCR and microarray the subpopulation of cells were shown to be very early progenitor cells with longer telomeres and enhanced expression of Oct-4 (Pochampally et al., 2004).

Nanog is an NK2-family homeobox transcription factor. It has been observed in mice that Nanog is key for the cells to remain in the undifferentiated state (Chambers et al., 2003). Nanog has been shown to be expressed by the ES cells as opposed to the MEF feeder layer, confirming its confinement to expression in pluripotent cells (Chambers et al., 2003). The over expression of Nanog in mouse ES cells acts to retain cell pluripotency and also nullifies the need for LIF and BMPs (Chambers, 2004). This effect has also been found in human bone marrow cells (along with forced expression of SOX-2), as well as maintenance of their expansion capabilities (Go et al., 2007). Upon differentiation of the mouse ES cells, mRNA expression of Nanog is downregulated (Chambers et al., 2003), leading to a significant downregulation of Oct 3/4 and loss of ES cell surface antigens, and differentiation toward extra-embryonic endodermal lineages (Hyslop et al., 2005b).

1.3.3 Markers of Pluripotent and Differentiated Embryonic Stem Cells

A summary of the markers used to identify pluripotent embryonic stem cells as well as those that have begun differentiation toward the three embryonic lineages is given in Table 1:1.

Marker Name	Cell Type	Significance
Alkaline phosphatase	Embryonic stem (ES), embryonal carcinoma (EC)	Elevated expression of this enzyme is associated with undifferentiated pluripotent stem cell (PSC)
Alpha-fetoprotein (AFP)	Endoderm	Protein expressed during development of primitive endoderm; reflects endodermal differentiation in PSC
Bone morphogenetic protein-4 (BMP-4)	Mesoderm	Growth and differentiation factor expressed during early mesoderm formation and differentiation
Brachyury	Mesoderm	Transcription factor important in earliest phases of mesoderm formation and differentiation; used as the earliest indicator of mesoderm formation
Cripto (TDGF-1)	ES, cardiomyocyte	Gene for growth factor expressed by ES cells, primitive ectoderm, and developing cardiomyocyte
GATA-4 gene	Endoderm	Expression increases as ES differentiates into endoderm
GCTM-2	ES, EC	Transcription factor uniquely expressed by ES cells either in or during the undifferentiated state of PSCs
Germ cell nuclear factor	ES, EC	Transcription factor expressed by PSCs
Hepatocyte nuclear factor-4 (HNF-4)	Endoderm	Transcription factor expressed early in endoderm formation
Nestin	Ectoderm, neural and pancreatic progenitor	Intermediate filaments within cells; characteristic of primitive neuroectoderm formation
Neuronal cell-adhesion molecule (N-CAM)	Ectoderm	Cell-surface molecule that promotes cell-cell interaction; indicates primitive neuroectoderm formation
OCT4/POU5F1	ES, EC	Transcription factor unique to PSCs; essential for establishment and maintenance of undifferentiated PSCs
Pax 6	Ectoderm	Transcription factor expressed as ES cell differentiates into neuroepithelium
Stage-specific embryonic antigen-3, 4 (SSEA-3,4)	ES, EC	Glycoprotein specifically expressed in early embryonic development and by undifferentiated PSCs
Stem cell factor (SCF or c-Kit ligand)	ES, EC, HSC, MSC	Membrane protein that enhances proliferation of ES and EC cells, hematopoietic stem cell (HSCs), and mesenchymal stem cells (MSCs); binds the receptor c-Kit
Telomerase	ES, EC	Enzyme uniquely associated with immortal cell lines; used for identifying undifferentiated PSCs
TRA-1-60	ES, EC	Antibody to a specific extracellular matrix molecule is synthesized by undifferentiated PSCs
TRA-1-81	ES, EC	Antibody to a specific extracellular matrix molecule synthesized by undifferentiated PSCs
Vimentin	Ectoderm, neural and pancreatic progenitor	Intermediate filaments within cells; characteristic of primitive neuroectoderm formation

Table 1:1 Markers used in the identification and characterisation of pluripotent and differentiated embryonic stem cells. Adapted from www.stemcells.nih.

1.3.4 Derivation of Skeletal Stem Cells/ Differentiation of Embryonic Stem Cells

In order to produce SSCs from human ES cells, a series of differentiation steps must occur. The first developmental step is the differentiation of human ES cells to the three germ layers, followed by germ layer specification. Naturally, during early development, three distinct embryonic lineages possess osteogenic potential. Neural crest cells, derived from the developing neuroectoderm and two lineages from the differentiating mesoderm (Heng et al., 2004). The attraction of deriving SSCs from human ES cells over other sources lies in the unlimited supply of SSCs that can be produced from ES cell sources.

Mesenchyme and embryonic cells can be induced to differentiate into mesenchymal tissues using similar techniques under appropriate conditions. The main components used in the culture media in order to differentiate the cells into osteoblasts (other than the standard 10-20% FCS-basal media solution) include dexamethasone, ascorbic acid (AA) and 1,25-dihydroxyvitamin D_3, (vitamin D_3). BMPs are often used to direct osteogenic differentiation, of the different isoforms; BMP-2, -6, and -9 were reported to be the most potent in promoting osteogenic differentiation of SSCs (Cheng et al., 2003). It is now known that AA induces matrix deposition and mineralization and dexamethasone modulates the production of cytokines that regulate the differentiation pathway, for example, down-regulating LIF production (Aubin, 1998, Barberi et al., 2005).

A summary of the approaches adopted to direct the differentiation of the cells can be seen in Figure 1:4, these include the formation of ES cell aggregates (embryoid bodies), co-culture with somatic cells, or growth on three-dimensional scaffolds.

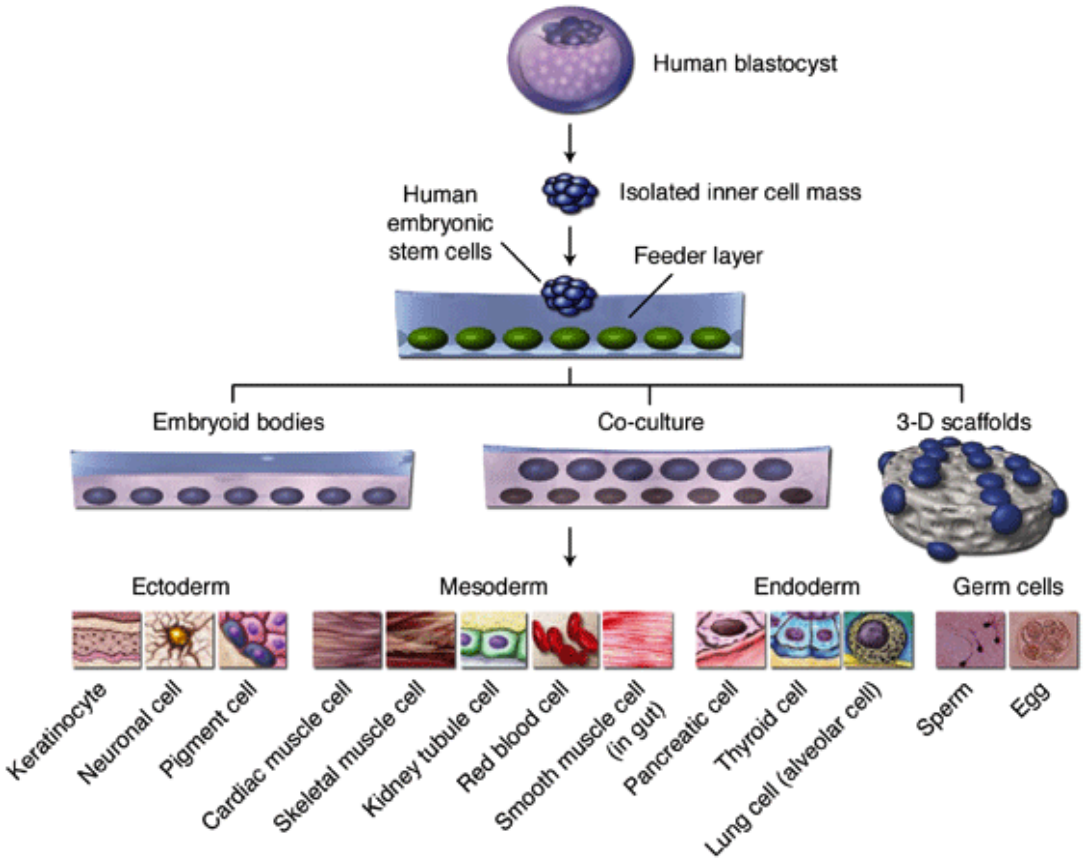

Figure 1:4 Derivation of a human embryonic stem cell line and differentiation strategies. Following isolation from the inner cell mass and culture on a feeder cell layer. The cell line can then be taken and differentiated into cell of the three embryonic lineages (ectoderm, mesoderm and endoderm) by using methods such as embryoid body formation, co-culture with somatic cells and culture on three-dimensional scaffolds. Image taken from Hyslop et al (2005a).

Most commonly, the culture of ES cells in suspension cultures to form embryoid bodies is used to achieve the spontaneous differentiation of ES cells and used as the initial step in differentiation strategies. There are several methods for inducing the formation of EBs from ES cells, the three basic methods are i) liquid suspension culture, in bacterial grade dishes, ii) culture in methylcellulose semisolid media and iii) hanging drop culture, reviewed by Kurosawa (2007). More recently, there have also been methods that include the use of round-bottomed 96-well plates and conical tubes, which require the use of set numbers of ES cells (Bauwens et al., 2008, Burridge et al., 2007, Ezekiel et al., 2007, Ng et al., 2005). The most suitable method for EB formation is in part dependent on the use of either mouse or human ES cells.

Suspension culture in bacterial grade dishes is suitable for both the differentiation of mouse and human ES cells. The cells are typically allowed to aggregate spontaneously and therefore the number of cells and the size of the aggregate varies, resulting in a heterogeneous EB population. However, heterogeneously sized EBs rapidly lose any synchrony in differentiation, making studies using these cells difficult to reproduce (Wartenberg et al., 1998). In order to improve the homogeneity in morphology and differentiation, rotating suspension culture was introduced, where the cells were placed on a horizontally rotating device at 50rpm (Zweigerdt et al., 2003), resulting in improved oxygen supply to the cells. Suspension culture has also been performed using low-adherence vessels to form spherical cell aggregates. Round-bottomed, low-adherence 96-well plates have been used, as they concentrate a known number of ES cells to the bottom of the well and allow cell-cell contact and aggregation. Ezekiel et al (2007) were able to form single embryoid bodies in a 96-well plate simply by culturing a known number in each individual well. They demonstrated a high throughput system with single mouse ES cells producing large numbers of uniform single-sized EBs. The addition of coating reagents to the surfaces of the 96-well plate that prevents cell adhesion to the plastic surfaces allows cells to aggregate and form an EB without the need for centrifugation.

Ng et al (2005) used centrifugation of 96-well plates and known numbers of human ES cells to promote homogeneously sized EBs. They also reported that the number of cells seeded into each well initially affected the level of hematopoietic differentiation in the resulting EBs. Another example of a centrifugation method using human ES cell cultures was reported by Burridge et al (2007). Again, a defined number of cells were centrifuged in V-96 well plates and the subsequent cardiomyocyte formation recorded in comparison to suspension culture. The authors were successfully able to produce EBs displaying a more homogenous size and tissue morphology and able to reproduce this across four human ES cell lines. In looking at cardiomyocyte differentiation, the authors found there were differences across the cell lines in the level of differentiation, and, furthermore, that the differentiation medium used played an important role in the differentiation of the cells. Similarly Ungrin et al (2008) demonstrated in human ES cells that the starting cell composition and inductive environment could be manipulated in order to form large numbers of well-defined aggregates which exhibited multi-

lineage differentiation and substantially improved self-organisation from single-cell suspensions.

In methylcellulose (MC) culture, when ES cells are seeded onto semi-solid methylcellulose media the ES cells tend to remain as single cells, isolated by the matrix of the methylcellulose. These single ES cells then develop into aggregates or EBs. This study showed that methylcellulose culture allows reproducible formation of EBs from single ES cells. Studies have suggested that this method is particularly suitable for the study of hematopoietic differentiation as hematopoietic cells are efficiently produced via EB formation in MC culture system (Wiles and Keller, 1991, Keller et al., 1993, Kennedy et al., 1997). Wiles et al (1991) suggested this may be due to the local accumulation of factors in the matrix of the MC surrounding EBs.

Finally, EBs can also be formed using the hanging drop method. This approach has proved popular in the culture of mouse ES cells. Hanging drops provide ES cells with an appropriate environment for the formation of EBs, with the rounded bottom of the drop providing a good area for cell aggregation. This method is more suitable for producing more homogenous EBs, as varying the number of cells in the initial suspension can control the number of cells aggregated in the hanging drop. Typically, 20-30μl drops containing 400-1000 ES cells are placed on the lid of petri dishes and inverted over petri dishes containing PBS to prevent the drops from drying out. After two days in culture, ES cells are placed in standard suspension culture conditions. Formation of human EBs in hanging drops has been reported by manually dissecting human ES cell colony pieces, however, again the size of the starting material remains heterogeneous and this remains a labour intensive method with low throughput (Yoon et al., 2006).

A number of studies have shown there are three main factors that affect the differentiation trajectory of ES cells. These are i) human ES cell composition, ii) colony size and, iii) EB size (Bauwens et al., 2008). Supporting the idea that the size of the EB is critical in the differentiation potential of the cells and the production of a more homogeneous cell population, Messana et al (2008) looked at three sizes of mouse EBs which were produced using standard suspension culture conditions. The three sizes of

EBs were cultured separately for three weeks in chondrogenic medium. The authors showed that small EBs had a greater potential than medium or large EBs for chondrogenic differentiation, since type II collagen and aggrecan expression was significantly upregulated in the small EBs in comparison to the medium and large sized EBs. Proteoglycans produced by the cells from the small EBs were greater than 50% compared to the other two groups. Additionally both Oct-4 and Sox-2 were greater expressed in the small EBs. Slight shifts in haematopoietic and endothelial differentiation were seen in the large and medium EBs.

For differentiation toward the osteogenic lineage, Cao et al (2005) studied differentiation using intact embryoid bodies. Cao and co-workers plated the EBs directly onto matrigel coated dishes and followed cellular outgrowth from the EBs for a total of 22 days. Cells were cultured in medium supplemented with known osteogenic promoting supplements and the authors observed distinct nodule-like structures (in the EB clumped cells), which expressed STRO-1 and bone specific alkaline phosphatase. They also reported the secretion of osteocalcin, a marker of mature osteoblasts (Bronckers et al., 1987), which peaked between day 12 and 14 in culture before reaching a plateau. Nakagawa et al (2009) compared the induction of chondrogenesis from human ES cells without the inclusion of an embryoid body step and supplementing the standard chondrogenic media with BMP-7 and TGF-β1. The authors concluded that this method was successful in the differentiation of the cells, with chondrogenesis assayed by measurement of GAG (glycosaminoglycan) levels, toluidine blue staining and histological analysis for type II collagen, as well as upregulation of *COL2A1* and the proteoglycan *Aggrecan*.

Strategies that do not involve EB formation have also been investigated for the differentiation of ES cells along the osteogenic and chondrogenic lineages. Previously the majority of studies performed have used mouse ES cells, although in the last few years increasing numbers of studies have used human ES cells. The protocols used have been varied, including, the use of different combinations of growth factors to promote the formation of osteoblast-like cells. Olivier et al (2006), obtained SSCs by using the scraped cells from the sides of human ES cell cultures which had spontaneously differentiated, however, these were found to maintain their multipotent potential when

replated. The human ES cells were cultured on γ-irradiated feeder cells and following sorting and expansion were shown to be able to differentiate into osteoblasts and adipocytes. Key to this investigation is that once the SSCs were produced, they could be used as feeder cells to support the growth of undifferentiated human ES cells, therefore not requiring feeder layers of animal origin.

In addition to the formation of embryoid bodies, a number of studies have been performed to investigate the effects of growth factors on ES cells. It is noteworthy that mouse ES cells cannot give rise to the trophectoderm and therefore there are likely to be different developmental potentials between mouse and human ES cells. Thus, it cannot be assumed that responses seen in the mouse will be the same as in human. For example, BMP signalling exerts different effects in stem cell cultures, promoting pluripotency in the mouse ES cells and differentiation to the trophoblast in human ES cells (Spagnoli and Hemmati-Brivanlou, 2006). Mouse and human ES cells may represent different stages of development and clearly display different requirements for growth and maintenance of the pluripotent state (Reubinoff et al., 2000, Thomson et al., 1998). However, the signalling pathways that regulate human ES cell differentiation are similar to those that regulate these processes in mouse ES cell cultures (Murry and Keller, 2008). For example, activin signalling leads to the efficient induction of definitive endoderm in human ES cell cultures, with molecular analysis showing that the induced populations progress through a PS stage to definitive endoderm in similar time frame to mouse cultures (D'Amour et al., 2005). Mesoderm induction from human ES cells is also comparable to mesoderm induction observed in the mouse (Murry and Keller, 2008).

Zur Nieden et al (2003) compared the morphologies of treated and non-treated mouse EBs which indicated that ascorbic acid and β-glycerophosphate were required for deposition and mineralization of extracellular matrix. This occurred as soon as 5 to 6 days after culture. Bielby et al (2004) initiated osteogenic differentiation using EBs derived from human ES cells, a method which at the time had only been applied to mouse ES cells. Following EB formation, the cells were harvested and replated in osteogenic medium. The positive staining of alizarin red and the presence of mineralized colonies indicated the differentiation of the cells down the osteoblast lineage. The supplementation with dexamethasone provided the greatest effect on bone

nodule formation, however the timing of supplementation was shown to be an important factor, with an increased response in dexamethasone treatment if applied later during the culture treatment. However, Karp et al (2006) found that culturing human ES cells without an EB stage led to seven-fold increase in the number of osteogenic cells and to spontaneous bone nodule formation after 10-12 days. This observation was in contrast to the EB method, which produced bone nodules after 4 weeks of culture in the presence of dexamethasone only.

In an investigation by Karner and colleagues (2007), four pluripotent stem cell lines were examined for their capacity to differentiate toward the osteoblastic lineage and their ability to then form a mineralised ECM. This included the use of an embryonic stem cell line that had been derived and maintained on commercially available human foreskin fibroblasts in comparison to culture on a MEF feeder layer to maintain the pluripotent state. The authors used cells cultured in monolayer and EB-derived cultures and found results which supported the findings of Karp et al (2006). Overall, it was concluded that the lineage potential was not dependent on the mode of differentiation but the cell line, with some cell lines appearing to have an increased tendency to follow the mesenchymal and osteoblastic lineage. The authors showed that the HS181 cell line possessed the highest osteogenic potential in monolayer and EB culture. However, it would be expected that the aggregation of human ES cells into three-dimensional structures in suspension would have an inductive effect.

A study performed by Sottile et al (2003) also used the formation of EBs in osteogenic conditions (50μM ascorbic acid phosphate, 10mM β-glycerophosphate and 100nM dexamethasone) to promote differentiation and used the formation of nodules as a marker of bone. The authors compared the time course of bone nodule formation to a human bone marrow stromal cell line. The study also included the omission of the EB step and found that mineralization was still observed but delayed. Kawaguchi et al (2005), found that upon addition of retinoic acid (RA) the overall mesoderm formation within EBs was reduced, with marked decrease in expression of brachyury. It was shown that RA-treatment on EBs was thought to be critical for quantative induction of mesenchymal lineages. Different growth factors were placed together with the RA-treated EBs and acted to induce and/or expand distinct mesenchymal sub-lineages. For example, when bone morphogenic protein 4 (BMP-4) was administered, adipogenesis is

suppressed, while the osteoblast phenotype is evident. Oct-4 expression is virtually eliminated in RA-treated EBs.

Experiments carried out by Schuldiner et al (2000), looked at the effects of 8 specific growth factors on the differentiation of human ES cells in culture and EBs, identifying growth factors which appeared to inhibit the expression of one set of germ layer cells while allowing differentiation into another. In order to achieve mesoderm formation, differentiation of the human ES cells was performed via an EB formation stage with TGF-β1 and activin A. Ectodermal/Mesodermal formation was induced by the addition of retinoic acid, epidermal growth factor (EGF), BMP4, and basic fibroblastic growth factor (bFGF). Induction into all three germ layers used nerve growth factor (NGF) and hepatocyte growth factor (HGF). Most of the growth factors could act to inhibit differentiation of specific cell types rather than giving an inductive affect, however, none tested could direct differentiation exclusively to one particular cell type.

Differentiation of human ES cells on three-dimensional polymer scaffolds has also been performed by Levenberg et al (2003). The authors found that the differentiation and organization of the cells was influenced by the scaffold and directed by the growth factors used. EBs were created and grown for 8/9 days before being trypsinized to obtain single cells which were seeded onto polylactic-co-glycolic acid (PLGA) or poly L-lactic acid (PLLA) scaffolds. The initial formation of EBs was observed to exhibit uniform growth and survival of the cells on the scaffolds compared to the use of undifferentiated ES cells. The addition to TGFβ-1 alone to the medium induced the formation of tissue that secreted a cartilage-like glycosaminoglycan extracellular matrix. The addition of retinoic acid to the media acted to induce ectodermal differentiation and Activin A and insulin like growth factor (IGF), the formation of structures with biochemical features found in developing liver (Levenberg et al., 2003).

Co-culture strategies to direct the differentiation of the mouse ES cells along the stromal lineage have also been reported by Buttery et al (2001). In this study, mouse calvarial osteoblasts from foetal mice were placed on transwell inserts and co-cultured with mouse ES cells dissociated from embryoid bodies. Differentiation toward the osteoblast lineage was characterised by the formation of bone nodules within an extracellular matrix of type I collagen and osteocalcin. The cells grown in co-culture showed a 5-fold increase in the number of nodules in comparison to cells cultured

without the foetal layer. In comparison to a number of other studies, the combination of dexamethasone, ascorbic acid and β-glycerophosphate was found to be most osteo-inductive on single ES cells, with the timing of stimulation also an important factor. Human undifferentiated ES cells have been co-cultured with irradiated neonatal or adult articular chondrocytes in high-density pellet mass cultures for 14 days. The co-cultured ES cells were then expanded on plastic and their differentiation potential toward the chondrogenic, osteogenic and adipogenic lineages compared to that of the undifferentiated ES cells. The authors demonstrated that the co-cultured ES cells could be expanded on plastic with a morphology and expression of surface markers similar to SSCs. Pellets formed from co-cultured cells were more heterogeneous and showed significantly increased cartilage matrix production (Bigdeli et al., 2009). A summary of all the differentiation studies discussed is given in Table 1:2.

Lineage	Method	Conditions	Reference;
Osteogenic	Suspension culture method of EB formation	Intact EBs were cultured for 22 days in osteogenic media and cellular outgrowth assessed	(Heng et al., 2004)
Hematopoietic	Forced aggregation of defined ES cell numbers to EBs in v-96 well plate	EBs formed by centrifugation method and cultured for 8-12 days in round bottomed well plates prior to transfer to tissue culture treated plates and differentiated further	(Ng et al., 2005)
Cardiomyocyte	Using same method as above, with conditions adapted	Four cell lines were tested, with EBs incubated for 2,4 or 6 days before transferring to suspension culture for 6 days to allow further differentiation	(Burridge et al., 2007)
Mesoderm, ectoderm, endoderm	Suspension culture method of EB formation followed by culture in low-attachment, non-tissue culture treated plates and finally plated onto tissue culture dishes	Prior to EB formation ES cells were plated at high density onto micropatterned matrigel islands. EBs were formed from the cells of these islands and differentiation trajectory observed for different sized ES cell aggregates cultured for a total of 16 days.	(Bauwens et al., 2008)
Hematopoietic	Methylcellulose culture of EBs	Dissociated EBs were seeded onto semi-solid methylcellulose media which then develop into EBs	(Keller et al., 1993, Kennedy et al., 1997, Wiles and Keller, 1991)
Chondrogenic	Suspension culture method of EB formation	EBs were organised into small, medium and large size (to determine the optimal size for differentiation). EBs were placed into adherent culture conditions and cultured for 3 weeks and chondrogenic differentiation assessed	(Messana et al., 2008)
Osteogenic	Suspension culture method of EB formation	Following growth for 2 days in culture EB media was supplemented with osteogenic growth factors and treatment was continued for 22 days. Osteocalcin secretion by spent media was assessed as well as molecular characterisation of osteogenic phenotype	(Cao et al., 2005)
Chondrogenic	Direct plating of ES cells from culture (omission of EB step)	Single cells were used for pellet cultures or plated directly into a culture dish, chondrogenic media was applied and the affects of the addition of BMP-7 and TGF-β1 assessed	(Nakagawa et al., 2009)
Osteogenic, adipogenic	Scraping of differentiated cells from sides of human ES cell cultures	Cells were cultured on an irradiated feeder layer and multipotent potential of the cells assessed	(Olivier et al., 2006)
Osteogenic	Embryoid body formation by hanging drop method	Following EB formation, EBs were cultured in 24-well plates. Medium used was supplemented at various time points with osteogenic factors.	(zur Nieden et al., 2003)
Osteogenic	Suspension culture method of EB formation	Following 5 days in suspension culture, cells harvested from EBs were replated in a medium containing osteogenic supplements. Cells were also implanted into SCID mice on a poly-D, L-lactide (PDLLA) scaffold; the cells had the capacity to give rise to mineralized tissue *in vivo*.	(Bielby et al., 2004)

Osteogenic	Direct culture of ES cells (omission of the EB stage)	Bone nodule formation was compared for cells cultured with/out an EB stage, cultured in dexamethasone only	(Karp et al., 2006)
Osteogenic	Culture of human ES cells in monolayer and as EBs	Undifferentiated cells were cultured either in suspension, (formation of EBs), or in monolayer, and both methods were in the presence of osteogenic supplements. Novel to our osteogenic differentiation study was the use of commercially available human foreskin fibroblasts to support the undifferentiated growth of the human ES cell colonies	(Karner et al., 2007)
Osteogenic	EB formation by suspension culture	EBs were formed in osteogenic media and remained in suspension culture conditions for the duration of the study	(Sottile et al., 2003)
Mesoderm	EB formation by suspension culture	EBs were treated with retinoic acid and then different growth factors applied and the affect on mesoderm lineage formation observed	(Kawaguchi et al., 2005)
Mesoderm	Treatment of ES cells in culture as well as EBs formed by	Differentiation of ES cells was by the formation of EBs with TGF-β1 and activin A. 8 different growth factors were used to direct the cells toward different mesoderm cells	(Schuldiner et al., 2000)
Mesoderm	Growth of ES cells on 3-D scaffolds	EBs were formed and then cultured on scaffolds as single cells in comparison to cells that had not undergone a differentiation step. 4 different growth factors were used to promote cell differentiation	(Levenberg et al., 2003)
Osteogenic	Co-culture of mouse ES cells and foetal mouse calvarial osteoblasts	Differentiation of ES cells toward the osteoblast lineage can be enhanced by supplementing serum-containing media with ascorbic acid, beta-glycerophosphate, and/or dexamethasone/retinoic acid or by co-culture with foetal murine osteoblasts.	(Buttery et al., 2001)
Chondrogenic, adipogenic, osteogenic	Co-culture of human ES cells and human articular chondrocytes	Cells were placed in co-culture for 14 days, and then expanded on plastic and their differentiation potential toward the adipogenic, chondrogenic and osteogenic lineages assessed	(Bigdeli et al., 2009)

Table 1:2 Overview of approaches taken for the differentiation of ES cells.

1.4 Induced Pluripotent Stem (iPS) Cells

Pioneering work by Yamanaka and Takahashi (2006) has led to a new field of stem cell research with the development of induced pluripotent stem (iPS) cells as a source of pluripotent stem cells. iPS cells are somatic cells that have been reprogrammed by the use of a number of (originally four key) factors to an embryonic-like state. Yamanaka and Takahashi (2006) successfully reprogrammed mouse embryonic fibroblasts and adult fibroblasts to pluripotent ES-like cells after viral-mediated transduction of a combination of 24 various transcription factors, finally narrowing down to four core factors which acted to reprogram the cells to an embryonic like state. The four transcription factors used were, Oct-3/4, SOX-2, c-myc, and Klf4, these were transferred using retroviruses and followed by selection for activation by the Oct-4 target gene Fbx15. The proteins acted to trigger the expression of other genes, which led the cells to become pluripotent. Oct-3/4 and SOX-2, function cooperatively as core transcription factors in maintaining pluripotency whereas c-myc and Klf4 are tumour related factors. When these cells were subcutaneously transplanted into nude mice, the resulting tumours contained a variety of tissues from all three germ layers (Takahashi and Yamanaka, 2006). Following on from this, Hanna et al, (2007) used mouse iPS cells to generate blood progenitor cells to treat a mouse with a humanized version of sickle cell anaemia. This study demonstrated the capacity and the potential of iPS cells to be introduced to the clinic. Although concerns exist, including the use of viral vectors and the presence of undifferentiated cells.

These cells exhibit similar characteristics to embryonic stem cells in the ability to form colonies, to display immortal growth characteristics, to form embryoid bodies in vitro and to form teratomas *in vivo*, as well as being able to differentiate into a variety of different cell types. However, despite their relative ease of production, iPS cells are as difficult to maintain undifferentiated in culture as embryonic stem cells, requiring defined culture conditions comparable to human ES cell culture. The pluripotent state of iPS cells has been found to be dependent on the continuous expression of the transduced OCT-4 and SOX-2 genes, whereas the endogenous OCT-4 and Nanog genes were either not expressed or were expressed at lower levels than in ES cells. The karyotype of mouse and human iPS cells has been investigated, with some abnormalities observed in a few lines, but the majority of murine and human iPS cell lines exhibit a normal

karyotype. However, over long term culture, as observed in some ES cells, chromosomal abnormalities can occur and therefore careful monitoring of iPS cells in culture will be essential (Amabile and Meissner, 2009).

Following the reprogramming of mice fibroblasts, Yu et al, (2007) reprogrammed human somatic cells, IMR90 foetal fibroblasts, using a different set of four factors, OCT-4, SOX-2, NANOG and LIN28. These were shown to have normal karyotypes, express telomerase activity, express cell surface markers and genes which characterise human ES cells, and maintain the developmental potential to differentiate into advanced derivatives of the three germ layers.

Similar to human ES cells, human iPS cells are potentially useful in studying the development and function of human tissues, with potential applications in discovering and testing new drugs and for transplantation medicine. A number of questions regarding iPS cells have been raised, including the actual differentiated state of the cells as well as their potential in disease models and for therapy. It has been suggested that those cells that have been successfully reprogrammed are actually progenitors rather than terminally differentiated cells (Rodolfa and Eggan, 2006). As with embryonic stem cells the therapeutic goal would be for custom made cells to be delivered to patients in the absence of vectors. In addition, some of the genes to the cells, as well as some of the genes themselves, may cause cancer (Cyranoski, 2008). Non-integrating adenoviral iPS (adeno-iPS) cells show DNA demethylation characteristic of reprogrammed cells, express endogenous pluripotency genes, form teratomas, and contribute to multiple tissues, including the germ line, in chimeric mice. Adenoviral reprogramming may provide an improved method for generating and studying patient-specific stem cells and for comparing embryonic stem cells and iPS cells (Stadtfeld et al., 2008). Other methods for iPS generation have been reviewed by Patel and Yang (2010), with the use of non-viral vectors becoming more common to address the issue of any unpredictable genetic dysfunctions.

Both ES cells and iPS cells present safety concerns due to their potential to form tumours. When these cells are transplanted in their undifferentiated state they form teratomas, which are tumours derived from all three germ layers. Currently the only way to ensure that these teratomas do not form is to differentiate the cells and to enrich

for the desired cell type and then screen for the presence of any undifferentiated cells (Murry and Keller, 2008). When performing these control procedures Laflamme and colleagues (2007), did not observe any teratoma formation in over 200 animals which had human ES cell derived cardiomyocytes transplanted.

1.5 Other Stem Cell Sources

Foetal-associated tissues are another potential source of cells for tissue engineering, however in order for these cells to be used, characterisation of the foetal cells is necessary in order to determine the process of normal development and to compare the pattern of secreted proteins which have been shown to differ depending upon the age of the cells. Such associated tissues are placenta, amniotic fluid and umbilical cord. In the UK, foetal tissue is collected and used in accordance with the Polkinghorne report, which states the requirement for written and informed consent of the (abortive) mother, with the ability for consent to be withdrawn at any time.

Cells obtained from the amniotic fluid, are not believed to be influenced by differentiation stimuli and may act in a manner which is more representative of the physiological processes of specific differentiation pathways. These cells would represent an ethically acceptable alternative to human ES cells (De et al., 2006). Supporting this idea is the identification of OCT-4 positive cells within amniotic fluid (Prusa et al., 2003). Menstrual blood has also been suggested as a source of stromal stem cells, and it has been demonstrated that these cells can easily be expanded and express multipotent markers such as OCT-4, SSEA-4 and c-kit at both the molecular and cellular level. The multipotency of the cells was also demonstrated by differentiation toward the chondrogenic, adipogenic, osteogenic, neurogenic and cardiogenic lineages (Patel et al., 2008).

Studies looking at the multipotentiality of foetal derived stem cells have been performed. Cui et al (2006) were able to demonstrate that human foetal articular chondrocytes could form cartilage in pellet culture, adipose cells in dense monolayer cultures, mineralize in an in vitro osteogenic assay and express neuronal markers in an in vitro neural assay. The authors also showed that culture-expanded articular chondrocytes exhibited differentiation patterns similar to that of SSCs from human bone marrow and other tissues. Another study compared the osteogenic capacity of SSCs

derived from human adult bone marrow, foetal bone marrow, umbilical cord, and adult adipose tissue, and concluded that foetal bone marrow derived SSCs had the most proliferative and osteogenic capacity of the stem cell sources examined. Zhang et al (2009) suggested that this enhanced osteogenic capacity as well as immunogenic privilege confirmed in these cells, made this cell source a good candidate for bone tissue engineering strategies. For osteogenesis modelling, Harris and co-workers (1995) established an immortalised human foetal osteoblastic cell line. Additionally, Montjovent et al (2004) demonstrated the properties of pre-natal cartilage like cells and developing bone cells, which showed enriched alkaline phosphatase activity when placed in osteogenic conditions as well as successful growth of the cells on 3-D scaffolds. The multilineage potential of foetal cells derived from the foetal femur has also been demonstrated (Mirmalek-Sani et al., 2005), as well as foetal cells at 14 weeks post conception (Campagnoli et al., 2001). Mirmalek-Sani et al (2005) observed an increased proliferation rate of the foetal cells compared to adult marrow populations.

Other sources of stem cells include adult tissues, and these stem cells are named according to the tissue from which they are derived. These adult tissue derived cells have the ability to differentiate into more than one cell type as well as cells of other lineages (Song and Tuan, 2004, Phinney and Prockop, 2007). Adult stem cells have been used to successfully treat leukaemia and related bone/blood cancers through bone marrow transplants. The use of these cells in therapy is not as controversial as the use of embryonic stem cells as their production does not require the destruction of an embryo.

Stem cells from various sources can potentially be differentiated toward skeletal cells. However, prior to this, an understanding of the bone physiology and composition is needed in order to accurately characterise the cells produced and assess their suitability for therapeutic application.

1.6 Bone Physiology and Composition

The skeletal system is a physical framework that acts to provide movement as well as mechanical and protective support. Bones can be classified according to their shape, gross appearance, macroscopic appearance and examination, and their developmental origin. Morphologically there are two forms of bone: cortical (compact), which provides the mechanical and protective functions and cancellous (spongy), which

provides the metabolic functions in bone (Marks and Hermey, 1996). Two types of bone formation process are apparent: intramembranous, in which mesenchymal progenitors condense and then differentiate directly into osteoblasts and, endochondral, in which mesenchymal progenitors condense to first form a cartilage model/template that is later replaced by bone in the process of endochondral bone formation. Endochondral bone formation is responsible for the formation of the majority of the bones in the body. In addition to the differences in the process of bone formation, it is known that separate embryonic lineages are involved in forming different parts of the skeleton (Aubin, 1998).

Bone is a specialised tissue comprised of an organic matrix, strengthened by calcium salt deposits. Type I collagen constitutes approximately 95% of the organic matrix, this is made intracellularly as tropocollagen which is then exported and associates into fibrils. The remaining 5% of the matrix is made up of proteoglycans and non-collagenous proteins (Marks and Hermey, 1996). The organic component of the matrix is also made up of non-collagenous proteins, including osteocalcin, bone sialoprotein (BSP), osteopontin and osteonectin, which are produced by bone cells and act to regulate bone mineralisation. Osteocalcin and BSP are both bone specific and comprise 20% and 15% respectively of the total non-collagenous proteins in bone (Hing, 2004). In terms of temporal expression, osteocalcin is the last to be expressed and acts as a biochemical indicator of bone turnover. A further function of osteocalcin is osteoclast recruitment (zur Nieden et al., 2003). BSP is a multi-functional protein which is expressed in the later stages of osteogenesis (zur Nieden et al., 2003). It is secreted by osteoblasts and modulates the vascularization of new bone (Alford and Hankenson, 2006). Osteopontin is secreted by osteoblasts during the early stage of osteogenesis.

The inorganic component of the matrix is predominantly crystalline mineral salts and calcium, present in the form of hydroxyapatite (Marks and Hermey, 1996). The matrix is initially unmineralised osteoid. The ECM of bone has been shown to be remodelled during growth and development as well as under various pathological conditions (Heng et al., 2004).

1.6.1 Long Bone Structure

The structure of a long bone (femur) can be seen in Figure 1:5. The structure of the long bone can be separated into several main areas. The central shaft of a long bone is called the diaphysis, which has a hollow centre, the medullary cavity containing the bone marrow. In children, long bones are filled with red marrow that is gradually replaced with yellow marrow with age. The diaphysis is cylindrical and is mostly made up of compact bone with only a small component of spongy bone on its inner surface around the medullary cavity. The end zone of the diaphysis is referred to as the metaphysis.

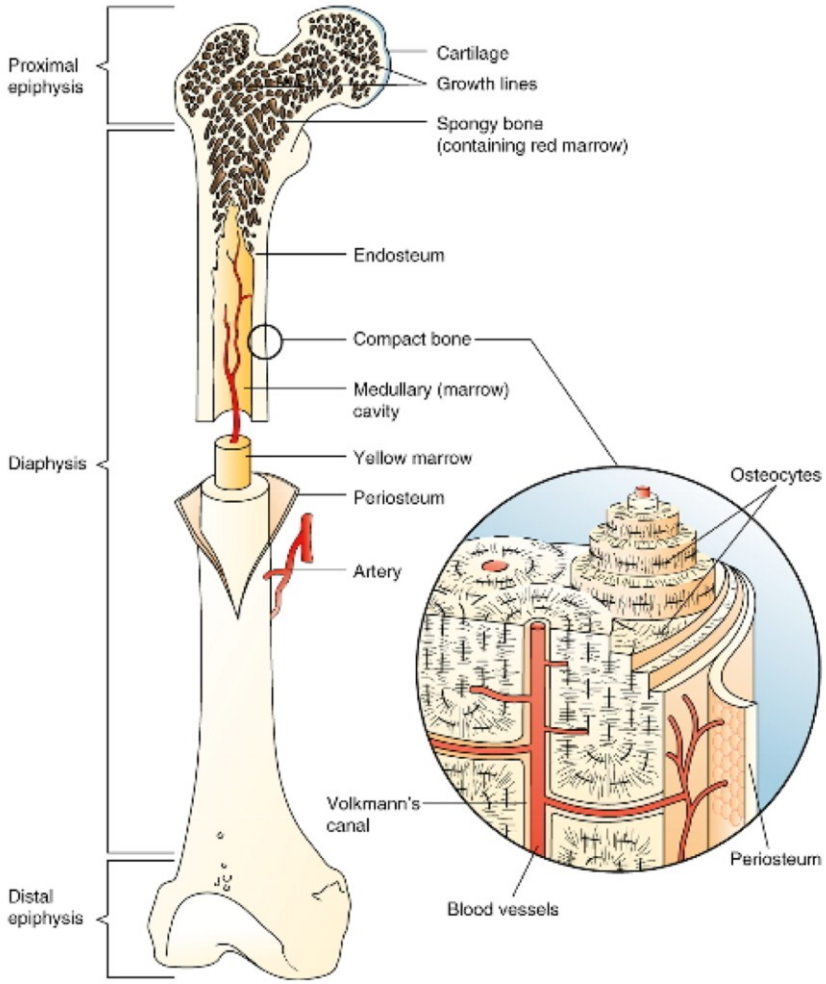

Figure 1:5 Structure of a long bone and composition of compact bone. The long bone is divided into three portions, the diaphysis and epiphysis (named proximal or distal in relation to their position in the torso) and is covered with periosteum and articular (joint) cartilage. The compact bone is composed of osteons. An osteon consists of concentric lamellae of bone matrix, mainly collagen fibres, surrounding a central canal called the Haversian canal, containing small blood vessels and nerves. Volkmann's canals link the Haversian canals of different osteons with one another and with the marrow cavity and provide the major route for blood vessels. Taken from: http://thepoint.lww.com.

At each end of the long bone, the epiphysis is found, which are described as proximal or distal in relation to the torso. The joint surface of each epiphysis is covered by a thin layer of articular (or hyaline) cartilage, which acts to cushion the opposing bone ends during joint movement and to absorb stress (Baron, 2003). The articular cartilage covers a layer of compact bone, beneath which lies the trabecular bone.

The metaphysis is the developmental zone between the epiphysis and the diaphysis. This is also referred to as the 'growth plate' or 'epiphyseal plate'. The growth plate grows during childhood as a layer of hyaline cartilage that allows the diaphysis of bone to grow in length, while the bone grows it ossifies near the diaphysis and the epiphysis (Baron, 2003).

The periosteum is a double-layered membrane consisting of an outer fibrous layer of collagen fibres and an inner layer of SSCs. The periosteum covers the surface of all bones except at the joints, and has a nerve and blood supply which enter the bone shaft via a nutrient foramen. The endosteum line internal bone surfaces and is composed of a single layer of connective tissue lining the surface of the medullary cavity. The cell population found in the bone marrow consists of haematopoietic and stromal stem cells (that have the ability to differentiate along different lineages), haematopoietic cells and osteoclasts as well as cells of the stromal lineage, including osteoblasts, chondrocytes and adipocytes.

1.7 Foetal Skeletal Development

The skeletal system develops from the paraxial and lateral plate (somatic layer) mesoderm and neural crest. During the 4th week of development, limb buds become visible. Initially these consist of a mesenchymal core derived from the somatic layer of lateral plate mesoderm that will form the bones and connective tissues of the limb. In 6-week old embryos the terminal portions of the limb buds become flattened to form the hand and foot plates. It is by the 6th week of development that the first hyaline cartilage models are formed as the mesenchyme in the buds begins to condense and differentiate into chondrocytes. The mould formed is termed the cartilage anlage. Control of the timing, shape and position of the mesenchymal condensations which occur relies on the homeobox (*Hox*) genes, with mammalian limb patterning determined by genes within the *Hox a, b, c* and *d* domains (Krumlauf, 1994).

1.7.1 Intramembranous Ossification

Intramembranous ossification occurs during embryonic development by the direct transformation of mesenchymal cells into osteoblasts. This type of bone formation is restricted to bones of the cranial vault, some facial bones and parts of the mandible and clavicle (Marks and Hermey, 1996).

1.7.2 Endochondral Ossification

Following formation of the cartilaginous mould, endochondral ossification is responsible for the growth and maturation of bone tissue. Ossification of the bones by endochondral ossification begins by the end of the embryonic period. Primary ossification centres are present in the long bones of all the limbs by week 12. From the primary centre in the diaphysis of the bone, endochondral ossification progresses toward the ends of the cartilaginous model. At birth the diaphysis of the bone is normally completely ossified, but both epiphysis are still cartilaginous (Marks and Hermey, 1996).

Development of long bones begins with a bone collar around the centre of the cartilage anlage (the primary ossification centre), leading to an early diaphysis that expands further toward each end of the bone through foetal development, shown in Figure 1:6. Invasion of a vascular supply and osteoprogenitor cell recruitment continues the growth and calcification process, forming the cortical bone and marrow cavity. Trabecular bone development occurs at a second ossification centre, with the growth plate facilitating the continual lengthening of the long bones throughout childhood and adolescence (Johnson, 2002).

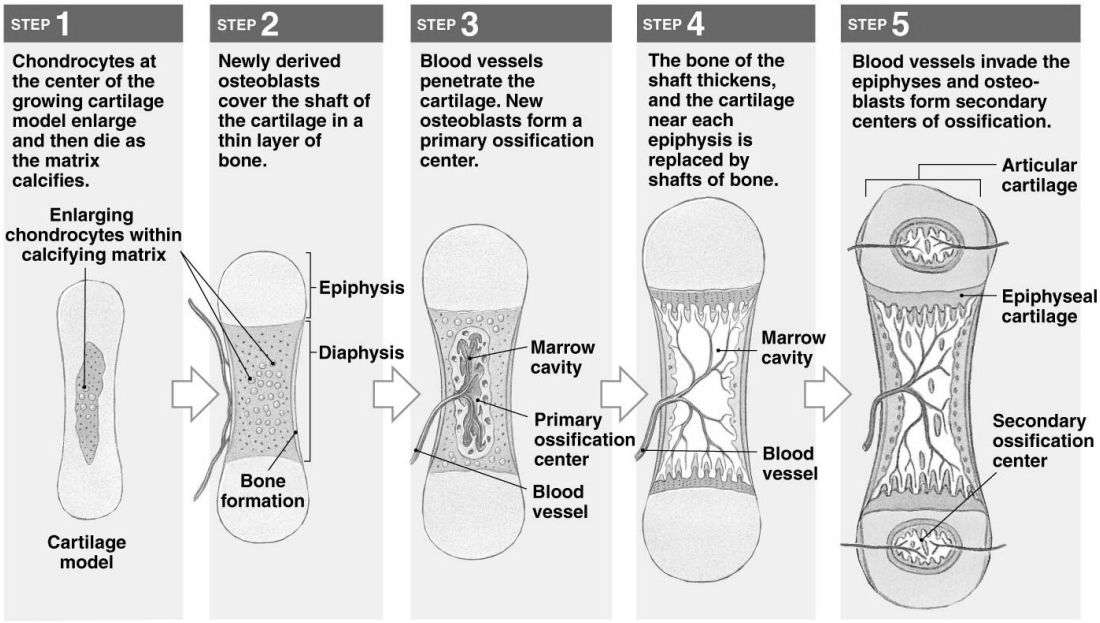

Figure 1:6 Process of endochondral ossification. Endochondral ossification is responsible for much of the bone growth in mammalian skeletons. The growth of the cartilage model in length is by the continuous cell division of chondrocytes, accompanied by secretion of extracellular matrix. The chondrocyte calcifies its matrix prior to undergoing apoptosis. Blood vessels then penetrate the calcified matrix, bringing in osteoblasts, which use the calcified cartilage matrix as a template to build bone. Adapted from www.welchclass.com, anatomy section.

The longitutidinal development of mammalian long bones depends upon the chondrocytic structures contained within the growth plate. The growth plate has an organised arrangement of cells that can be divided into histological zones that highlight the progression and maturation of chondrocytes within the same section.

Bone remodelling is a continual process, with the activities of osteoblasts and osteoclasts closely coordinated during skeletal growth. The process of bone remodelling results in no net bone formation and is tightly regulated, allowing bone tissue to adapt its internal structure and mass to mechanical demands ensuring maximal strength with minimal bone mass (Klein-Nulend et al., 2005). The remodelling process is illustrated in Figure 1:7, during bone remodelling, old bone is resorbed by osteoclasts and replaced with new osteoid, secreted by osteoblasts. Osteoclasts are then activated and the resorption process takes approximately 10-14 days. Osteoblasts are then recruited which proliferate and differentiate into mature osteoblasts and secreting new bone matrix. The matrix then mineralises to generate new bone and the remodelling process is complete.

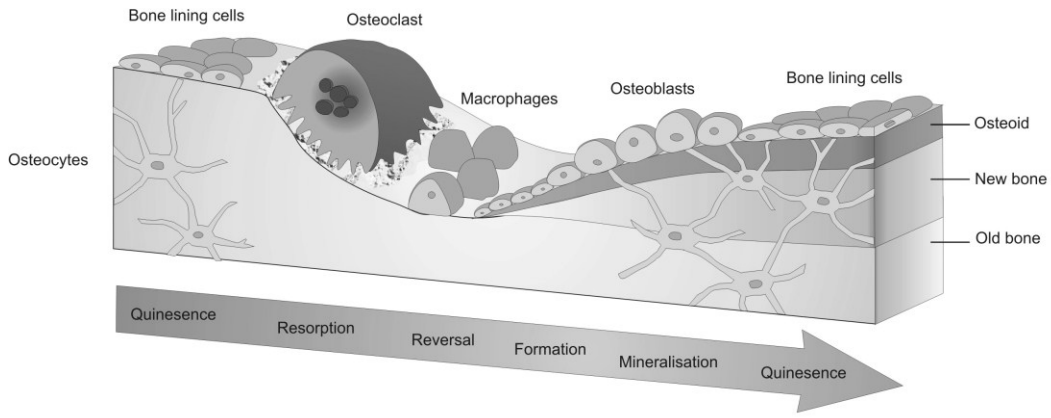

Figure 1:7 The bone remodelling process. The resorption process takes approximately 10-14 days with osteoclasts responsible for resorption of the old bone. Osteoblasts are then recruited which proliferate and differentiate into mature osteoblasts which secret new bone matrix. The matrix then mineralises to generate new bone and the remodelling process is complete. Figure adapted from York.ac.uk Research Image Library.

1.8 Bone Cells

The process of bone development involves a number of distinct phases, including, migration of cells with osteogenic potential to the site of future skeletogenesis; this is followed by mesenchymal-epithelial interactions, leading to condensation/aggregation of mesenchymal cells and finally differentiation along the chondrogenic or osteogenic lineages. The development of the osteogenic lineage includes the secretion of a complex extracellular matrix. There are four main bone cells; these are osteoblasts, osteocytes, osteoclasts, and bone lining cells. Osteoblasts are the small, mononuclear cells responsible for bone formation.

Osteoblasts are derived from the osteoprogenitor cells remaining from embryonic development, which are capable of self-renewal and maintenance. These cells are located near to the bone surface, and their primary function is to produce osteoid and manufacture hormones such as prostaglandins which act on bone itself (Baron, 2003). Osteoblasts produce alkaline phosphatase, a chemical that has a role in the mineralisation of bone, as well as other matrix proteins. Alkaline phosphatase is a marker, albeit non-specific, of osteoblasts in culture. Type I collagen is also synthesised by osteoblasts and deposited in layers in mature bone, called lamellae. The orientation of the fibres allows for a high density of collagenous filaments.

Osteocytes originate from osteoblasts and are in essence osteoblasts trapped by the bone matrix they produce. The space that they occupy is known as a lacuna. Osteocytes have many canaliculi (small channels found in ossified bone) which reach out to osteoblasts, for the purpose of communication, as the cells are thought to regulate the bones' response to stress. Overall the functions of osteocytes include bone formation, matrix maintenance and calcium homeostasis.

Osteoclasts are large multinucleate cells located on bone surfaces and are the cells responsible for bone resorption by reshaping the deposited matrix (Baron, 2003). During bone development, osteoclasts which are located in lacunae, are required to degrade the cartilage matrix for vascular invasion in endochondral ossification. Furthermore, osteoclasts are also involved in bone growth and shape modification in endochondral ossification. After skeletal maturation, osteoclasts continue to play a critical role in bone maintenance by participating in bone remodeling. Bone formation and reabsorption is a continual process and a dynamic equilibrium exists between both processes.

Finally, bone lining cells are former osteoblasts that have become flattened, mononucleate cells which line the surface of most bones. Bone lining cells regulate the movement of calcium and phosphate in and out of bone, and have receptors for hormones and signalling molecules that initiate bone remodelling and osteoclastic resorption.

1.9 Markers of Bone

The identification of osteogenesis related transcription factors and osteoblast specific markers has increased our understanding of the differentiation process. Differentiated osteoprogenitors express markers such as osteopontin (OP), which is expressed at an early stage and alkaline phosphatase (AP). The osteogenic cells are capable of producing extracellular organic matrix, *in vivo*, including associated bone markers, bone collagen 1 and osteocalcin (OCN), which act as markers of the mature osteoblast phenotype. Bone sialoprotein (BSP), a protein of the matrix appears at the time of the occurrence of mineral. Osteogenesis can be demonstrated by specific staining for calcium deposition in matrix, for example using von Kossa or Alizarian Red staining. A list of the typical markers used is given in Table 1:3.

Marker Name	Cell Type	Significance
Bone-specific alkaline phosphatase (BAP)	Osteoblast	Enzyme expressed in osteoblast; activity indicates bone formation
Hydroxyapatite	Osteoblast	Mineralized bone matrix that provides structural integrity; marker of bone formation
Osteocalcin (OC)	Osteoblast	Mineral-binding protein uniquely synthesized by osteoblast; marker of bone formation
Bone morphogenetic protein receptor (BMPR)	Mesenchymal stem and progenitor cells	Important for the differentiation of committed mesenchymal cell types from mesenchymal stem and progenitor cells; BMPR identifies early mesenchymal lineages (stem and progenitor cells)
CD34	Hematopoietic stem cell (HSC), satellite, endothelial progenitor	Cell-surface protein on bone marrow cell, indicative of a HSC and endothelial progenitor; CD34 also identifies muscle satellite, a muscle stem cell
CD34+Sca1+ Lin- profile	Mesenchymal stem cell (MSC)	Identifies MSCs, which can differentiate into adipocyte, osteocyte, chondrocyte, and myocyte
CD44	Mesenchymal	A type of cell-adhesion molecule used to identify specific types of mesenchymal cells
c-Kit	HSC, MSC	Cell-surface receptor on BM cell types that identifies HSC and MSC; binding by foetal calf serum (FCS) enhances proliferation of ES cells, HSCs, MSCs, and hematopoietic progenitor cells
Colony-forming unit (CFU)	HSC, MSC progenitor	CFU assay detects the ability of a single stem cell or progenitor cell to give rise to one or more cell lineages, such as red blood cell (RBC) and/or white blood cell (WBC) lineages
Fibroblast colony-forming unit (CFU-F)	Bone marrow fibroblast	An individual bone marrow cell that has given rise to a colony of multipotent fibroblastic cells; such identified cells are precursors of differentiated mesenchymal lineages
CD146	Bone marrow fibroblasts, endothelial	Cell-surface protein (immunoglobulin superfamily) found on bone marrow fibroblasts, which may be important in hematopoiesis; a subpopulation of Muc-18+ cells are mesenchymal precursors
Stem cell antigen (Sca-1)	HSC, MSC	Cell-surface protein on bone marrow (BM) cell, indicative of HSC and MSC
STRO-1 antigen	Stromal (mesenchymal) precursor cells, hematopoietic cells	Cell-surface glycoprotein on subsets of bone marrow stromal (mesenchymal) cells; selection of Stro-1+ cells assists in isolating mesenchymal precursor cells, which are multipotent cells that give rise to adipocytes, osteocytes, smooth myocytes, fibroblasts, chondrocytes, and blood cells
Collagen types II and IV	Chondrocyte	Structural proteins produced specifically by chondrocyte
Sulfated proteoglycan	Chondrocyte	Molecule found in connective tissues; synthesized by chondrocyte

Table 1:3 Markers commonly used to characterise cells found in bone, cartilage and bone marrow and their significance. Adapted from www.stemcells.nih.

1.10 Cartilage

Cartilage is highly specialised connective tissue composed of chondrocytes and extracellular matrix. Cartilage has little capacity to regenerate due to the absence of

blood vessels, nerves or a lymphatic system. Chondrocytes form only 1–5% volume of the articular cartilage and are sparsely spread in the matrix. Chondrocytes receive nutrients via diffusion across the matrix, since the entire tissue is avascular (Bhosale and Richardson, 2008). Chondrocytes synthesise all matrix components and regulate matrix metabolism. Chondrocytes organise collagen, proteoglycan and non-collagenous proteins into a unique and highly specialised tissue. The composition, structure and functions of chondrocytes vary depending on the depth from the surface of the cartilage. Morphologically there are four named zones, from top to bottom; superficial zone, transitional zone, middle or deep zone, and the calcified cartilage zone. As cartilage is avascular, nutrition of the tissue is dependent on diffusion of molecules through the cartilage matrix, to and from the synovial fluid (Dijkgraaf et al., 1995). Cartilage can be characterised as cells (chondrocytes) embedded within their own matrix, consisting of 40% collagen and 60% proteoglycans, molecules with a protein backbone and glycosaminoglycan (GAG) side chains.

Cartilage can be divided into three major types, elastic, fibrous, hyaline, according to their structure, and morphological appearance. Hyaline cartilage consists of predominantly type II collagen and proteoglycan and forms the skeletal mould during foetal development. Hyaline cartilage represents the most abundant cartilage type in the body. Fibrous cartilage provides great compression strength to the meniscus, perichondrium and invertebral discs through an organised matrix of collage type I and II, as found in bone. Elastic cartilage consists of elastin protein fibres that together with type II collagen provide a strong yet elastic tissue as present in the outer ear, and laryngeal structures.

Sox-9 is required for cartilage formation, with the maintenance of the chondrogenic phenotype confirmed by the expression of type II collagen and aggrecan (Bi et al., 1999, Healy et al., 1999). Maturation of chondrocytes to a hypertrophic state results in the expression of type X collagen. This is then followed by chondrocyte apoptosis and infiltration of osteoblasts during endochondral ossification (Provot and Schipani, 2005), which can be seen in Figure 1:6.

1.11 Tissue Engineering

With an increasingly ageing population, skeletal degeneration due to osteoarthritis or trauma and bone loss has become a major healthcare problem with significant socio-economic consequences. Currently treatments for cartilage degeneration and bone loss are limited and the long-term outcomes unclear. This has led to a need for an alternative strategy for cartilage and bone regeneration. One such strategy is tissue engineering.

Tissue engineering is the use of a combination of cells, an extracellular matrix or scaffold and growth factors, which when combined will produce a three-dimensional construct which can be used to repair and/or replace portions of whole tissue. The central paradigm shown in Figure 1:8 is a simplified version and the paradigm also now includes mechanical forces and bioreactors. The term regenerative medicine is often used synonymously with tissue engineering, although this tends to place more emphasis on the use of stem cells to produce tissue (Mason and Dunnill, 2008). The development of models based on the interaction and integration of cells and biomaterials can also help us in the understanding of the basic mechanisms of bone and cartilage physiology. The models generated should mimic these tissues by resembling their organisation, mechanical properties and their physiological responses to different stimuli (Tortelli and Cancedda, 2009).

Monolayer culture has played an important role in bone and cartilage physiology, with osteogenic and chondrogenic cells being intensively investigated using the traditional two-dimensional culture systems. This has been successful in allowing researchers to investigate cellular differentiation and ECM deposition; however, these approaches cannot faithfully mimic bone and cartilage. The complex organisation between the cells and ECM is strictly dependent on the three-dimensional environment in which they are organised (Tortelli and Cancedda, 2009).

Briefly, the disadvantages which have been identified in tissue engineering models using human ES cells are that as yet the genetic stability of ES cells during extended culture has not been defined and undifferentiated cells must be removed to preclude teratoma formation (Metallo et al., 2008). In contrast, the major advantage of using ES cells is the scalable expansion of the cells at an early stage of the tissue engineering

process. Large quantities of clonally derived undifferentiated cells can be induced along a particular differentiation pathway to produce an ample supply of functional cells (Metallo et al., 2008). The current tissue engineering strategies taken using ES cells are well reviewed by Metallo et al (2008) and Jukes et al, (2009).

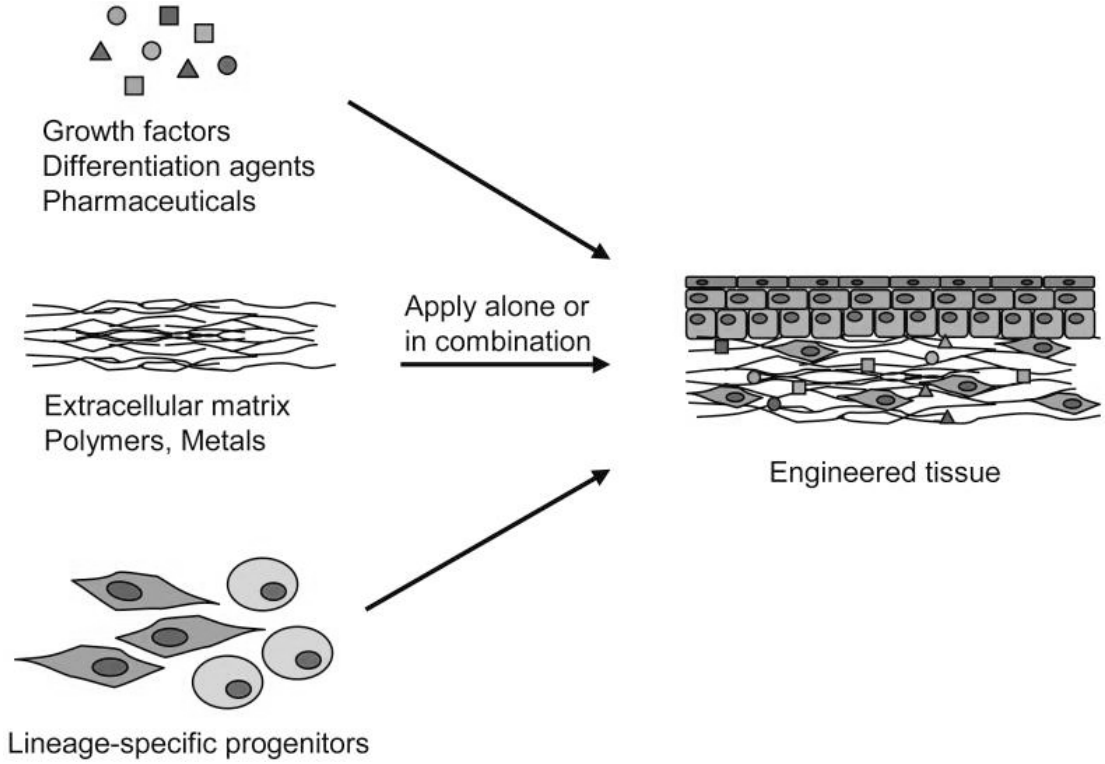

Figure 1:8 Central paradigm of tissue engineering, simplified model. Any combination of the above components may be included to construct engineered tissues. Physical supports/scaffolds provide a 3-D environment for stem cells to grow and interact. The addition of tissue inducing factors such as growth factors acts to mediate endogenous or exogenous cell growth and differentiation (no consideration for mechanical forces is given in this schematic). Image modified from Metallo et al (2008).

1.11.1 Biomaterials/Scaffolds

A number of biodegradable and bioresorbable materials, as well as scaffold designs, have been experimentally and/or clinically studied. For bone and cartilage tissue engineering the design of biomaterials which mimic the *in vivo* environment is a promising area for tissue engineering strategies, with the continued advances made in this area of research, the incorporation of human ES cell derivatives is likely to enhance the ability of tissue engineers to produce a functional bone or cartilage construct. Ideally a scaffold should have the following characteristics: i) three-dimensional and highly

porous with an interconnected pore network for cell growth and flow transport of nutrients of metabolic waste; ii) biocompatible and bioreasorbable with a degradation and resorption rate which can be controlled and match cell/tissue growth in vitro and/or *in vivo*; iii) suitable surface chemistry for cell attachment, proliferation, and differentiation and iv) mechanical properties to match those of the tissue at the implantation site (Hutmacher, 2000).

A number of materials have been used for bone regeneration, including ceramics or materials based on hydroxyapatite (HA), ceramic forms of β-tricalcium phosphate and composites of both hydroxyapatite and β-tricalcium phosphate (Shin et al., 2003, Rose et al., 2004). Scaffolds based upon organic (aliphatic) polyesters have the advantage of having FDA (Food and Drug Administration, USA) approval (Freed et al., 1994). Scaffolds have also been based on corals and marine sponges (Green et al., 2003). An approach taken, which is of particular relevance in these studies, is the co-culture of human umbilical vein endothelial cells (HUVEC's) and human osteoblast-like cells and the interaction on a scaffold of a porous bioactive glass ceramic construct. The study clearly demonstrated that the scaffolds were able to support both endothelial and human osteoblast cell proliferation both in mono and co-culture. Proliferation of human osteoblast cell cells seeded in the scaffolds was consistently shown to be greater than those observed on commercial HA scaffolds (Deb et al., 2010). These materials have been extensively reviewed by Hutmacher (2000) and Tortelli and Cancedda (2009) however, this falls outside the scope of this thesis.

1.11.2 Growth Factors

The process of bone tissue engineering is influenced by the presence of appropriate growth factors and inductive signals that effect the replication and differentiation of undifferentiated cells, resulting in the increase or decrease of a cell population. The use of appropriate growth factors can be used to stimulate differentiation towards a particular pathway. Transcription factors also play an important role as proteins that are involved in the regulation of gene expression, and play fundamental roles in osteoblast and chondrocyte differentiation.

For osteogenic differentiation in foetal cell populations, Jaiswal et al (1997), routinely used the combination of ascorbate and dexamethasone. Ascorbic acid 2-phosphate

(ascorbate) is a long acting derivative of ascorbic acid (vitamin C) and is therefore used as relevant substitute. Ascorbate has been used for human osteoblasts in *in vitro* cultures is an enzyme co-factor activity for collagen synthesis (Takamizawa et al., 2004). The use of dexamethasone, a glucocorticoid hormone, in osteogenic differentiation has also been established (Jaiswal et al., 1997, Cheng et al., 1994).

For chondrogenic differentiation, SSCs are typically cultured in a three-dimensional system by pelleting out of the growth medium and culture in the absence of serum and in the presence of TGF-β3. As the cells differentiate an extracellular matrix consisting typically of type II collagen, secreted by the chondrocytes can be detected. For osteogenic differentiation, the cells are cultured in ascorbic acid, β-glycerol phosphate and dexamethasone. Cultures can be assayed for the release of alkaline phosphatase, an osteogenic differentiation marker (Jaiswal et al., 1997, Pittenger et al., 1999). Human osteoblast cells are unable to develop mineralised bone matrix in monolayer culture, however the cells will deposit collageneous and non-collagenous proteins. For this reason they are termed 'osteogenic' or 'bone-like' cells rather than osteocytes (terminally differentiated state) found in native bone.

1,25-dihydroxyvitamin D_3, (vitamin D_3) is often used in combination with ascorbic acid and dexamethasone and has been established to induce a dose-dependent osteogenic response in human bone marrow stromal cells, with increased alkaline phosphatase, type I collagen and osteocalcin expression (Beresford et al., 1984, Beresford et al., 1986, Franceschi and Young, 1990).

Another group of osteo-inductive factors are the bone morphogenic proteins (BMPs). These proteins are critical in the formation of new skeletal tissue (Wozney, 1992). BMP-2, BMP-4 and BMP-7 are expressed throughout limb development, with a threshold level of BMP signalling required for the onset of chondrogenesis. Limbs that are therefore deficient in BMP-2 and BMP-4 fail to form, and there is severe impairment of osteogenesis (Bandyopadhyay et al., 2006). BMPs represent a subfamily within the transforming growth factor-β superfamily (Wozney, 1992). Studies have been undertaken looking at the effects of BMPs on osteogenic and chondrogenic differentiation and their possible clinical applications in bone repair (Li and Wozney,

2001, Yoon and Lyons, 2004, Partridge et al., 2002). Specifically BMP-2 has shown promise for use in bone tissue engineering strategies, (Partridge et al., 2002, Li and Wozney, 2001, Bessa et al., 2008).

The transforming growth factor-β proteins are also understood to play vital roles in the formation of bone and cartilage. Four types of transforming growth factor-β peptides have been identified (TGF-β1, -β2, -β3 and β5), and are understood to play essential roles is bone development, with TGF-β3 in particular identified for use in chondrogenic differentiation (Pittenger et al., 1999). A pellet method in combination with TGF-β3 has been identified as a suitable model for the maintenance of a chondrogenic phenotype (Tare et al., 2005).

To promote adipogenic differentiation, SSCs are cultured in medium together with 3-isobutyl-1-methylxanthine (IBMX), dexamethasone, insulin and indomethacin (Pittenger et al., 1999). Adipogenesis can be confirmed by morphology, with accumulation of lipid-rich vacuoles. Adipocytes will express peroxisome proliferation-activated receptor γ (PPAR-γ), lipoprotein lipase (LPL) and fatty acid binding protein aP2.

1.11.3 Bioreactors

A further approach to successful tissue engineering involves the use of bioreactor technology to culture tissue engineered constructs. Bioreactor technologies intended for use in tissue engineering strategies have been to grow functional cells and tissues for transplantation, and for controlled in vitro studies on the regulation effect of biochemical and biomechanical factors on cell and tissue development (Korossis et al., 2005). Bioreactors typically provide physical stimuli, efficient and uniform mixing of cells on three-dimensional scaffolds and can facilitate the maintenance and diffusion of nutrient levels and pH. Thus, bioreactors have the potential to improve the formation of functional tissue. Bioreactors thus need to provide the appropriate physical stimulation to cells, continuous supply of nutrients, such as glucose and amino acids, biochemical factors and oxygen, diffusion of chemical species as well as continuous removal of waste products of cellular metabolism. Additionally the bioreactor, typically, has to be able to operate over long periods of time (Korossis et al., 2005).

Increasing evidence suggests that mechanical forces are important modulators of cell physiology and may increase the bioactivity of cells within bio-artificial matrices, and therefore may possibly improve or accelerate tissue regeneration in vitro (Butler, 2000). Various studies have demonstrated the validity of this principal, particularly in muscoskeletal tissue engineering. For example, cyclical mechanical stretch was found to: i) enhance proliferation and matrix organization by human heart cells seeded on gelatin-matrix scaffolds, ii) improve the mechanical properties of tissues generated by skeletal muscle cells suspended in collagen or Matrigel, and iii) increase tissue organization and expression of elastin by smooth muscle cells seeded in polymeric scaffolds (reviewed by Martin et al (2004)).

Little is known about the specific mechanical forces that are most suitable for a particular tissue. Engineered tissues at different developmental stages may require different regimes of mechanical conditioning due to the increase in extracellular matrix. With these factors in consideration bioreactors provide controlled environments for reproducible and accurate applications of specific regimes of mechanical forces to 3-D constructs (Demarteau et al., 2003).

Cartilage tissue engineering is an attractive target since cartilage is avascular, is composed of only one cell type and has a relatively simple composition and structure. Several types of bioreactor systems have been developed to enhance cartilage and bone formation, ranging from spinner flasks to perfusion and rotating-wall bioreactors. To culture individual cells in a bioreactor, microcarrier suspensions can be used, in which carriers are suspended in a reactor with continuously stirred media which is changed periodically to encourage cell growth. Typically, artificial tissue constructs are primarily cultured in rotating bioreactor vessels or perfusion culture systems. The use of these bioreactors are well reviewed in (Butler, 2000, Klein-Nulend et al., 2005, Martin et al., 2004, Schulz and Bader, 2007).

1.11.4 Animal Models

The development of tissue engineering strategies requires extensive preclinical experimentation using appropriate animal models. The success of any treatment strategy usually requires validation in an animal model prior to clinical application. Animal models were developed to test bone repair by tissue engineering approaches, mimicking

real clinical situations. The major considerations which must be made for any animal model, include the choice of defect, animal age, the anatomic site, the size of legion and the micromechanical environment (Cancedda et al., 2003). Additionally to the normal considerations for tissue engineering animal models, biomechanical considerations are also important, however little common criteria have been reported.

For tissue engineering strategies, it is essential to choose an appropriate animal model that can cover a number of questions posed by the study. However, more than one animal model may be required. The main questions are related to the selection of an appropriate cell source, scaffold material(s), growth factors (and concentration of) and the mode of application (carrier systems and release mechanisms). Particularly, in the case of bone tissue engineering the local mechanical forces on the new construct could also play a decisive role in the success or failure of the procedure (Buma et al., 2004). Buma and colleagues suggested that the simplest model that should be utilised, would use small animals and would be able to answer many questions posed by the study. The authors suggested the use of bone chamber models which are easy to insert, can be placed at loaded or non-loaded areas of the bone and generally multiple chambers can be placed in a single animal, depending on the size of the chamber. However the authors also suggested that the final pre-clinical test should be performed in large animals using a similar surgical technique comparable to the final procedure in humans.

1.11.5 Organotypic Culture

Organotypic culture involves growing cells in a three-dimensional environment, which, in part, more closely mimics the conditions *in vivo*. This approach has been used in neuronal tissue expansion. Gahwiler (1981) first utilised this protocol for the culture of hippocampal slices. The majority of neuronal research using this cell culture system has looked at slice cultures of rat brain slices. Since Stoppini et al (1991) introduced a simple method of culture of hippocampal slices on semi-porous membranes, study of central nervous system function and dysfunction has dramatically increased the use of these membranes. In this system, explanted tissues were placed onto a culture insert containing a semi-porous membrane and were maintained at an air–liquid interface inside a small drop of fluid, with the cultures fed by medium on the underside of the membrane. Organotypic cultures have allowed the cultivation of cells previously

unavailable in *in vitro* culture providing a platform for studies of neural physiology, pharmacology, morphology, development and endocrinology.

Additionally the organotypic model has also been used for drug screening studies. Pringle and colleagues (2003) used the culture system to detect novel neuroprotective compounds. Furthermore, drug testing can also be performed for cells cultured using the organotypic model as an *in vitro* representation of the tumour microenvironment, providing a model which is more biologically relevant and technically challenging than traditional 2-D culture systems (Benbrook, 2006).

Research into expansion of the other cell types using the organotypic culture model has also been performed. Stark et al (1999) used organotypic co-cultures to cultivate normal epidermis from keratinocytes. This was achieved by seeding keratinocytes on a collagen matrix in which suspended fibroblasts had previously been gellified.

A novel organotypic model has also been established for the human endometrium, in which primary epithelial cells have been shown to retain their steroid hormone responsiveness. The organotypic culture model enabled contact with the extracellular matrix of neighbouring cells (essential for epithelial cells to display a differentiated morphology and function) both *in vivo* and *in vitro* (Blauer et al., 2005).

1.12 Dielectrophoresis

In order to establish a protocol for tissue engineering, the fields of electronics and engineering have started to combine with biology in order to generate facile technologies in which cells can be characterised and separated from heterogeneous cell populations to aid in characterisation and isolation of cell types. As yet, there is no protocol that successfully enables the separation of pure bone stem cells due to a lack of markers for bone stem cell populations.

Dielectrophoresis (DEP) offers a novel method by which, in this case, bone cells can be identified and separated based on their unique dielectrophoretic potential, removing the need for biochemical labels and tags that in some cases remain to be identified. The

DEP phenomenon has been widely applied to the manipulation, separation and analysis of cellular and viral particles (Hughes, 2002b, Jones, 2003).

DEP falls under the nanotechnology area of electronics that is of interest in biological and chemical analysis. This is also referred to as 'Lab-on-a-Chip' technology, which is the miniaturisation and integration of lab apparatus and processes onto a single chip. The concept first emerged in 1994, to describe an integrated system for cell identification which would have previously required large amounts of laboratory equipment (Effenhauser and Manz, 1994). This allows experimentation on particles, micrometers in size, suspended in small volumes of liquid, and provides the potential for quick, inexpensive sample analysis. Part of the application of 'Lab-on-a-Chip' is alternating current (AC) electrokinetics, which is a group of methods used to manipulate microscopic particles/cells suspended in a solution, using electric fields. DEP is an example of an alternating current (AC) electrokinetic technique that measures the movement of the particles and can be used to manipulate, separate and analyse cellular scale particles (Effenhauser and Manz, 1994).

AC electrokinetics was first described by Herbert Pohl (1978), as a process which can be used to characterise the properties of different particles. These properties can then be used to infer chemical and/or biological properties. DEP and other AC techniques such as travelling-wave dielectrophoresis (TWD) and electrorotation (ER) utilise the differences in the electric polarisability of particles and the surrounding liquid (Hughes, 2002c). When a cell is suspended in an electric field, the cell polarises and will acquire a dipole. The direction and magnitude of the induced dipole is dependent on the frequency and magnitude and the dielectric properties of the cell and the medium in which it is present (Pohl, 1978). Pohl described how bio-particles such as bacteria, cells and viruses could be characterised by their dielectric properties. This has lead to the use of dielectrophoresis in order to make a distinction between different bacteria types (Marks et al., 1994), to detect changes in cell cytoplasmic properties (Labeed et al., 2006) and to detect the viability of cells (Huang and Holzel, 1992). The main factors that determine the dielectric properties of a cell are the surface charge, membrane capacitance and the conductivity of the cytoplasm. These properties, together, make up the dielectric 'fingerprint' of the cell. Conductivity (σ) is the measurement of a materials ability to conduct an electric current. For cells, energy is stored in the form of

induced charges at the interfaces which define their structure (e.g. at membranes or cell walls) with energy dissipation taking the form of ionic current flow around the cell surface and through the cytoplasm (Pethig et al., 2004). DEP can be used to determine the dielectric properties of particles by examining their behaviour across a wide frequency range. In order to extract the dielectric parameters from dielectric data, modelling techniques are used in order to find best fit parameters (Huang et al., 1996) in order to determine the membrane and cytoplasmic properties, providing information on the biological state of the cells. Typically this involves the determination of a frequency where the dielectric force of a particle is zero, and determining the dielectric properties of the membrane (Burt et al., 1990). Using this same method studies have been undertaken looking at cellular responses to toxic compounds (Ratanachoo et al., 2002), changes in the membrane upon apoptosis (Wang et al., 2002) and cancer cell transformation (Huang et al., 1996). Through the use of a broader frequency range (e.g. 1Hz- 20MHz) the properties of the cytoplasm can also be determined and used to examine the effects of antibiotics on bacteria (Johari et al., 2003). This also makes DEP a valuable tool for screening applications.

1.12.1 Theory

DEP is defined as the induced motion of particles in non-uniform electric fields. A polarisable particle in a uniform electric field will experience no net movement, as the forces induced by the interaction between each of the dipole charges and the electric field are equal and opposite, there is no net movement of the particle. A non-uniform electric field is one in which there is no net electrical force imposed on any particles resulting in the generation of field gradient. If a dielectric particle is suspended in an electric field, it will polarise. The magnitude and direction of this induced dipole depends on the frequency and magnitude of the applied electric field and the dielectric properties of the particle and the medium (Hughes, 2002c). Particles that experience such forces can be made to exhibit a variety of motions including attraction to and repulsion from the regions of high electric field by changing the frequency of the applied electric field. This property ensures that DEP can be further classified by direction (Jones, 1995), as shown in Figure 1:9.

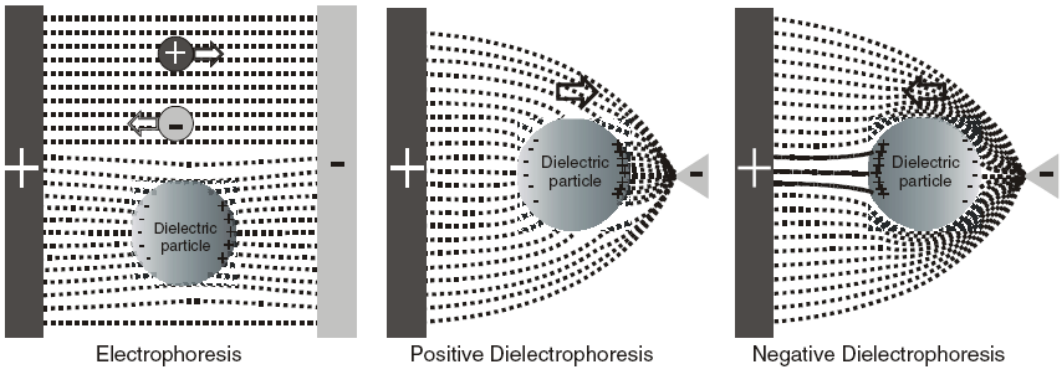

Figure 1:9 Positive and negative DEP in electrophoresis affected charged particles. Although there is polarisation of the particles by the electric field the charges cancel out so that there is no net force or movement. In dielectrophoresis, the presence of a non-uniform electric field the particles (and the surrounding medium) polarise to a different extent on opposite sides of the particle and therefore experience a net force. If the particle is more polarisable than the surrounding medium, it moves towards the field gradient (positive DEP), however if it polarises less than the surrounding medium negative DEP occurs and the particle is repelled and moves away from the field gradient. Image taken from Hoettges et al, (2007).

In DEP if the particle is more polarisable than the medium surrounding the particle, the dipole aligns with the field and the force acts up the field gradient toward the region of highest electric field, therefore, there will be net movement of the particles toward the electrode, this effect is termed positive dielectrophoresis. If the particle is less polarisable than the medium, the dipole aligns against the field and the particle is repelled from the regions of high electric field, called negative dielectrophoresis (Pethig et al., 2004).

The interaction of the electric field and the charges on each side of the dipole act to generate a force. Coulomb's law states that a charge of q1 generates an electric field E, and it is this electric field that induces a force on a second charge q2 according to the following equation 1;

$$F = k_{\mathrm{e}} \frac{q_1 q_2}{r^2},$$

Equation 1; Coulomb's law; the magnitude of the electrostatic force (*F*) on a charge (q_1) due to the presence of a second charge (q_2), is given by the above equation. *r* is the distance between the two charges and k_e a proportionality constant. A positive force implies a repulsive interaction, while a negative force implies an attractive interaction.

If there is an electric field gradient across the cell, the magnitude of the forces on either side of the cell will be different, with the cell experiencing net movement in the direction of the increasing field strength. The particle will always move along the direction of the greatest increasing electric field regardless of the field polarity, as the dipole will re-orient itself with the applied polarity and the force is always governed by the field gradient rather than the field orientation (Labeed, 2004). This force is termed dielectrophoresis (DEP).

The dielectrophoretic force, F_{DEP}, acting on a spherical body can be used to obtain parameters such as permittivity and conductivity. The equation is shown below (equation 2), where r is the particle radius, εm is the permittivity of the suspending medium, ∇ is the Del vector operator, where E^2 is the gradient of the strength of the applied electric field squared and the equation contained in the curly arrows is the real part of the Clausius-Mossotti (CM) factor given by the equation 3.

$$F_{\mathrm{DEP}} = 2\pi r^3 \varepsilon_m \mathrm{Re}\left\{\frac{\varepsilon_p^* - \varepsilon_m^*}{\varepsilon_p^* + 2\varepsilon_m^*}\right\} \nabla \left|\vec{E}\right|^2$$

Equation 2; Dielectrophoretic equation, the factor contained in the brackets is known as the real part (Re) of the Clausius-Mossotti function and contains all the frequency dependence of the DEP force.

$$K(\omega) = \frac{\epsilon_p^* - \epsilon_m^*}{\epsilon_p^* + 2\epsilon_m^*}$$

Equation 3; Clausius-Mossotti factor; which is derived from the complex permittivity of the particle and the medium, which are represented by ε_p and ε_m are shown respectively.

The permittivity (ε) of the particles and medium are both frequency dependent and therefore the Clausius-Mossotti (CM) factor is frequency dependent. This is due to the fact that the polarisability of the cell (which has a complex, heterogeneous structure with multiple layers) has contributions from the different internal compartments of the cell, which in turn have unique kinetics. At lower frequencies (<100kHz) the cell appears insulating and therefore less polarisable than typical ionic media, resulting in the cells experiencing negative DEP. Positive DEP is experienced at higher frequencies,

(~1-100MHz) where the CM factor compares the cytoplasm and media conductivities. In this case if the cells were in a higher conductivity solution even at the higher frequencies they would experience negative DEP (Labeed, 2004). At the highest frequencies, the CM factor compares the cytoplasmic and media permittivity. For these cells, this is likely to result in negative DEP as the cytoplasmic proteins impart a net permittivity that is lower than that of water. By varying the frequency the properties of the various cellular compartments can be determined (Labeed, 2004). As previously mentioned, the cells will experience positive or negative DEP based on the applied frequency, the cellular electrical properties and the conductivity (or permittivity) of the solution. As conductivity is the easiest to adjust this is the most commonly used variable in studies (Jones, 2003, Voldman, 2006). Additionally, it is important to consider the choice of suspending medium. For example, higher conductivity medium can lead to heating effects in the medium, which can cause damage to cells. A similar effect can some times be observed at high frequencies. Ideally the optimum operating conditions would be determined and applied in the experiment and device design (Voldman, 2006). An example of this is the importance of resuspending cells in an environment which is iso-osmotic, for example by the addition of appropriate molarities of sugars which do not affect medium conductivity. For the purposes of sorting, the conductivity of the medium can be manipulated so that differences in the cytoplasmic properties can be used as a means to sort the cells.

Characterisation of cells is based on physical phenomena occurring inside the cell, such as changes in conductivity (which reflects the ability of a cell to carry charge) and permittivity (reflecting the ability to store electric charge), for both the cytoplasm and the membrane. A simple model is shown in Figure 1:10 of the single shell model, showing the cell surrounding a core and a suspended in a dielectric medium.

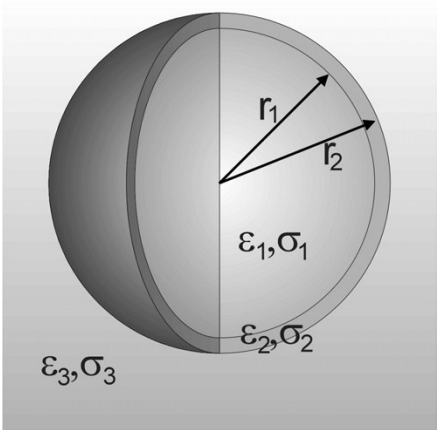

Figure 1:10 A schematic of the single shell model, showing the shell surrounding a core and suspended in a dielectric medium. Values r_1 and r_2 represent the inner and outer radii of the membrane (Broche et al., 2005).

A typical spectrum showing the relative polarisability of a single shelled particle as a function of frequency is shown in Figure 1:11. There are three plateaux, at a low frequency (negative DEP), intermediate frequency (positive DEP) and high frequency (negative DEP). Fx_1 and Fx_2 indicate the lower and upper crossover frequencies respectively, where the CM factor equals zero. This displays two characteristic dispersions, one rising at lower frequency and one falling at a higher frequency. The frequency where the polarisability crosses from negative to positive for a homogenous sphere allows the direct determination of the properties of the sphere from the CM factor by equalling zero, however for a shelled sphere the expression becomes more complicated (Broche et al., 2005). Some studies have been performed in order to derive expressions for the lower crossover frequency, but the upper frequency has largely been ignored due to limitations with signal generation equipment.

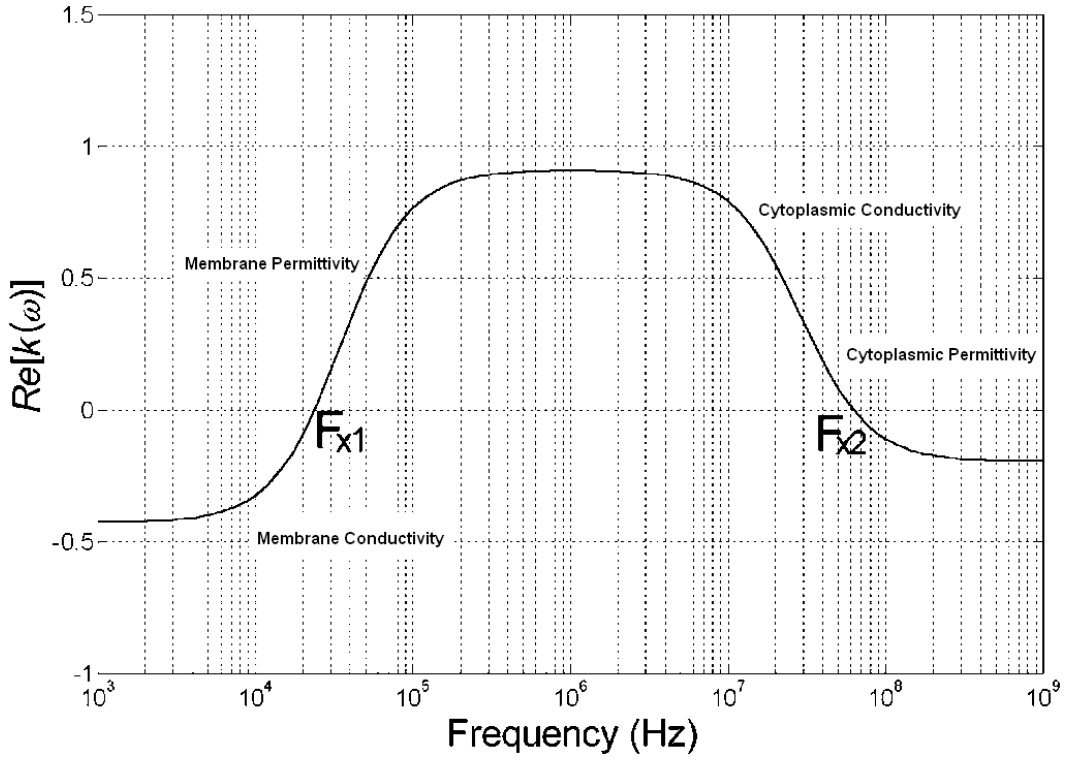

Figure 1:11 A typical spectrum showing the relative polarisability (Re[*K(w)*]) of a single shelled particle as a function of frequency. There are three plateaux shown, a low frequency (negative DEP), intermediate frequencies (positive DEP) and high frequency (negative DEP). The transition between each plateau is approximately one decade. Both upper and lower crossover frequencies are indicated by Fx_1 and Fx_2 respectively, this is the point where (Re[*K(w)*]) = 0. Also indicated are the regions of the curve, which are affected by different cellular properties, with the cytoplasmic effects at the higher frequencies and membrane effects at lower frequencies. Image modified from (Broche et al., 2005).

Pohl (1978) described the observation that a particle will be pulled strongly toward the region of highest electric field in a non-uniform field. The movement of the cell toward this high electric field means that the cell must have a higher specific polarisability than the surrounding water. Pohl described a number of ways that this high polarisability can be obtained. As the cell is largely water, there are dissolved intracellular regions of numerous polar molecules-proteins, sugar, DNA and RNA, all of which can contribute to polarisation. There are structured regions that can act as capacitative regions, for example, lipid membranes across which electrolytes can act to produce charge distribution. Finally, there are also structured areas in the surface where ionic double layers can produce large depolarisations.

Pethig et al (1996), used yeast cells to show collection of the cells arising from both positive and negative DEP using castellated electrode design, and the two forms of collection differed significantly as functions of the frequency of the applied non-uniform electric field and of the conductivity of the suspending medium. Gascoyne et al (2002), used positive and negative DEP to characterise normal, leukemic and differentiation-induced leukemic mouse erythrocytes as a function of frequency in the range $5x10^2$-10^5 Hz, which were shown to be significantly different. The group also showed that DEP could be used to separate the cells upon choosing a suitable frequency and cell suspension medium.

By using DEP as a characterisation technique, the subsequent dielectric properties obtained can be used to provide the basis for separation of cells. Marks et al (1994) determined a frequency range 10kHz-100kHz for the effective electrical conductivity values from gram-positive and gram-negative bacteria. This information enabled experimental conditions to be selected that could be used to separate different microorganism species using DEP.

1.12.2 Microfluidics

Microfluids deals with the behaviour, precise control and manipulation of fluids on a micro scale, typically featuring, small volumes and device sizes that have low energy consumption. Microfluidics is a multidisciplinary field, emcompassing engineering, physics, chemistry, microtechnology and biotechnology. Microfluidics also incorporates the 'Lab-On-A-Chip' technologies. The behaviour of fluids at the microscale can differ from the 'macrofluidic' behaviour, with factors such as surface tension, energy dissipation and fluidic resistance start to dominate the system. Microfluidics studies the changes in these behaviours and how these properties can be exploited for new uses. There are a number of DEP based microfluidics devices, which are used for the cell sampling, trapping and sorting, based upon mechanical and electrical principals on a single cell level (Andersson and Van den Berg, 2003). Microfluidic devices and their uses have been extensively reviewed by Erickson and Li (2004), Huh et al (2005) however, this falls outside the scope of this thesis.

1.12.3 DEP for Biological Characterisation

Pohl and Hawk (1966) described the first means of physically separating live and dead cells using a high-frequency non-uniform electric field to cause selective dielectrophoresis of yeast cells. Living cells separated from the dead cell population remained viable after the separation process. Consequently, DEP has been used to detect and separate viable from non-viable cells, since the technique is sensitive enough to detect populations of cells that are behaving differently at specific frequencies. As cells have characteristic dielectric properties, determined by their physiological properties, DEP can detect physiological changes associated with trans-membrane signalling events and changes in cell life cycle for example changes in the cytoplasm were detected in apoptosis (Labeed et al., 2006). DEP has also been used to examine the effects of drugs on cells (Hubner et al., 2005b, Hübner et al., 2007, Labeed et al., 2003). The dielectric properties of the cells treated with drugs were altered, namely a reduction of the cytoplasmic conductivity of the treated cells compared to control cells (Hubner et al., 2005a). Separation of cells by DEP has also been demonstrated for CD34+ cells in the bone marrow which can be separated from human blood (Stephens et al., 1996, Talary et al., 1996) as well as breast cancer cells from blood (Becker et al., 1995). It has also been reported that breast carcinoma and the surrounding tissues display different dielectric properties (Surowiec et al., 1988). There has also been some literature on the stimulation of osteoblasts by dielectrophoretic manipulation. Zou and colleagues (2006) used micro-electro-mechanical systems (MEMS) technology, as a platform for the study of osteoblast cellular response to local, mechanical, topographic and biochemical cues. The authors also investigated the use of DEP to manipulate and position osteoblasts in the system and found that dielectrophoresis ‘may have an anabolic effect on osteoblasts’ based on the viability values for cells exposed to DEP being three times higher than the control cells.

1.13 Current Challenges

To date the ideal source of bone cells that can eventually be used clinically for skeletal tissue engineering is largely unknown. Lacking, is a comparative (using an identical system) of SSCs derived from embryo, foetal and adult sources. This requires information on the presence, activity and plasticity of the skeletal stem cells derived

from ES cells as well as information of their differences and/or similarities to the physiology of adult SSCs.

A possible line of investigation is the study of the molecular basis of multipotency of SSCs. There is evidence that differentiation can be reversed and alternative lineages derived. For example, Song and Tuan (2004) showed that fully differentiated osteoblasts are able to differentiate into fully functional lipid-producing adipocytes or chondrocytes and visa versa, indicating the plasticity of SSCs.

A key issue is the ability to understand the developmental physiology of skeletal cells and their differentiation pathway. As mentioned previously, an advantage to using human ES cells rather than SSCs for osteoregulation is that ES cells can, potentially, provide an unlimited supply of differentiated osteoblasts and osteoprogenitor cells for transplantation. However, given limitations in our current knowledge as well as the issue of ethics, it is likely that SSCs derived from bone marrow offer facile translational opportunities to the clinic than embryonic derived SSCs.

This investigation will focus on the formation of new skeletal tissue, the elucidation of the processes involved in foetal, and human ES cell differentiation, development characterisation, physiology and proliferation to bone tissue. Pivotal will be the molecular characterisation of the embryonic and foetal skeletal progenitor stem cells in both the undifferentiated and differentiated state. Unique to the current studies published will be the use of conditioned media obtained from foetal femur derived cells cultured in osteogenic conditions. This will be compared to co-culture studies of the foetal femur cells with human ES cells in both monolayer culture and organotypic 3-D pellet culture. Analysis of the differentiation studies will include histological and molecular characterisation of the cells. Further to this, we will look at additional characterisation the foetal cell population looking at STRO-1 (osteoprogenitor precursor) and 7D4 (chondroprogenitor precursor) expression as well as looking at the potential of isolated positive cell fractions for chondrogenesis and osteogenesis.

1.14 Aims and Objectives

Central to the formation of new skeletal tissue is the characterisation of the initial starting population as well as the elucidation of the processes involved in skeletal cell differentiation. In addition, the ability to derive protocols for skeletal cells from ES cell populations will prove invaluable and generate new models for differentiation. This project will also examine interactions between the embryonic and foetal stem cell populations.

Specifically;

- Characterisation of human embryonic stem cells using the HUES-7 cell line as a model.
- Characterisation of human foetal femur-derived cells using novel antibodies for the selection of osteo- and chondroprogenitor cell populations.
- Characterisation of skeletal stem cell populations using dielectrophoresis, as a potential strategy to sort cells.
- To examine the differentiation potential of human ES cells using interactions with human foetal femur-derived populations, in co-culture systems and the use of conditioned medium derived from foetal femur-derived cell populations to examine the interaction with human ES cells.

Chapter 2 Materials and Methods

2.1 Materials

All tissue culture plastics were obtained from Elkay, Basingstoke, UK or Griener Bio-One, Gloucester, UK and biochemical reagents were obtained from Sigma-Aldrich, Dorset, UK unless otherwise stated. Rat anti-mouse IgM MicroBeads for MACS (473-01) and MACS columns (473-06) were obtained from Miltenyi Biotec LTD, Bisley, UK. PicoGreen® dsDNA Quantitation reagent (P7589), Cell Tracker Green™ CMFDA (5-chloromethyl-fluorescein diacetate, C7025), Ethidium Homodimer-1 (E1169) Tris-EDTA (Tris-hydrochloric acid EDTA, T9285), alkaline buffer solution (A9226), alkaline phosphatase assay kit with Sigma 104® phosphatase substrate (104-0) and AP standard (104-1), Naphthol AS-MX Phosphate 0.25% (855) and Fast Violet B Salts (F1631) were all ordered from Sigma-Aldrich UK. Additional histological supplies were purchased from VWR International Ltd, Leicestershire, UK, including Alcian blue 8GX (343291G), Sirius red F3B (341492F) and molybdophosphoric acid (292713W). Type I collagen polyclonal antibody was a gift from Dr Larry Fisher, NIH, Bethesda, USA. Sox-9 polyclonal antibody (AB5535) was obtained from Chemicon International (part of Millipore, Hertfordshire, UK). 7D4 monoclonal antibody was a gift from Prof. Bruce Caterson, Cardiff University. STRO-1 monoclonal antibody was gifted from Dr J. Beresford, University of Bath. DAPI (4',6-diamidino-2-phenylindole) nuclear counter stain (D3571) was purchased from Molecular Probes, Invitrogen, Paisley, UK. Secondary antibodies were purchased from DAKO, Cambridgeshire, UK. Molecular biology reagents were purchased from Invitrogen Life Tech, Paisley, UK and Promega Ltd, Southampton, UK, including TRIzol solution (15596-018), Superscript™ first-strand synthesis system (11904-018), SuperScript™ III Reverse Transcriptase (18080-044). RNA was cleaned up using the Zymo RNA-clean up kit (R1013) from Cambridge Biosciences, Cambridge, UK. Primers utilised for molecular analysis were ordered from Sigma-Genosys, Dorset UK, a list of primer sequences and amplicon size are given in section 2.9.3.

2.1.1 Image capture

Slides and tissue culture images were captured and processed with Carl Zeiss Axiovision software Version 4.7 via an AxioCam HR digital camera on an Axiovert 200 inverted microscope (Carl Zeiss AG, Germany). FISH images were captured with Carl Zeiss AxioObserver Z1. All other photographs were captured with a Canon

Powershot G2 digital camera. X-ray photography was performed on a Faxitron® Specimen Radiography System MX-20 Digital with Faxitron® Specimen DR software (Faxitron® X-ray Corporation, USA).

2.2 Solutions

2.2.1 General Solutions

20xSSC; 175.3g NaCl, 88.2g sodium citrate in 1 litre distilled water.

0.1M citrate buffer, PH 6; 2.1g citric acid monohydrate in 900 ml water, PH with NaOH and make up to 1 litre.

TE (Tris/EDTA) Stock (1x); dilute from 100x TE stock: 500µl (0.5 ml) of TE in 50 ml distilled water.

2.2.2 Staining solutions

2.2.2.1 Alcian Blue/Sirius Red staining

Alcian Blue: 1.5 g Alcian blue 8GX in 300 ml distilled water with 3 ml acetic acid

Molybdophosphoric Acid: 3g molybdophosphoric acid in 300 ml distilled water

Sirius Red: 0.3g Sirius Red F3B in 200 ml distilled water and 100ml saturated picric acid

Haematoxylin Weigerts A: 10g haematoxylin in 1 litre methanol.

Haematoxylin Weigerts B: 6g Ferric Chloride in 500 ml distilled water and 5ml concentrated HCl.

Acid Alcohol: 20 ml HCl in 2 litres 50% methanol.

2.2.2.2 Alkaline Phosphatase staining

Activating Buffer pH=7.4; 75ml stock A made up to 100 ml and 81 ml stock B made up to 100 ml. Additional 100 ml distilled water and 600mg magnesium chloride.

Stock A: Tris Maleate; 12.1g Tris, 11.6 g maleic acid in 500 ml distilled water.

Stock B: Sodium Hydroxide; 4g sodium hydroxide in 500 ml distilled water.

Naphthol AS-B1 Stock Solution pH 8.3; 4.36g Tris in 180 ml distilled water. Mix separately: 25mg Naphthol AS-B1 Phosphate, 10 ml Dimethyl Formamide and 10 ml distilled water.

2.2.2.3 Von Kossa staining

1% Silver Nitrate; 0.5g (500mg) Silver Nitrate in 50 ml of distilled water.

2.5% Sodium Thiosulfate; 7.5g Na Thiosulfate in 300 ml distilled water

Van Gieson Counterstain; 180mg Acid Fuchsin in 100 ml saturated picric acid and 100 ml distilled water.

2.2.2.4 Oil Red O staining – Stock solution

Oil Red O in 99% Isopropanol; 1 ml Oil Red O powder in 100 ml 99% Isopropanol.

2.2.2.5 Oil Red O staining – Working solution

Mix 3ml filtered Oil Red O stock solution with 2 ml distilled water. Leave for 1 hour to mix before applying to cells.

2.2.3 Biochemistry Assays

Alkaline Phosphatase assay buffer; 5 ml 2-AMP Alkaline Buffer Solution (Sigma A9226) in 10 ml distilled water with 30µl Igepal CA-630 (Sigma I3021-50).

Alkaline Phosphatase substrate; 0.04g Phosphatase Substrate (Sigma P47441G)**,** 10 ml 2-AMP alkaline buffer solution in 20 ml distilled water.

2.3 Tissue Culture

2.3.1 Human Bone Marrow Cells

Human bone marrow samples were obtained from haematologically normal patients undergoing routine total hip replacement surgery for a fractured neck of femur or as a result of osteoarthritis. Only tissue that would have been discarded was used with the approval of the Southampton and South West Hants Local Research Ethics Committee (LREC 194/99).

Primary cultures of bone marrow cells were established as follows: marrow aspirates were washed in α-MEM and passed through a 70µm cell strainer. The suspended cells were then centrifuged at 1100rpm for 4 minutes at 18^{o}C. The cell pellet was resuspended and plated into culture flasks. Non-adherent cells and red blood cells were removed via a PBS wash and media change after one week, followed by media changes every 3 days. Cell cultures were maintained in basal medium, α-MEM (Minimum

Essential Medium alpha modified) containing 10% FCS and penicillin/streptomycin at 37^{o}C and 5% CO_2. When the cells reached confluence, after approximately 12-14 days, the cells were utilised for differentiation studies.

2.4 Foetal Femur Cultures

Human foetal femurs were obtained following termination of pregnancy according to guidelines issued by the Polkinghome Report and with Southampton University NHS Trust ethical approval. The femurs were placed in sterile PBS and the surrounding muscle removed with forceps as detailed in Mirmalek-Sani et al (2005). Femurs were dissected and processed in one of two ways. The total explants were plated into T25 flasks in 5ml basal media, which was changed weekly or treated with 1mg/ml collagenase B overnight before centrifugation at 1100rpm for 4 minutes at 4^{o}C. The cell pellet was resuspended and plated into tissue culture flasks. The cells were maintained at 37^{o}C with 5% CO_2. Foetal age was calculated by measuring foot length and given in weeks post conception (WPC) shown in table 2:1. Carnegie staging (O'Rahilly and Muller, 1987, Bullen and Wilson, 1997) was used to determine the ages of embryos for which the foot length could not be measured and was determined by looking at the anatomy and features of the embryo, a table of standard staging criteria is provided in table 2:2.

2.4.1 Cell Passage

Prior to trypsin treatment, the cells were washed with 1x PBS and detached following the addition of 1x Trypsin/EDTA for 10 minutes at 37^{o}C. Once cells were detached, the trypsin was inactivated by the addition of α-MEM containing 10% FCS. The cells were centrifuged at 1100rpm for 4 minutes at 4^{o}C. After resuspension the cell number was determined using a haemocytometer and cells passaged at the required density.

Foetal foot length (mm)	Days post conception (DPC)	Weeks post conception (WPC)
3.75	52	7.5
4.0	53	7.5
4.5	54	7.5
5.0	55	7.5
5.5	56	8.0
6.0	59	8.5
6.5	61	8.5
7.0	63	9.0
7.5	65	9.0
8.0	68	9.5
8.5	70	10.0
9.0	72	10.0
9.5	73	10.5
10.0	77	11.0

Table 2:1 Foetal age in weeks and days post conception as determined by measurement of foetal foot length.

Carnegie Stage	Approx. age (days)	Size (mm)	Key developmental features
13	28 - 32 (week 5)	4 - 6	leg buds, lens placode, pharyngeal arches Somite Number 30
14	31 - 35	5 - 7	lens pit, optic cup
15	35 - 38	7 - 9	lens vesicle, nasal pit, hand plate
16	37 - 42 (week 6)	8 - 11	nasal pits moved ventrally, auricular hillocks, foot plate
17	42 - 44	11 - 14	finger rays
18	44 - 48 (week 7)	13 - 17	ossification commences
19	48 - 51	16 - 18	straightening of trunk
20	51 - 53 (week 8)	18 - 22	upper limbs longer and bent at elbow
21	53 - 54	22 - 24	hands and feet turned inward
22	54 - 56	23 - 28	eyelids, external ears
23	56 - 60	27 - 31	rounded head, body and limbs

Table 2:2 Standard staging criteria for the classification of human embryos. Adapted from UNSW Embryology.

2.4.2 Immunoselection of Osteoprogenitor Populations

2.4.2.1 Magnetically Activated Cell Sorting (MACS)

STRO-1 positive marrow stromal cells from human bone marrow were immunoselected with the antibody STRO-1 using MACS as previously described (Howard et al., 2002). The process was as follows; using the same protocol for preparation of the marrow cells, red blood cells were removed via centrifugation with Lymphoprep solution. Cells were resuspended at $1x10^8$ cells per 10ml of blocking solution (HBSS with 5% FCS, 5% human normal AB serum and 1% BSA) and incubated with the STRO-1 antibody hybridoma for 1 hour. Following two washes with MACS Buffer (HBSS (Hank's Buffered Salt Solution)) containing 1% BSA (bovine serum albumin) cells were incubated with MACS anti-IgM beads for 45 minutes, before passing the cell suspensions through a MACS column in the presence of a magnet to give the negative fraction. The column was then washed using MACS buffer, and in the absence of the magnet, 3ml MACS buffer was passed through the column to yield the STRO-1^+ cell fraction. The STRO-1^+ culture was maintained in basal medium until confluent and then utilised for studies as specifically detailed in each section.

2.4.2.2 Fluorescence Activated Cell Sorting (FACS)

Flow cytometry allows measurements of various particle/cellular properties suspended in a fluid stream. In essence, single cells are passed through a flow chamber in which they encounter a LASER beam light source. The cellular properties influence the way in which the light is scattered and subsequently information regarding the relative size and granularity of a cell is obtained. Typically fluorescent probes are used which bind to specific cell associated molecules.

Fluorescence activated cell sorting (FACS) is a specialised form of flow cytometry which provides a method of sorting a heterogeneous population of cells into two or more containers, one cell at a time, based upon the specific light scattering and fluorescent characteristics of the cell. The principal of (FACS) is shown in Figure 2:1. Briefly, the cell suspension is passed through a fluidics system which forces the cells, individually, down a narrow nozzle. The nozzle is vibrated at an optimal frequency to produce droplets which are at a fixed distance. Just before the stream breaks into droplets, the fluorescent characteristic of the cell is measured by the scanning of the

cells with a blue laser. The laser light is scattered by the cells and characteristics of the cells determined. An electrical charge must be produced in order to sort the cells, based on mathematical/statistical parameters. The charge is applied directly to the stream via a stream charging wire in the nozzle. Once charged the droplets fall through and electrostatic deflection system which diverts the droplets into the containers based on their charge. The number of cells deflected into each tube is recorded as well as the fluorescent intensity for each of the cells.

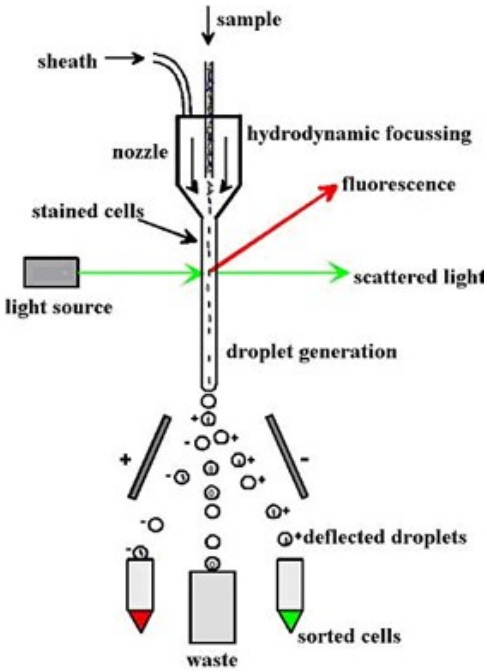

Figure 2:1 Principals of fluorescence activated cell sorting (FACS). Cells pass through a thin nozzle, which forces the cells to travel down one cell at a time. A laser is then directed at the cells which scatter the light according to the size and granularity of the cells. The fluorescent characteristic of the cell is determined and a charge applied to the cells in order to sort them into positively and negatively charged/stained fractions. Image taken from http://medschool2.ucsf.edu/ molecular methods web module.

2.4.2.3 FACS of human foetal femur derived populations

Freshly isolated foetal femurs were grown for 12 days as described in section 2.4. Cells were harvested using trypsin-EDTA and passed through a 70µm cell strainer before performing a cell count. Individual cell aliquots were centrifuged at 12,000rpm for 5 minutes and incubated on ice with the appropriate antibodies as follows; typically, $1x10^6$ cells were used for the unlabelled (FACS buffer only) and mouse IgM isotype control, (MOPC-104E, Sigma) whilst the remaining cells were split equally and stained

with either a 1:2 dilution of STRO-1 or 1:50 dilution of 7D4 antibody. Cells were washed twice in FACS buffer (0.5mM EDTA, 1% BSA solution in PBS) and incubated for a further 30 minutes on ice with a 1:200 dilution of goat anti-mouse IgM-Alexa 488 secondary antibody (Invitrogen, UK). After two further washes in FACS buffer, cells were finally resuspended in a maximum of 250µl FACS buffer (dependent upon cell density) and kept on ice before analysis and sorting on a Becton, Dickinson FACSAria™ cell sorter (BD, Oxford, UK). The positively stained cell fractions were expressed as a percentage of the gated events (10,000 events per reading, including cells). Cells were gated to exclude debris and dead cells. The isotype control (mouse IgM) was used to establish a gate to provide positively stained cell population equivalent to 0% of the total cells. Stained samples were then loaded and the percentage of the total cell population determined. Analysis was carried out using the BD FACSDiva software (BD Biosciences, Oxford, UK).

2.4.3 Osteogenic Conditions

For the promotion of osteogenic differentiation, cell cultures were grown in osteogenic media (α-MEM with 10% FCS, 100µM ascorbate (ascorbic acid 2-phosphate) and 10nM dexamethasone. Media was changed every 3 days.

2.4.4 Chondrogenic Conditions

For the promotion of chondrogenic differentiation, cell cultures were grown in chondrogenic media (α-MEM supplemented with 10ng/ml TGF-β_3, 10nM dexamethasone, 100µM ascorbate (ascorbic acid 2-phosphate) and 10µl/ml 100x ITS Supplement Solution – Insulin, Transferrin, Selenium). Media changes were performed every 3 days.

2.4.5 Adipogenic Conditions

For the promotion of adipogenic differentiation, sub-confluent monolayer cultures of cells grown in basal conditions were transferred to adipogenic media (α-MEM with 10% FCS and 0.5mM IBMX (3-isobutyl-1-methylxanthine), 10nM dexamethasone, 10µg/ml insulin (in the form of 100x ITS Supplement Solution – Insulin, Transferrin, Selenium) and 100µM indomethacin). Adipogenic media was replaced with basal medium supplemented with insulin only on days 3, 7, 11 and 15 of culture for 24 hours

only, with adipogenic media changes between. After day 15, insulin-only supplemented media was used to maintain the cells with media changes performed every 3 days.

2.5 WST-1 Assay for Cell Proliferation

Cell proliferation was assayed using the WST-1 reagent colorimetric assay (1644807, Roche, Germany). Cleavage of the tetrazolium salt, WST-1, by the mitochondria of viable cells in culture produced an absorbance value in direct proportion to cell number. Foetal femurs were collected and dissected as previously mentioned and samples were digested overnight in collagenase B (10mg/ml) in α-MEM. Foetal cells were plated at $1x10^4$ cells per well of a 48-well plate and after 24 hours, six wells were incubated with a 1:10 dilution of WST-1 reagent in basal medium. After 4 hours at 37°C absorbance at 450nm was recorded (arbitrary units) on a ELX-800 Universal Microplate Reader Bio-Tek Instruments, Inc. (USA) with Bio-Tek KC4 Kineticalc for Windows Ver.3.01, Rev.7 software. Cultures were returned to the incubator and cell culture maintained at 37°C and assay was repeated on a further six wells each day until day 8. Cell proliferation curves were analysed using SigmaPlot for Windows Ver.9.0 (Systat Software Inc., USA).

2.6 Human Embryonic Stem Cell Culture

Protocols for human ES cells culture were adapted from those described in Laslett et al., 2003; Hoffman and Carpenter, 2005; Thomson et al., 1998, as well as in-house protocols.

2.6.1 Preparation of media

1. Mouse Embryonic Fibroblast (MEF) medium consisted of 10% foetal calf serum (FCS) DMEM (Dulbecco's Modified Eagle's Medium) and penicillin/streptomycin.
2. Human ES cell medium contained KO-DMEM (Knock-out DMEM), 13% KO-SERUM, 1.3% Penicillin/Streptomycin, 1.3% Non-essential amino acids, 1.3% Glutamax, 650µl 50mM β-mercaptoethanol and 10ng/ml bFGF (Peprotech, USA. Reconstituted according to manufacturers instructions).
3. Embryoid body media consisted of KO-DMEM, 10% FCS, 1% Glutamine, 1% non-essential amino acids, and 3.5µl mercaptoethanol.

2.6.2 Culture of Human ES Cells on MEFs

Prior to the use of the MEFs as a feeder layer, MEF cells were expanded and finally mitotically inactivated by irradiation of the cells using gamma irradiation at 3000 rads. MEFs were then placed into 1ml aliquots and stored long term in liquid nitrogen. To prepare the MEF feeder layer, the frozen vials were thawed rapidly in warm water and spun at 1100rpm for 4 minutes at 18^{o}C. MEFs were then resuspended in MEF media and plated at a seeding density of 1x10^{5} cells per well of a 6 well plate. Prior to addition, MEFs wells were gelatin coated for a minimum of 30 minutes. MEFs were plated out at least 1 day prior to use to allow enough time to settle and could be kept for up to 4 days with MEF media. The human ES cells were passaged onto the MEF layer and media changed daily. Cells were allowed to grow until passage was required or signs of differentiation occurred.

2.6.3 Culture of Human ES Cells on Matrigel

2.6.3.1 Preparation of Matrigel

To prepare the matrigel aliquots, matrigel was slowly thawed overnight at 4^{o}C. On ice and using pre-chilled pipettes and eppendorfs, 5ml of KO-DMEM was added to the bottle and mixed well. 400µl aliquots were then made and placed at -20^{o}C. To prepare the plates, to each 400µl aliquot 5.6ml of ice cold KO-MEM was added, 1ml was then added to each well and the plates stored at 4^{o}C for use the following day. The plates were kept for up to 4 weeks at 4^{o}C prior to use.

2.6.3.2 Preparation of Conditioned Medium

MEF cells prepared as described in section 2.5.2 were cultured only with human ES cell medium. Media changes were performed daily with the conditioned medium directly used on cells cultured on matrigel or pooled and frozen down for later use.

2.6.4 Cell Passage

After washing the ES cells with PBS, the cells were treated with 1ml per well of collagenase IV and incubated at 37^{o}C for 5-10 minutes, until the edges of the human ES cell colony began to curl. The collagenase was then removed and replaced with the appropriate amount of human ES cell media for the ratio of the split before scraping the well. A minimum 1:3 ratio was used to split the cells. The cells were then added drop wise around a new MEF coated well plate to ensure an even distribution. Following

passage, a media change was performed after 48 hours. If there was a significant amount of spontaneous differentiation, a sterile pipette was used to pick off the differentiated cells prior to passage.

2.6.5 Embryoid Body Formation – Suspension Culture Method

Human embryonic stem cell line 7 (HUES-7) cells were treated with 1ml per well of collagenase IV and incubated at 37^{o}C for 10 minutes. The collagenase was then removed and replaced with 1ml per well of MEF media and centrifuged at 1000rpm for 4 minutes. The pellet was resuspended in 10ml of EB media and placed into a non-tissue culture treated petri dish. Media changes were undertaken every 3-4 days.

2.7 Histological Analysis

2.7.1 Alkaline Phosphatase Staining

Cells cultured on tissue culture plastic were fixed in 95% v/v ethanol. Alkaline phosphatase activity was demonstrated with Napthol AS-MX Phosphate and Fast Violet B Salts following incubation at 37^{o}C for up to 60 minutes. Samples were then rinsed with distilled water to stop the reaction and air-dried. Photographs were then taken within 3 days.

2.7.2 Oil Red O Staining

Stock solution of Oil Red O was made up as described in section 2.1. Cells previously fixed in Formal Calcium were washed with 60% Isopropanol. 1ml of Oil Red O working solution was added per well and left to stain for 15 minutes. Wells were then rinsed 3 times with excess water to remove lipid droplets released from cells. Finally, 1ml of PBS was added to wells to visualise under light microscope, within 1 hour of staining.

2.7.3 Fixation and Embedding

Pellet and tissue samples for alkaline phosphatase staining were fixed in 95% v/v ethanol, all remaining samples were fixed with 4% w/v paraformaldehyde. Samples to be embedded in paraffin wax were dehydrated for 1 hour in graded ethanol stages of 50%, 90% and 100% (absolute) ethanol. In the final 100% ethanol stage, 2 drops of 1% eosin solution were added to stain the sample pink in order to aid visibility during the embedding stage. Samples were then placed twice in chloroform for 35 minutes and

finally soaked in paraffin wax at 60^{o}C twice for 45 minutes. Samples were embedded in hot wax and placed on a cooling surface at 2-4^{o}C to solidify. The blocks were stored at 4^{o}C prior to sectioning.

2.7.4 Slide Preparation

Paraffin wax embedded samples were removed from cold storage at 4^{o}C and trimmed of any excess wax, and marked for orientation. Using a Microm 330 microtome, sections were cut at 7µm and placed in a water bath at 37^{o}C and allowed to spread and separate before being transferred onto pre-heated glass slides (Fisher Scientific, Leicester, UK) on a 37^{o}C hotplate and left for 30 minutes. Slides were placed into a drying oven at 37^{o}C for 2-3 hours then stored at 4^{o}C. Prior to staining, the slides were warmed to room temperature.

2.7.5 Alcian Blue/Sirius Red Staining

Prior to Alcian Blue/Sirius Red staining, excess wax covering the sections was removed via two washes in histoclear. The sections were rehydrated through graded methanol steps of 100%, 90% and 50%. Sections were soaked in a water bath followed by nuclear counter-staining with Weigert Haematoxylin solutions A and B for 10 minutes and dipped 3 times in acid methanol. Slides were then rinsed in water and stained with 0.5% Alcian Blue for 30 minutes. After 20 minutes (pre-treatment/staining) with 1% molydophosphoric acid, samples were stained using 0.1% Sirius Red for 60 minutes and dehydrated through reverse graded methanol (50%, 90% and 100%). The slides were finally mounted with dibutyl phthalate xylene (DPX) and glass cover slips. Sirius Red stains collagens within the bone matrix while Alcian Blue stains proteoglycans within cartilage.

2.7.6 Von Kossa Staining

The sections were rehydrated through graded methanol steps, as for Alcian blue/Sirius red staining and transferred to water. 1% silver nitrate (1ml/slide) was added to the sections, which were then left under UV light for 20 minutes. Slides were rinsed thoroughly in running water prior to treatment with 2.5% sodium thiosulphate for 8 minutes and rinsed once more. A counter stain was then performed with alcian blue for 1 minute, and Van Giesen for 5 minutes. Finally, the slides were dehydrated through alcohols, starting at 90% methanol, placed through histoclear and mounted in DPX.

Deposits of calcium or calcium salt can be visualised. Pink sections of the slide stain osteoid and brown/black represent mineralized matrix.

2.7.7 Immunocytochemistry of Monolayer Cultures and Paraffin Sections

After removal of excess wax and rehydration of the samples, endogenous peroxidase activity was blocked with 3% H_2O_2. Sections were incubated overnight at 4^{o}C with the relevant primary antibody. Negative controls were performed by replacing the primary antibody incubation step with 1% BSA in PBS. All steps thereafter were performed as described below.

For SOX-9 staining, prior to blocking endogenous peroxidase activity, a heat step was performed using 0.01M-citrate buffer, which acts as an epitope retrieval. The solution is designed to break the protein cross-links that can mask the antigen/epitope in paraffin embedded sections.

After thorough washing (in high salt, low salt, TRIS), the appropriate biotin-linked secondary antibody was added for 1 hour and samples left in the dark. The samples were developed using 3-amino-9-ethyl-cardazole (AEC) in acetate buffer containing H_2O_2, to give a red/brown stain. The slides were counter stained with light green for 1 minute 20 seconds and alcian blue for 45 seconds. Finally, the slides were mounted with glycerol jelly.

For staining of HUES-7 embryonic stem cells (fixed on chamber slides using ice cold ethanol), a fluorescence technique was used. After dehydration, a permeabilisation step was performed (required for cells but not for tissue sections). Again, the relevant primary antibody was left overnight at 4^{o}C and the remaining protocol employed. Finally, slides were mounted in DAPI containing mounting medium.

2.8 Alkaline Phosphatase Staining for Ethanol Fixed Sections

Sections were de-waxed and rehydrated through histoclear and descending methanol as detailed above and washed briefly in the water bath before being left in activating buffer overnight, at room temperature. AS-B1/fast red mixture (AS-B1 stock solution mixed with 70mg fast red) was filtered onto the slides and then left for 1 hour at 37^{o}C. Slides

were washed with water and counterstained in light green for 1 minute and stained in alcian blue for 2 minutes and finally mounted using glycerol jelly.

2.9 Fluorescent In-Situ Hybridisation (FISH) on Paraffin Embedded Tissue Sections

Sections on superfrost-plus slides were heated at 37^{o}C for up to 1 hour, and washed twice in histoclear for 10 minutes in order to remove all the paraffin from the sections. The slides were rehydrated in an ethanol series (100%, 100% 90% and 50%) for 10 minutes each and into water. Sections were microwaved in 0.1M citrate buffer (pH 6) for 10 minutes and immediately transferred into distilled water and washed several times.

Slides were rinsed in 2xSSC (solutions are given in section 2.13) and then placed into 2xSSC at 75^{o}C for 2 minutes, followed by denaturation in 70% formamide/2xSSC for a further 3 minutes. Dehydration was performed through three-minute washes in 70%, 90% and 100% ethanol. The slides were then air-dried and treated at 80^{o}C for 5 minutes on a heat block to denature the DNA. 1μg X and Y chromosome DNA probes (kindly provided by Professor David Wilson) were applied to the sections. 0.2μl of 0.2mM Texas red (Y chromosome) or green (X chromosome) was used for the probes. A cover slip was added and sealed. Slides were transferred for hybridisation to the ThermoBrite machine (ThermoBrite Statspin S500-24. Abbott Molecular, Berkshire, UK) and heated to 82^{o}C (Techne Dri Block DB-2-D, VWR International Ltd, Leicestershire, UK) for 2 minutes before being left at 37^{o}C overnight. Post hybridisation, slides were washed 3 times for 5 minutes at 60^{o}C in 0.1xSSC. Finally, slides were mounted and counter stained with Vector Shield (containing DAPI).

For use as a positive control, blood cells in metaphase (kindly provided by Professor David Wilson) were used, which were taken through the same ethanol and heat treatment steps as the sample slides.

2.10 Biochemistry Assays

Cells grown on monolayer culture in well plates were initially fixed with 95% ethanol and air-dried. For each assay, the cell layer from each well was scraped in 0.05% v/v Triton-X with a freeze-thaw process. This was repeated three times to provide lysed samples.

2.10.1 Alkaline Phosphatase

Alkaline phosphatase was measured through colorimetric dephosphorylation of p-nitrophenol phosphate. Alkaline phosphatase activity was measured using, typically, 10µl of cell lysate from each well incubated with 100mM p-nitrophenol phosphate (pNPP) as a substrate in 90µl 2-amino-2-methyl-1-propanol alkaline buffer solution. The reaction was timed and stopped with 100µl of 1M sodium hydroxide (NaOH). The turnover of pNPP was used to quantify alkaline phosphatase activity, which was measured by the absorbance values at 410nm on an ELx800 spectrophotometer. Results were expressed as nmol pNPP/hr.

2.10.2 PicoGreen dsDNA Quantification

DNA content was determined using PicoGreen dsDNA quantification reagent (Molecular Probes, Invitrogen, Paisley, UK). This is an ultra sensitive fluorescent nucleic acid stain for quantification of double-stranded dsDNA in solution. 10µl of cell lysate samples were added with 90µl Tris-EDTA (Tris-HCL Ethylenediamine Tetra-acetic Acid) buffer and 100µl of 1:200 dilution of PicoGreen regent in Tris-EDTA buffer. Fluorescence was measured immediately on an FLx cytofluor microplate reader (Biotech Instruments Inc, USA) using 480nm excitation and 520nm emission. Specific activity results were calculated and expressed as nmol pNPP/ng DNA/hr.

2.11 Molecular Analysis

2.11.1 RNA Extraction

Cells were washed with PBS and 1ml of TRIzol reagent (a mono-phasic solution of phenol and guanidine isothiocynate) was added to a T75 flask and left for 5 minutes. The flask was then scraped and the solution transferred on ice, to diethylpyrocarbonate (DEPC)-treated eppendorf tubes and stored at -80°C or on ice to be used immediately for RNA extraction. TRIzol is a strong denaturant which acts to maintain the integrity of RNA while breaking down cells and dissolving components. To extract the RNA, 200µl chloroform was added to the tube. The solutions were vortexed and centrifuged at 12,000g for 15 minutes to separate the solution into an aqueous and organic phase, with the top aqueous phase containing the RNA exclusively. The aqueous phase was transferred into a new tube and the RNA recovered by the addition of 500µl isopropyl ethanol and incubation at room temperature for 10 minutes to precipitate the RNA. The tubes were then placed at -20^{o}C for a minimum of 1 hour and up to 12 hours. The tubes

were then centrifuged at 12,000g for 10 minutes to produce a visible white pellet of RNA. The supernatant was removed and the RNA pellet washed with 75% ethanol in ultra pure water (UPW) and centrifuged again at 7,500g. The ethanol was discarded and the pellet left to dry on ice for no longer than 1 min so as not to decrease the solubility. Finally, depending on the size of the pellet, the pellet was dissolved in up to 100µl of heated UPW. The RNA concentrations were quantified by the absorbance value at 260nm using a NanoDrop® ND-1000 UV-Vis Spectrophotometer (Thermoscientific, USA).

RNA clean up was performed (particularly important for quantitative PCR) using the Zymo DNA-free RNA kit (Cambridge Biosciences, Cambridge, UK), which removes DNA from RNA preparations via DNase I treatment followed by adsorption of the RNA onto the matrix of the ZymoSpin column provided. The RNA was washed 2x then eluted with up to 17µl volume of RNase-free water. UPW heated to 65°C was used to elute the RNA. The RNA samples were then placed at -80°C or used immediately for complementary DNA (cDNA) synthesis.

2.11.2 cDNA Synthesis

cDNA synthesis was performed using the SuperScript© First-Strand Synthesis System for RT-PCR. The protocol used was adapted as follows; the RNA/Primer mixtures were prepared in DEPC treated eppendorfs containing 10µl total solution of the DNA-free RNA, 10mM dNTP, Oligo dT and ultra pure water. The solution was incubated at 65^{o}C for 5 minutes and then placed back on ice for 1 minute. To this 10µl of solution made up of 10X RT Buffer, 25mM MgCl2, 0.1M DTT, RNase OUT recombinant RNase Inhibitor and Reverse Transcriptase was added and incubated at 42^{o}C for 50 minutes. To terminate the reaction the tubes were incubated at 70°C for 15 minutes before finally cooling on ice. At this point the cDNA was placed at -20°C for storage or used for the PCR reaction.

2.11.3 Real-time PCR

For real-time PCR, ready made SYBR-Green master mix (2x concentration) was used. To 12.5µl master mix, 2.5µl forward and reverse primers (5µM working concentration) were added and the total solution (24µl per reaction) was loaded in triplicate into a 96-well PCR plate. 1µl of cDNA was then added to each well. The plate was loaded into

the Applied Biosystems (Life Technologies, USA), 7500 Real Time PCR System and the reaction run. Thermocycler conditions were typically, 50^{o}C for 2 minutes, 95^{o}C for 10 minutes, followed by 40 cycles at 95^{o}C for 15 seconds and 60^{o}C for 1 minute. An additional stage was added, 95^{o}C for 15 seconds, 60^{o}C for 1 minute and 95^{o}C for 15 seconds. Data was then analysed using the Applied Biosystems 7500 System SDS Software, version 1.3.1 programme. Fold induction and expression levels for each target gene were calculated using the delta-delta Ct method, also known as the comparative Ct method, where [delta][delta]Ct=[delta]Ct,$_{sample}$-[delta]Ct,$_{reference}$. Here, [delta]CT,$_{sample}$ is the Ct value for any sample normalized to an appropriate endogenous housekeeping gene. In this case, β-Actin was used for all studies, as it has been shown that GAPDH is less stable for use as an housekeeping gene (Sellayah et al., 2008).

Primer sequences used are shown in table 2:3. All primers used relating to osteogenic and chondrogenic genes were designed by Dr Rahul Tare, and all primers for pluripotency and early differentiation genes were designed by Dr Fay Chinnery.

Gene	Primer sequences	Amplicon size
Human β- Actin	F: 5'ggc atc ctc acc ctg aag ta 3' R: 5'agg tgt ggt gcc aga ttt tc 3'	82 bp
Human Runx-2	F: 5'gta gat gga cct cgg gaa cc 3' R: 5'gag gcg gtc aga gaa caa ac 3'	78 bp
Human ALP	F: 5'gga act cct gac cct tga cc 3' R: 5'tcc tgt tca gct cgt act gc 3'	86 bp
Human Col1a1	F: 5'gag tgc tgt ccc gtc tgc 3' R: 5'ttt ctt ggt cgg tgg gtg 3'	52 bp
Human Osteocalcin	F: 5'ggc agc gag gta gtg aag ag 3' R: 5'ctc aca cac ctc cct cct g 3'	102 bp
Human Osteonectin	F: 5' gag gaa acc gaa gag gag g 3' R: 5' ggg gtg ttg ttc tca tcc ag 3'	95bp
Human Bone Sialoprotein (BSP)	F: 5' cag ttc aga aga gga gg 3' R: 5' tca gcc tca gag tct tca tc 3'	100bp
Human Sox9	F: 5'ccc ttc aac ctc cca cac ta 3' R: 5'tgg tgg tcg gtg tag tcg ta 3'	74 bp
Human Col2a1	F: 5'cct ggt ccc cct ggt ctt gg 3' R: 5'cat caa atc ctc cag cca tc 3'	58 bp

Table 2:3 Forward and reverse primers used for qPCR for genes commonly used to characterise bone/cartilage differentiation. Primers were designed to flank two exons or were intron spanning.

Gene	Primer sequences	Amplicon size
Human OCT-4	F: 5'ctc acc ctg ggg gtt cta tt 3' R: 5'agc taa gct gca gag cct ca 3'	76 bp
Human SOX-2	F: 5'caa gat gca caa ctc gga ga 3' R: 5'gct tag cct cgt cga tga ac 3'	95 bp
Human Nanog	F: 5' gct ttg aag cat ccg act gt 3' R: 5'agt ctc cgt gtg agg cat ct 3'	113 bp
Human Brachyury (mesoderm)	F: 5' agg tac cca acc ctg agg ag 3' R: 5' gct gga cca att gtc atg g 3'	135 bp
Human BMP4 (mesoderm)	F: 5' tcc aca gca ctg gtc ttg ag 3' R: 5' ggg atg ctg ctg agg tta aa 3'	148 bp
Human SOX-1 (ectoderm)	F: 5'gga atg gga gga cag gat tt 3' R: 5'aac agc cgg agc aga aga ta 3'	132 bp
Human SOX-17 (endoderm)	F: 5'ctg cca ctt gaa cag ttt gg 3' R: 5'gag gaa gct gtt ttg gga aca 3'	138 bp

Table 2:4 Forward and reverse primers used for qPCR. Pluripotency genes and genes for early mesoderm/ectoderm/endoderm differentiation. Primers were designed to flank two exons or were intron spanning.

2.12 Dielectrophoresis

2.12.1 Cell Culture

MG-63 (human osteoblast like) and SAOS-2 (sarcoma osteogenic) cell lines were maintained in basal medium (DMEM containing 10% FCS) at 37^{o}C, supplemented with 5% CO_2. STRO-1 positive cells were maintained in standard media and culture conditions. The cells were maintained by routine passage at 70-80% confluence. Prior to treatment with trypsin, cells were washed with 1x PBS and detached by adding 1x trypsin/EDTA for 10 minutes at 37^{o}C. Once detached the trypsin was inactivated by the addition of DMEM containing 10% FCS. The cells were then centrifuged at 1100rpm for 4 minutes at 4^{o}C.

2.12.1.1 Cell Preparation

Cells were prepared by repeated washing to remove as much of the standard culture media as possible. The cells were detached from the plastic using trypsin-EDTA for 5

minutes, then spun at 1100rpm for 4 minutes at 4°C. The pellet was then resuspended in conductivity medium and washed twice before being finally resuspended in 1ml of conductivity medium. The conductivity medium was made up of 8.5% sucrose and 0.3% glucose in distilled water, and made up to the required conductivity, typically 100μS using PBS. It is a requirement that the cells were washed so many times as the cross-over of culture media is likely to make the final conductivity higher. This is particularly a problem as the cells were resuspended in a small volume, meaning that the percentage of media carried over was greater.

2.12.2 Microwell System

The microwell is a three-dimensional electrode made up of alternating layers of metal and insulator.

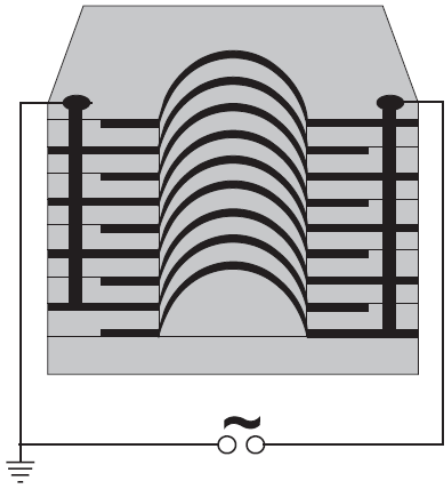

Figure 2:2 Schematic diagram of single well electrode. The three-dimensional well electrode is made from alternating layers of thick copper tape separated by an insulating polymide layer and adhesive. Holes of 0.7mm diameter are drilled through the layers so that the walls of the holes have electrodes of alternating potential separated by insulating layers (Hubner et al., 2005).

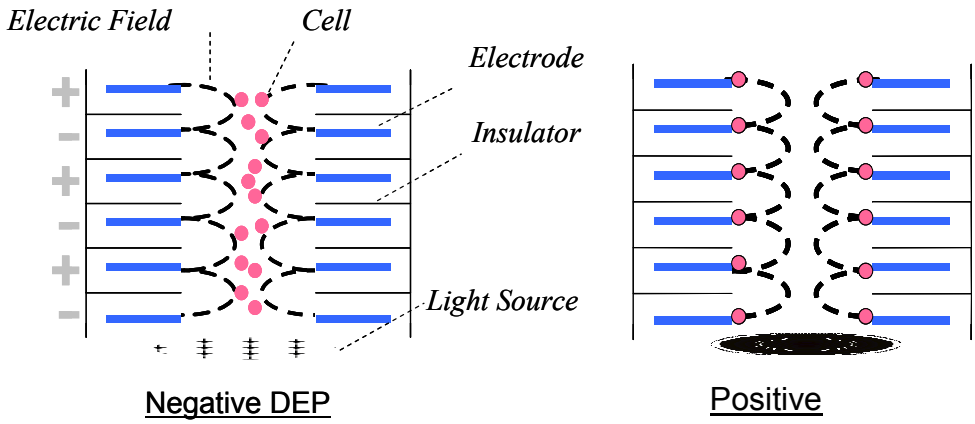

Figure 2:3 Schematic of cross section of well, showing the position of the cells during positive and negative DEP. In negative DEP, cells move toward the region of lowest electric field strength (the centre of the well) and therefore decrease the light intensity in the centre of the well. In positive DEP the cells will collect at the electrode edge increasing the light intensity in the centre of the well. Note that the electric field does not span the diameter of the well.

If positive DEP is occurring, the cells will collect at the electrode edge (the outer part of the well), therefore increasing the light intensity in the centre of the well. When displaying negative DEP, cells move toward the region of lowest electric field strength, which is the middle of the well, producing an increase in light intensity at the edges of the well and a decrease in the centre of the well. The greater the dielectrophoretic response, the greater the difference in light intensity between the two regions.

The experimental set up is shown in Figure 2:4. For each experiment, approximately 1µl of cell solution was injected into the well. Using a signal generator, electrodes were energised with $10V_{pk\text{-}pk}$ using a sinusoidal signal at a range of frequencies from 1kHz-20MHz at 5 points per decade. Light transmitted through the wells was viewed at 4x magnification under a Nikon Eclipse E400, with a Photonic Science Coolview camera connected to a PC running Photolite to capture the images. One image was taken every 3 seconds for a total of 1 minute, with the first image being taken before the application of the electric field. The analysis was carried out using the MatLab script to determine the change in light intensity in relation to the initial picture frame. The entire diameter of the well was analysed (although the highest electric field was found at the perimeter of the well, with it not reaching the centre of the well) as well as being split into 10

different bands, analysed separately or in various combinations to show the overall movement of the cells. The light intensity across the well was normalised with respect to the initial conditions in the well, due to any potential changes in starting cell concentrations.

As stated in the system the high electric field is found at the perimeter of the well and the low found in the centre. Light is passed through the well and MatLab captures the images of the well at set time intervals, this is then compared to the initial image taken and the change in light intensity calculated. If positive DEP is occurring, the cells will collect at the electrode edge (the outer part of the well), therefore increasing the light intensity in the centre of the well. When displaying negative DEP, cells move toward the region of lowest electric field strength, which is the middle of the well, producing an increase in light intensity at the edges of the well and a decrease in the centre of the well. The greater the dielectrophoretic response, the greater the difference in light intensity between the two regions.

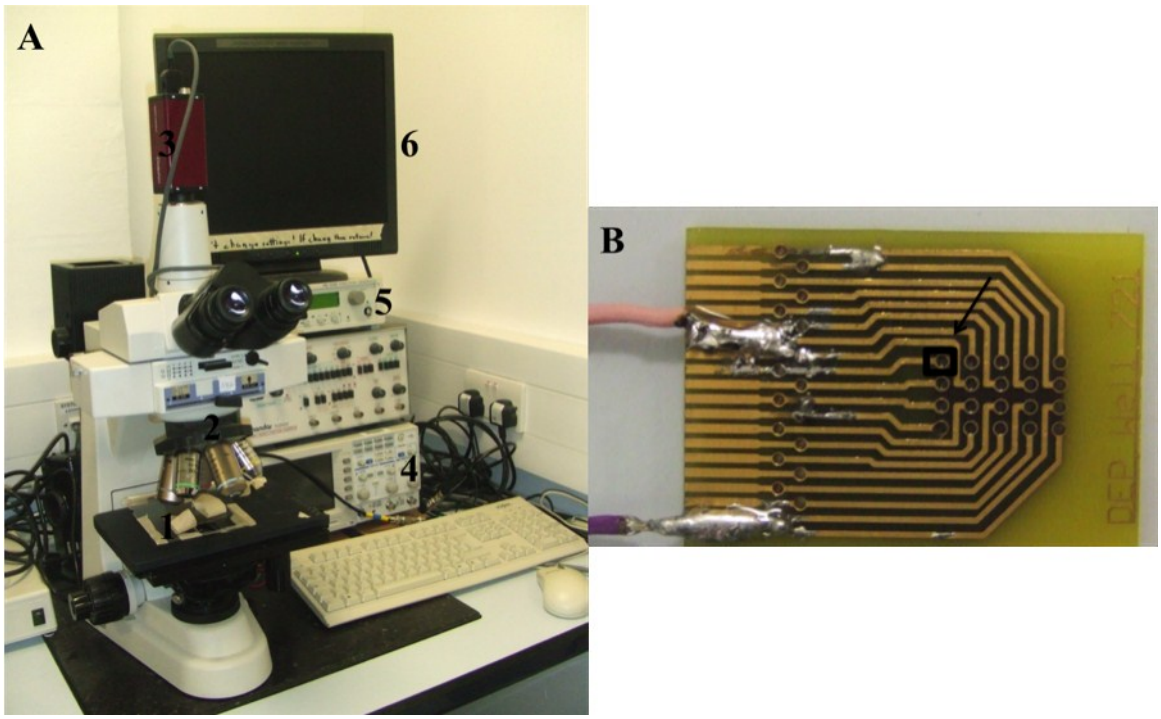

Figure 2:4 A) DEP well chip experimental set-up: this includes the well device (1/B) placed on an upright microscope at 4x objective (2) and connected to a camera (3). The device electrodes for the well which was to be used was connected to a signal generator (4/5) to produce the DEP force. All of the named devices were connected to a computer (6) and

operated and analysed via MatLab. B) Well chip device, with a single well indicated by the arrow.

2.12.3 Data Analysis

In order to generate the data and model the results, MatLab (The Math-works Inc, Nantick MA) script was used. The programme works by analyzing the change in light intensity in relation to the first picture taken without the applied electric field. The light intensity is normalised with respect to the initial conditions in the well since it is possible that changes can occur due different initial cell concentrations. A total of 23 frequencies were run determined by a logarithmic scale.

The entire diameter of the well is monitored during the course of the experiment. The well is divided into 10 segments that are monitored separately. For the characterisation analysis, segments 7-10 are analysed exclusively, this is in part due to the possibility that in the centre of the well, random motion is likely to occur (Hubner et al., 2005).

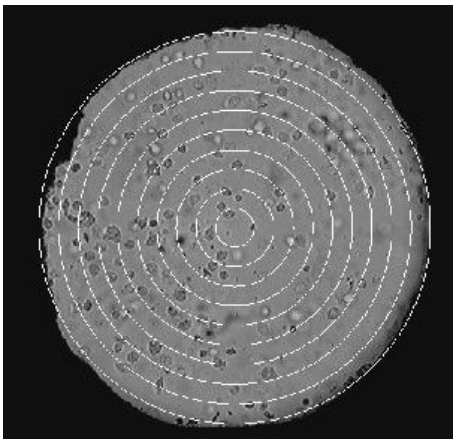

Figure 2:5 Image showing initial detection of well by the MatLab script. Image shows cell distribution at the start if the experimental run and bands dividing the well. The three outer bands 7-10 are used for analysis.

For each experimental run, data was plotted and a model applied. The model includes: cell radius, membrane thickness, permittivity and conductivity, cytoplasmic conductivity and permittivity and medium permittivity and conductivity. In order to generate the model, typical values were applied and then adjusted in order to achieve the best fit of the curve to the points. The individual values obtained for each cellular property were then averaged. At this point, the dielectrophoretic characteristic of the

cell can be said to be determined. Each part of the model curve represents a component above and are represented in one log10 region.

2.12.4 DEP Channel Device

The channel device was fabricated on glass slides using techniques as described in Wang et al., 2007 and Flanagan et al., 2007. The conditions used were that as optimised by Flanagan et al (2007). Each channel device contained 3 groups of electrodes lying on the floor of the channel each group containing 16 electrodes. When a frequency is applied cells can be trapped along the electrode sides if the DEP force is greater than that of the flow and if the cell is experiencing positive or negative DEP. The cell preparation for the channel device differed from the well chip only in that a cell count was taken to determine if there were enough cells to run the experiment. A cell concentration of $8x10^5$-$1x10^6$/ml was needed, of which less than a 200µl volume of cells was needed to run the experiment.

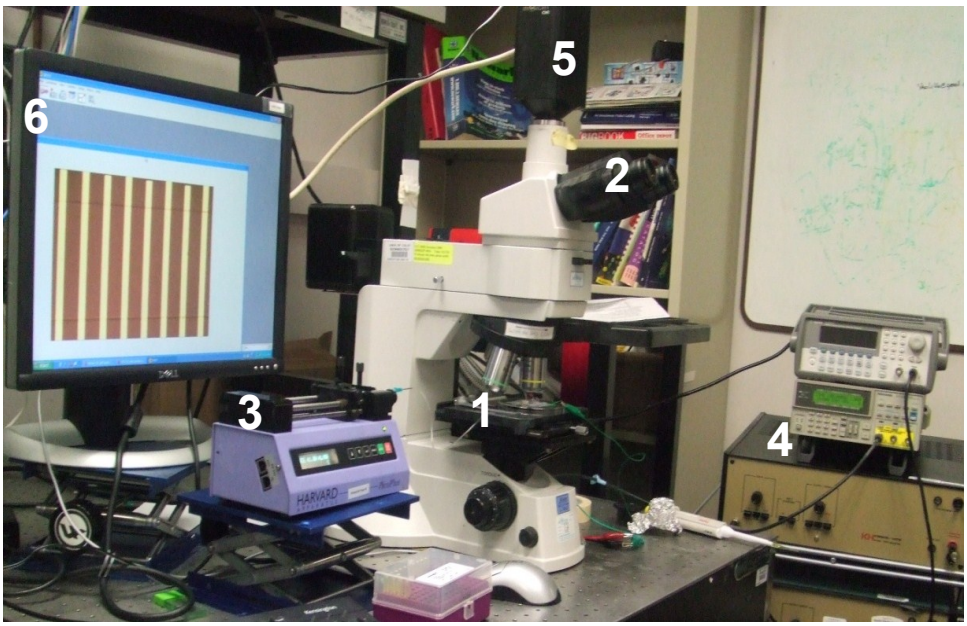

Figure 2:6 Experimental set-up of channel device: this includes the channel device (1) placed on an upright microscope (2) and connected to a syringe pump (3) via the device outlet to control the fluid flow. The device electrode for the region of the device that was to be used was connected to a function generator (4) to produce the electrical force. The microscope was set to 10x magnification with a colour camera (5) attached, which was connected to the computer. The image shown on the screen (6) is that which was recorded and analysed, it shows 8 of the 16 electrodes in one portion of the channel device.

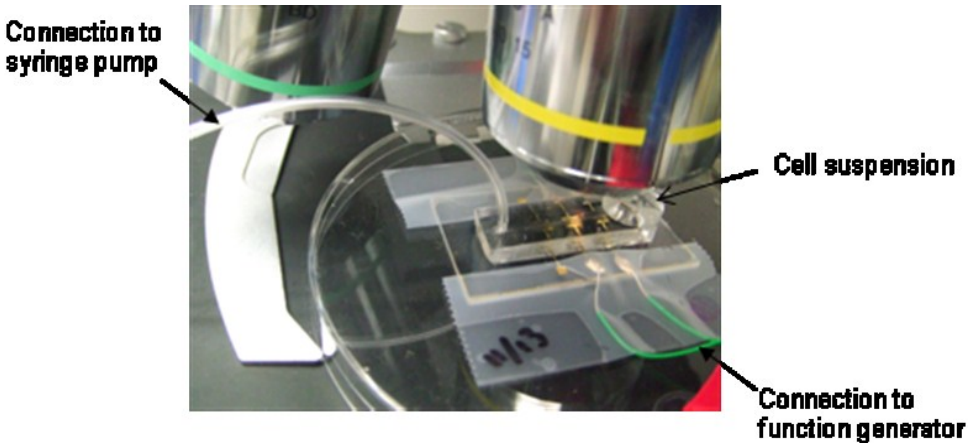

Figure 2:7 Microscope stage portion of the channel device experimental setup: Microscope focussed on one of the three sets of electrodes that are connected to the function generator. Cells were loaded into the device by placing 50µl cell suspension over the inlet.

The device was placed on the stage of an upright microscope and the channel region of the device visualised with the 10x objective. The microchannel outlet of the DEP device was connected to a syringe pump (Pico Plus, Harvard Apparatus, MA) using Teflon tubing. Prior to the addition of cells, fluid flow was initiated and the channel cleaned with trypsin-EDTA followed by washing with DEP buffer. A high flow rate (40µl/min) was used to fill the channel and tubing with fluid before stabilizing the rate at 2µl/min for the experimental runs (which had been found to be the optimal flow rate for the device). A function generator was used to produce an AC signal (8 V with the frequency ranging between 25kHz – 10MHz) to provide the DEP force in the channel. A colour digital camera was attached to the microscope and the CamStudio screen recorder used to capture movies (100 frames/second) of the cells trapped at each frequency. The cells were recorded for 5 seconds before applying the DEP force with recording continuing for a further 5 seconds. Three video segments per frequency were captured.

2.12.4.1 Data Analysis

To calculate the percentage of trapped cells at each frequency, a 5 second frame of the videos were viewed (PFV, Photoron, Ltd.) and the cells flowing through the channel manually counted. The cells trapped by the electrodes in the last frame of the videos were also counted and the figure expressed as a percentage of the total cells. In the system, the high electric field is found at the perimeter of the well and the low electric

field found in the centre. Light is passed through the well and MatLab captures the images of the well at set time intervals, this is then compared to the initial image taken and the change in light intensity calculated.

2.13 Statistics

Statistical analysis was performed using unpaired t-tests to compare mean values between two groups and a one-way ANOVA was performed to compare mean of three or more experimental groups, followed by a Newman-Keuls post-hoc test to identify significance between groups. All experiments were repeated at least 3 times (unless otherwise stated), values were expressed as mean ± standard deviation (SD). Graphical representation of p-values were assigned as * $p<0.05$.

Chapter 3 Characterisation of human embryonic stem cells and foetal femur derived cell populations.

3.1 Introduction

3.1.1 Human Embryonic Stem Cells

Although there is a wealth of research looking at various differentiation strategies for ES cells, there is also a significant amount of research into optimising the culture conditions of ES cells and an understanding of the factors and pathways involved in the maintenance of pluripotency (see section 1.3). To date, there has been substantial characterisation of the stem cell lines (Ware et al., 2006) with the largest study being conducted by the Stem Cell Initiative, (Adewumi et al., 2007) which examined a total of 59 cell lines worldwide. Despite the identification of diverse genotypes, derivation and culture maintenance techniques, the authors found that all cell lines exhibited similar expression patterns for several markers of human ES cells. The ES cell lines examined expressed the glycolipid antigens SSEA3 and SSEA4, the keratan sulfate antigens TRA-1-60, TRA-1-81, GCTM2 and GCT343, and the protein antigens CD9, Thy1 (also known as CD90), tissue-nonspecific alkaline phosphatase and class 1 HLA, as well as the genes strongly associated with development, NANOG, OCT-4, TDGF1, DNMT3B, GABRB3 and GDF3. However, the cell lines were not identical, with differences found in expression of several lineage markers, and although several imprinted genes showed generally similar allele-specific expression patterns some gene-dependent variation were observed.

The current studies have used the human embryonic stem cell line 7 (HUES-7), derived by Cowan et al, (2004). HUES-7 cells exhibit typical human ES cell characteristics, displaying a high ratio of nucleus to cytoplasm, prominent nucleoli, and compact colony morphology. The HUES cell lines were found strongly positive for a number of molecular markers of undifferentiated pluripotent human stem cells, including octamer binding protein-3/4 (OCT-3/4), stage-specific embryonic antigen (SSEA), SSEA-3, SSEA-4, TRA-1-60, TRA-1-81, and alkaline phosphatase. HUES-7 cells were expanded and distributed at passage 11 (therefore all data on passage number seen is n+11). However the prolonged culture of these cells (and other stem cell lines) typically results in chromosomal abnormalities in chromosomes 2, 12 and 17 (Draper et al., 2003, Andrews et al., 2005). Karyotyping of the HUES-7 cell line utilised here revealed the addition of chromosomes 12 and 17 (48XY).

An overview of the differentiation studies performed in the literature thus far is given in section 1.3.3. The majority of differentiation studies performed to date using the HUES-7 cell line have centred on cardiomyocyte differentiation. Denning et al (2006) performed a parallel investigation of the HUES-7 and BG01 cell lines comparing their proliferation and cardiac differentiation, in parallel to the BG01 cell line. Denning and co-workers found that using the same culture technique (formation of EBs from a MEF feeder layer, followed by culture in FBS-containing medium) produced spontaneously contracting EBs in both BG01-EBs and HUES-7 EBs. The mean beat rate was comparable at 37.2 ±2.3 and 41.1 ±3.1 beats/minute for BG01-EBs and HUES-7-EBs, respectively. The derived cardiomyocytes expressed cardiac genes and responded to pharmacological stimulation (Denning et al., 2006). A transgenic approach was also taken to enrich the cardiomyocytes derived from the HUES-7 cells and found that parental and transgenic HUES-7 cells had a similar morphology, pluripotency marker expression, differentiation, and cardiomyocyte physiology (Anderson et al., 2007).

3.1.2 Human Foetal Femur Derived Cells

A developing area of research has been the characterisation of foetal-derived tissues obtained from aborted foetuses. However, the properties of these cells in comparison to ES cells and adult stem cells remains less well defined due, in part to, the absence of reliable markers for these cells. It has previously been shown that cells derived from the human foetal femur are multipotent and able to differentiate along the osteogenic, chondrogenic and adipogenic lineages via the use of specific differentiation factors. The single cell clonal multipotentiality of these cells has also been demonstrated (Mirmalek-Sani et al., 2005).

The use of osteogenic inducing agents in foetal cell populations has been addressed by Jaiswal et al (1997), who routinely used the combination of ascorbate and dexamethasone to differentiate the cells toward the osteogenic lineage. Ascorbate has shown to be an enzyme cofactor required for collagen synthesis (Takamizawa et al., 2004). The use of dexamethasone, a glucocorticoid hormone, in osteogenic differentiation has also been established in numerous studies (Jaiswal et al., 1997, Cheng et al., 1994).

1,25-dihydroxyvitamin D_3, (vitamin D_3), often used in combination with ascorbate and dexamethasone, has been shown to induce a dose-dependent osteogenic response in human bone marrow stromal cells, with increased alkaline phosphatase, type I collagen and osteocalcin expression (Beresford et al., 1984, Beresford et al., 1986, Franceschi and Young, 1990).

An important group of osteo-inductive factors are the bone morphogenic proteins (BMPs), which are critical in the formation of skeletal tissue (Wozney, 1992). BMPs are a subfamily within the transforming growth factor-β superfamily (Wozney, 1992). A number of studies have been undertaken looking at the effects of BMPs on osteogenic and chondrogenic differentiation and their possible clinical applications in bone repair (Li and Wozney, 2001, Yoon and Lyons, 2004, Partridge et al., 2002). Specifically BMP-2 has shown promise for use in tissue engineering strategies for orthopaedic application (Partridge et al., 2002, Li and Wozney, 2001, Bessa et al., 2008).

The transforming growth factor-β peptides are also understood to play vital roles in the formation of bone and cartilage, with TGF-β3, in particular, identified for use in chondrogenic differentiation (Pittenger et al., 1999). A pellet method in combination with TGF-β3 has also been identified as a suitable model for the maintenance of a chondrogenic phenotype (Tare et al., 2005).

3.1.2.1 Characterisation of Human Foetal Cells using Progenitor Markers.

The isolation and subsequent expansion of skeletal stem cells has, to date, been undertaken using a small panel of monoclonal antibodies. However, as yet, there is no unique marker for the skeletal stem cell. A comprehensive table of skeletal stem cell markers is given in section 1.8. One of the antibodies identified, STRO-1 (Gronthos and Simmons, 1995, Gronthos et al., 1999, Simmons and Torok-Storb, 1991b), recognises a trypsin-resistant cell surface antigen present on a subpopulation of human bone marrow cells. Gronthos and colleagues (1994) first reported on the use of STRO-1 monoclonal antibody to reduce heterogeneity of the stromal cell population, with expression of STRO-1 demonstrated to reside primarily in the colony forming units-fibroblastic (CFU-F). As yet the epitope for STRO-1 remains to be characterised, however it is known that the antibody does not bind to myeloid cells, megakaryocytes or macrophages (Gronthos et al. 1994).

7D4 is a novel monoclonal antibody, which recognises proteoglycan sulphation motifs homologous to Versican (a large aggregating proteoglycan), and has been used to determine chondroprogenitor populations in bovine cartilage sections (Hayes et al., 2008b). In addition, the 7D4 antibody was used in flow cytometric analysis to select for chondrocytes from the metabolically active superficial zone of adult bovine cartilage (Hayes et al., 2008a, Hayes et al., 2008b).

3.2 Aims

The aims of the current studies were;

- To characterise the undifferentiated human embryonic stem cell profile of the HUES-7 cell line,
- To determine the phenotype of human derived foetal cells through molecular, biological and histological techniques.
- To derive human skeletal cell populations from foetal cell populations and direct their differentiation along the skeletal lineages using selected growth factors,
- Selection and expansion of osteoprogenitor and chondroprogenitor populations using specific markers from foetal femur-derived cell populations and their subsequent characterisation.

3.3 Materials and Methods

3.3.1 Reagents and Materials

All reagents including tissue culture reagents were obtained from Sigma-Aldrich, UK, unless otherwise stated. Penicillin/Streptomycin was purchased from Lonza, Cambridge, UK. Foetal calf serum was purchased from Invitrogen, Paisley, UK. Collagenase B was purchased from Roche Diagnostics Ltd., East Sussex, UK. Type I collagen polyclonal antibody was a gift from Dr Larry Fisher, NIH, Bethesda, USA. Sox-9 polyclonal antibody (AB5535) was obtained from Chemicon International (part of Millipore, Hertfordshire, UK. 7D4 monoclonal antibody was a gift from Prof. Bruce Caterson, Cardiff University. STRO-1 monoclonal antibody (STRO-1 hybridoma gifted from Dr J. Beresford, University of Bath). DAPI (4',6-diamidino-2-phenylindole) nuclear counter stain (D3571) was purchased from Molecular Probes, Invitrogen, Paisley, UK. The secondary antibody, Anti-Mouse IgM Alexa-488 was purchased from Invitrogen, Paisley, UK. Pluripotency markers OCT-4, SSEA-3 and TRA-1-60 were purchased from Santa Cruz Biotechnology, Germany and SOX-2 from Millipore, Hertfordshire, UK and corresponding secondary antibodies were purchased from Sigma-Aldrich, Dorset, UK and Molecular Probes, Invitrogen, Paisley UK. All molecular reagents (including primer sets) were purchased from Invitrogen, Paisley, UK or Sigma-Aldrich, Dorset, UK. Primer sequences are given in section 2.10.3.

All images were captured with Carl Zeiss Axiovision software via AxioCam HR digital camera or Canon Powershot G2 digital camera.

3.3.2 Human Embryonic Stem Cell Culture

HUES-7 cells were routinely cultured and maintained on a MEF feeder layer as described in detail in section 2.5. Media changes were performed daily and the cells passaged at confluence, which was approximately every 3-4 days. After washing the cells with PBS, the cells were treated with 1ml per well of collagenase IV and incubated at 37^{o}C for 3-4 minutes, until the edges of the colony began to lift. The collagenase was then removed, and replaced with the appropriate amount of human ES cell media (for the ratio of the split) prior to cell harvest. A maximum 1:3 split ratio was used for cell passage. The cells were then added drop wise around a new MEF coated well plate to ensure even distribution. Following passage, media change was performed after 48

hours. If there was a significant amount of spontaneous differentiation, the differentiated cells were removed from the culture by picking off the differentiated colonies with a sterile pipette prior to passage. If required, collagenase treatment for up to 10 minutes was used for confluent colonies or wells displaying higher than usual levels of differentiation.

Prior to commencement of differentiation studies, cells were cultured on MEF free conditions using matrigel plates. A minimum of two passages was performed to ensure removal of MEF cells. MEF conditioned media was used to maintain the pluripotent state of the cells, and was prepared by the application of human ES cell medium to MEF cells subsequently cultured overnight. The conditioned medium was then directly used on matrigel culture plates or pooled and frozen for later use.

3.3.3 Embryoid Body Formation

Embryoid body formation was performed as follows. HUES-7 cells were treated with 1ml per well of collagenase IV and incubated at 37^{o}C for 10 minutes. The collagenase was removed and replaced with 1ml per well of MEF media and spun at 1000rpm for 4 minutes. The cell pellet was then resuspended in 10ml of MEF media and placed into a non-tissue culture treated petri dish and maintained at 37°C with 5% CO_2. Media changes were undertaken every 3-4 days with 80-90% media removal (whilst taking care to ensure that EBs were not removed) and replacing with fresh media.

3.3.4 Foetal Cell Isolation

Human foetal femurs were obtained and processed as previously described (section 2.3). Briefly, femurs were dissected and plated into T25 flasks in 5ml collagenase B (1mg/ml) and digested overnight. Cells were then plated at appropriate densities in basal medium and maintained at 37°C in 5% CO_2. Cells were passaged using a Tris-EDTA solution in PBS before re-plating in appropriate differentiation medium, given in sections 2.2.3-2.2.5. Cells utilised for FACS were grown for 12 days in basal media. Foetal age was measured by foot length to give an age weeks post conception (WPC, see section 2.3.1). For histological analysis whole femurs were fixed in 4% PFA and embedded in paraffin wax before sectioning at 7μm.

3.3.5 Alcian Blue/Sirius Red Staining

Paraffin wax embedded samples were processed through histoclear to remove excess wax before rehydration through graded methanol (100%, 90% and 50%) and into distilled water. Rehydrated sections were nuclear counter-stained with Weigert Haematoxylin solutions A and B for 10 minutes. Samples were then dipped 3 times in acid methanol, rinsed in water and stained with 0.5% Alcian Blue for 30 minutes. Samples were treated in 1% molydophosphoric acid for 20 minutes and finally left for 60 minutes in 0.1% Sirius Red, and dehydrated through reverse graded methanol (50%, 90% and 100%) and histoclear. Sections were mounted with DPX.

3.3.6 Von Kossa Staining

Histological sections were rehydrated through graded methanol steps, as detailed in section 3.3.5 and transferred into distilled water. Silver nitrate was then added to the sections, and exposed to UV light for 20 minutes. Slides were then rinsed thoroughly in running water before treating with sodium thiosulphate and a further rinse step. A counter stain was performed using Alcian Blue for 1 minute, and van giesen for 5 minutes. Finally, slides were dehydrated as described in 3.3.5 and mounted in DPX.

3.3.7 Immunofluorescence

Sections were blocked with 1% BSA in PBS. Foetal cells fixed in 4% paraformaldehyde (w/v), were incubated overnight with a 1:2 dilution of STRO-1 human monoclonal antibody (unpurified tissue culture supernatant from the STRO-1 hybridoma provided by Dr J. Beresford, University of Bath) or 1:200 dilution of 7D4 primary antibody. A 1:50 dilution of Alexafluor 488 conjugated anti-mouse IgM secondary antibody was applied and, following three PBS washes, samples were incubated with 1:100 4',6-diamidino-2-phenylindole (DAPI) stain for 5 minutes. Cultures were washed in PBS and visualised with appropriate fluorescent filters with a Carl Zeiss Axiovert 200 microscope.

3.3.8 Immunocytochemistry

3.3.8.1 Fluorescent Method

Cells were fixed in 4% paraformaldehyde (w/v) and washed with PBS before blocking for 5 minutes with 1% BSA in PBS and overnight incubation at 4^{o}C with the appropriate primary antibody. Isotype and negative controls were performed by

replacing the primary antibody incubation step with isotype antibody or 1% BSA in PBS respectively. Slides were washed in 3x 5 minutes washes with PBS, the appropriate fluorescently tagged secondary antibody was applied and incubated for 1 hour in the dark. Washes were repeated and DAPI nuclear stain was applied for 5 minutes before final washes and visualisation under fluorescence microscope.

For embryonic stem cell staining an additional 1 hour blocking step was used prior to addition of the primary antibody. For nuclear markers this consisted of 0.01% Triton X-100 and donkey serum, while for surface marker staining, the blocking solution did not contain Triton X-100.

3.3.8.2 AEC Method

For type I and II collagen staining the same protocol as described in 3.2.8.1 was used, with the exception of the application of a secondary antibody conjugated with biotin. Samples were developed using 3-amino-9-ethyl-cardazole (AEC) in acetate buffer containing H_2O_2. Sections were mounted with glycerol jelly.

For SOX-9 staining, prior to blocking endogenous peroxidise activity, an antigen retrieval heat step was performed using 0.01M citrate buffer for 10 minutes.

3.3.9 PicoGreen dsDNA Quantification and Alkaline Phosphatase Specific Activity Quantification

DNA content was determined using PicoGreen dsDNA quantification reagent (Molecular Probes). 10µl of cell lysate was combined with 90µl Tris-EDTA (Tris-HCL Ethylenediamine Tetra-acetic Acid) buffer and 100µl of 1:200 dilution of PicoGreen reagent in Tris-EDTA buffer. Fluorescence was measured immediately on an FLx cytofluor microplate reader using 480nm excitation and 520nm emission. Alkaline phosphatase activity was measured using 10µl of cell lysate from each well incubated with 100 mM p-nitrophenol phosphate (pNPP) as a substrate in 90µl 2-amino-2-methyl-1-propanol alkaline buffer solution. The reaction was timed and stopped using 100µl of 1M sodium hydroxide (NaOH). The turnover of pNPP was used to quantify alkaline phosphatase activity, which was measured by the absorbance values at 410nm on an ELx800 spectrophotometer. Results were expressed as nmol pNPP/hr. The alkaline phosphatase specific activity was calculated and expressed as nmol pNPP/ng DNA/hr.

3.3.10 WST-1 Assay for Cell Proliferation

Cell proliferation was assayed using the WST-1 Reagent colorimetric assay (1644807, Roche, Germany). Cells were plated at $1x10^4$ cells per well in a 48 well plate and following 24 hours, six wells were incubated with a 1:10 dilution of WST-1 reagent in basal medium. After 4 hours, at 37°C, absorbance at 450nm was recorded (arbitrary units) on an ELX-800 Universal Microplate Reader, Bio-Tek Instruments, Inc. (USA) with Bio-Tek KC4 Kineticalc for Windows Ver.3.01, Rev.7 software. Cultures were returned to incubators at 37°C and the assay repeated on a further six wells daily until day 7. Cell proliferation curves were analysed with SigmaPlot for Windows Ver.9.0 (Systat Software Inc., USA).

3.3.11 RNA Extraction and PCR Analysis

A detailed description of the RNA isolation and cDNA synthesis process is given in section 2.11. Briefly, cells were treated for 30 minutes with collagenase B before total RNA was extracted using TRIzol reagent, subjected to DNAse treatment (DNA-free RNA kit) and reverse transcribed using the Super-Script First-strand synthesis system for RT-PCR. Real-time qPCR was performed using the Applied Biosystems 7500 system. Samples were run in triplicate and values were calculated using the comparative Ct method and normalized to β-actin expression. Data was expressed as the mean ± SD.

3.3.12 Fluorescence Activated Cell Sorting (FACS)

Cells isolated from human foetal femurs were grown for 12 days in basal culture (described in section 2.3). Cells were treated with trypsin-EDTA and passed through a 70μm cell strainer in order to obtain single cells before counting and separated into four groups; i) unlabelled, ii) isotype control, iii) STRO-1 and, iv) 7D4 labelled populations. The primary antibody was incubated for 1 hr before washing and a further 1 hr incubation with the appropriate secondary antibody with a fluorescent labelled tag. The cells were finally resuspended in 200-500μl volumes depending upon the initial cell density. Cells were sorted using a BD FACSAria™flow cytometer (BD, Oxford, UK). Unstained and isotype control samples were used to place gates around the live and stained cell populations. Gates were adjusted for each sample and necrotic cells and debris excluded. An isotype control was also used to set the positive cell population gate. Stained samples were then applied and the percentage of the total cell population determined. Cells were then sorted at a medium flow rate using the purity setting, which

selected for only positive cells in and around a single droplet. This compromised the total yield obtained but gave positive populations with greater than 85% purity. Following sorting, cells were expanded in culture and at confluence were utilised for co-expression, molecular, biochemical and growth kinetic studies, using the protocols as previously described in sections 3.2.

3.3.13 Statistics

Statistical analysis was performed using unpaired t-tests to compare mean values between two groups and a one-way ANOVA was performed to compare the mean of three or more experimental groups, followed by a Newman-Keuls post-hoc test to identify significance between groups. All experiments were repeated at least 3 times (unless otherwise stated), values were expressed as mean ± standard deviation (SD). Graphical representation of p-values were assigned as * $p<0.05$.

3.4 Results

3.4.1 Establishment of Human Embryonic Stem Cell Culture and Characterisation

HUES-7 human embryonic stem (ES) cells, were cultured on MEFs and matrigel and maintained in standard culture conditions as described in section 2.5. Figure 3:1 A and B, show a typical pluripotent embryonic stem cell colony, defined morphologically by tight compact cells, with a defined border. Figure 3:1 C and D shows a pluripotent colony cultured under feeder free conditions on matrigel. Upon differentiation, loss of the defined border of the colony is observed with the cells exhibiting different morphologies, as seen in Figure 3:1 E. The colony exhibits a well-defined edge and the cells are less compact in comparison to cells cultured on the MEF layer. For use in differentiation studies, the ES cells were cultured in feeder free conditions on matrigel. In order to ensure that no MEF cells were present in the culture, ES cells were passaged a minimum of three times prior to use in differentiation studies. As well as the use of the cell morphology to determine the pluripotent state, immunocytochemistry revealed the expression of the nuclear pluripotency markers OCT-3/4, SOX-2 and NANOG (Figure 3:2). Positive staining of the surface markers TRA-1-60, SSEA-3 and alkaline phosphatase was also observed (Figure 3:3).

3.4.2 Embryoid Body Formation

A simple way in which the embryonic stem cells can be differentiated is through the formation of embryoid bodies (EBs). EBs are cell aggregates formed naturally when the cells are in suspension culture and in the absence of bFGF. The EB structure closely mimics that of the *in vivo* environment and results in the differentiation of cells to all 3 germ layer lineages (Itskovitz-Eldor et al., 2000).

Embryoid bodies were allowed to grow for 7 days. Within the dish there was no uniform shape or size (due to the suspension culture protocol, as described in section 2.5.5). Figure 3:4 A and B show the growth of the EBs at day 1 and 3 of culture. From day 5 vesicle outgrowth was observed, as seen in Figure 3:4 C and D. There was also some adherence of individual cells and whole EBs to the plastic with a variety of cell morphologies observed.

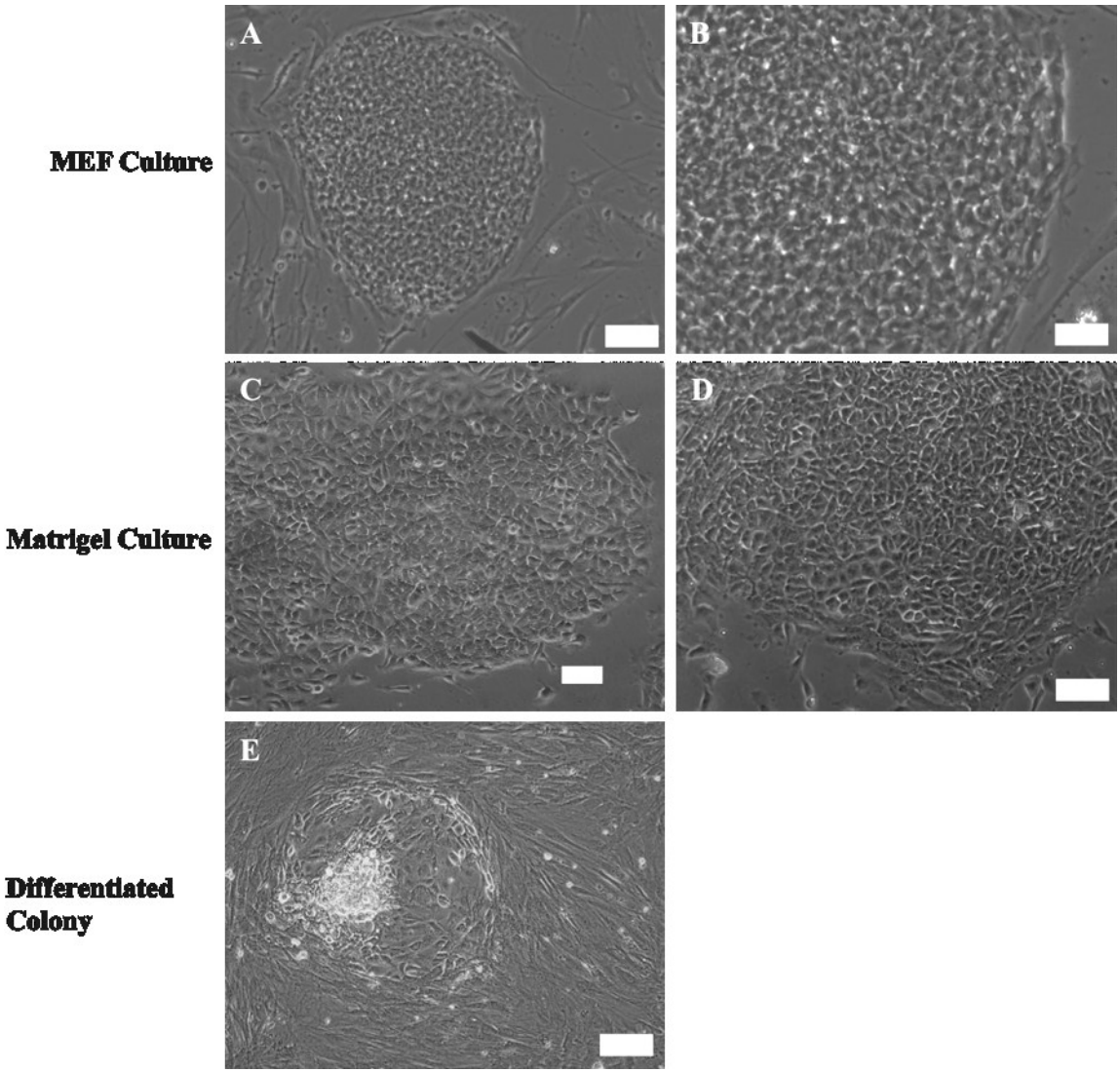

Figure 3:1 HUES-7 embryonic stem cells. A) Human embryonic stem cell colony- defining features indicating the pluripotent state include defined edges with B) tight compact cells, C) and D) colonies grown on matrigel, free of MEFs. These colonies still show a defined border with less compact cells. E) Differentiated colony, note loss of border and different cell morphologies appearing. Scale bars represent 100µm except for B) and D) that represent 50µm.

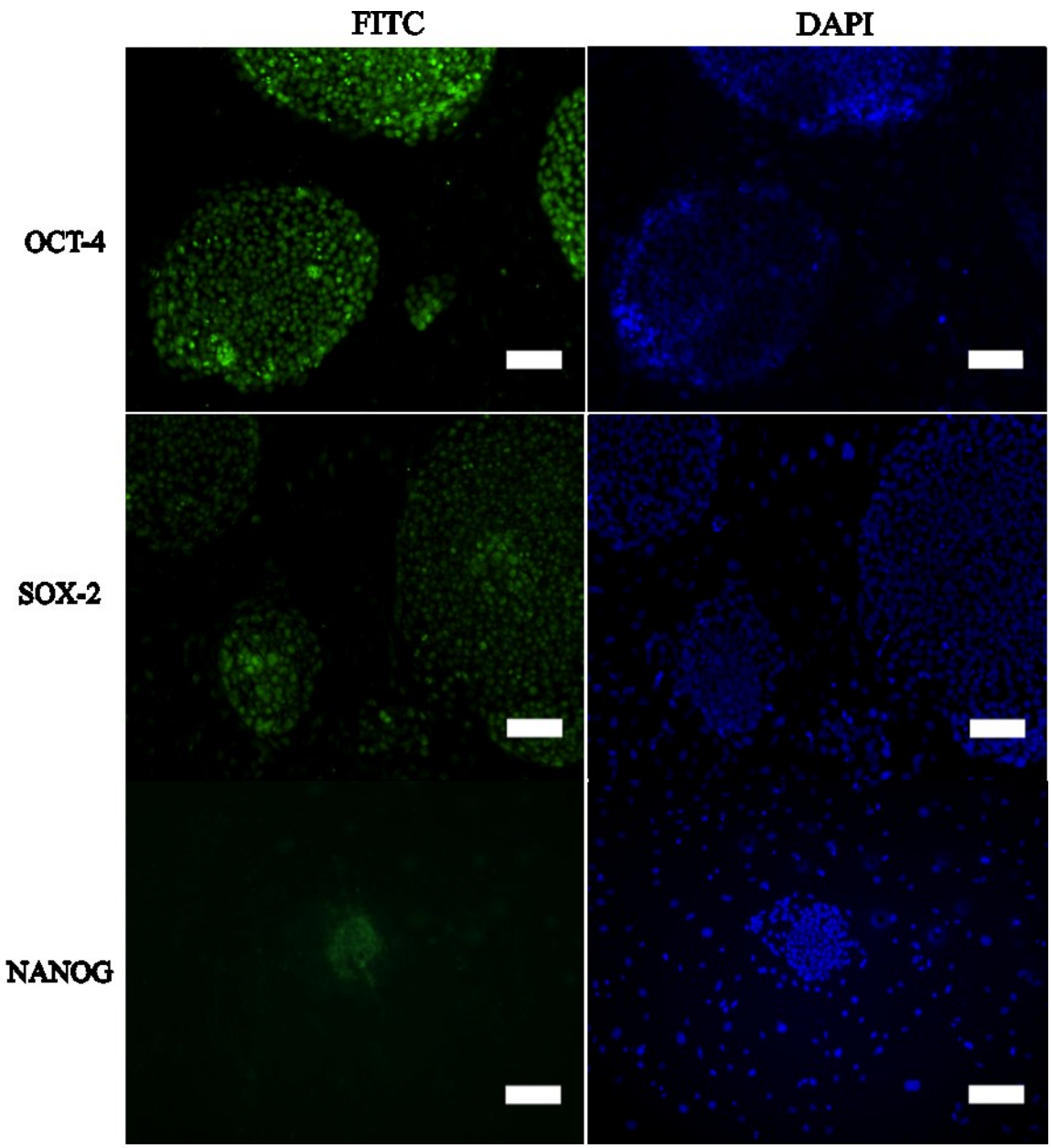

Figure 3:2 HUES-7 embryonic stem cells displaying positive staining for nuclear pluripotency markers OCT-4, SOX 2 and NANOG. Scale bars represent 100µm.

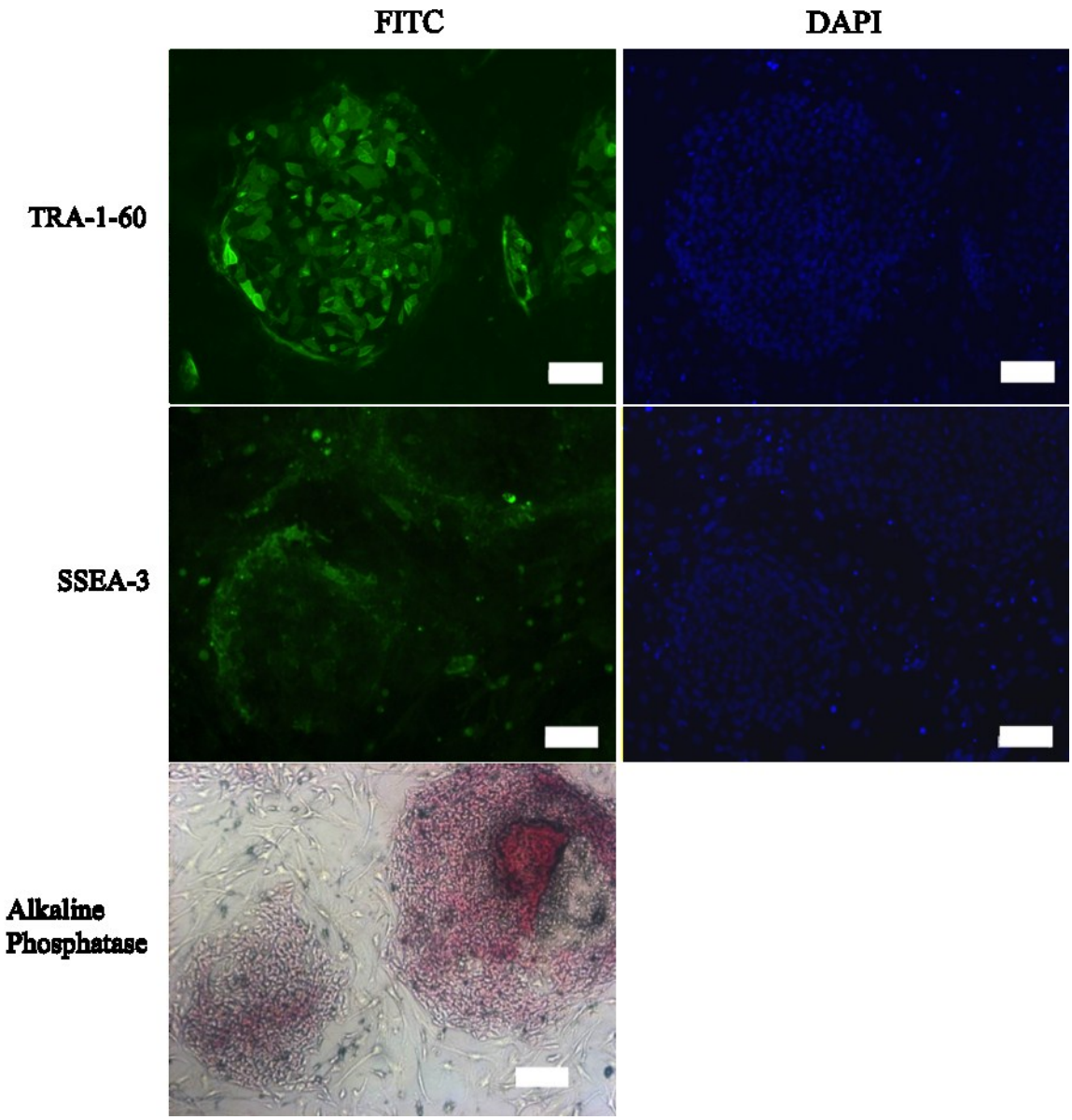

Figure 3:3 HUES-7 embryonic stem cells displaying positive staining for the surface markers, TRA-1-60, SSEA-3 and alkaline phosphatase. Cells were stained following passage and culture for 72 hours. Scale bars represent 100µm with the exception of alkaline phosphatase bar that represents 200µm.

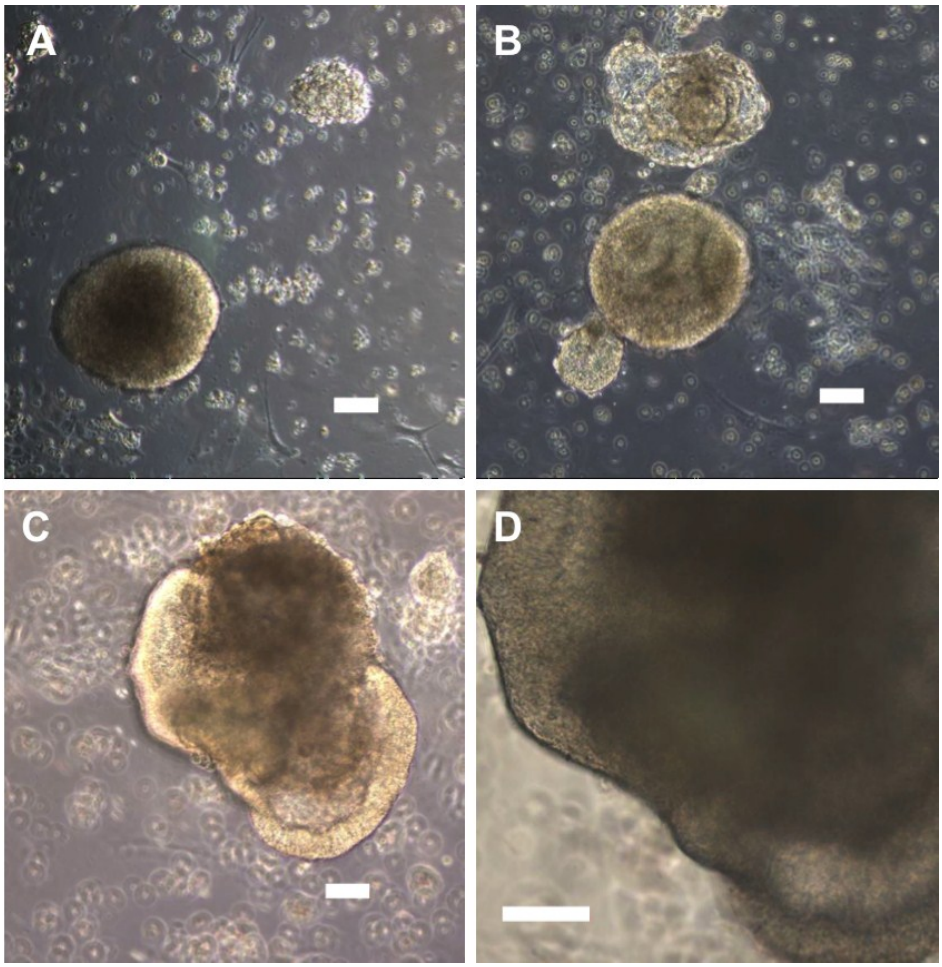

Figure 3:4 Embryoid bodies in culture at A) day 1, B) day 3, C) and D) day 5. Scale bars represent 100µm apart from D) represents 200µm.

3.4.3 Establishment of Foetal Femur Derived Cell Cultures

Foetal femurs were obtained at between 7.5 to 12 weeks post conception and processed as described in section 2.3 and expanded in culture for characterisation and differentiation studies. Upon collection, the femur was surrounded by skeletal muscle tissue (Figure 3:5 A), which was stripped away in order to reveal the femur alone, (Figure 3:5 B). Histological analysis of the foetal femurs revealed a predominantly cartilaginous anlage with an emergent bone collar visible by eye upon collection. Early mineralization of the bone collar was confirmed by CT analysis (Figure 3:5 C).

In the foetal femur the presence of type I and some type II collagen was confirmed by immunostaining (Figure 3:6 A and B respectively). The presence of type II collagen illustrates cartilaginous matrix deposition. A predominantly cartilaginous anlage was observed in sections stained with Alcian blue/Sirius red, revealing a proteoglycan-rich matrix and collagen (Figure 3:6 C). The emergent bone collar showed collagenous matrix deposition. Chondrocytic cells within the matrix lacunae were visible. Positive staining for the transcription factor SOX-9 (Figure 3:6 D) confirmed the chondrocytes were at an early stage of differentiation. Von Kossa staining illustrated the secretion of some osteoid by osteoblasts of which a negligible proportion had undergone mineralisation (Figure 3:6 E). At this stage of development, no vascularisation was observed.

Cellular outgrowth of foetal cells was observed from explant cultures (Figure 3:7 A) and could be passaged and utilized for studies. However, cells obtained from overnight Collagenase B digests were regularly used for experiments. Cells obtained from collagenase digest were observed to grow rapidly in culture and displayed a characteristic fibroblastic morphology (Figure 3:7 B). The foetal cells reached confluence following 7 days in culture when seeded at a density of 200 cells/cm^2 (Figure 3:7 C).

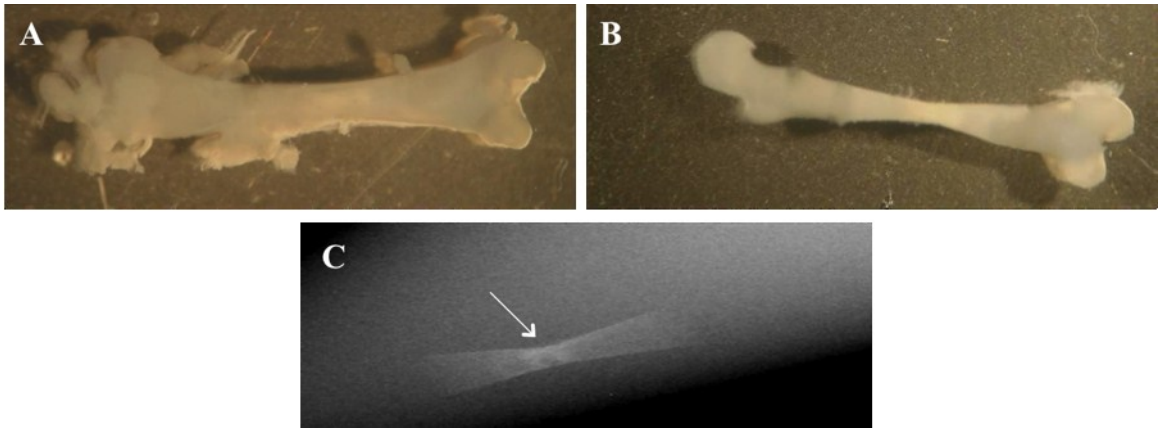

Figure 3:5 A) Foetal femur upon collection. B) Foetal femur following initial processing, a visible bone collar can be seen. C) CT image showing foetal femur with negligible mineralisation as indicated by the arrow. Femurs were collected at 7.5-12 weeks post conception and were typically between 4-10mm in length.

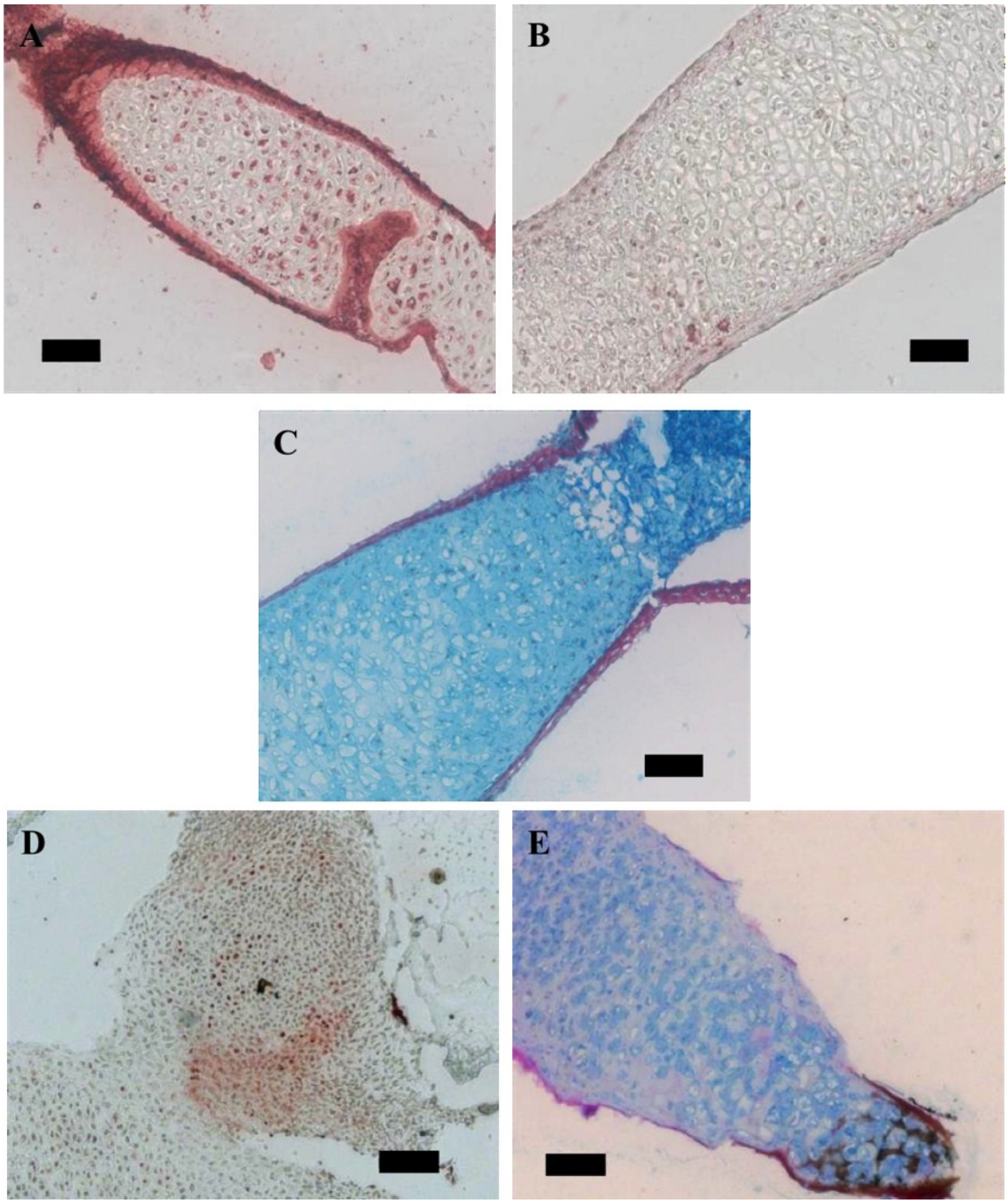

Figure 3:6 Whole foetal femur H988, A) type I collagen stain, B) type II collagen staining for hyaline cartilage, C) Alcian blue and Sirius red staining. Alcian blue stains for proteoglycans within cartilage while Sirius red stains collagen within the bone matrix. D) SOX-9 stain revealing early chondrocytes, and D) Von Kossa staining. The pink areas show osteoid whilst the brown regions show mineralisation. The section was counterstained with alcian blue. Scale bars represent 100µm.

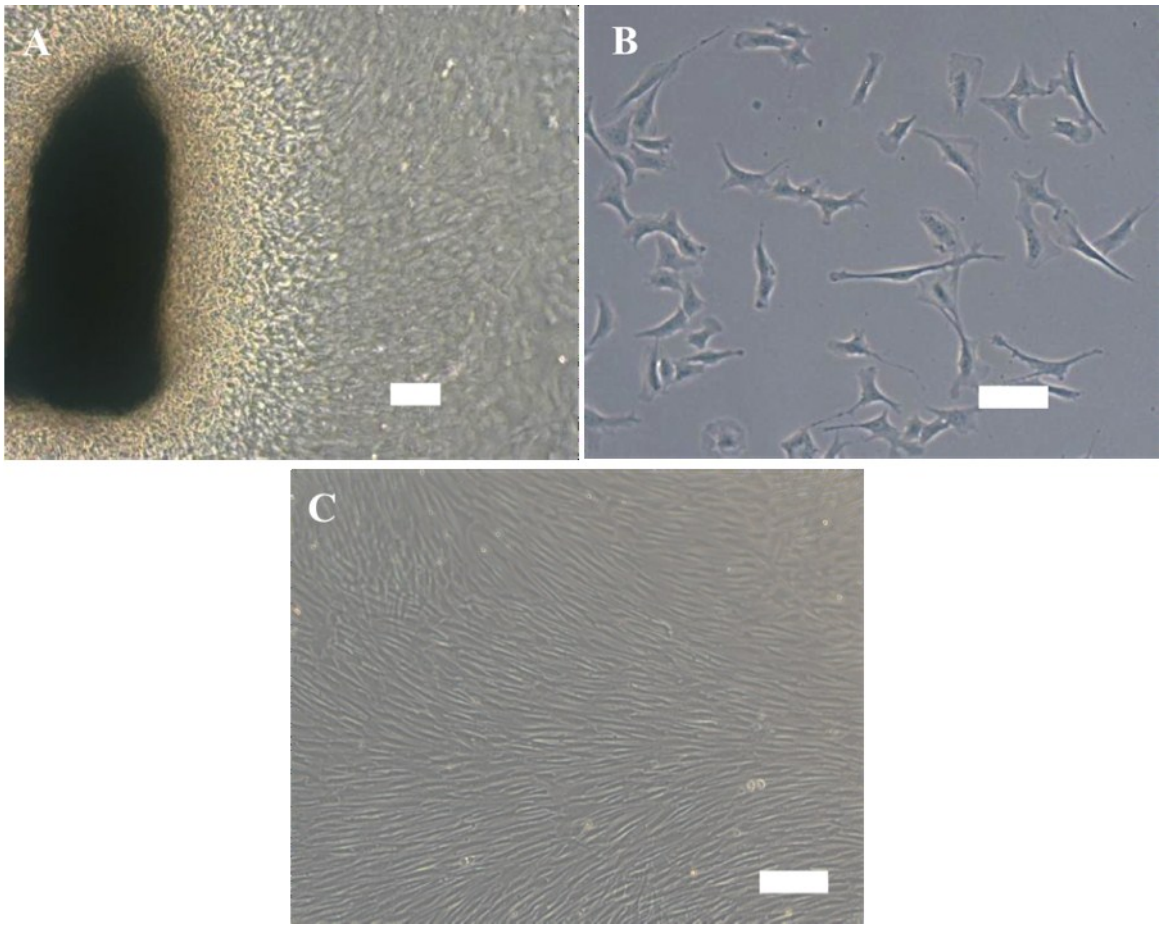

Figure 3:7 Foetal femur derived cellular outgrowth. A) femur explants after 7 days in culture. B) Cells extracted following a collagenase B digest after 48 hours, and C) after 7 days in culture (at confluence) in basal conditions. Scale bars represent 100µm.

3.4.4 Differentiation of Foetal Femur Cell Populations

The multipotentiality of the foetal femur derived cells was shown by the directed differentiation of the cells down the osteogenic, chondrogenic and adipogenic lineages. Some type I collagen staining was observed in basal conditions as shown in Figure 3:8 A. The osteogenic phenotype was confirmed with the positive staining of type I collagen in the cells, as shown in Figure 3:8 B. When the cells were cultured with chondrogenic culture media this gave rise to chondrogenic tissue, as demonstrated by the deposition of matrix containing type II collagen (Figure 3:8 C). Following 21 days in culture adipocytes were observed in the foetal cell cultures and the phenotype confirmed with Oil Red O staining for lipid vacuoles (Figure 3:8 D). The enzymatic activity of alkaline phosphatase (Figure 3:9), another marker of osteogenic differentiation and new bone turnover, was observed in selected foetal cells. After 7 days in osteogenic culture, extensive alkaline phosphatase activity was observed in comparison to basal conditions (Figure 3:9).

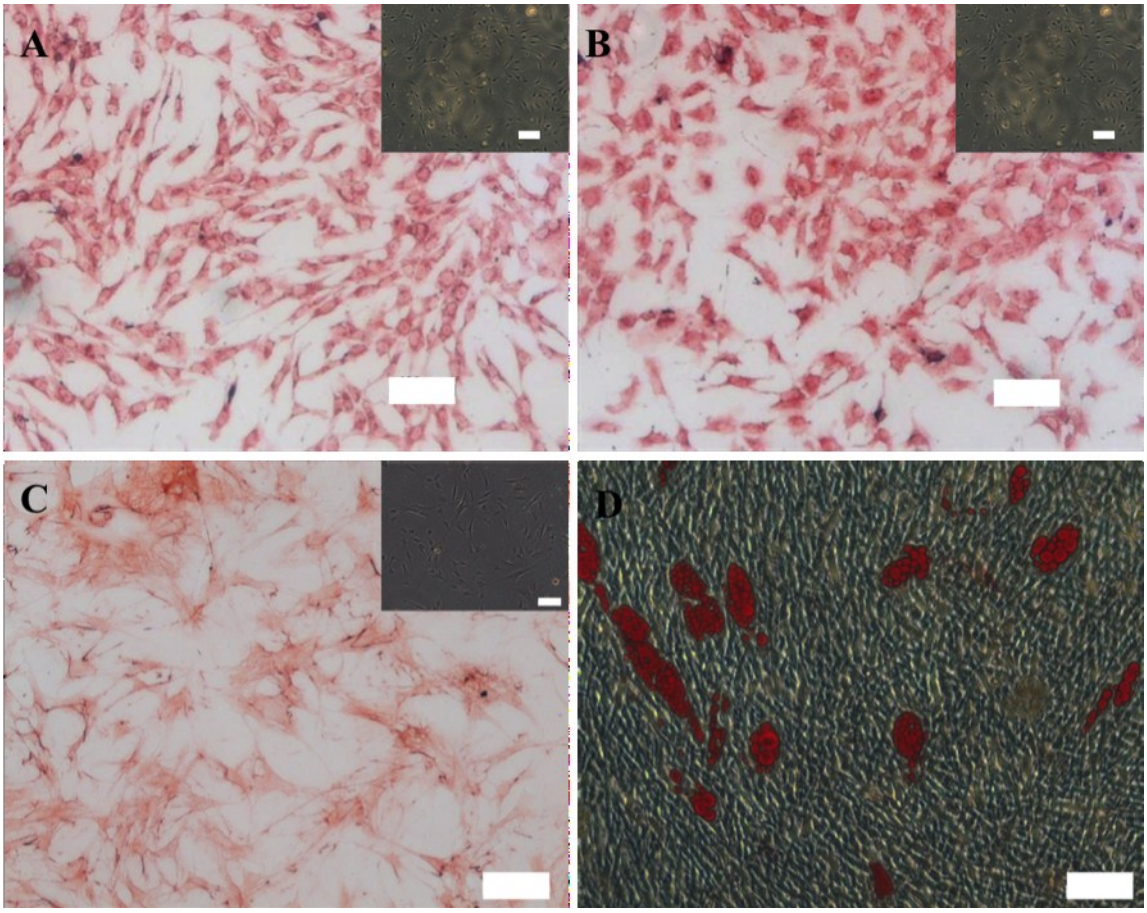

Figure 3:8 Type I Collagen staining of cells grown for 7 days in A) basal and B) osteogenic conditions C) Type II collagen staining for cells grown in basal conditions for 7 days. D) Foetal cells grown in adipogenic conditions for 21 days stained with Oil Red O. Inserts show negative controls. Scale bars represent 100µm.

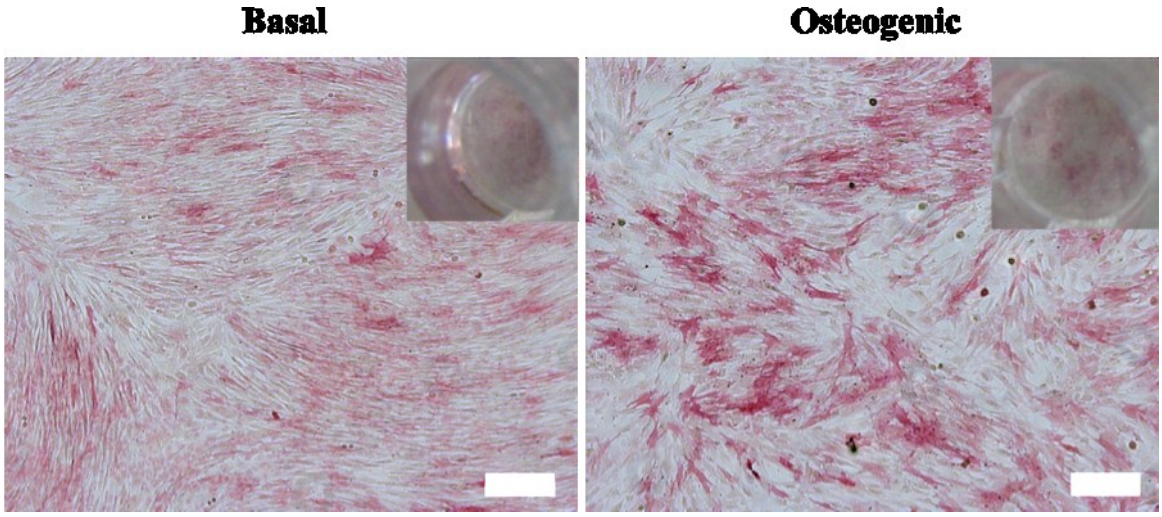

Figure 3:9 Alkaline phosphatase staining of foetal cells grown in basal and osteogenic conditions following 7 days in culture. Inserts show stained wells. Scale bars represent 100µm.

3.4.5 Human Foetal Femur–Derived Cell Proliferation

The WST-1 turnover assay was utilised in order to determine population doubling time over several days in culture recorded by absorbance readings at 450nm. 7 data points were taken, with the first 5 proving sufficient to determine the growth curve (based on the assumption of linear growth). Any data above 3-3.5AU were excluded due to saturation of the assay at this level as seen by the plateau of results following day 6 in culture.

Estimation of the population doubling time, based on these results utilised a single dataset, 2 parameter exponential growth function, displayed below:

$$y = ae^{bx}$$

Where 'a' is the initial cell number, 'e' is the exponential function, 'b' is the rate of change and 'x' is the doubling time (in days). Derivation of the equation (shown in appendix 1) gives a simplified version needing only the 'b' value:

$$\frac{\ln(2)}{b} = x$$

Calculation of the results obtained from the logistic curve plots are shown in Table 3.1, and give an estimated doubling time for the human foetal femur-derived cells of 21.4± 3 hours.

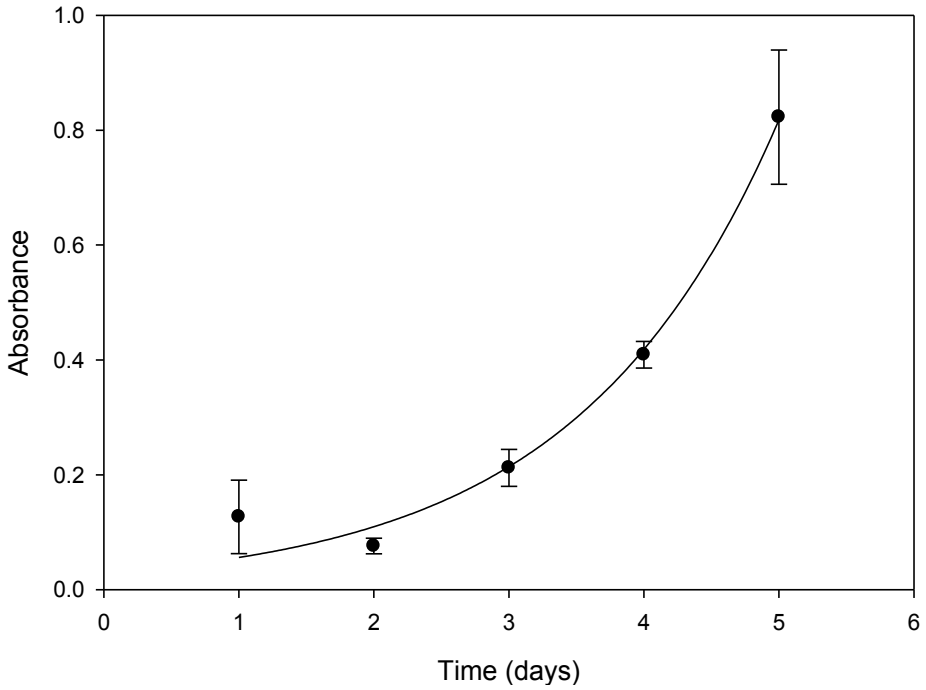

Figure 3:10 Analysis of human foetal cell population doubling by WST-1 reagent assay. Sample H1186 foetal cell proliferation over 5 days assayed by WST-1 reagent. Analysis of the growth curve gives an estimated doubling time of 21.5 hours. Results are expressed as mean values ± SD (n=1, 6 replicates).

Collection No.	Age (WPC)	r^2 value	Doubling time (hours)
H1186	7.5	0.9934	21.5
H1187	9	0.9994	18.71
H1200	7.5	0.9917	23.7
H1203	7.5	0.9830	24.8
H1244	9	0.9989	18.71
H1288	8.5	0.9980	20.8

Table 3:1 Population doubling times for human foetal femur-derived cells. Calculations derived from WST-1 assay results. Femur collection number shown with foetal age (weeks post conception), giving a mean population doubling time of 21.37 ±2.5 hours, n=6.

3.4.6 Further Characterisation of Foetal Femur Derived Cell Populations using Progenitor Markers STRO-1 and 7D4.

3.4.6.1 Long Term Expression of STRO-1 and 7D4

Both STRO-1 and 7D4 were found to be expressed in cultures of foetal femur tissue. However, STRO-1 positive staining was exclusively observed in culture, whereas 7D4 staining was observed in the foetal femur and cell culture. The expression of STRO-1 in the whole foetal femurs could not be determined in both paraffin fixed sections or frozen femurs which had been processed (including decalcification) and sectioned using the cryostat. Femur explants were plated out and allowed to adhere, from the cell outgrowths expression of STRO-1 (Figure 3:11) was seen as early as day 1, and maintained for 3 days and beyond. 7D4 positive staining could be observed in the foetal femur located, specifically in the hypertrophic chondrocytes (Figure 3:12).

From fresh isolation, foetal cells were directly plated and allowed to grow for up to 21 days in basal conditions. Expression of STRO-1 was observed at 7, 14 and 21 days of culture (Figure 3:13) after which monolayer cultures became detached. Similarly, expression of 7D4 was also observed at days 7, 14 and 21 (Figure 3:14).

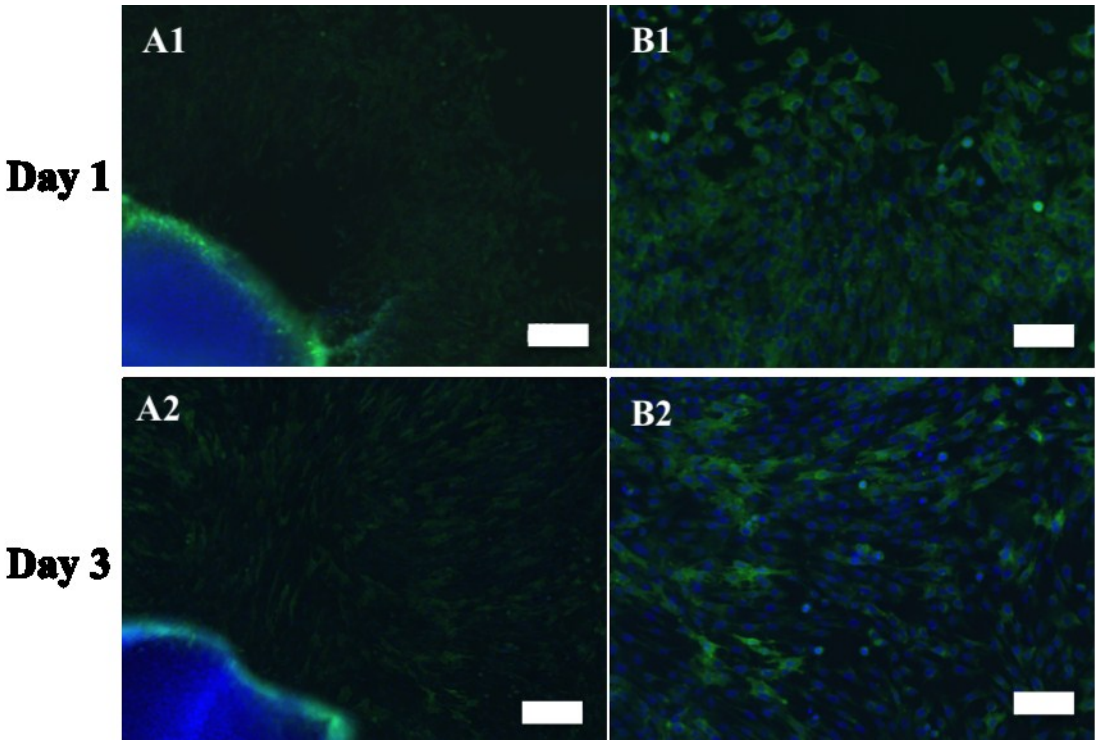

Figure 3:11 STRO-1 positive staining seen in explant cultures of foetal femurs as early as day 1 following adherence and cell growth from explant culture. Scale bars for A1-2 represent 200μm. Scale bars for B1-2 represent 100μm.

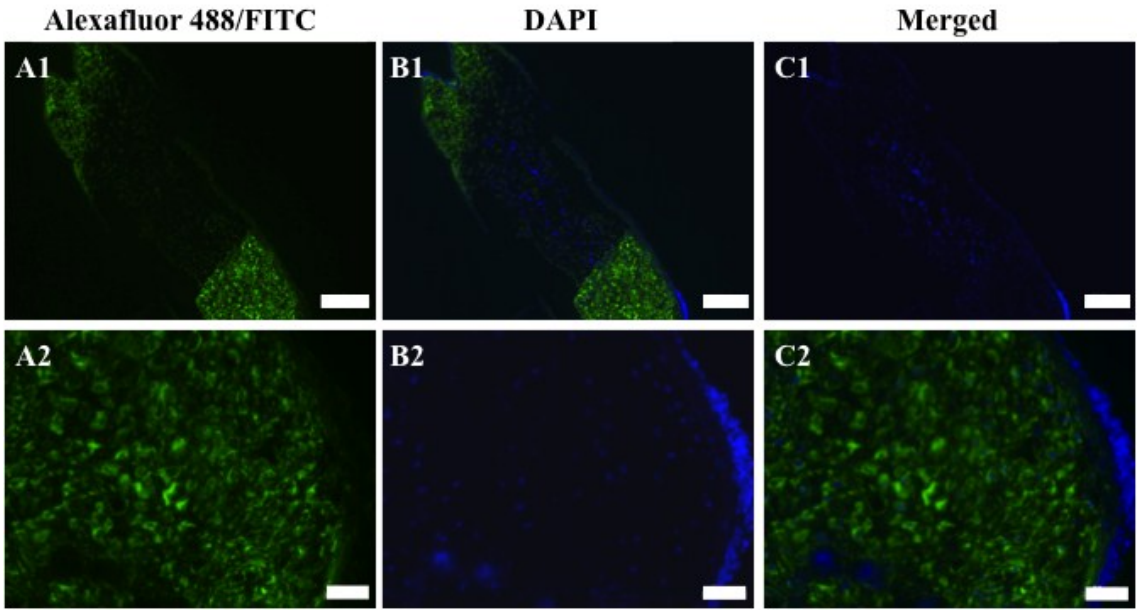

Figure 3:12 Positive staining for 7D4 expression in foetal femur, mostly found in the hypertrophic chondrocytes. Scale bars for A1-3 represent 50μm and B1-3 represent 200μm.

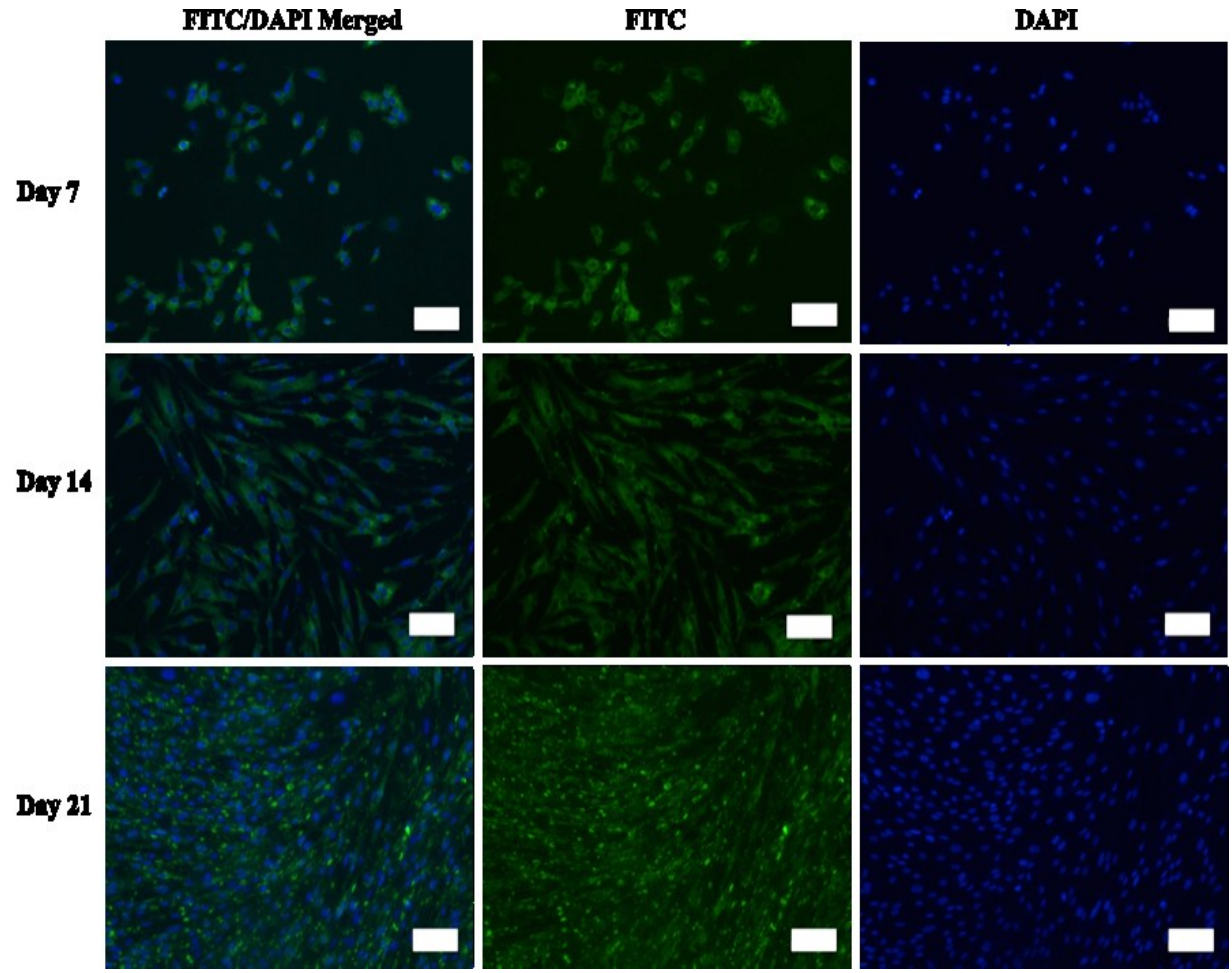

Figure 3:13 Long-term expression of STRO-1 in unselected foetal cell populations. Sample H1177. Expression was observed for up to 21 days in culture. Scale bars represent 100µm.

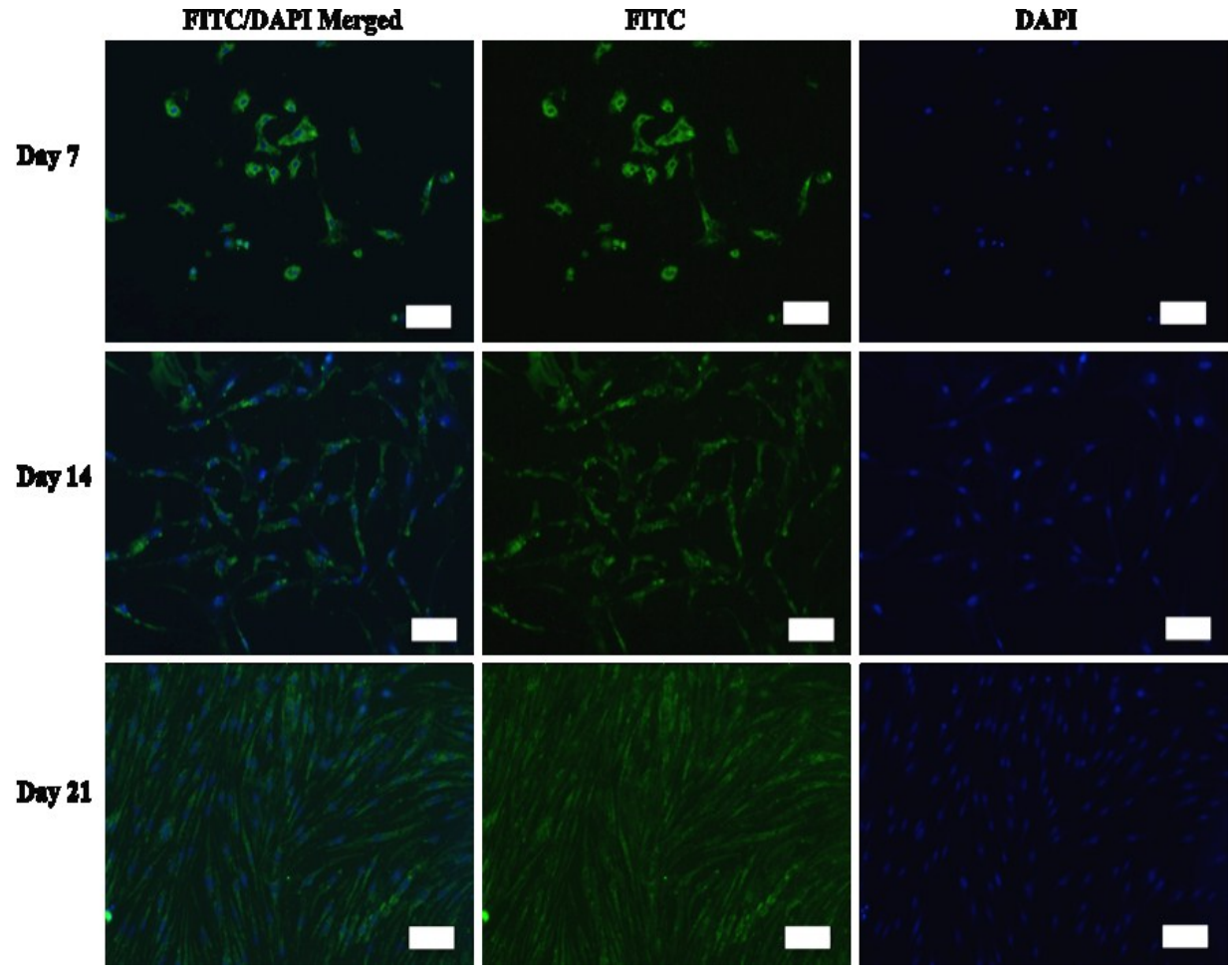

Figure 3:14 Long-term expression of 7D4 in unselected foetal cell populations. Sample H1177. Scale bars represent 100μm.

3.4.6.2 Cell Sorting by Fluorescence-Activated Cell Sorting (FACS)

Quantification of the STRO-1 positive and 7D4 positive fractions within the human foetal cell populations was analysed by FACS. Results were obtained following the analysis of 10,000 events (cells) to give plots of forward and side scatter as an indication of cell size and granularity respectively. The area P1, as shown in Figure 3:15, was determined to be the majority of the cell population and was gated to exclude any dead cells or debris. Isotype controls and labelled cells (shown in Figure 3:16) were analysed to give a cell distribution plot and for fluorescence. Cells were observed to cluster into two populations with the first population omitted from the gate in order to eliminate any potentially dead cells which would have taken up the dye. Calculations of STRO-1^{+} fractions in foetal cells before and after sorting are given in Table 3.2, and range from 0.2-12% of the cell population. Purities greater than 85% were achieved post sort.

Florescent images of the cells taken immediately after staining (Figure 3:17) confirm the small percentage population of STRO-1 and 7D4 positive cells. Images of the cells in culture immediately post sort (Figure 3:17) demonstrate the high percentage purity obtained following sorting, and following one day in tissue culture, the recovery of the cells as well as fluorescent signal expression.

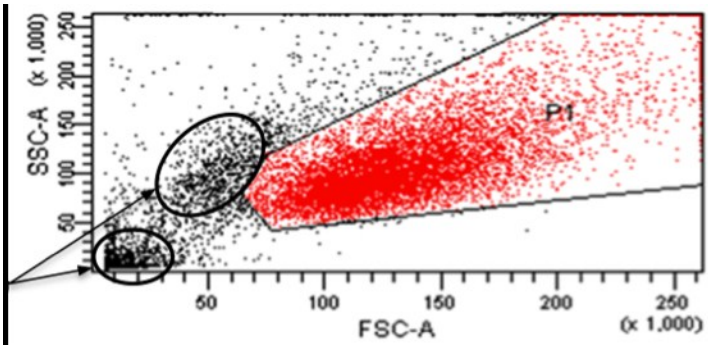

Figure 3:15 Flow cytometry scatter plot for unlabelled human foetal femur cells. The intensity of the right-angle light scatter or side scatter (denoting granularity) is plotted against the forward scatter (denoting size) for each cell. The marked area (P1) shows the gate for those cells to be analysed. Areas circled indicate cell debris and possible dead cell population excluded from analysis.

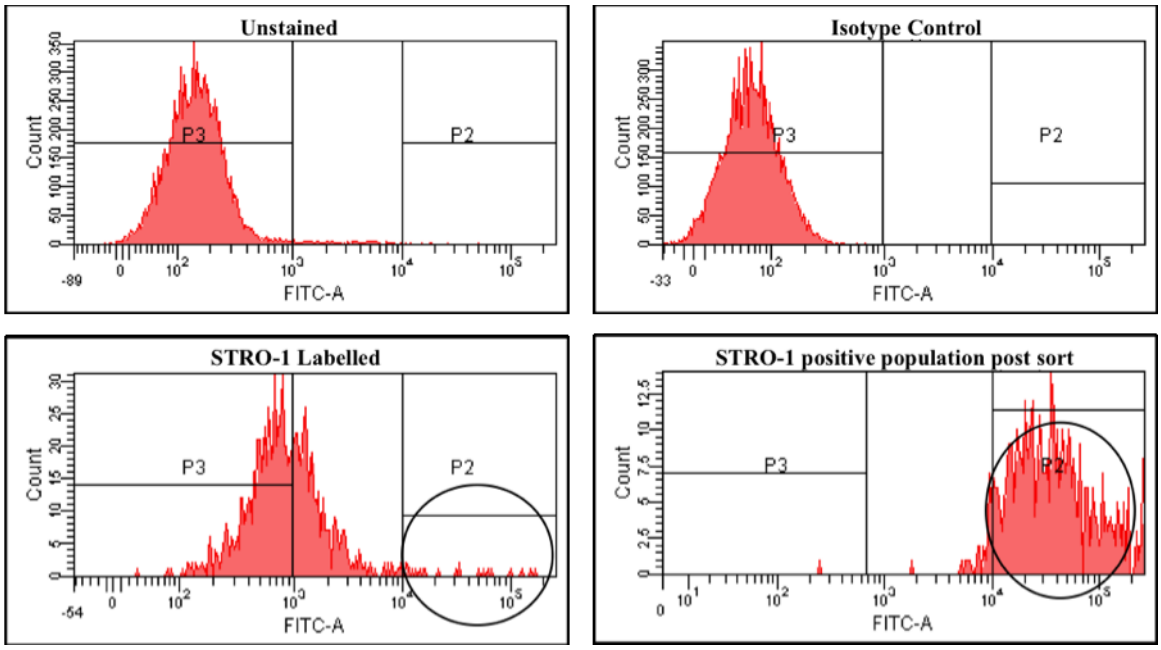

Figure 3:16 Example of histograms obtained showing fluorescent profile of unstained and isotype control (mouse IgM particles) cells, used in order to place the gates P2 and P3 (positive and negative cell fractions respectively). The plot of STRO-1 labelled cells are those prior to sort indicating approximately 5% of the total cell population based on the gate placed. The STRO-1 positive cells, post sort, show 95% purity with negligible contamination of the P3 population.

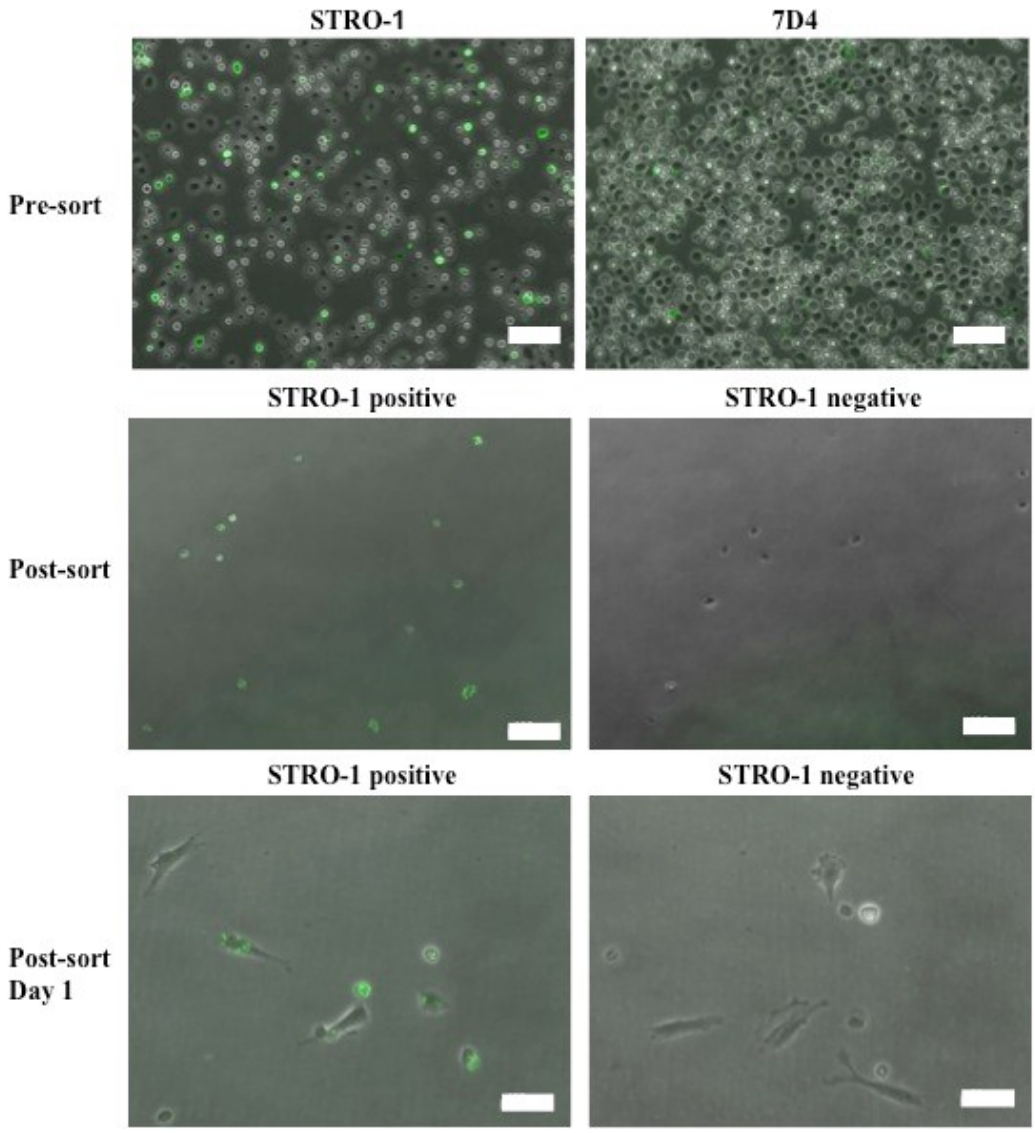

Figure 3:17 STRO-1 and 7D4 stained cells pre- and post- sort from a haemocytometer. Images were taken at day 1 post sort and confirmed a positive and viable cell population. Scale bars represent 100μm.

Sample	% STRO-1 positive	% 7D4 positive	% Purity post sort STRO-1	% Purity post sort 7D4
H1168	4.6	3.4	-	-
H1177	2.6	$< 1^{(*)}$	-	-
H1179	2.0	$< 1^{(*)}$	-	-
H1203	3.7	3.4	85.0	41.6
H1204	7.8	2.4	90.4	37.5
H1208	2.7	$< 1^{(*)}$	$96.2^{(**)}$	-
H1209	1.7	$< 1^{(*)}$	79.9	-
H1212	0.6	0.8	$75.7^{(**)}$	-
H1214	10.2	$< 1^{(*)}$	-	-
H1217	9.5	$< 1^{(*)}$	-	-
H1221	10.0	0.2	-	-
H1232	9.0	5.1	$99.7^{(**)}$	$94.2^{(**)}$
H1244	6.7	0.1	95.2	-
H1271	10.0	0.4	92.6	65.0
H1285	1.3	0.3	78.9	46.2
H1288	12.6	0.1	$98.7^{(**)}$	$50.3^{(**)}$
Average	**5.9**	**1.6**	**89.2**	**55.8**
St Dev	3.9	1.8	8.7	21.1

Table 3:2 FACS samples utilised, showing initial percentages of the STRO-1 and 7D4 cell fractions positively labelled and percentage purity obtained following sort. * although a percentage of less between 0-1% was recorded this matched, or was less than the isotype control levels and therefore no sorting was undertaken. ** indicates those cells which went through a two-fold purity sort process. – indicates those cells which were not successfully sorted.

Upon sorting cells were expanded in culture under basal conditions and grown to confluence before being utilised for immunocytochemistry, biochemical, molecular and growth kinetics studies. In culture, each of the sorted cell populations displayed the same fibroblastic morphology as the unsorted foetal femur cells (Figure 3:18). Similarly, growth in basal, osteogenic or chondrogenic culture conditions showed no significant differences in the cells morphology. Upon performing co-expression staining following 2 days in culture, positive staining for both STRO-1 and 7D4 (Figure 3:19) was observed irrespective of the cells previously being sorted as positive or negative for STRO-1 and 7D4.

Cells were then cultured for 7 days in basal, osteogenic and chondrogenic media conditions. Immunocytochemistry revealed the presence of both type I and type II collagen (Figure 3:20-3:22) in all three unsorted/sorted cell populations. Particularly strong type I and II collagen staining was observed in the STRO-1 positive cell population (Figure 3:21) cultured in basal media compared to the unsorted population (Figure 3:20). Strong staining of type I and II collagen was observed in the STRO-1 negative cell population (Figure 3:22). STRO-1 negative sorted cells showed weaker staining of type I and II collagen in both media conditions, with the exception of type II collagen staining in osteogenic conditions, which was the greatest of the three cell populations.

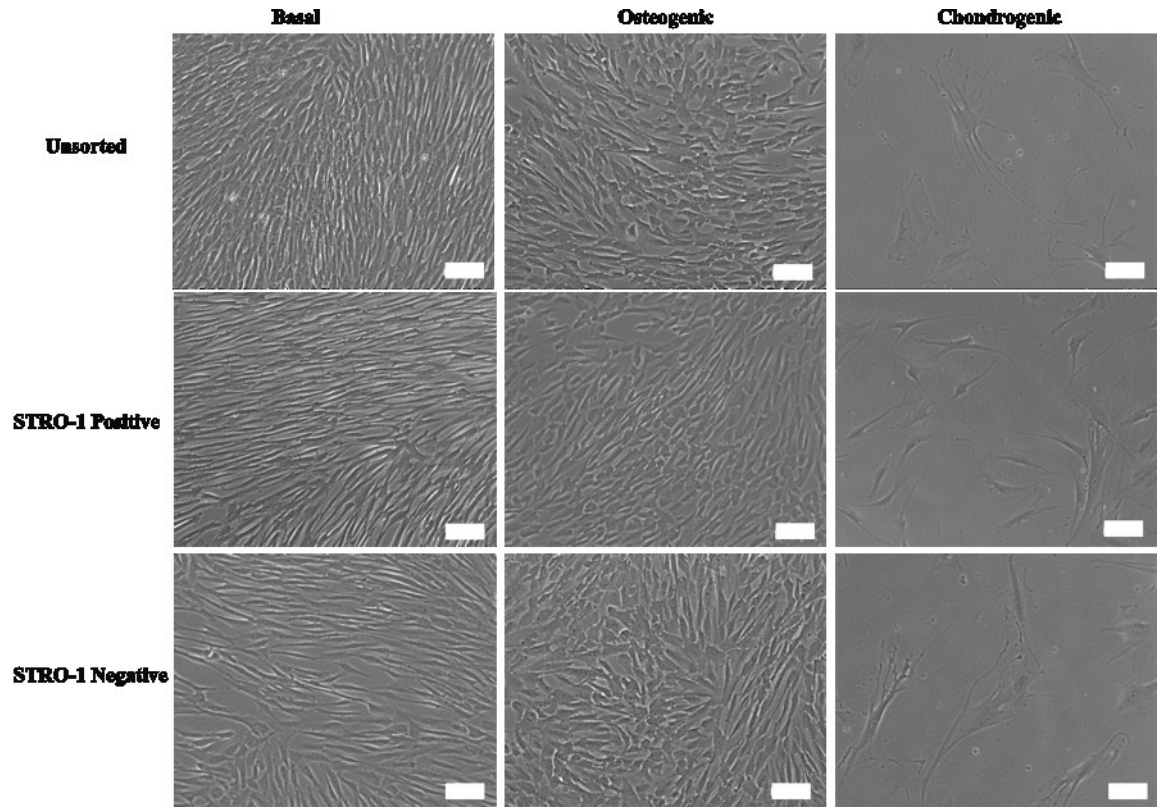

Figure 3:18 Following sorting, selected cells were expanded in culture and showed no difference in cell morphology across the groups. Scale bars represent 200μm.

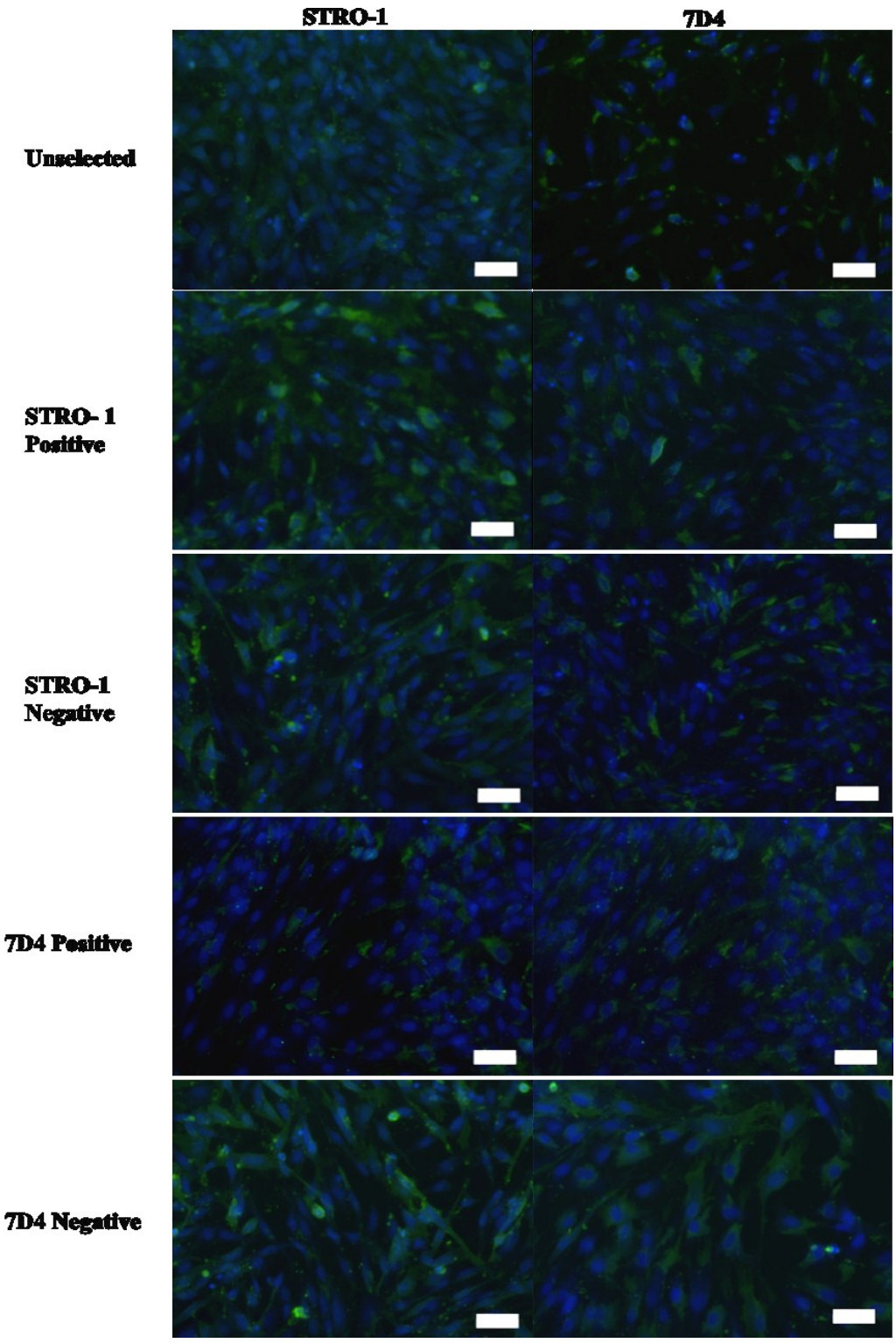

Figure 3:19 Co-expression staining of STRO-1 and 7D4 cells post sort and overnight culture. STRO-1 positive cells stained exhibited positive staining with 7D4, and equally 7D4 positive sorted cells exhibited positive staining for STRO-1. Scale bars represent 50μm.

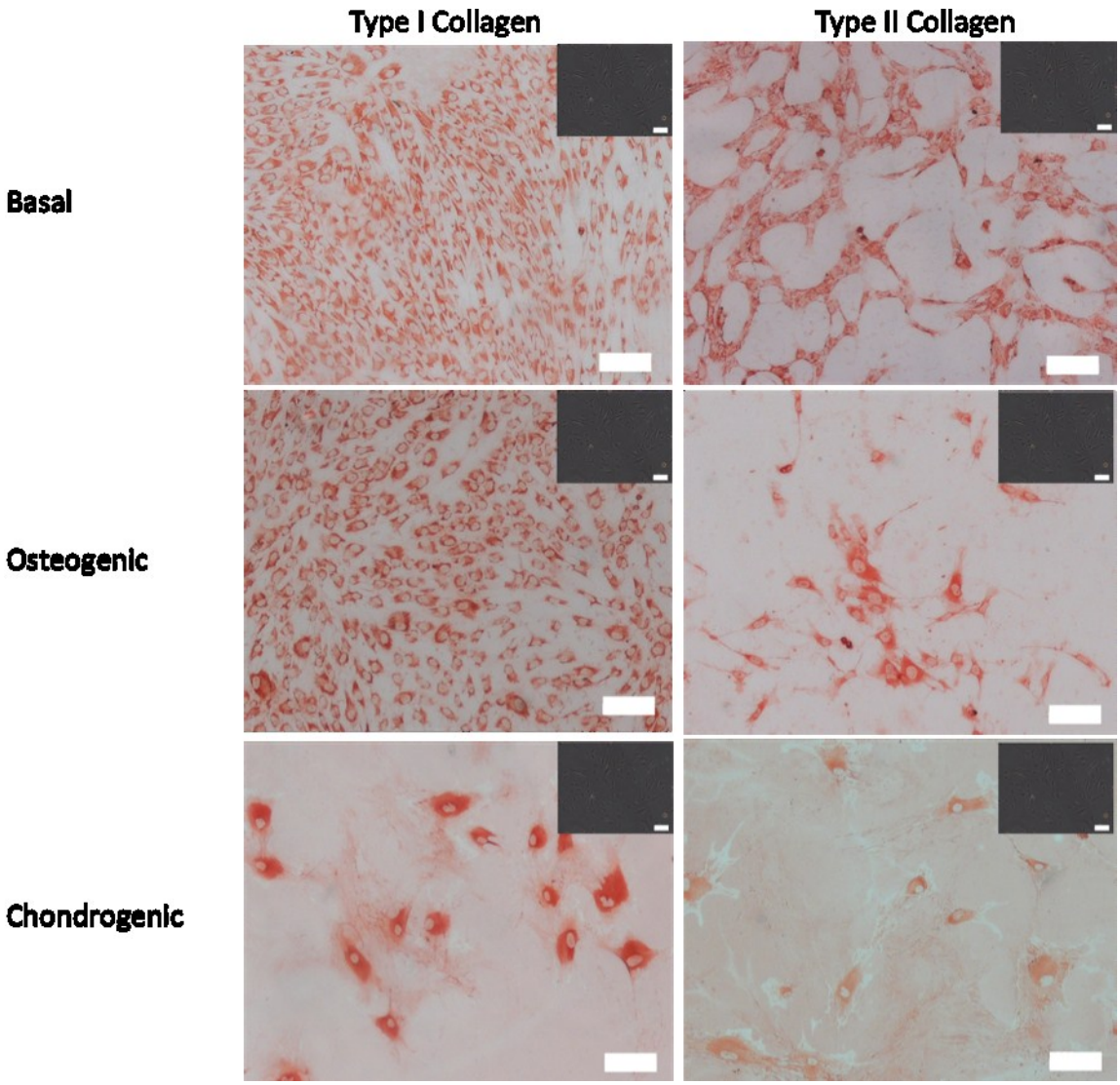

Figure 3:20 Unselected foetal cell population H1271 after 7 days in culture in basal osteogenic or chondrogenic media. Type I and II collagen staining using the AEC method with negative control cells shown in inserts. Scale bars represent 100μm.

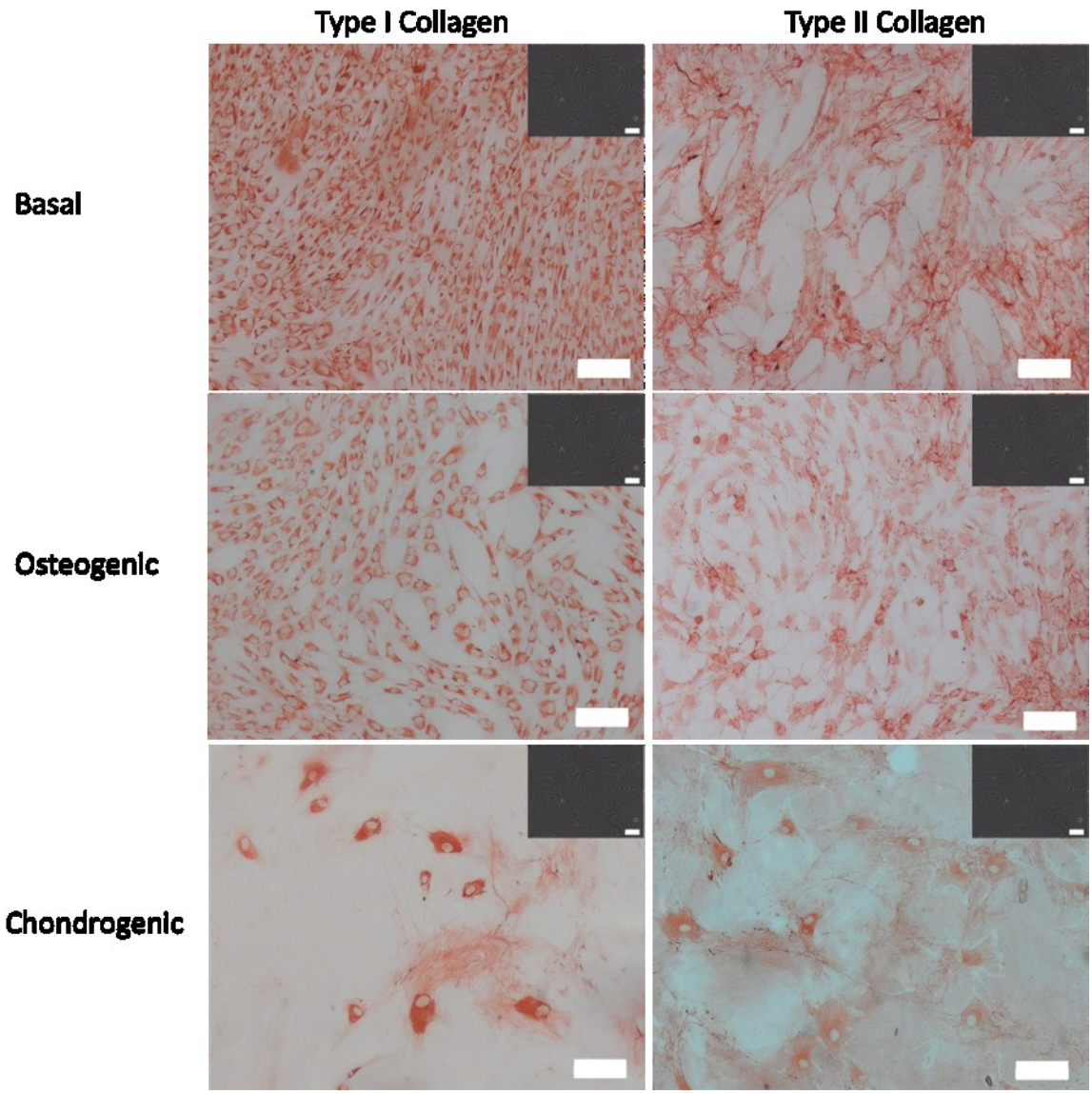

Figure 3:21 STRO-1 positive cell sorted foetal population H1271 after 7 days in culture in basal, osteogenic, or chondrogenic media. Type I and II collagen staining using the AEC method with negative control cells shown in inserts. Scale bars represent 100μm.

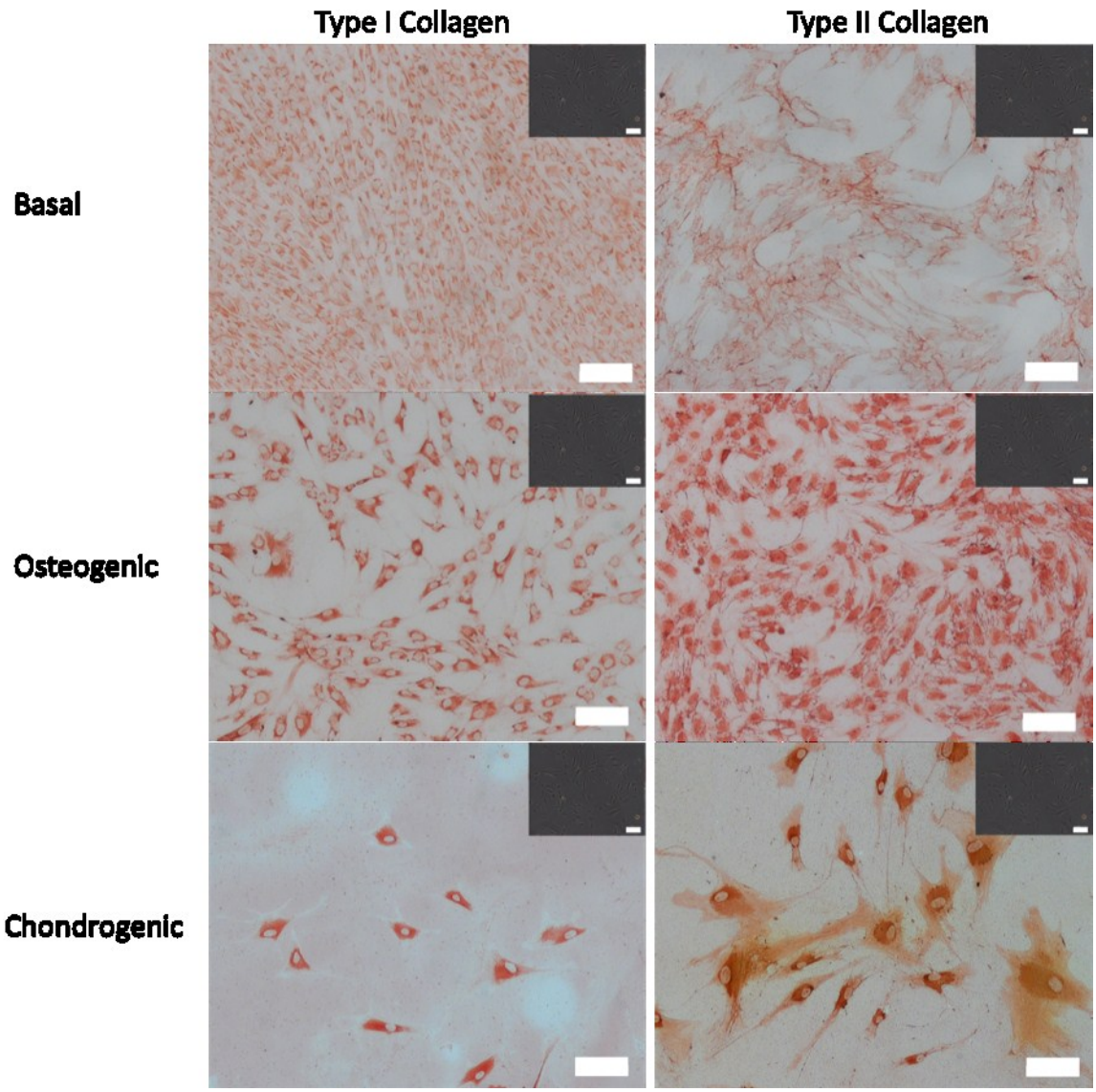

Figure 3:22 STRO-1 negative cell sorted foetal population H1271 after 7 days in culture in basal, osteogenic, or chondrogenic media. Type I and II collagen staining using the AEC method with negative control cells shown in inserts. Scale bars represent 100μm.

3.4.7 STRO-1 Population Doubling Time for FACS Populations

STRO-1 positive cells were observed to double every 19.86 ± 6 hours with no correlation observed with sample age. In contrast, unselected cells were observed to double every 21.4 ± 3 hours while the negative cell fraction was calculated to double every 22.4 ± 3 hours.

Collection No.	Age (WPC)	r^2 value	Doubling time (hrs)
H1203	7.5	0.9559	14.5
H1244	9	0.9970	16.07
H1271	8	0.9517	28.1
H1288	8.5	0.9958	20.8

Table 3:3 Population doubling times for STRO-1 positive selected human foetal femur-derived cells. Calculations derived from WST-1 assay results. Femur collection number shown with foetal age (weeks post conception), giving a population doubling time of 19.86 ±6 hours.

Collection No.	Age (WPC)	r^2 value	Doubling time (hrs)
H1203	7.5	0.9713	25.8
H1271	8	0.9570	18.6
H1288	8.5	0.9948	22.9

Table 3:4 Population doubling times for STRO-1 negative selected human foetal femur-derived cells. Calculations derived from WST-1 assay results. Femur collection number shown with foetal age (weeks post conception), giving a population doubling time of 22.4±3 hours.

3.4.8 Alkaline Phosphatase Specific Activity

Alkaline phosphatase specific activity was observed to double in the unselected cell populations, where basal conditions showed approximately 0.07 $nmol^{-1}$ μg DNA^{-1} hr^{-1} compared to 0.14 $nmol^{-1}$ μg DNA^{-1} hr^{-1} in the cells cultured in osteogenic conditions. A significant doubling of the alkaline phosphatase specific activity between the unselected and STRO-1 positively selected cells was observed (Figure 3:23), where the specific activity in the osteogenic cultured cell was 0.4 $nmol^{-1}$ μg DNA^{-1} hr^{-1}. A significant difference in expression between basal and osteogenic cells of all groups was observed. Equally, a significant difference was seen between the unselected and STRO-1 populations, as well as the STRO-1 positive and STRO-1 negative cell populations. Histological analysis confirmed the biochemical data shown in Figure 3:24.

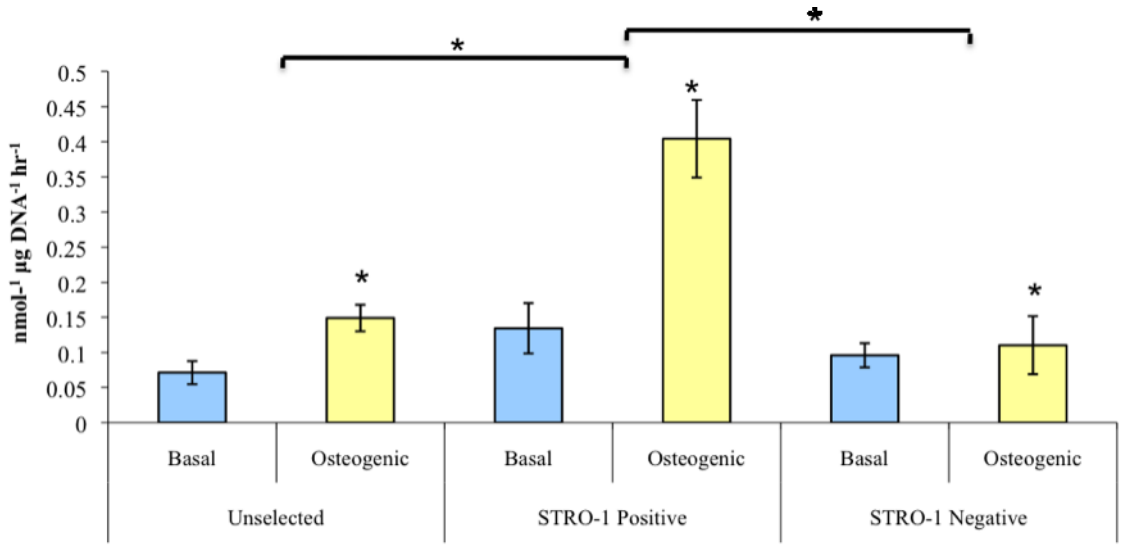

Figure 3:23 Alkaline phosphatase specific activity for unselected and STRO-1 selected cells. After 7 days in culture Sample H1271, 8 replicates. All values were expressed as mean ± standard deviation (SD). * depicts significance p<0.05.

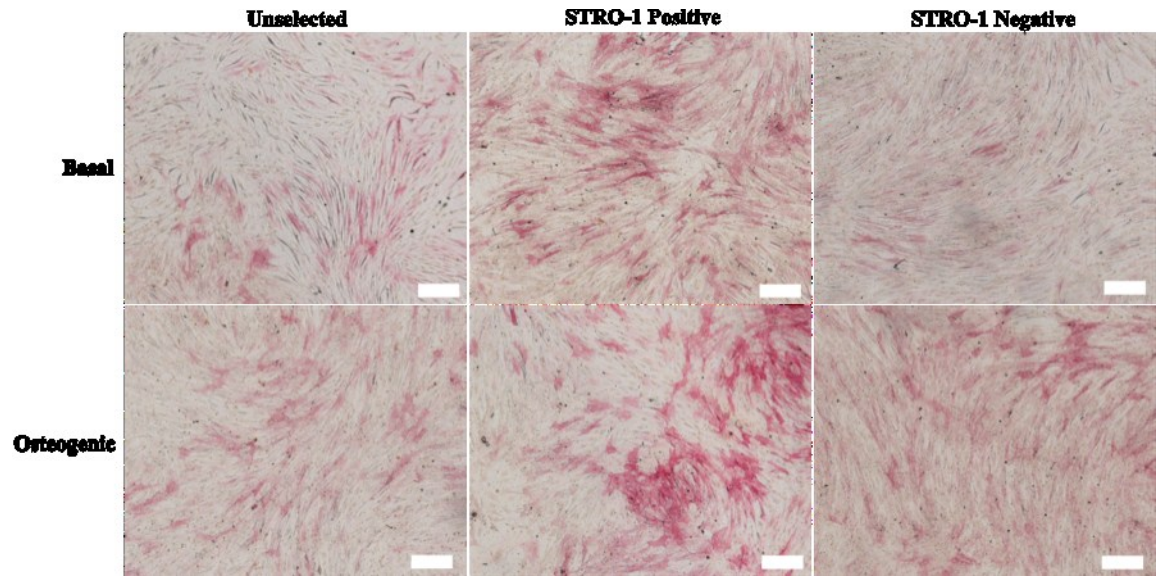

Figure 3:24 Alkaline phosphatase staining of unselected and STRO-1 positive and negative selected cells after 7 days in culture. Sample H1271. Scale bars represent 100µm.

3.4.9 Molecular Characterisation of Selected and Unselected Cell Populations

Following sorting and expansion in culture, cells were seeded at appropriate densities and grown for up to 21 days in basal, osteogenic and chondrogenic conditions. Samples were analysed at 7 and 21 days. The data presented represent, n=4 of the unselected cell population, n=3 of the STRO-1 positive FACS cells and n=2 of the STRO-1 negative FACS cells. Only 1 successful sort of 7D4 positive and negative cells was obtained giving n=1 and therefore this data will not be used but has been placed in appendix 2. The data set H1271 has been displayed here in order to demonstrate the trends seen across all sorted and unsorted cells.

The data has been split into two sections. The expression levels of the osteogenic markers alkaline phosphatase, osteocalcin and Runx-2 were measured, with type II collagen, SOX-9 and RUNX-2 again used as chondrogenic markers. The Ct values for Type I collagen were found to be equal to or greater than that of β-actin and therefore the expression levels of type I collagen could not be determined. This is likely to be due to the high levels of type I collagen produced by fibroblastic cells. Expression levels of the genes at days 7 and 21 for each media treatment group were compared. For statistical analysis, expression levels of the treatment groups were compared to the unsorted cell population as well as comparison between the STRO-1 positive and negative cell populations.

In basal conditions, alkaline phosphatase expression was significantly increased in both the STRO-1 positive and negative cell populations at day 7 and 21 (Figure 3:25). With a significant difference observed between the STRO-1 positive and negative cells. RUNX-2 expression also showed a significant increase in expression at day 7 of culture in the STRO-1 positive and negative cell fractions. However, by day 21 of culture, RUNX-2 expression was decreased in the STRO-1 positive cell fraction (Figure 3:25). Finally, of the osteogenic markers no significant change in expression was observed in day 7 or 21 of culture in the STRO-1 positive cell fraction (Figure 3:25). A significant increase in Type II collagen expression was observed at day 21 of culture, which was also significant in comparison to the STRO-1 negative cell population (Figure 3:26). Significant decreases in SOX-9 expression at day 7 and 21 were observed for both STRO-1 selected populations (Figure 3:26).

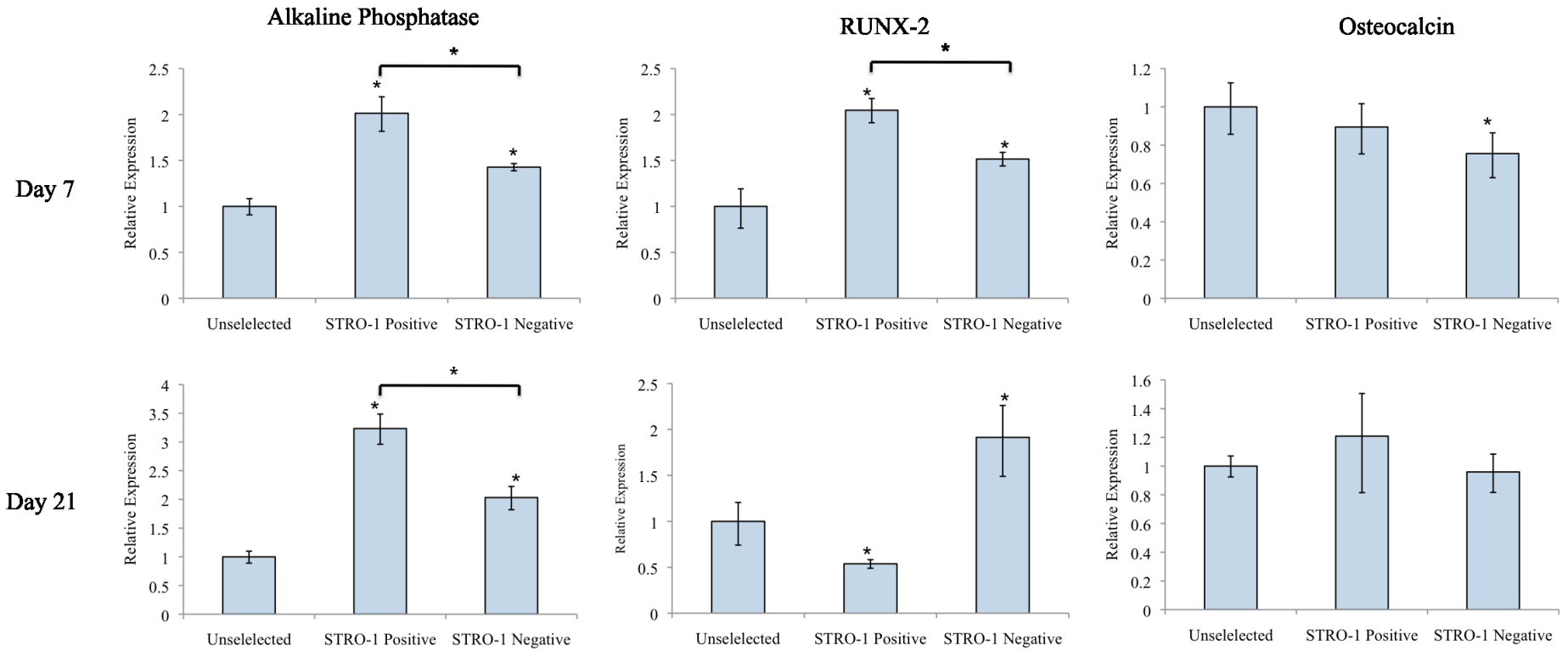

Figure 3:25 Unselected, STRO-1 positive and STRO-1 negative cell groups cultured in basal media. Expression levels were observed following 7 and 21 days in culture. Expression of osteogenic markers alkaline phosphatase, RUNX-2 and osteocalcin relative to β-actin. Relative expression of the sorted cell populations was calculated against unselected cells set at 1. * indicates significance $p<0.05$ relative to the unselected cell population, as well as between STRO-1 positive and negative cell populations.

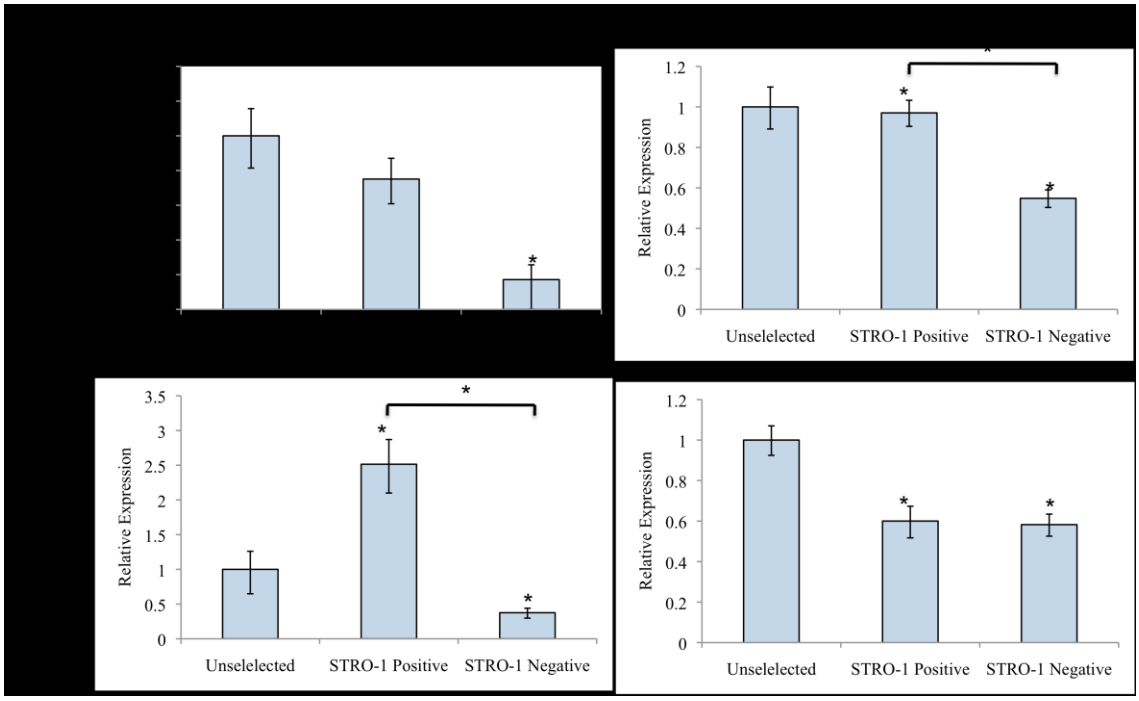

Figure 3:26 Unselected, STRO-1 positive and STRO-1 negative cell groups cultured in basal media. Chondrogenic markers, Type II collagen and SOX-9 expression relative to β-actin. Expression levels were observed following 7 and 21 days in culture relative to β-actin. Relative expression of the sorted cell populations was calculated against unselected cells set at 1. * indicates significance $p<0.05$ relative to the unselected cell population, as well as between STRO-1 positive and negative cell populations.

In osteogenic conditions, for alkaline phosphatase the greatest expression was observed in the STRO-1 positive sorted cell population with a significant increase at both day 7 and 21 of culture. By day 21 of culture alkaline phosphatase expression in the STRO-1 negative fraction had decreased compared to both the STRO-1 positive and unselected cell populations (Figure 3:27). RUNX-2 expression was found to be significantly higher in the STRO-1 negative cell population compared to the unselected and STRO-1 positive cell fractions, with this observed at both day 7 and 21 of culture (Figure 3:27). Osteocalcin expression was significantly decreased for both STRO-1 populations at both day 7 and 21 (Figure 3:27). Type II collagen in the STRO-1 positive population was increased more than two fold at day 7, with a two fold reduction in expression observed in the STRO-1 negative cell population. However, by day 21 of culture no significant changes in expression were observed across the three groups (Figure 3:28). Finally, SOX-9 expression was reduced approximately two fold in STRO-1 positive and negative cell populations at both day 7 and 21 of culture (Figure 3:28).

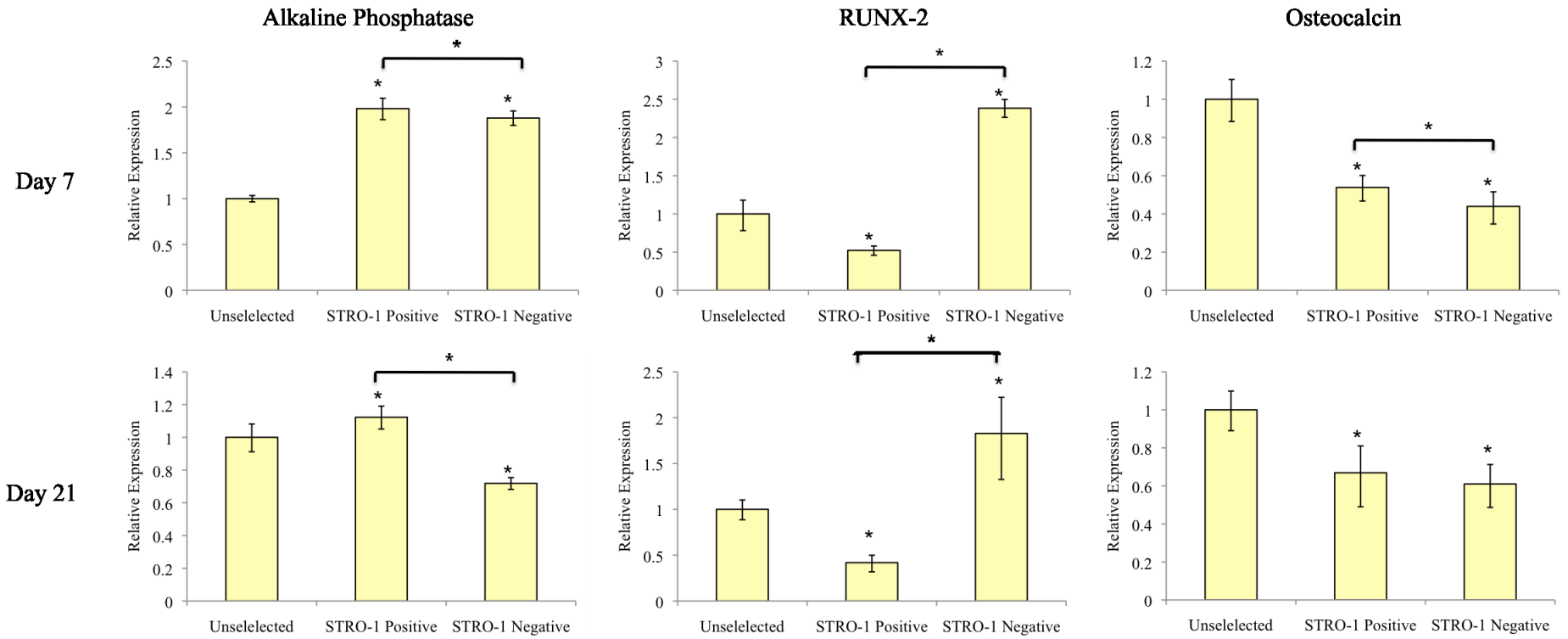

Figure 3:27 Unselected, STRO-1 positive and STRO-1 negative cell groups cultured in osteogenic media. Expression levels were observed following 7 and 21 days in culture. Expression of osteogenic markers alkaline phosphatase, RUNX-2 and osteocalcin relative to β-actin. Relative expression of the sorted cell populations was calculated against unselected cells set at 1. * indicates significance $p<0.05$ relative to the unselected cell population, as well as between STRO-1 positive and negative cell populations.

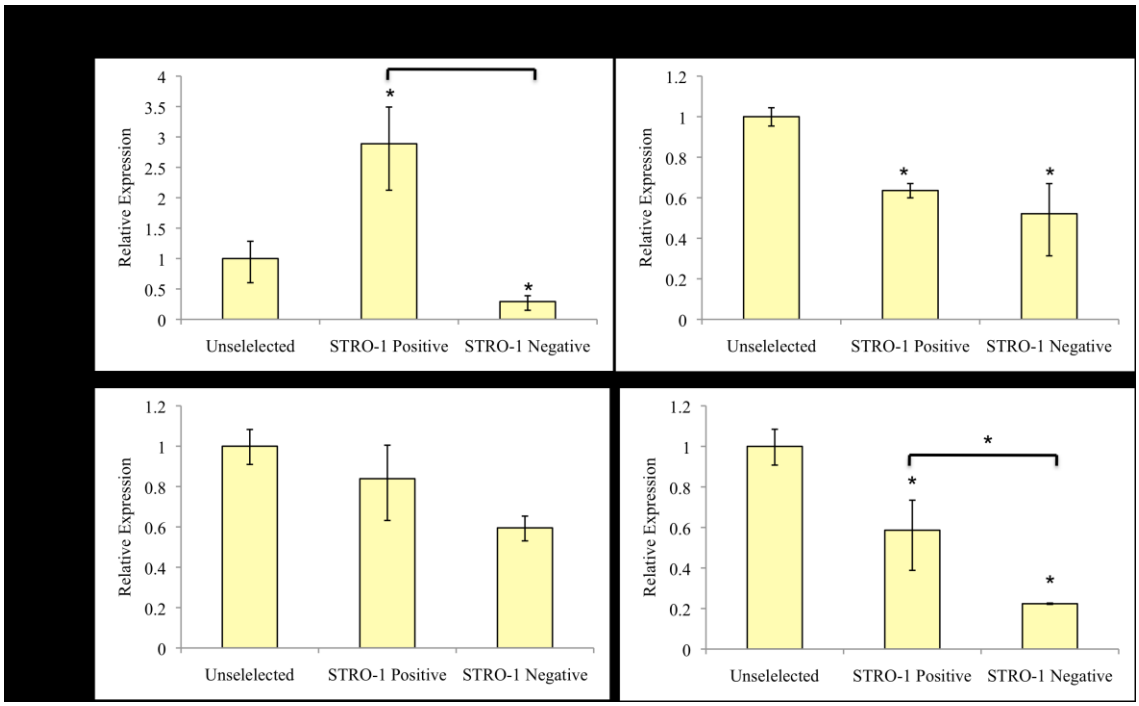

Figure 3:28 Unselected, STRO-1 positive and STRO-1 negative cells cultured in osteogenic media. Chondrogenic markers, Type II collagen and SOX-9 expression relative to β-actin. Expression levels were observed following 7 and 21 days in culture. Relative expression of the sorted cell populations was calculated against unselected cells set at 1. * indicates significance $p<0.05$ relative to the unselected cell population, as well as between STRO-1 positive and negative cells.

In chondrogenic conditions, alkaline phosphatase expression was observed to be greatest in the STRO-1 positive cell fraction. A significant difference was observed between the expression levels of the STRO-1 positive and negative cell populations at both time points of culture (Figure 3:29). RUNX-2 expression showed the greatest difference at days 7 and 21. At day 7, STRO-1 positive cells showed nearly a two-fold increase in expression, with expression levels minimal in the STRO-1 negative cell population. However, by day 21 of culture, the greatest expression was observed in the STRO-1 negative cell population whilst expression in the STRO-1 positive population remained comparable to the unselected cell population (Figure 3:29). Osteocalcin expression levels were observed to reduce in both the STRO-1 sorted cell populations compared to the unselected cells at both days 7 and 21 of culture (Figure 3:29). When determining the expression of chondrogenic markers, Type II collagen expression was observed to be significantly greater in the STRO-1 positive selected cell population compared to the STRO-1 negative cells, which displayed minimal expression at day 7. By day 21 of culture, expression levels of Type II collagen were comparable with not significant differences observed across the cell groups (Figure 3:30). Finally, SOX-9 expression showed the greatest increase in expression in the cells cultured in chondrogenic condition, a significant increase in expression was observed in the STRO-1 positive cell fraction at day 7 of culture (Figure 3:30). However, as with Type II collagen expression, SOX-9 expression levels at day 21 were comparable across the groups with no significant changes in expression observed.

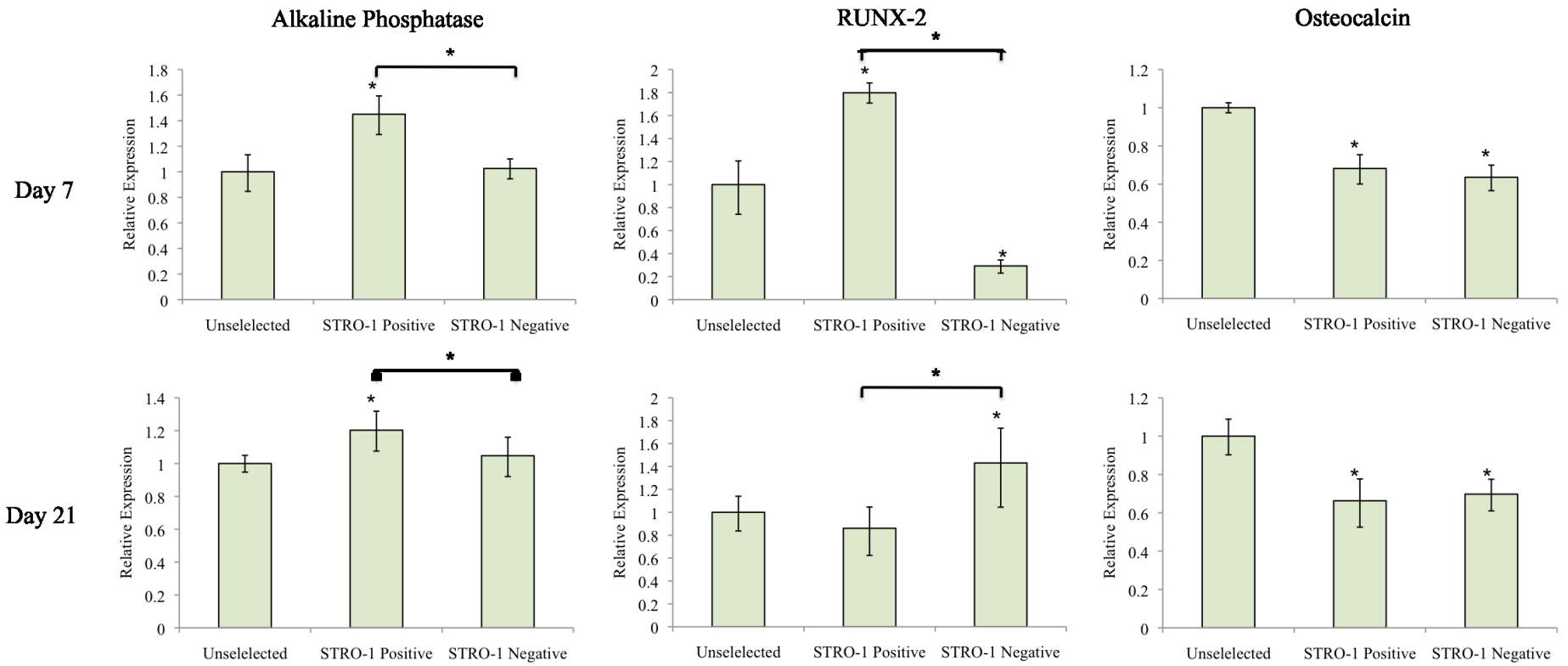

Figure 3:29 Unselected, STRO-1 positive and STRO-1 negative cell groups cultured in chondrogenic media. Expression of osteogenic markers alkaline phosphatase, RUNX-2 and osteocalcin relative to β-actin. Expression levels were observed following 7 and 21 days in culture. Relative expression of the sorted cell populations was calculated against unselected cells set at 1. * indicates significance $p<0.05$ relative to the unselected cell population, as well as between STRO-1 positive and negative cell populations.

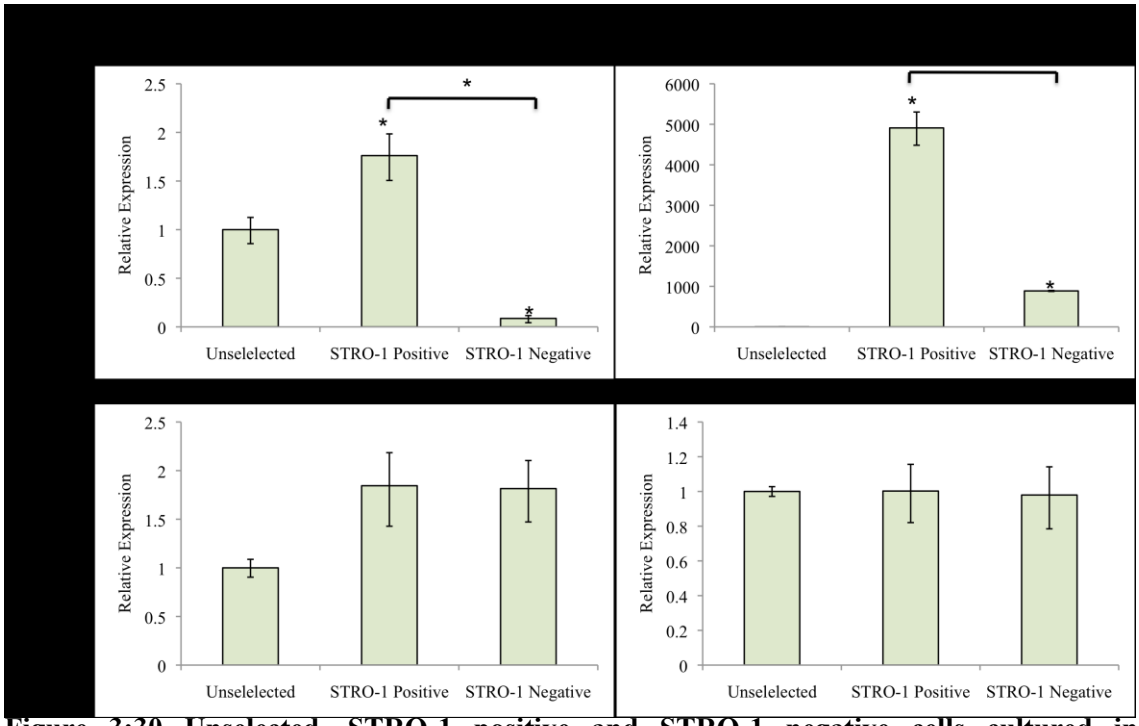

Figure 3:30 Unselected, STRO-1 positive and STRO-1 negative cells cultured in chondrogenic media. Chondrogenic markers, Type II collagen and SOX-9 expression relative to β-actin. Expression levels were observed following 7 and 21 days in culture. Relative expression of the sorted cell populations was calculated against unselected cells set at 1. * indicates significance $p<0.05$ relative to the unselected cell population, as well as between STRO-1 positive and negative cells.

3.5 Discussion

With an increasingly ageing population, the development of our understanding of embryonic stem cell and skeletal stem cell biology will be key in future reparative strategies. In order to develop successful tissue regeneration strategies, sufficient progenitor cell populations must be provided. These studies examined the phenotypic properties and differentiation strategies for the HUES-7 embryonic stem cell line (Cowan et al., 2004). This cell line shows similarities to other reported human ES cell lines, with a high ratio of nucleus to cytoplasm, prominent nucleoli, and compact colony morphology. The cells were found to be strongly positive for a number of molecular markers of pluripotency including, OCT 3/4, SOX-2, NANOG, TRA-1-60, SSEA-3 and alkaline phosphatase. Successful formation of EBs was also performed using the suspension culture protocol and culturing the cells in standard EB media (Kurosawa, 2007). The EBs were successfully cultured for 7 days in media, and although in non-adherent culture conditions, some adherence of whole EBs was observed. Further differentiation strategies and characterisation of EBs has been carried out in this series of studies and results are given in sections 4.3.1 and 4.4.

These studies examined the phenotypic properties for human embryonic stem cell populations and cells derived from the human foetal femur, collected at 7.5-12 weeks post conception. The isolation of cells from explant cultures and collagenase digest were both successful in expanding foetal femur-derived populations. Evaluation of the starting material revealed that those cells derived from the foetal femur included epiphyseal chondrocytes and were surrounded by a perichondrium/periosteum, which consisted of an outer fibroblastic layer and an inner layer of non-committed mesenchymal cells. Relatively small numbers of differentiated osteoblasts were present along the central diaphysis, as indicated by the presence of a thin bone collar. It is not known whether any cell type preferentially grew out from the explants, theoretically these cells could have been derived from the cut edges of the epiphysis (early chondrocytes) or from the perichondrium (fibroblastic or skeletal stem cells). Since the majority of the cell types present in the foetal femurs were epiphyseal chondrocytes, it is probable that the starting cells were early chondroprogenitor and mesenchymal progenitor populations. For cells obtained through collagenase digest it is expected that this will contain both chondroprogenitor and mesenchymal progenitor cell populations.

The multipotency of the human foetal femur populations was determined by the differentiation of the cells down the osteogenic, chondrogenic and adipogenic lineages. The culture of foetal femur-derived populations in the presence of dexamethasone, isobutyl methylxanthine (IBMX), insulin and indomethacin favoured adipogenesis, while culture in presence of TGF-β3 favoured chondrogenesis. The expression of alkaline phosphatase in confluent cultures of human foetal femur-derived cells would indicate a predominantly osteoprogenitor phenotype, as confirmed by both histological and biochemical analysis. The multipotential differentiation of femur-derived cells from 8–11 week post conception foetal tissue has been demonstrated (Mirmalek-Sani et al., 2005) with the observations confirmed by Cui and co-workers (2006). The multipotency of the foetal femur-derived cells suggests a population of skeletal progenitor cells able to differentiate as a result of external cues and/or factors.

These studies have established isolation protocols and examined the phenotypic properties for cell populations derived from human foetal femurs, collected at 8–11 weeks post-conception. Isolation from explants cultures, as demonstrated in adult-derived bone chips, was successful in expanding foetal femur-derived populations. Current approaches to isolate adult mesenchymal stem cells have centred predominately on the isolation and expansion of these early progenitors from adult marrow fibroblast populations (Bruder et al., 1997; Jaiswal et al., 1997; Kadiyala et al., 1997). This is in large part due to the low incidence, indeterminate morphology and undefined biochemical phenotype of the mesenchymal stem cell (Horwitz, 2002). The skeletal stem cell gives rise to a hierarchy of bone cell populations artificially divided into a number of developmental stages including; mesenchymal stem cell (MSC), determined osteoprogenitor cell (DOPC), preosteoblast, osteoblast and ultimately, osteocyte (Bianco et al., 2001; Friedenstein, 1976; Pittenger et al., 1999; Jiang et al., 2002; Verfaillie, 2002).

The suitability of human foetal femur derived cells as a model for the study of osteogenesis has previously been studied (Mirmalek-Sani et al., 2005). The use of modulatory agents to induce osteogenesis such as ascorbate and dexamethasone has been routinely described in the literature. The molecular data obtained in these studies further support the use of these agents for the purpose of osteogenic differentiation. Ascorbate has been demonstrated to have a proliferative effect in cultures of MG-63

cells (an osteoblast-like osteosarcoma cell line) (Takamizawa et al., 2004). Enhanced osteogenesis has been reported by a number of groups, following the use of ascorbate at 100μM in basal medium together with dexamethasone at 10nM (Jaiswal et al., 1997; Beresford and Owen, 1998). This effect also observed in the foetal femur-derived cell populations with significantly increased alkaline phosphatase activity and type I collagen expression (Mirmalek-Sani et al., 2005). Another known osteoinductive agent, bone morphogenetic protein-2 (BMP-2), has been used to promote new bone formation (Wozney and Rosen, 1998). The effects of BMP-2 on increasing human skeletal cell proliferation has also be demonstrated (Akino et al., 2003).

Although derived from the cartilaginous anlage of femur tissue at 7.5–12 WPC, foetal femur-derived cells displayed an osteoprogenitor phenotype with expression of type I collagen, alkaline phosphatase and STRO-1 in basal culture conditions. The maintenance of STRO-1 expression in foetal femur derived cells at 21 days and over passage confirms the presence of a progenitor cell sub-population of within the culture that maintains its phenotype. In contrast, in adult-derived cultures a loss of expression has been observed after 14 days of culture and following passage (Shi et al., 2002, Simmons and Torok-Storb, 1991a, Simmons and Torok-Storb, 1991b, Stewart et al., 1999).

Histological and molecular analysis indicated that the foetal femur-derived cells displayed an undifferentiated skeletal phenotype rather than a cartilaginous phenotype with expression of type I collagen and STRO-1 in explant/collagenase digest cell cultures. The maintenance of STRO-1 and 7D4 expression in foetal femur derived cells for up to 21 days in culture, confirms a sub-population of progenitor cells within the foetal femur with a capacity to maintain their phenotype. In human bone marrow cultures, it has been shown that STRO-1 is maintained up to 14 days in culture (Simmons and Torok-Storb, 1991b, Stewart et al., 1999, Shi et al., 2002). Gronthos and co-workers (1994) found that the heterogeneity of the stromal cell population could be reduced by isolation using the monoclonal antibody STRO-1, which recognises a trypsin-resistant cell surface antigen present on a sub-population of bone marrow cells. Although the epitope for STRO-1 remains to be characterised, the cells expressing STRO-1 have been found to include predominantly the adherent, high growth potential, colony forming units-fibroblastic (CFU-F). It is known that the antibody does not bind

to myeloid cells, megakaryocytes or macrophages (Gronthos et al., 1994). In human bone marrow cell populations, STRO-1 positive cell populations demonstrated delayed onset in mineral formation, and reduced capacity for the development of mineralised bone tissue over time. Additionally the STRO-1 positive cells lacked expression of markers typically associated with mature bone cells such as bone sialoprotein and osteocalcin (Gronthos et al., 1999). Cell surface expression of the STRO-1 and alkaline phosphatase antigens was assessed using human bone marrow cells sorted using FACS. Cells expressing the STRO-1-/ALP+ and STRO-1-/ALP- phenotypes appeared to represent fully differentiated osteoblasts, while the STRO-1+/ALP+ subset represented an intermediate preosteoblastic stage of development (Gronthos et al., 1999).

The 7D4 antibody was used to recognise chondroprogenitor populations within the human foetal femur. 7D4 recognises novel sulphation motifs in chondrotin sulphate chains of versican. Versican performs a functional role during early events of limb skeletogenesis as it is essential for pre-cartilage aggregation and subsequent cartilage differentiation (Williams Jr et al., 2005). Although positive staining for STRO-1 was observed in culture, staining was not observed in the whole foetal femur, although expression was observed from cells from explants as early as day 1 of culture and maintained for 3 days and beyond. However, 7D4 expression in whole sections of the foetal femur was observed in the hypertrophic, pre-hypertrophic chondrocytes and the proliferative zones.

The long-term expression of STRO-1 and 7D4 could only be determined to 21 days as monolayer cultures detached from tissue culture surfaces, even with the lowest possible seeding concentration at day 0. The expression of the STRO-1 positive cell fraction was found to comprise 5.9% of the foetal femur-derived cell population in the samples examined. In contrast the STRO-1 positive cell fraction was found to equate to 10% of the bone marrow mononuclear cells (Simmons and Torok-Storb, 1991b). Expression of the 7D4 positive cell fraction was determined as 1.6% of the cell population. Due to the high standard deviation observed for both STRO-1 and 7D4 positive cells in the foetal femur populations, a larger sample set would be needed to reduce the standard deviation observed. Within the STRO-1 positive cell fraction, positive staining for 7D4 was observed and equally the 7D4 positive cell fraction staining positive for STRO-1. This would suggest one of two things about the sorted cell populations i) the presence of a

sub-fraction of cells which express either STRO-1 or 7D4 or ii) a common subset of cells exist which express STRO-1 and 7D4.

A study by Yang and colleagues, (2007), observed only 0.5% of cells were STRO-1 positive in dental pulp cells, which was lower than the 9% positive population exhibited in other studies. The authors hypothesized that this low number may be the result of the cell population sorted from the complete primary cell culture rather than from the single-colony-derived cell populations. Compared with clonogenic methods, which necessitate visual inspection and personal selection (Gronthos et al., 2002), FACS requires a relatively standardized skill and can be more helpful to isolate a stable and homogeneous population (Yang et al., 2007). Further, they suggested the very low percentage of STRO-1 positive cells could be due to the long time in primary culture before selection was applied (Simmons and Torok-Storb, 1991b, Yang et al., 2007). However, expression of both STRO-1 and 7D4 was shown for up to 21 days in culture, so this reasoning would not explain the low percentages observed in these studies. On the other hand, differences in the primary cell population as suggested by Yang and colleagues (2007) may be the reason for the variation in STRO-1 positive and 7D4 positive percentage observed.

Examination of the cell proliferation rates indicated a doubling time 21.37±2.5 hours for the human foetal femur-derived cells. The population doubling time of the STRO-1 positive sorted cells was observed to be 19.86 ±6 hours and the STRO-1 negative portion 22.4±3. These doubling times are comparable to the observed times for unsorted foetal femur-derived cells. The literature has found the doubling time of human embryonic stem cells to be 24-48 hours, dependent and individual for each clonal line (Cowan et al., 2004; Park et al., 2004) and indicates that these times are comparable with the doubling times recorded for the foetal cells. Suva and colleagues (2004) calculated the mean doubling times of adult stromal cells at 2.1 days (range 1.6–6.7 days), independent of age, with a sample range of 27–81 years (mean patient age of 59 years). Further studies would be needed in order to verify the doubling time calculated here, for example, growth in serum replacement media to allow a better comparison with the ES cell lines. However, foetal cells clearly have faster doubling time than human ES cells and adult stromal cells and therefore act as a good half way model for the study of skeletal cell differentiation.

FACS was used to derive STRO-1 positive and negative cell populations. Although cell sorting was achieved with 80% purity or greater, following return to culture, and staining of the cells, positive staining of STRO-1 and 7D4 was observed in the negatively sorted cell populations. Gronthos and colleagues, (1999), using FACS sorting of STRO-1 and alkaline phosphatase positive and negative groups in human bone marrow cells, found that those cells which had initially lacked any cell surface expression of STRO-1 and alkaline phosphatase, were subsequently found to express alkaline phosphatase. Similarly, STRO-1 and alkaline phosphatase positively stained cells, were later found to lose expression of STRO-1 following re-culture. It would be expected that the cells contained in the STRO-1 negative cell fraction, would represent the remainder of cells in the population, which show a more differentiated phenotype. The onset of STRO-1 and 7D4 expression in culture, following sorting, may imply plasticity in cell development. Cell culture factors such as media volume, percentage foetal calf serum, incubation time and seeding density have been suggested to either reduce or increase the expression of STRO-1 (Thomas, 2008). This may contribute to the molecular differences observed as well as the lack of expression of STRO-1 seen in the whole foetal femur.

Molecular analysis indicated that the foetal femur-derived cells displayed an undifferentiated skeletal phenotype rather than a cartilaginous phenotype as suggested by the expression of alkaline phosphatase expression in basal conditions, while culture in osteogenic conditions resulted in expression of osteocalcin. A significant increase in alkaline phosphatase expression was observed in osteogenic conditions at both days 7 and 21 of culture. This was observed in the positively sorted cell fraction, as well as the negatively sorted fraction compared to the unsorted cell population. However, a significant difference in expression was observed between the positively and negatively sorted fractions. Osteogenic precursors are known to be present in the STRO-1 positive fraction of human bone marrow, and expression of alkaline phosphatase provides an early indication of osteogenic differentiation (Walsh et al., 2000).

A significant loss in type II collagen expression was observed in the majority of STRO-1 negative cells in all media conditions. Higher expression levels were recorded in the STRO-1 positive fractions in both osteogenic and chondrogenic conditions at day 7 of culture. The expression of type II collagen in the STRO-1 positive fraction is consistent

with the data presented by Simmons (1991b) and suggests that the STRO-1 fraction has predominantly osteogenic propensity. An increased expression of type II collagen by STRO-1 positive populations has also been demonstrated by Yu and colleagues (2010) in dental pulp stem cells.

As osteocalcin is used as a marker of more mature bone cells, the decreased expression observed in the sorted cell populations compared to the unsorted cell population, may be explained by the presence of progenitor cells in the STRO-1 positive cell fraction. It would be anticipated that the STRO-1 negative cell fraction consists of a more differentiated cell population, since a proportion of the progenitor cell population is removed by FACS. Thus, a decrease in osteocalcin expression would not be expected in comparison to the unsorted cell population. RUNX-2 expression in all conditions showed the same pattern with increased expression at day 7 of culture compared to the unsorted cell population, which was decreased by day 21 of culture. RUNX-2 is an important transcription factor necessary for osteoblast differentiation and bone formation and is an early osteoblastic marker. Gain-of-function studies in chick embryos suggest that osteochondroprogenitor differentiation proceeds via a balance of SOX-9 and RUNX-2 levels, where higher SOX-9 levels lead to chondrogenesis and higher RUNX-2 levels lead to osteogenesis (Eames et al., 2004). SOX-9 is required in several successive steps of the chondrocyte differentiation pathway during endochondral bone formation *in vivo*. SOX-9 is needed for the commitment of undifferentiated mesenchymal cells to a cell type that is both a chondroprogenitor and an osteoprogenitor and later in the differentiation process is needed for differentiation and proliferation of chondrocytes (Akiyama et al., 2002). Since, Sox-9 expressing cells are said to mark osteochondroprogenitor cells (Kawakami et al., 2006), the increase in SOX-9 expression observed in the STRO-1 positive fraction would support this. SOX-9 expression levels followed a similar pattern to Runx-2 with the exception of chondrogenic conditions at day 7 where an increase in expression was observed in the positive and negative STRO-1 cell fractions, corresponding with the high SOX-9 expression levels needed to lead to chondrogenesis (Eames et al., 2004).

Walsh and colleagues (2000) suggested a time dependent expression of STRO-1 which is related to bone function and differentiation, and therefore would suggest an implication in the development of the cells. The similarities seen in the expression

patterns of the STRO-1 positive and negative cells could be due to the presence of a progenitor cell population in the negative fraction, following expression of STRO-1 in these cells. This temporal expression would also explain the positive staining of STRO-1 and 7D4 in the negatively sorted cell fractions following re-culture.

In summary these studies have demonstrated the foetal femur-derived cell population to be a valid model for the studies of differentiation of the cells toward skeletal lineages. The multipotentiality of the cells has been demonstrated using typical bone and cartilage differentiation factors. Most significantly the isolation and culture of the STRO-1 positive cell population has revealed the cells have an osteogenic propensity, with increased alkaline phosphatase specific activity for STRO-1 positive cells compared to the unselected cell fraction.

In order to develop these studies further, molecular characterisation of the 7D4 positive and negative cell fractions would establish if these cells demonstrate a chondrogenic propensity. As yet it is unclear if the 7D4 positive and STRO-1 positive populations are distinct or have proportions of cells within the population, which express both antigens. Additionally, CD146 (cluster of differentiation 146) also known as the melanoma cell adhesion molecule (MCAM), is a cell adhesion molecule currently used as a marker for endothelial cell lineage. However, CD146 has been identified as a marker for skeletal progenitors (Sacchetti et al., 2007). Using the same studies presented here, determination of the percentage of CD146 positive cells in the foetal femur derived population and their potential for differentiation toward bone and cartilage could be determined in parallel to the STRO-1 and 7D4 studies. Determination of the relative proportions of each of the markers would add a further dimension to the characterisation studies of the foetal femur cells.

Chapter 4 Differentiation of human embryonic stem cells towards the osteogenic and chondrogenic lineages

4.1 Introduction

4.1.1 Embryonic Stem Cell and Foetal Femur-Derived Cell Differentiation

Various groups have performed studies looking at the multipotentiality of foetal derived stem cells. Thus, the multilineage potential of foetal cells derived from the foetal femur has been demonstrated (Mirmalek-Sani et al., 2005), as well as foetal cells at 14 weeks post conception (WPC). Campagnoli et al (2001) observed an increased proliferation rate of the foetal cells compared to adult marrow populations. The studies performed successfully demonstrated the differentiation potential of the derived cells toward the osteogenic, chondrogenic and adipogenic lineages.

Similarly, strategies for the differentiation of human ES cells and EB formation have been described in detail in section 1.3.4 and summarised in Table 1:2. A typical differentiation approach is the formation of embryoid bodies (EBs). EBs are cell aggregates that are formed naturally when embryonic stem cells are grown in non-adherent cell culture conditions, the growth of which mimics a number of the stages involved in the developing embryo. Culture of ES cells using EBs results in the formation of cells of the three embryonic germ layers and EBs have been used as the ES cell source in a number of differentiation experiments (Kawaguchi, 2006, Kawaguchi et al., 2005, Khoo et al., 2005). Extensive reviews of the strategies which can be taken for EB formation are given by Itskovitz-Eldor and Schuldiner (2000) and Kurosawa (2007). The formation of cardiomyocyte cells (Burridge et al., 2007), as well as differentiation toward the osteogenic lineage (Cao et al., 2005, Heng et al., 2004, Bielby et al., 2004) has been reported using EB formation approaches.

To date few studies have been performed utilising co-cultures of foetal and embryonic stem cell populations as a differentiation strategy. Buttery et al (2001) utilised calvarial osteoblasts from foetal mice and co-cultured these with mouse cells dissociated from embryoid bodies on transwell inserts. Differentiation towards the osteoblast lineage was characterised by the formation of bone nodules within an extracellular matrix of type I collagen and osteocalcin. The cells grown in co-culture displayed a 5-fold increase in the number of nodules formed in comparison to cells cultured in the absence of a foetal layer. Using human undifferentiated ES cells, Bigdeli and colleagues (2009), co-cultured ES cells with irradiated neonatal or adult articular chondrocytes in (high-

density) pellet mass cultures for 14 days. The co-cultured ES cells were then expanded on plastic and their differentiation potential along the chondrogenic, osteogenic and adipogenic lineages compared to that of the undifferentiated ES cells. The authors demonstrated that the co-cultured ES cells could be expanded on plastic with a morphology and expression of surface markers similar to SSCs.

As for adult differentiation along the osteogenic and chondrogenic lineages, the differentiation factors used for the promotion of osteogenic differentiation of ES cells are typically, ascorbate-2-phosphate, dexamethasone and BMP-2, and for chondrogenic differentiation, ascorbate-2-phosphate, dexamethasone, ITS and TGF-β_3.

Dexamethasone is a synthetic glucocorticoid shown to enhance differentiation of osteogenic cells from precursor cells, such as ES cells and adult stem cells. Dexamethasone has been show to enhance cell growth as well as the induction of alkaline phosphatase activity (Coelho and Fernandes, 2000), and to promote osteogenic differentiation and maturation (Walsh et al., 2001).

Ascorbic acid 2-phosphate (ascorbate) combines the phosphorous component of β-glycerolphosphate to produce a stable and long acting derivative of ascorbic acid (vitamin C) has proved a relevant substitute to ascorbic acid. Ascorbate is an enzyme cofactor activity important for collagen synthesis and has been used in various *in vitro* cultures of bone cell studies (Takamizawa et al., 2004). For promotion of osteogenic differentiation in foetal cell populations, Jaiswal et al (1997), routinely used the combination of ascorbate and dexamethasone.

Bone morphogenetic proteins (BMP) have been shown to induce osteogenic differentiation and subsequent tissue mineralisation as detailed in 1.11.1. BMPs are a member of the transforming growth factor beta superfamily. Polypeptides belonging to this family function as morphogens by mediating physiological processes such as cell growth and differentiation, tissue morphogenesis and regeneration, immune response, hormonal mechanisms and bone induction. BMP 2, 4 and 7 have been shown to play a critical role in bone formation and bone healing (Lieberman et al., 2002).

TGF-β3 is part of the TGF-β superfamily, members of which play an important role in physiological and pathological processes. TGF-βs are expressed ubiquitously by a wide variety of cell types, including bone and soft tissue. TGF-β_3 in particular has been found to be involved in bone formation. Bone formation can be achieved earlier by co-delivery of BMP-2 and TGF-β_3 in contrast to delivery of BMP-2 or TGF-β_3 individually, suggesting that TGF-β_3 interacts synergistically with BMP-2 during the formation of bone. However, the role of TGF-β_3 in osteogenesis remains limited (Hao et al., 2008). TGF-β superfamily has been acknowledged to be one of the most effective for chondrogenesis in vitro, while TGF-β_3 has been observed to be upregulated in dedifferentiated human chondrocytes (as reviewed in Hao et al (2008)).

4.1.2 Organotypic Culture

EBs provide an effective 3-D culture system for the differentiation of ES cells along the embryonic germ lineages. Differentiation of human bone marrow cells toward the cartilage lineage has also been performed using a 3-D pellet system (Tare et al., 2005). The organotypic culture system provides an alternative 3-D culture model. In this model, cells are cultured at a liquid-air interface in an environment that mimics in part that *in vivo*. Typically, this protocol is utilised for the culture of whole tissue sections and has been adapted for the culture of cells. Gahwiler (1981) updated the classic organotypic model for the culture of hippocampal slices. Stoppini et al (1991) used explanted tissues on a culture insert containing a semiporous membrane and maintained the tissue at an air–liquid interface within a small drop of fluid. The cultures were fed by medium on the underside of the membrane.

This same organotypic model has also been applied to drug screening, Pringle and colleagues have used the culture system to detect novel neuroprotective compounds (Pringle et al., 2003). Furthermore, Benbrook and colleagues (2006) cultured tumour cells in the organotypic model as *in vitro* representation of the tumour microenvironment.

The organotypic cell model has been applied to a variety of cell types. Stark et al (1999) have used organotypic co-cultures to cultivate normal epidermis from keratinocytes. A novel organotypic model has also been established for the human endometrium, in

which primary epithelial cells retain their steroid hormone responsiveness (Blauer et al., 2005).

The work in this chapter details a novel *ex vivo* organotypic culture model that has been designed to mimic at least in part, the 3-D skeletal tissue architecture through representative cell-cell and matrix interactions traditionally found only in *in vivo* models of skeletal tissue. Moreover, the potential of the co-culture system as a tissue-engineering model has also been assessed.

4.1.3 Aims

The aims of these current studies were,

- To differentiate HUES-7 ES cells via an embryoid body step toward the mesoderm lineage.
- To differentiate the human ES cells using foetal femur-derived cell conditioned media along the mesoderm/osteogenic lineage.
- To determine the differentiation potential of the foetal and embryonic cells in a 2-D co-culture culture system.
- To establish a 3-D model by which embryonic and foetal cells could be grown in a co-culture system to promote the differentiation of the cells toward bone and cartilage

4.2 Materials and Methods

4.2.1 Reagents and Materials

All reagents including tissue culture reagents were obtained from Sigma-Aldrich, Dorset, UK and Greiner Bio-One, Gloucester, UK unless otherwise stated. Penicillin/Streptomycin was purchased from Lonza. Foetal calf serum was purchased from Invitrogen. Collagenase B was purchased from Roche Diagnostics Ltd., East Sussex, UK. DAPI (4', 6-diamidino-2-phenylindole) nuclear counterstain (D3571) and Vybrant cell tracker was purchased from Molecular Probes, Invitrogen, Paisley, UK. Type I collagen polyclonal antibody was a gift from Dr Larry Fisher, NIH, Bethesda, USA. Sox9 polyclonal antibody (AB5535) was obtained from Chemicon International, (part of Millipore, Hertfordshire, UK). DAPI (4',6-diamidino-2-phenylindole) nuclear counter stain (D3571) was purchased from Molecular Probes, Invitrogen, Paisley, UK. Pluripotency markers OCT-4, SSEA-3 and TRA-1-60 were purchased from Santa Cruz, Biotechnology, Germany and SOX-2 from Millipore and secondary antibodies were purchased from Sigma-Aldrich, Dorset, UK and Molecular Probes, Invitrogen, Paisley, UK. Early differentiation antibody BMP-4, was purchased from Ab-Cam. Brachyury, AFP, SOX-1 and SOX-17 antibodies were purchased from R&D. Corresponding secondary antibodies were purchased from Molecular Probes, Invitrogen, Paisley, UK or Chemicon (part of Millipore, Hertfordshire, UK). All molecular reagents (including primer sets) were purchased from Invitrogen, Paisley, UK or Sigma-Aldrich, Dorset, UK, primer sequences given in section 2.10.3. Probes and positive controls used for FISH were kindly provided by Professor David Wilson, University of Southampton.

All images were captured using Carl Zeiss Axiovision software via AxioCam HR digital camera or Canon Powershot G2 digital camera. FISH images were captured using Carl Zeiss Axiovision software via Carl Zeiss AxioObserver Z1.

4.2.2 Human Embryonic and Foetal Cell Culture

4.2.2.1 Human Embryonic Stem Cell Culture

Human ES cells (HUES-7) were routinely cultured and maintained on MEF feeder layer as described in section 2.5. The addition of collagenase for up to 10 minutes for very confluent colonies or wells displaying higher levels of differentiation enabled the

release of differentiated regions of cells. Human ES cell conditioned media was obtained by pooling the media from ES cells from the daily media changes and freezing at -20^{o}C for later use. The media was filter sterilised before addition to foetal cell cultures.

Prior to differentiation studies, ES cells were under feeder-free conditions on matrigel coated plates. A minimum of two passages was performed to ensure the complete removal of MEF cells. The use of MEF conditioned media was a prerequisite to maintain the pluripotent state of the cells, and this was prepared by overnight incubation of human ES cell medium on MEF cells. The medium was then directly used on matrigel culture plates or could be pooled and frozen for use at a later date.

4.2.2.2 Embryoid Body Formation

Human ES cells cultured on MEFs were treated with 1ml per well of collagenase IV and incubated at 37^{o}C for up to 10 minutes. The collagenase was then removed and replaced with 1ml per well of MEF media and spun at 1000rpm for 4 minutes. The pellet was resuspended in 10ml of EB media and placed into a non-tissue culture treated petri dish and maintained at 37°C with 5% CO_2. Media changes were performed every 3-4 days by gently tipping the petri dish, and allowing the EBs to settle before removing as much media as possible without taking up the EBs and replacing with fresh media. For EBs grown in osteogenic or chondrogenic conditions, the necessary factors (given in section 2.4.3 and 2.4.4) were added directly to the EB media and cells cultured the same way.

4.2.2.3 Foetal Cell Culture

Human foetal femurs were obtained and processed as previously described in section 2.3. Briefly, femurs were dissected and plated into T25 flasks in 5ml collagenase B (1mg/ml) and digested overnight. Cells were then plated at appropriate densities in basal medium and maintained at 37°C with 5% CO_2. Cells were passaged using a Tris-EDTA solution in PBS before re-plating in appropriate differentiation medium. For the promotion of osteogenic differentiation, cell cultures were grown in osteogenic media (α-MEM with 10% FCS, 100μM ascorbate (ascorbic acid 2-phosphate) and 10nM dexamethasone. For the promotion of chondrogenic differentiation, cell cultures were grown in chondrogenic media (α-MEM supplemented with 10ng/ml TGF-β_3, 10nM

dexamethasone, 100µM ascorbate (ascorbic acid 2-phosphate) and 10µl/ml 100x ITS Supplement Solution – Insulin, Transferrin, Selenium).

4.2.2.4 Preparation of Foetal Conditioned Medium

At confluence foetal cells were passaged and plated out at appropriate densities with osteogenic or chondrogenic media. Media changes were performed every two days, with the media taken off, aliquoted and immediately frozen and stored at -20^{o}C. Prior to application on embryonic stem cells, the media was filter sterilised and used neat or as a 50/50 mix with embryonic stem cell media (prepared as described in section 4.2.2).

4.2.2.5 Organotypic/3-D Culture Model

The organotypic culture model is a 3-D construct in which single or multiple cell types can grow and interact in an environment that mimics, in part, that found *in vivo*. Cells were grown as a pellet culture on the organotypic model. Cells were grown to confluence before treatment for 30 minutes with collagenase IV and trypsin/EDTA to obtain single cells. A cell count was performed and the suspension made up to a cell concentration of $3x10^5$ cells/ml. 1ml aliquots were then placed in 15ml falcon tubes and centrifuged at 400g for 10 minutes. The tubes were cultured in an incubator at 37°C with 5% CO_2 for 2 days to allow a cluster of cells to form. Pellets were then transferred into the organotypic culture system (Figure 4:1). In brief, pellets were placed on top of a confetti membrane (1 pellet/membrane) within a well insert (up to 6 pellets per insert), as shown in Figure 4:1. 1ml of differentiation media was placed in the well and the cells cultured for up to 28 days in the incubator at 37°C with 5% CO_2.

Pellets were also formed containing a mix of foetal and embryonic stem cells. In this instance the same protocol was followed however a 50/50 mix of the cells was used to give an overall starting cell concentration of $3x10^5$ cells/pellet.

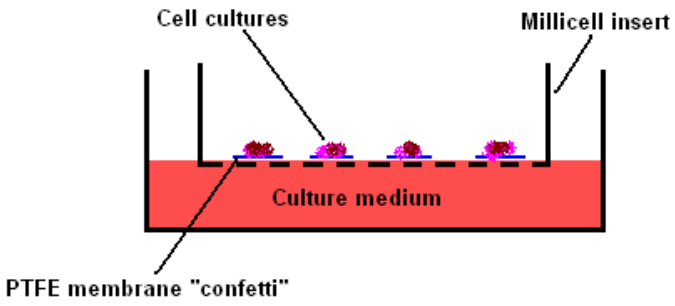

Figure 4:1 Organotypic culture set up. The cell cultures (pellets) were grown for 3 days in pellet culture conditions before being placed on the PTFE confetti membrane within the cell culture insert. Pellets were cultured with either osteogenic or chondrogenic media.

4.2.2.6 Fluorescent In-Situ Hybridisation (FISH)

Sections on superfrost glass slides were de-waxed and rehydrated through an ethanol series and prepared for FISH as described in section 2.6.3. Briefly, following a citrate antigen retrieval step, slides were rinsed in 2xSSC and then placed into 2xSSC at 75^{o}C for 2 minutes, followed by denaturation in 70% formamide/2xSSC for a further 3 minutes. Dehydration was performed using three-minute washes in ethanol. The slides were then air-dried and treated at 80^{o}C for 5 minutes on a heat block to denature the sections. X and Y chromosome DNA probes were applied to the sections. A cover slip was added and sealed. Slides were transferred to a Thermobrite machine and heated to 82^{o}C for 2 minutes before being left at 37^{o}C overnight as the hybridisation step. Post hybridisation, slides were washed 3 times for 5 minutes at 60^{o}C in 0.1XSSC. Finally, slides were mounted and counter stained with Vector Shield (containing DAPI). Slides were visualised using a Carl Zeiss AxioObserver Z1.

4.2.3 RNA Extraction and PCR Analysis

Foetal cells were treated for 30 minutes with collagenase B before total RNA was extracted using TRIzol reagent, subjected to DNAse treatment (DNA-free RNA kit) and reverse transcribed using the Super-Script First-strand synthesis system for RT-PCR as described in section 2.10. Real-time qPCR was performed using the Applied Biosystems 7500 system for quantifying the expression of osteogenic and chondrogenic markers (primer sequences are given in section 2.11.3). Samples were repeated in triplicate and values were calculated using the comparative Ct method and normalized to β-actin expression, and expressed as the mean ± SD.

4.2.4 Statistics

Statistical analysis was performed using unpaired t-tests to compare mean values between two groups and a one-way ANOVA was performed to compare mean of three or more experimental groups, followed by a Newman-Keuls post-hoc test to identify significance between groups. All experiments were repeated at least 3 times (unless otherwise stated), values were expressed as mean ± standard deviation (SD). Graphical representation of p-values were assigned as * $p<0.05$.

4.3 Results

4.3.1 Embryoid Body (EB) Formation

One approach for the differentiation of human ES cells is through the formation of embryoid bodies, which are cell aggregates, formed spontaneously under non-adherent cell culture conditions and in the absence of FGF2. Initial EB formation was attempted with ES cells that had been cultured using feeder free conditions. No EB formation was observed. EBs were only successfully formed when using ES cells that had been cultured on a MEF feeder layer. A number of protocols were then attempted to form EBs of a uniform size and shape for subsequent differentiation studies. Protocols were adapted from Ng et al (2005) and Ezekiel et al (2007), however, these proved unsuccessful for the formation of EBs due to apoptosis of the cells and/or the failure of the cells to aggregate. The standard suspension culture protocol was then utilised (Kurosawa, 2007), with successful formation of EBs, although this protocol did not result in pellets of any uniform size or shape. EBs were formed successfully under both static and rotating culture conditions (Figure 4.2). EBs from static culture displayed a less uniform size and shape, whereas, under rotating conditions, the EBs formed were found to be more uniform, of larger size and more prone to aggregating.

In order to push the differentiation of the cells toward the mesoderm lineage cells were grown in suspension culture using standard EB media with osteogenic and chondrogenic factors applied, given in section 4.2.2.3 (Figure 4.3). Under these conditions, the EBs appeared to be larger in size and greater in number compared to control medium. This was particularly true for ES cells grown in chondrogenic conditions as shown in Figure 4:3 C. EBs were stained with alkaline phosphatase in order to determine any change in expression; however for both osteogenic and chondrogenic conditions no loss of expression in alkaline phosphatase was observed over 15 days in culture (Figure 4:4). Following EB formation, the EB was placed into culture dishes where cell adhesion and cell outgrowth was observed within 24 hours. The cells which grew out of the EBs displayed similar cell morphologies (Figure 4:5), however due to the high confluence of the cells following 7 days in culture, immunostaining for type I and type II collagen was unable to give a true representation of matrix production (data not shown).

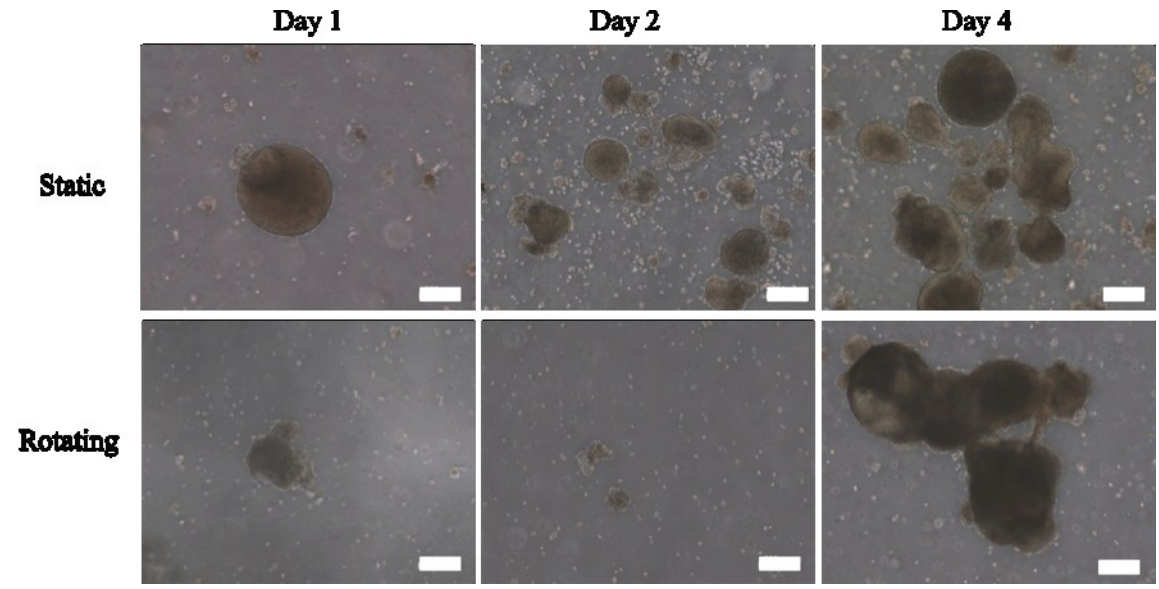

Figure 4:2 Embryoid bodies grown in rotating or static culture for 4 days. Scale bars represent 100μm.

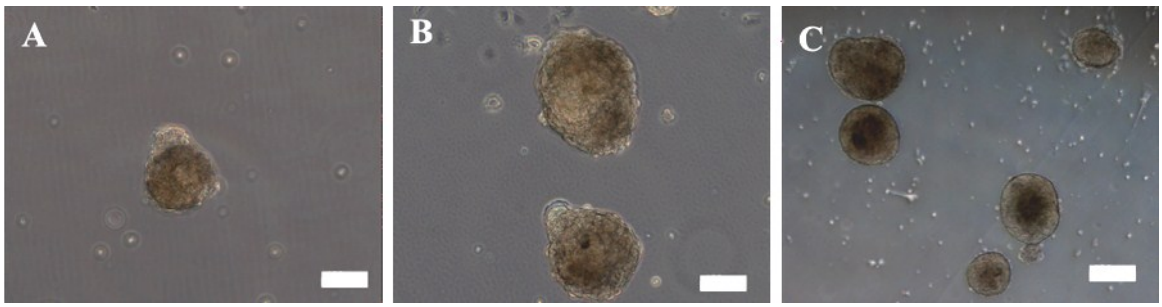

Figure 4:3 Embryoid bodies grown in A- EB (basal), B- osteogenic, C-chondrogenic conditions at day 5 of culture. Scale bars show 100μm except for C, which represent 200μm.

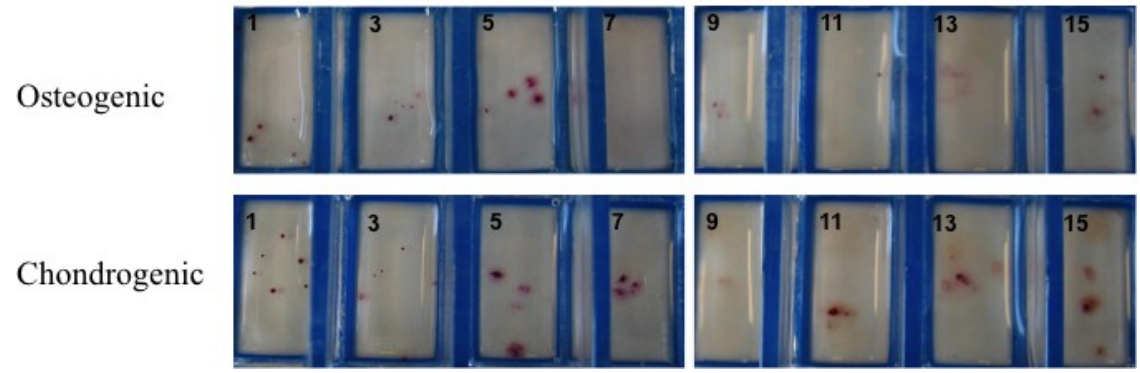

Figure 4:4 EBs grown in osteogenic and chondrogenic media conditions respectively for up to 15 days in culture stained for alkaline phosphatase expression. Numbers represent days in culture.

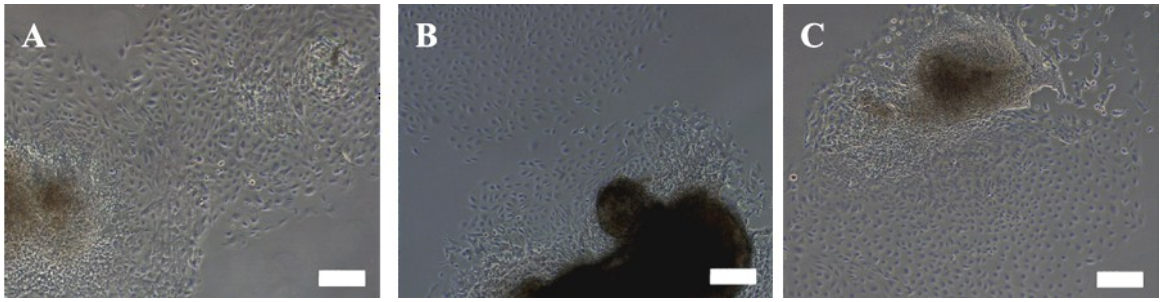

Figure 4:5 Embryoid bodies cultured in A) EB (basal), B) osteogenic, C) chondrogenic conditions at day 3 of culture on tissue culture plastic. Scale bars represent 200μm.

4.3.2 EB Molecular Characterisation

Molecular characterisation was performed following culture of EBs for 5 days in standard EB media as well as EB media supplemented with osteogenic and chondrogenic growth factors. The expression levels of pluripotency markers (Figure 4:6) as well as markers of early differentiation (Figure 4:7 and 4:8) were determined. The study was repeated three times, however due to great variation in differentiation levels observed, individual data sets are shown.

In two out of three studies, loss in expression of OCT-4 and SOX-2 was observed in comparison to human ES cells grown in monolayer culture. Expression of the pluripotency marker NANOG was reduced in all three studies undertaken.

Expression levels of mesoderm differentiation markers Brachyury and BMP-4 were minimal with the exception of two media conditions, embryoid body media and chondrogenic media, with a 6 fold and 4 fold increase in expression respectively (Figure 4:7). In the case of SOX-1 (an ectoderm marker), for 2 of 3 of the experimental runs an increase in expression levels was observed in the three media condition groups. For endoderm differentiation the marker SOX-17 was utilised, with some increased expression seen, however, no overall pattern was observed, with increases in expression seen in different media conditions for each experimental run (Figure 4:8).

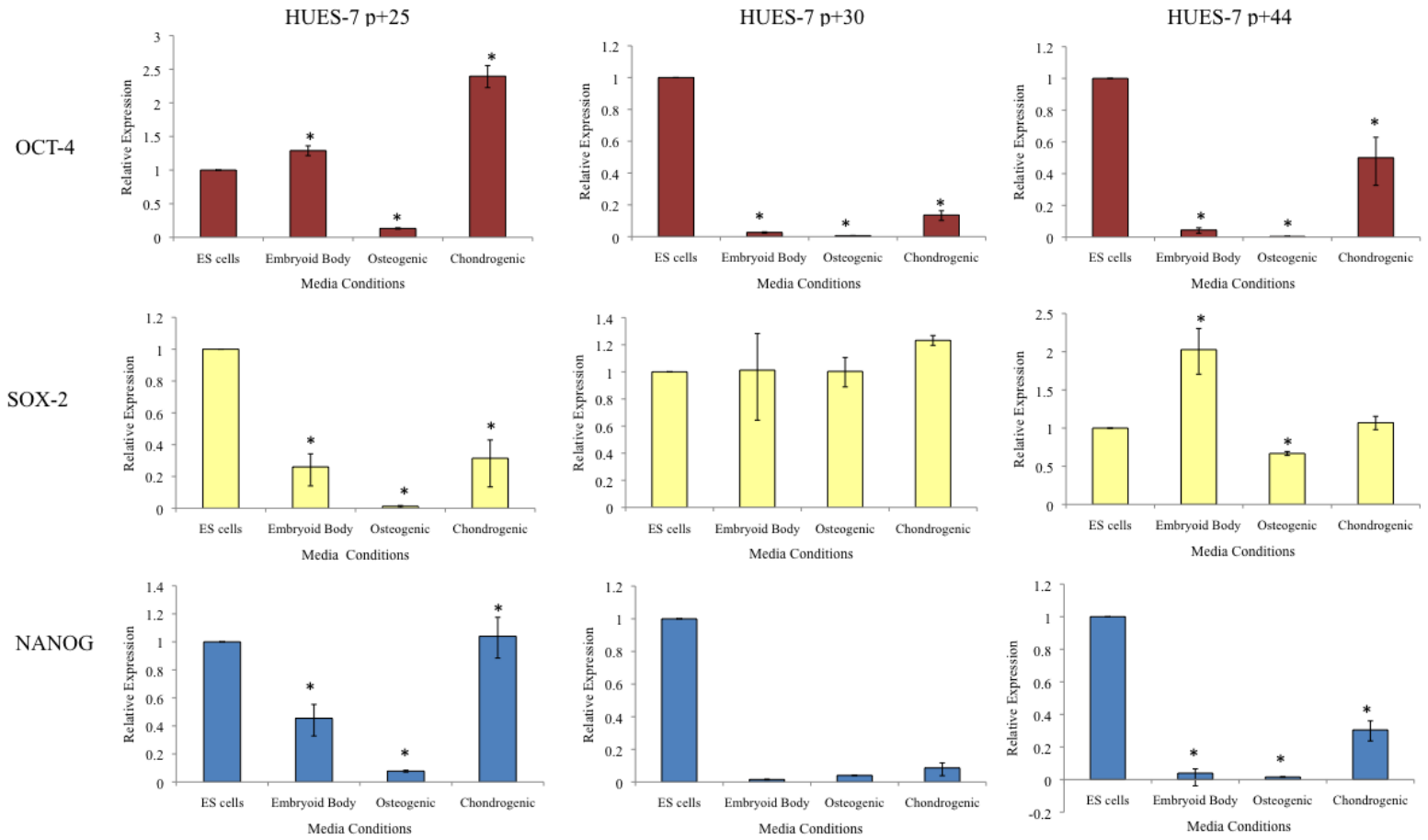

Figure 4:6 Pluripotency marker expression in 5 day old embryoid bodies cultured in standard embryoid body media, osteogenic or chondrogenic media conditions. Expression levels are given relative to β-actin. Undifferentiated stem cells were used as comparative and set at 1. * indicates significance $p<0.05$ relative to the undifferentiated ES cell population.

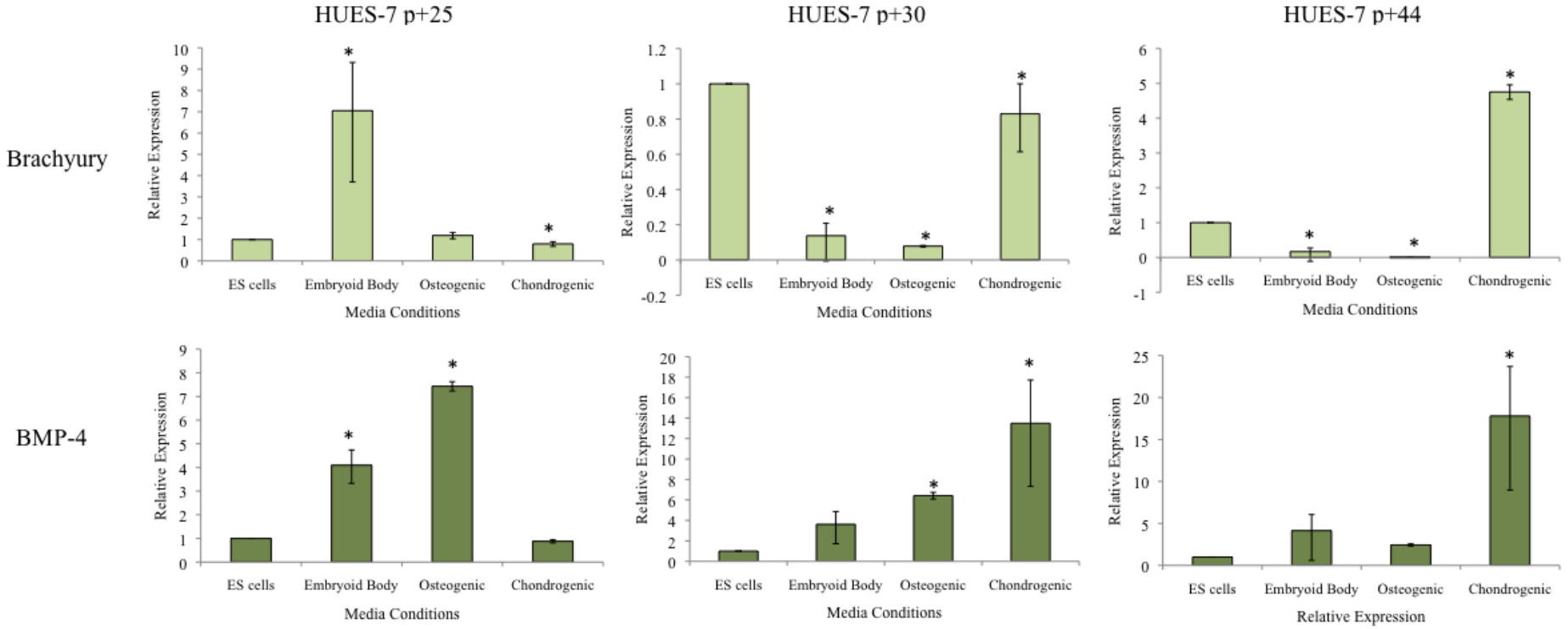

Figure 4:7 Early differentiation marker expression in 5 day old embryoid bodies cultured in standard embryoid body media, osteogenic or chondrogenic media conditions. Expression levels are given relative to β-actin. Brachyury and BMP-4 were used as markers of mesoderm differentiation with Undifferentiated stem cells were used as comparative and set at 1. * indicates significance $p<0.05$ relative to the undifferentiated ES cell population.

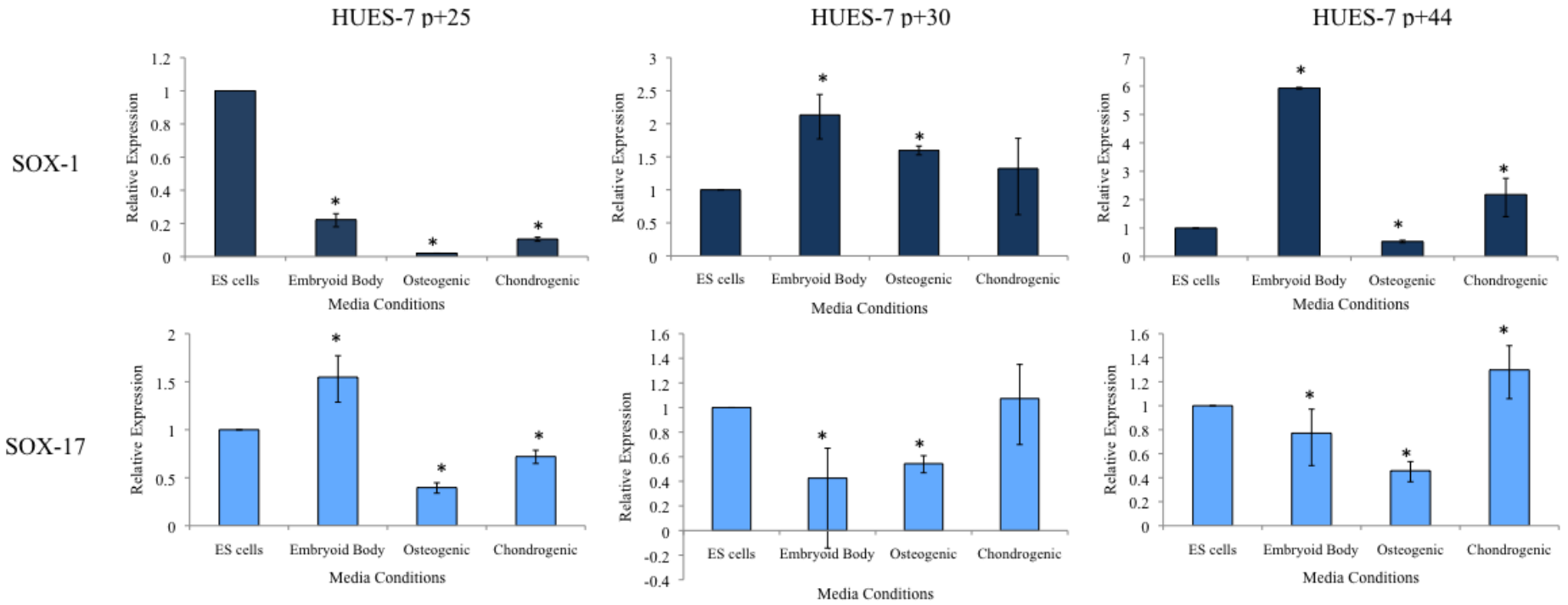

Figure 4:8 Early differentiation marker expression in 5 day old embryoid bodies cultured in standard embryoid body media, osteogenic or chondrogenic media conditions. Expression levels are given relative to β-actin. Sox-1 and Sox-17 used as markers of early ectoderm and endoderm differentiation respectively. Undifferentiated stem cells were used as comparative and set at 1. * indicates significance $p<0.05$ relative to the undifferentiated ES cell population.

4.3.3 Co-culture of Human ES Cells on a Foetal Cell Layer

In order to determine the differentiation potential of human ES cells grown in a monolayer co-culture system, ES cells were passaged as normal onto a confluent foetal cell layer. Cells were cultured for 7 days with MEF conditioned media or osteogenic media. ES cells grew as colonies on the foetal layer (Figures 4:9 and 4:10) in MEF conditioned media (basal) and osteogenic media conditions.

In both MEF conditioned media and osteogenic conditions, expression of alkaline phosphatase was observed, in both the ES colonies as well as the foetal cells. Greater staining observed for both ES and foetal cells grown in osteogenic conditions (Figure 4:9 and 4:10 B). Equally, following cytohistochemistry, in both media conditions, there was a loss of expression of pluripotency markers in the ES cell colonies (Figure 4:9 and 4:10 C-E). No expression of type I or II collagen (Figure 4:9 and 4:10 F-G) was seen in the ES cell colonies in either media condition, although minimal expression of type I collagen was seen in MEF conditioned media treated foetal cells compared to those cultured in osteogenic conditions which showed greater expression.

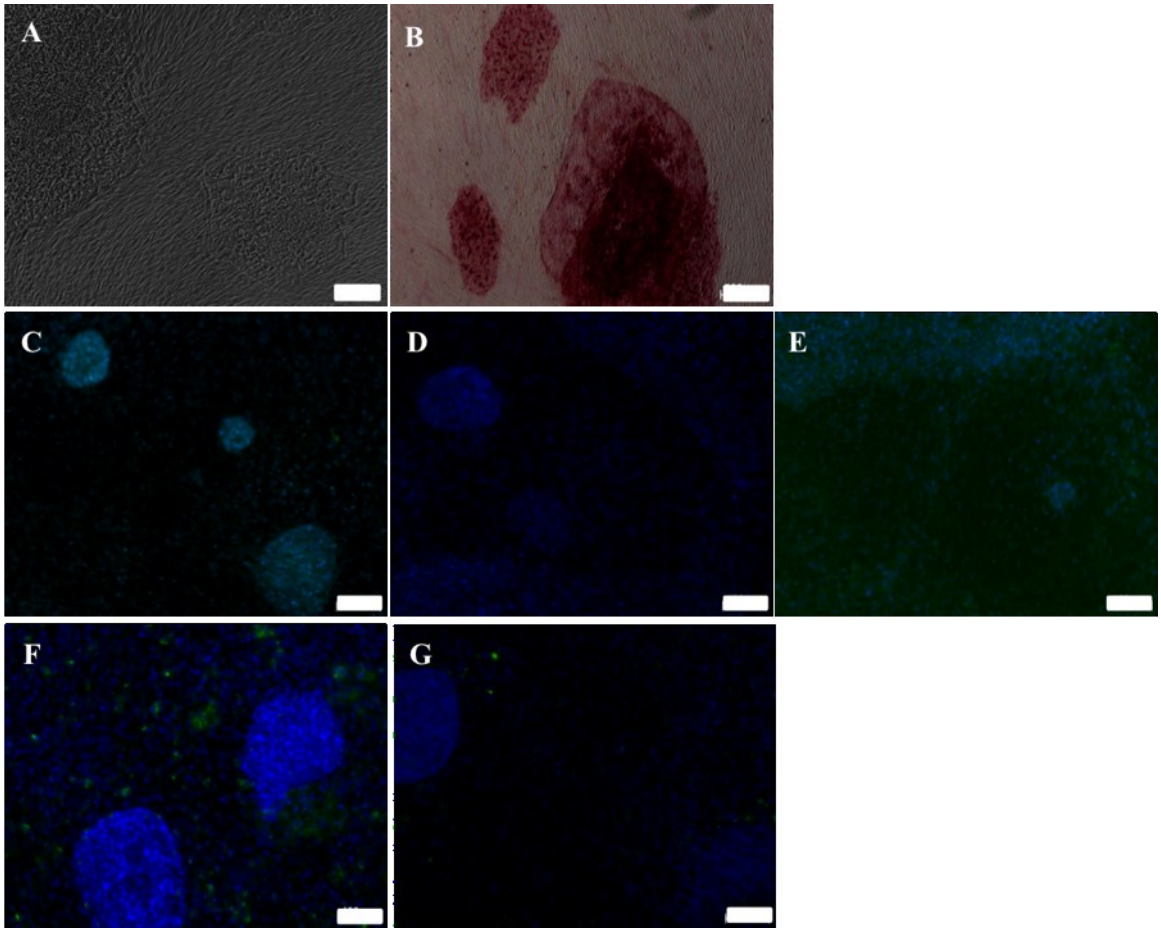

Figure 4:9 Human ES cells cultured on foetal cell layer in basal media. A) Phase image showing ES cell colonies growing on top of a foetal cell layer. B) Alkaline phosphatase staining. C)-E) Pluripotency marker staining, OCT-4, SSEA-3 and TRA-1-60. F) Type I, and G) Type II collagen staining. Scale bars A)-B) show 200μm and C)-G) show 100μm.

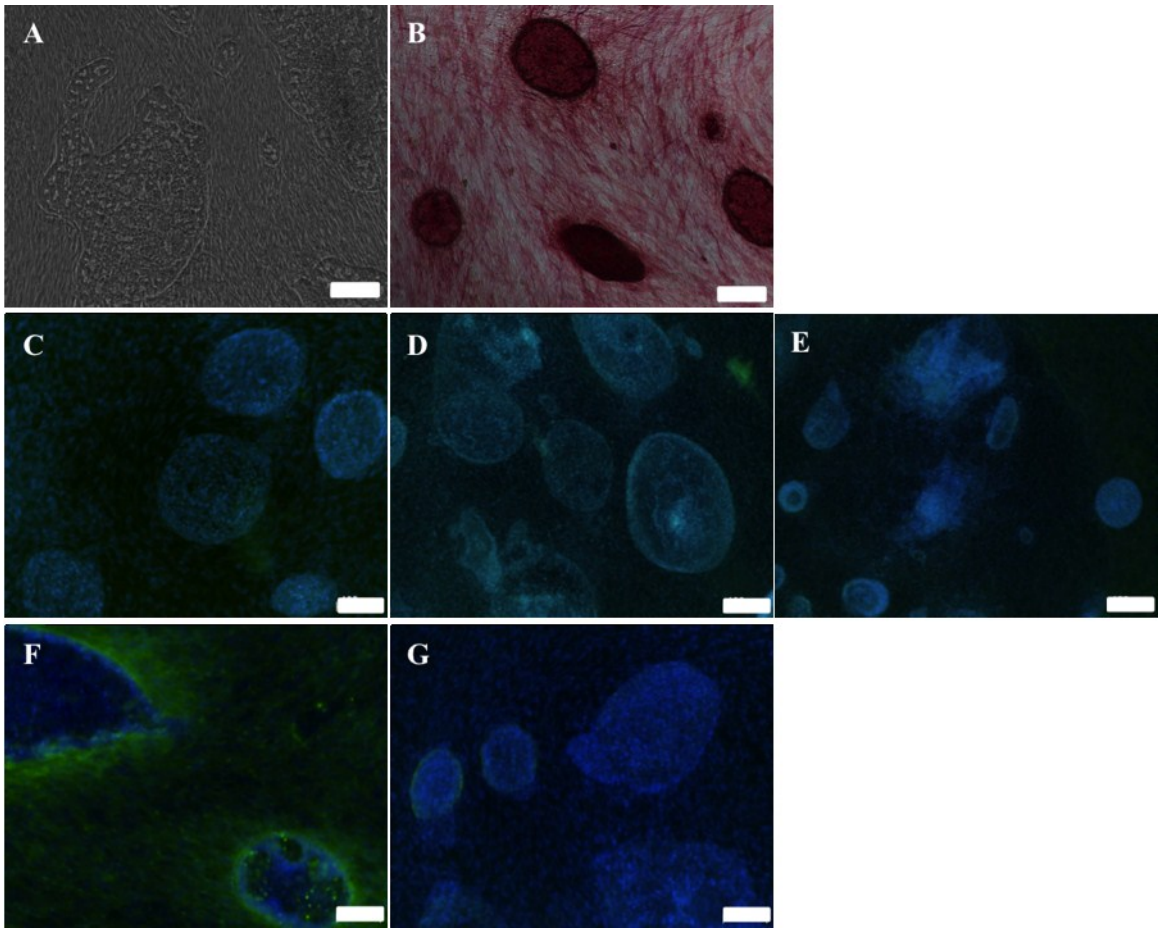

Figure 4:10 Human ES cells cultured on foetal cell layer in osteogenic media. A) Phase image showing ES cell colonies growing on top of a foetal cell layer. B) Alkaline phosphatase staining. C)-E) Pluripotency marker staining, OCT-4, SSEA-3 and TRA-1-60. F) Type I, and G) Type II collagen staining. Scale bars A)-B) show 200μm and C)-G) show 100μm.

4.3.4 Single Cell Co-culture of Human ES Cells and Foetal Cells

In addition to culturing the cells as embryoid bodies, 2-D culture systems were also utilised to determine any differences in the differentiation potential of the ES cells. One of the 2-D culture systems adopted was the co-culture of single ES cells and foetal cells compared to single cells grown in isolation in basal and osteogenic conditions for 7 days. ES cells that were cultured alone displayed less cell adherence to the tissue culture plastic following two days in culture compared to foetal cells and as a result, fewer cells in total were present by the end of the study at 7 days. This is shown in the live/dead and alkaline phosphatase staining images (Figure 4:11-4:12 D-I). In the mixed populations cultures, the effect of a colony of ES cells within the foetal cell layer can be seen (Figure 4:11-4:12 F and I). However, these cells show a different morphology to pluripotent ES cell colonies, which are distinct from the foetal cells. Alkaline phosphatase staining was observed in both the foetal and ES cells, with stronger staining seen in osteogenic culture conditions. Live/dead staining revealed viability of both cell types in both basal and osteogenic conditions (Figure 4:11-4:12 G-I), with FITC green staining representing the live cell population.

Biochemical assays to determine the alkaline phosphatase specific activity (Figure 4:13) in the three cell populations were performed. As expected foetal cells in osteogenic conditions had increased alkaline phosphatase specific activity, which was observed in 3 of the 4 populations. In contrast this was not observed in the mixed cell cultures. The difference in alkaline phosphatase specific activity between the foetal only and the mixed cell populations was found to be significant in two of the four studies performed. ES cells displayed negligible amounts of alkaline phosphatase specific activity, which when calculated against the standard curve, in some cases resulted in negative activity levels.

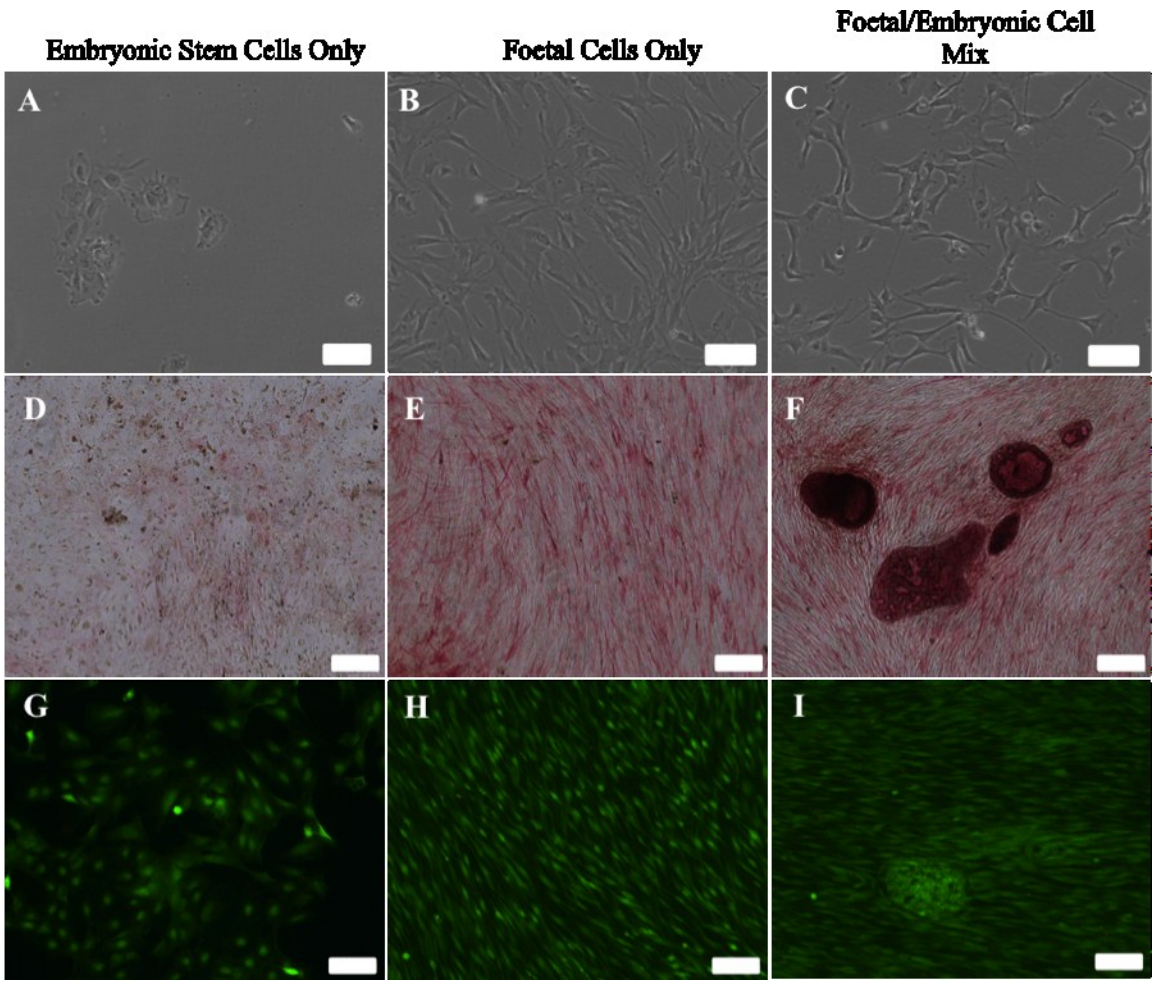

Figure 4:11 Human ES and foetal cells grown in basal conditions. A)-C) cells in culture at day 2. D)-F) Alkaline phosphatase staining of cells at day 7 and G)-I) Live/dead staining of cells at day 7. All scale bars represent 100μm with the exception of D)-F) which represent 200μm. Images shown are representative of n=4 different populations.

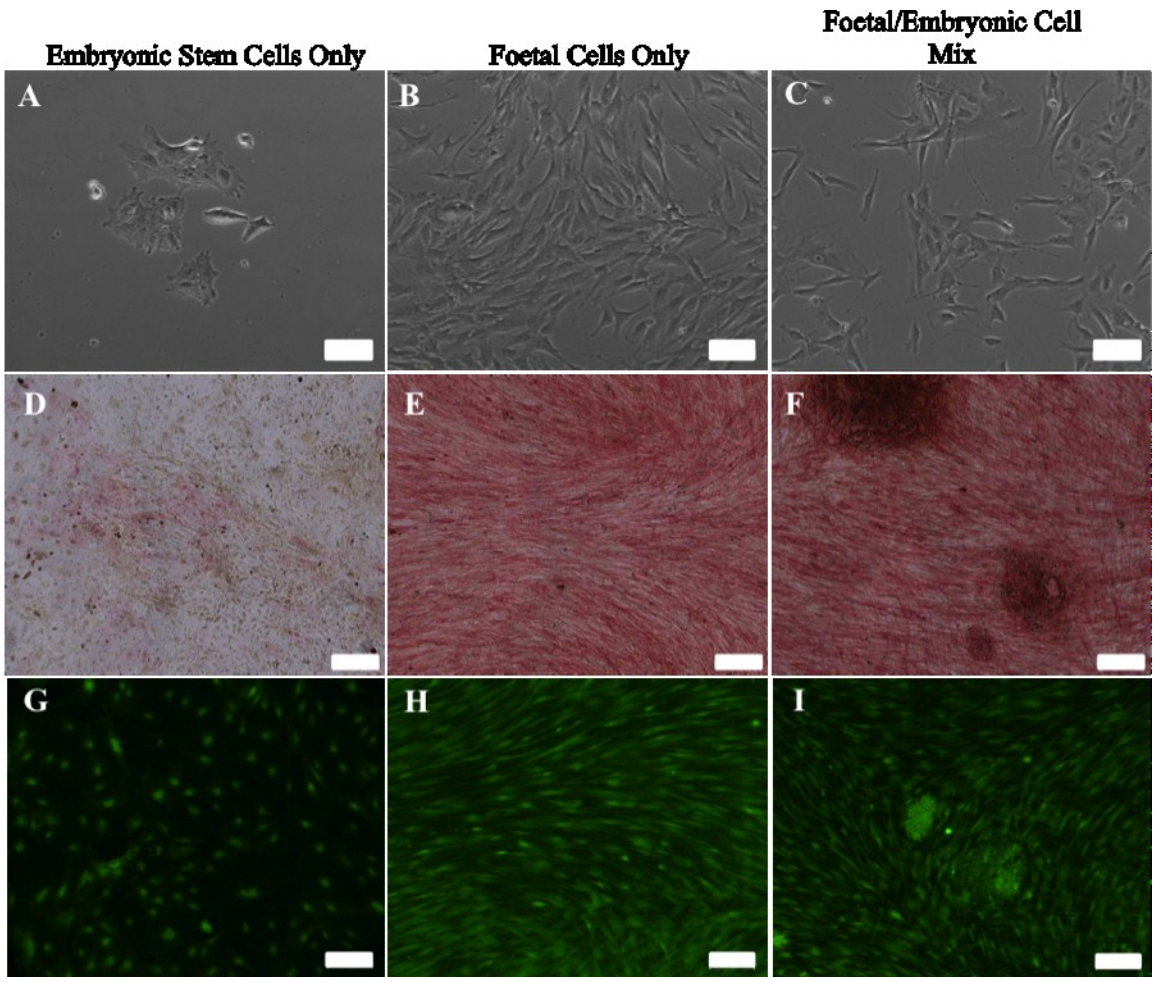

Figure 4:12 Human ES and foetal cells grown in osteogenic conditions. A)-C) cells in culture at day 2. D)-F) Alkaline phosphatase staining of cells at day 7 and G)-I) Live/dead staining of cells at day 7. All scale bars represent 100μm with the exception of D)-F) which represent 200μm. Images shown are representative of n=4 different populations.

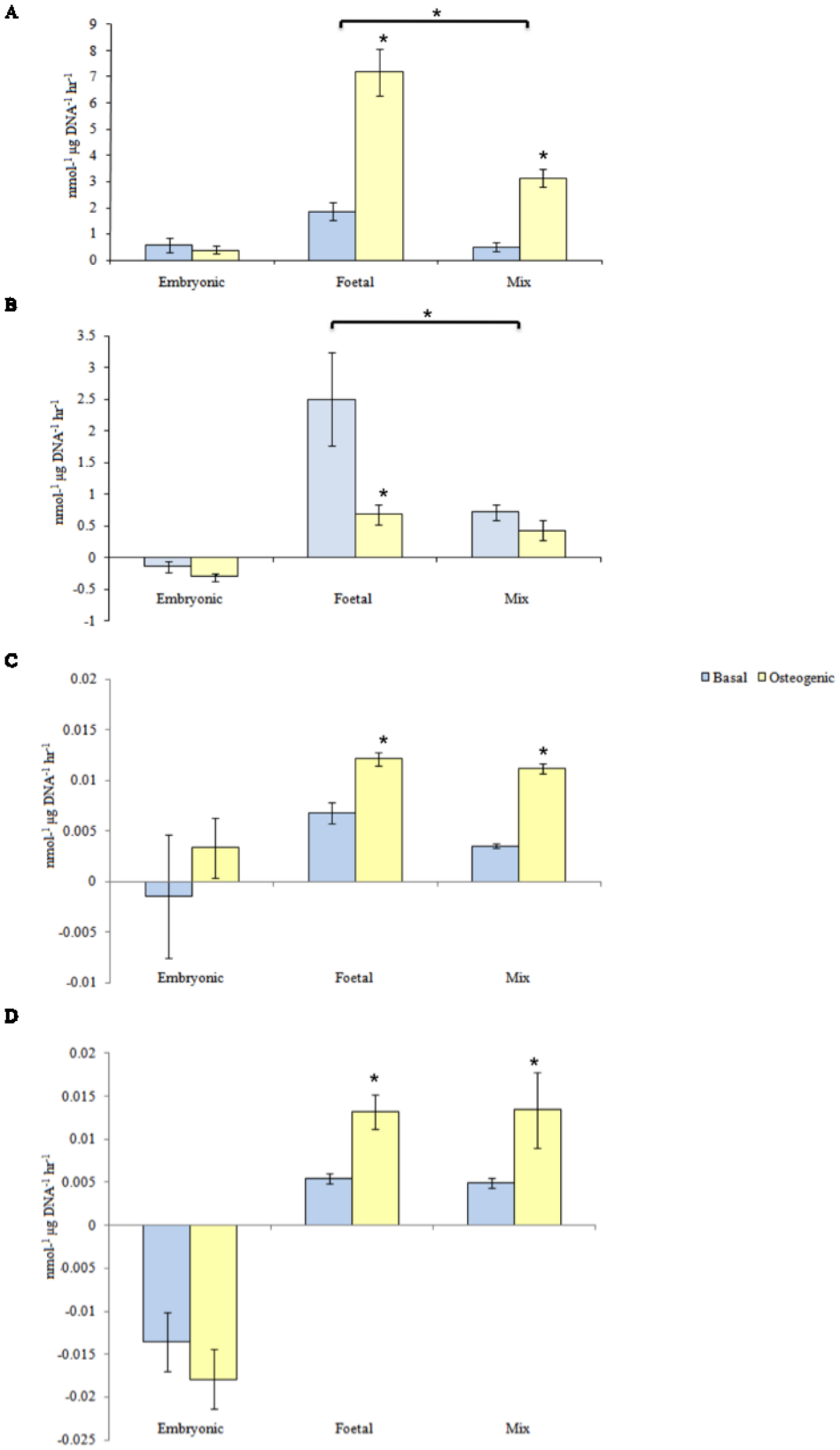

Figure 4:13 Alkaline phosphatase specific activity for single embryonic and foetal cells and co-cultured (mix) cell populations. Four separate populations are shown, A) H1229, B) H1300, C) H1132 and D) H1138. * indicates significance $p<0.05$.

4.3.5 Single Cell Culture System

A further example of a 2-D culture system utilised was the single cell culture of human ES cells. Following culture on matrigel and the removal of the fibroblast layer over three passages, cells were treated with trypsin and single cells obtained, which were then plated out and cultured with osteogenic media from foetal cells (osteogenic conditioned media). The cells were cultured over a total of 10 days (8 days in the case of one data set where day 10 cells were lost), with cells being harvested for qPCR at days 0, 2, 4, 6, 8 and 10 for molecular characterisation of expression levels of pluripotency and differentiation markers. The data shown is for four individual cell data sets, given the large differences in the expression levels seen across the data sets. As the data obtained was inconsistent across the studies, the overall trend will be discussed.

For the pluripotency marker, OCT-4, a loss of expression was observed in 3 of the 4 data sets over the 10 day time course. SOX-2 and NANOG expression was lost in all 4 experimental data sets over the 10 day time course (Figure 4:14).

SOX-1 expression (Figure 4:15) was minimal in two of the experimental data sets, with variable expression seen in the remaining two data sets. Although the overall trend shows minimal expression of SOX-1 in the cultures. SOX-17 expression (Figure 4:15) in three of experimental data sets was observed to peak followed by a loss in expression. The peaks in expression were not observed at the same days in culture. However, as with SOX-1 expression, SOX-17 expression was minimal/lost over the time course of the studies. This was also the case for expression of Brachyury (Figure 4:16), which was negligible in two of the experimental data sets, with variable expression seen in the remaining two data sets, and therefore no overall pattern could be determined. BMP-4 another mesoderm differentiation marker was also assessed and shown to be expressed in variable levels, with peaks in expression seen at various time points (Figure 4:16). The increase in BMP-4 expression was consistently high in the four groups, with a reproducible value obtained at day 2 of culture. This also correlates to the data obtained for EB differentiation in section 4.3.2 Alkaline phosphatase expression (Figure 4:16) was also measured, again showing no consistent pattern of expression, with an overall loss observed in only two of the experimental data sets.

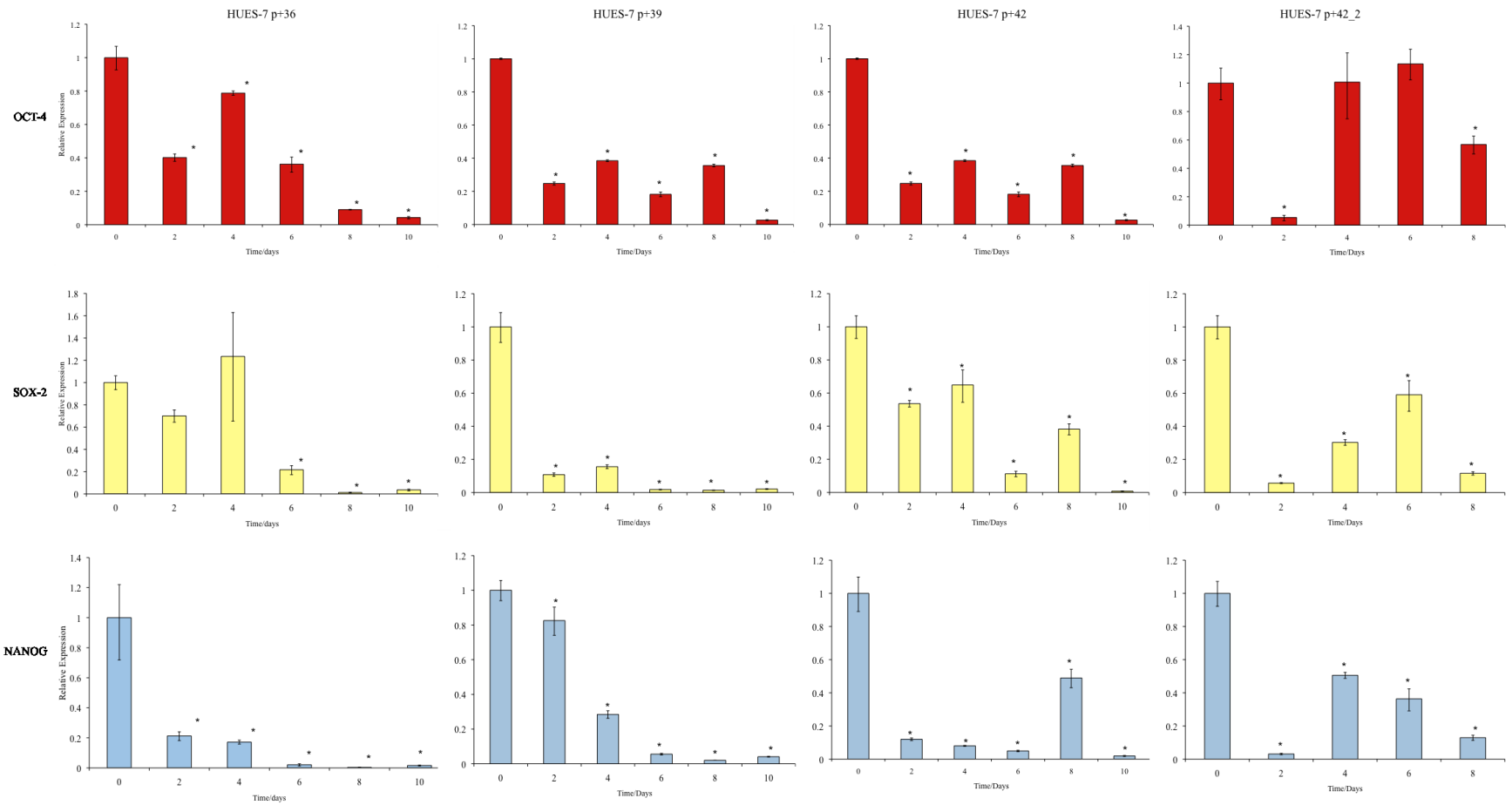

Figure 4:14 Pluripotency marker expression relative to β-actin levels. Single human ES cells were cultured with osteogenic foetal cell conditioned media for 10 days in culture. Expression levels were observed at days 2, 4, 6, 8 and 10. Cells at day 0 are undifferentiated human ES cells prior to trypsin treatment and were set at 1 to compare relative expression levels. A total of four repeats were performed. * indicates significance $p<0.05$ relative to the undifferentiated day 0 ES cell population.

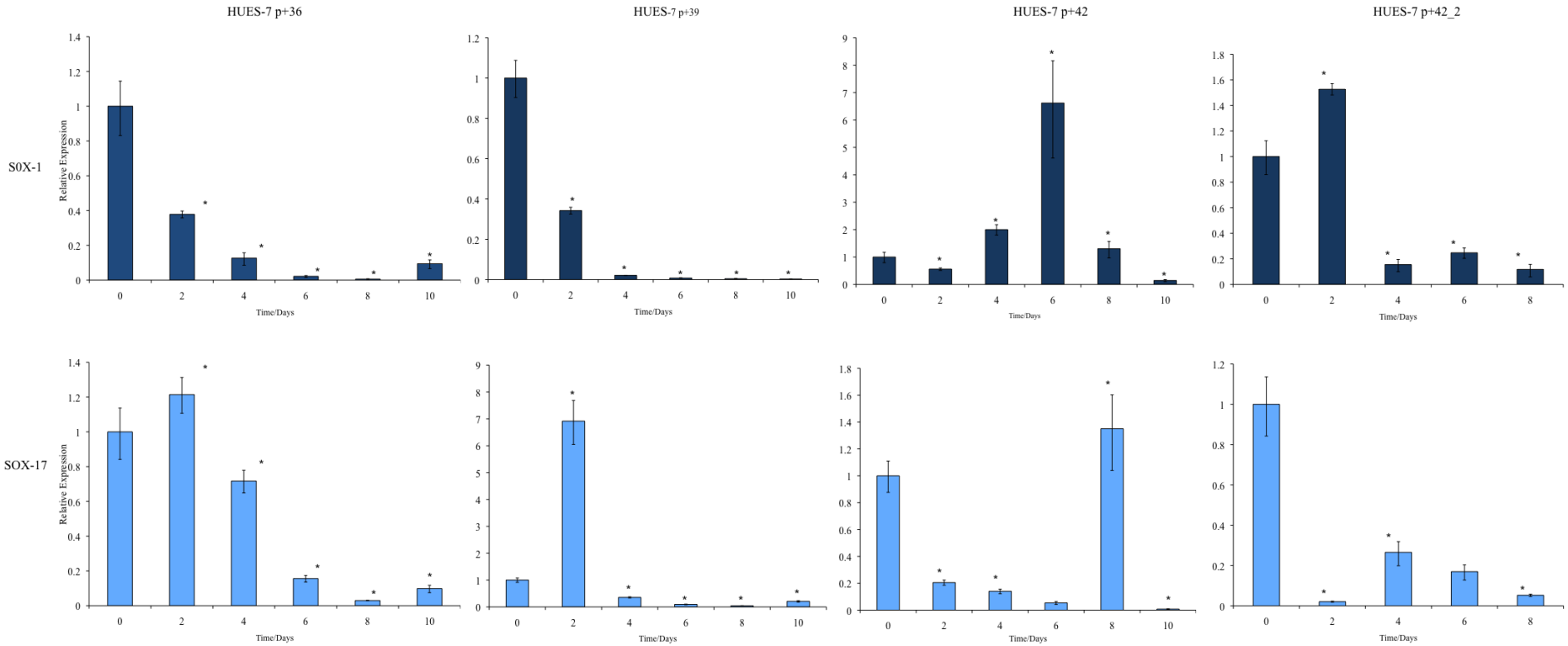

Figure 4:15 Differentiation marker expression relative to β-actin levels. Single human ES cells were cultured with osteogenic foetal cell conditioned media. Expression levels were observed at days 2, 4, 10 and 12 in culture. Cells at day 0 are undifferentiated human ES cells prior to trypsin treatment and were set at 1 to compare relative expression levels. * indicates significance $p<0.05$ relative to the undifferentiated day 0 ES cell population.

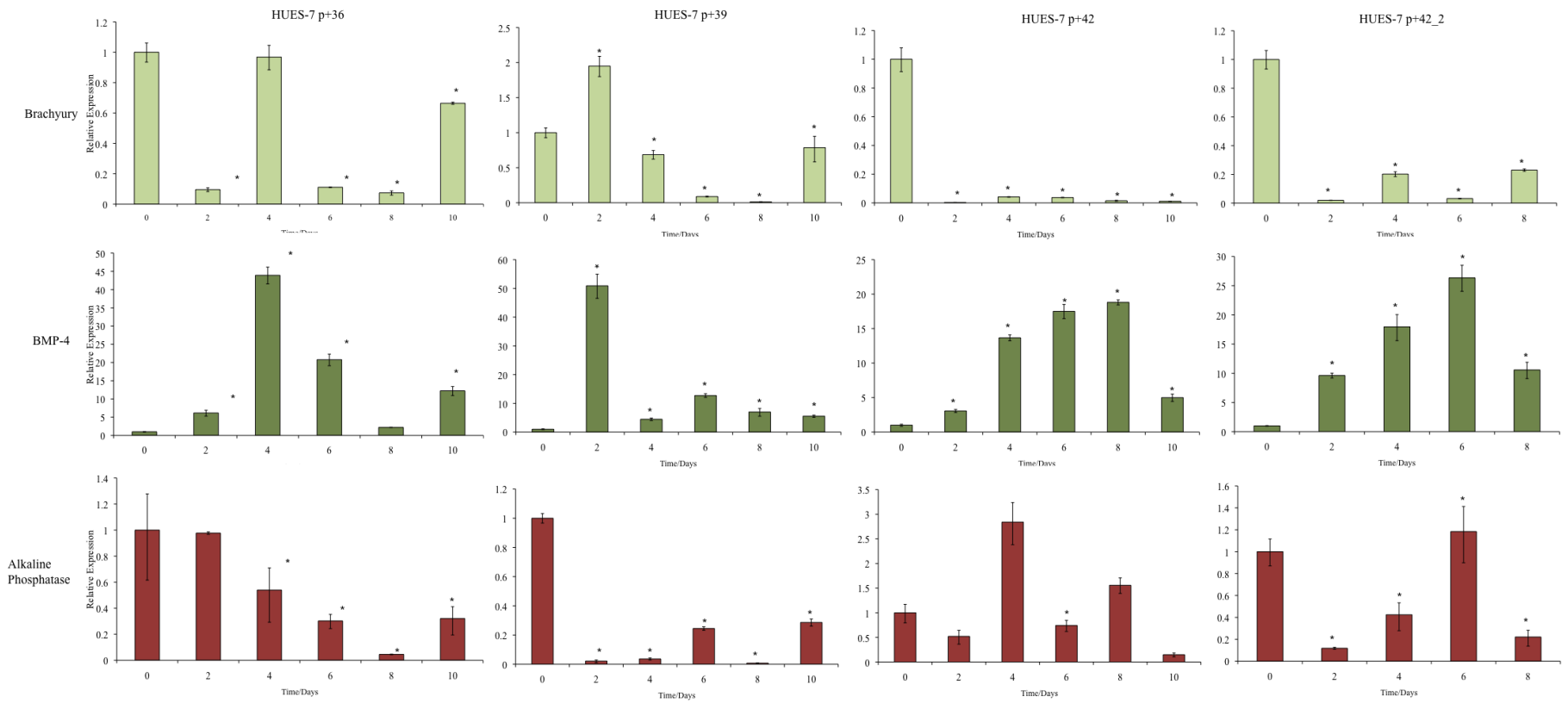

Figure 4:16 Differentiation marker expression relative to β-actin levels. Single human ES cells were cultured with osteogenic foetal cell conditioned media. Expression levels were observed at days 2, 4, 10 and 12 in culture. Cells at day 0 are undifferentiated human ES cells prior to trypsin treatment and were set at 1 to compare relative expression levels. * indicates significance $p<0.05$ relative to the undifferentiated day 0 ES cell population.

4.3.6 Culture of Foetal Femur Derived Cells in Human ES Cell Conditioned Medium

After a number of approaches to examine the effect of foetal cells on the human ES cell population, the effect of the application of human ES cell conditioned media on foetal cells was investigated.

In order to observe the affect of the addition of human ES cell conditioned medium on foetal femur-derived cells, following daily ES cell media changes, media was pooled and filter sterilised prior to application on foetal cells, either as 100% conditioned media or 50% conditioned media, where the remaining 50% media was human ES cell media. The cells were cultured for 3 days, with media changes taking place every other day. Morphologically the cells had a fibroblastic appearance and did not appear significantly different to foetal cells cultured in standard conditions (Figure 4:17). Cells were then treated with TRIZOL, RNA extracted, and qPCR performed. The data obtained for four separate patients is shown in Figures 4:18 and 4:19. Due to the patient variation the data could not be averaged, however a general trend was observed across the four data sets. For each of the genes analysed, the expression at day 0 of the foetal cells prior to media addition was set at 1 and all data relative to β-actin expression. Type II collagen, SOX-9 and SOX-1 expression was observed to decrease in three of the four patient samples in both 100% and 50% ES cell conditioned media. In all patient samples, there was a loss of expression of alkaline phosphatase. RUNX-2 and BSP expression was greater in 3 of the 4 patient samples, with the greatest increase observed in the cells treated with 50% conditioned media in the case of RUNX-2. Osteonectin expression showed the greatest variation across the two sample groups as well as across patients with 2 of the 4 showing a decrease in expression.

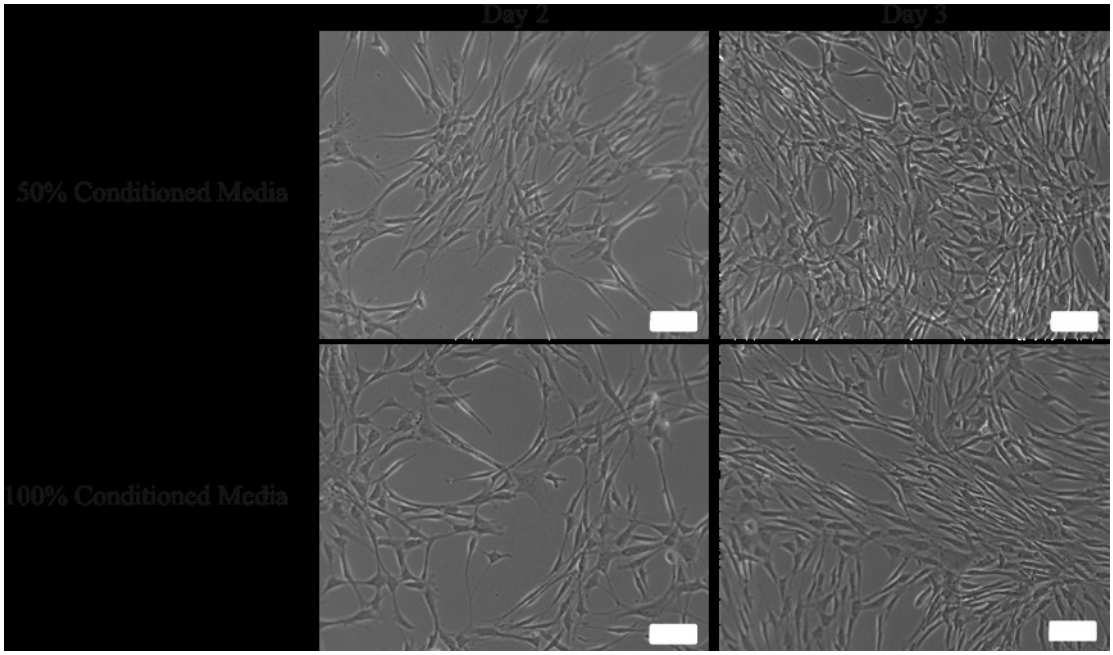

Figure 4:17 Foetal femur-derived cells in culture in both 50% and 100% ES cell conditioned medium at day 2 and 3. Scale bars represent 100μm.

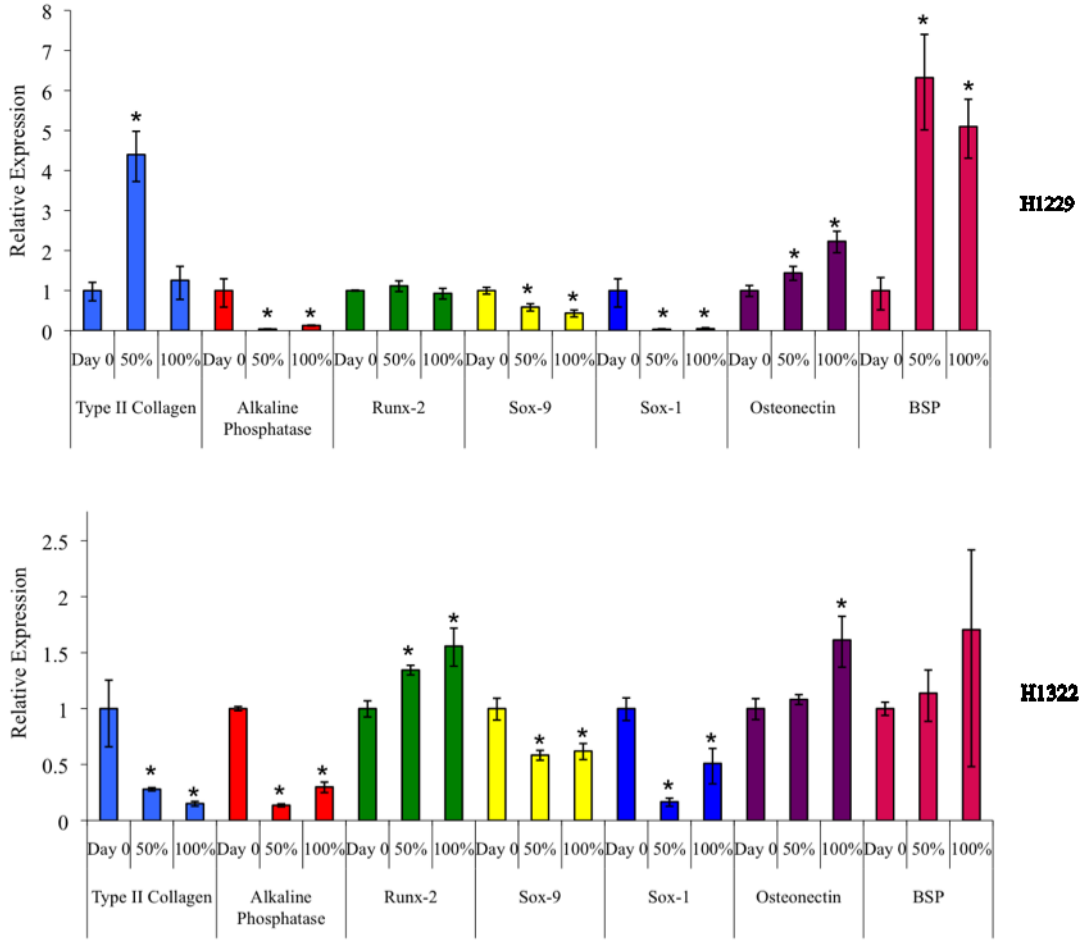

Figure 4:18 Gene expression relative to β-actin levels. Foetal femur cells were cultured with 50% or 100% human ES cell conditioned media for 3 days. Cells at day 0 are human foetal cells prior to the addition of conditioned media and were set at 1 to determine relative expression levels. * indicates significance $p<0.05$ relative to the day 0 foetal cell population.

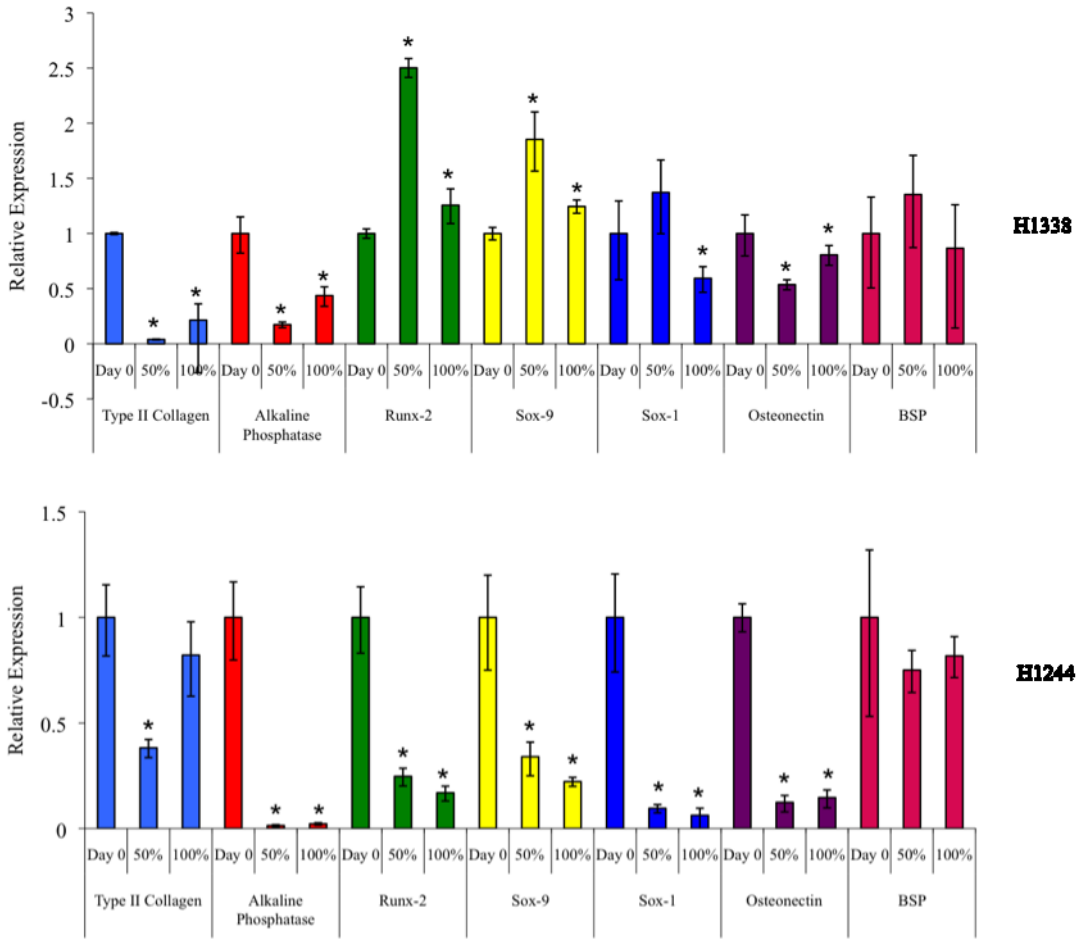

Figure 4:19 Gene expression relative to β-actin levels. Foetal femur cells were cultured with 50% or 100% human ES cell conditioned media for 3 days. Cells at day 0 are human foetal cells prior to the addition of conditioned media and were set at 1 to determine relative expression levels. * indicates significance $p<0.05$ relative to the undifferentiated day 0 ES cell population.

4.3.7 Organotypic/3-D Culture Model

Equal numbers of foetal and embryonic stem cells were trypsinized and mixed as single cells and centrifuged to form a pellet (Figure 4:20 A), and left in the incubator under standard conditions for 3 days before being added to the organotypic culture system (Figure 4:20 B). The cells were left in culture for up to 28 days in osteogenic and chondrogenic conditions with pellets being harvested at days 1, 7, 14 and 28. In order to identify the cells, foetal cells alone were labelled with Vybrant® CDFA SE Cell tracer (Molecular Probes, Invitrogen, UK), a long lasting cell tracker, so that the viability of the cells could be determined visually using a fluorescence microscope. It was previously observed that the addition of Vybrant® to the embryonic cells and the pellet formation protocol compromised the viability of the cells and therefore no pellets were formed. The labelling of foetal cell populations with Vybrant was an unsuccessful protocol for determining the location of the foetal cells in relation to the embryonic cells due to leaching of the dye to all cells as demonstrated in Figures 4:21 and 4:22. In order to indentify the location and differentiation of the cell types, Fluorescent In-Situ Hybridization (FISH) was performed.

The HUES-7 cell line are karotypically male (Cowan et al., 2004), whereas the foetal cells were previously determined also by FISH to be karyotypically female. We therefore examined for the presence of the Y chromosome in the cells to determine the location of the embryonic population confident that the remaining unstained populations would be the female, foetal cell population. The study was repeated a further three times using the male human ES cell population and a female foetal cell population with FISH used to determine the location of the cells within the pellet following sectioning.

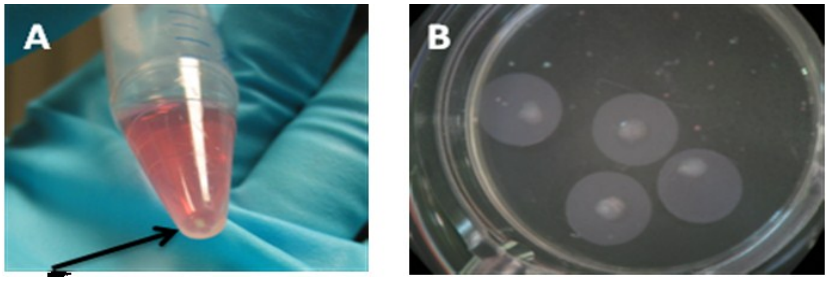

Figure 4:20 Experimental set up. A; pellet as indicated by arrow, following centrifugation of the cells, pellets were allowed to form in culture for 3 days in basal conditions before placing onto B; confetti membrane within tissue culture insert.

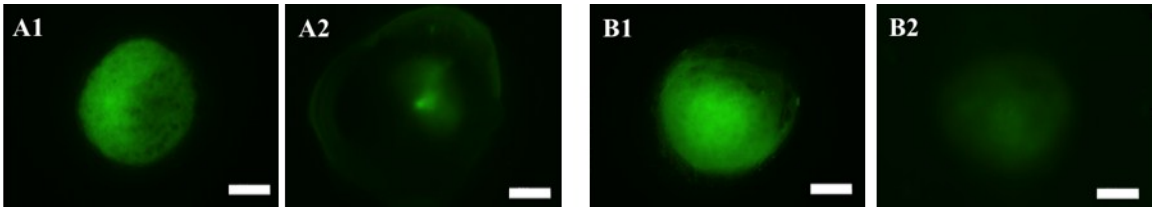

Figure 4:21 Mixed foetal and ES cells in vitro labelled with vibrant, long lasting cell tracker A1-2; Osteogenic pellets grown at days 2 and 25 respectively, B1-2; chondrogenic pellets at days 2 and 25 of culture. Over the course of the 28 days there was a reduction in the fluorescent intensity of the labelled cells. Scale bars represent 500μm.

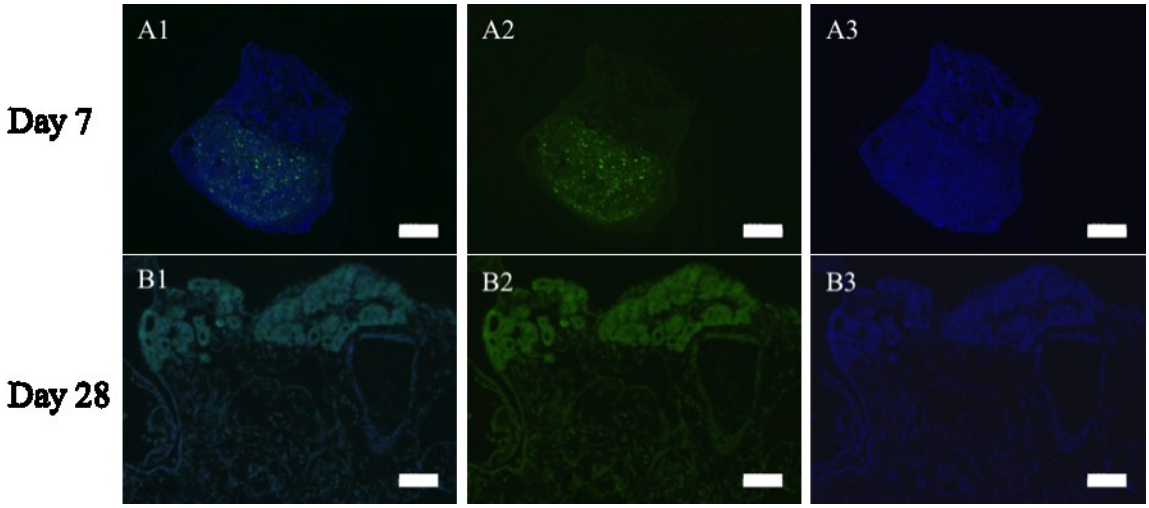

Figure 4:22 Example of vybrant staining as seen following processing and sectioning with a DAPI counter-stain, at days 7 and 28 of culture. Images A-B1 FITC and DAPI merged, A2-B2 FITC alone, and A-B3 DAPI nuclear stain alone. Scale bars A1-3 represent 200μm and B1-3 100μm.

4.3.7.1 Optimisation of FISH Protocol

Due to the fixation and processing of the cells in 90% ethanol and paraffin wax, it was necessary to adjust the FISH protocol accordingly; this is described in section 4.2.2.6. The Y chromosome probe was labelled with Texas Red and the X chromosome probe labelled with FITC. Cells in the metaphase stage of mitosis were used as a positive control as the chromosomes are visible at 100x magnification. Figures 4:23 and 4:24 show cells in metaphase that have positive labelling for the XX and XY chromosomes respectively. In all cases, a highspot/concentrated stain indicates successful labelling. All cells were counterstained with DAPI. The addition of a citrate step and denaturing solution was successful in acting as an antigen retrieval step and allowed the penetration of the Y chromosome probe. Figure 4:25 indicates the difference in staining achieved by the addition of a citrate step and denaturing solution. Standard FISH techniques resulted in a high level of background staining with no specific staining seen (Figure 4:25 A1 and A3). However clear highspots of positive staining was seen in those cells with the additional citrate step (Figure 4:25 B1 and B3). Due to the high levels of background green/red stain still observed (even with inclusion of the citrate step), for the purposes of identification of two cell populations in the co-culture pellets, only the Y chromosome (Texas Red) probes were added in the hybridisation step to identify the embryonic cell population. The assumption made is that any unstained cells were the foetal cell population. This was successful in enabling the identification of the embryonic cell population, with some background staining observed, but highspots of Texas Red stain identifying the Y chromosome.

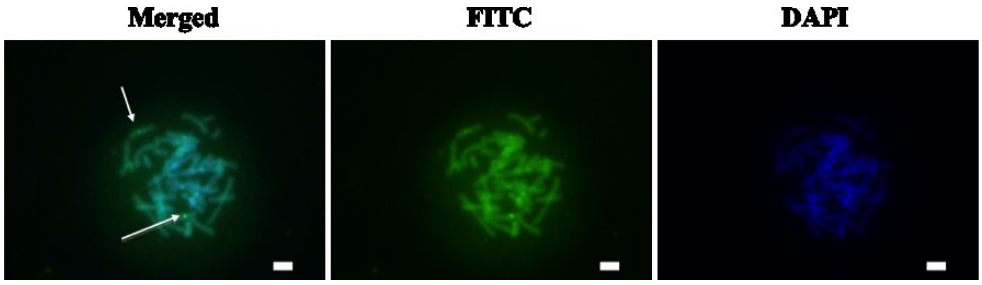

Figure 4:23 FISH on metaphases showing the presence of two X chromosomes (FITC labelled probe) and confirming the female sex cell. Scale bars represent 5μm. Arrows highlight X chromosomes.

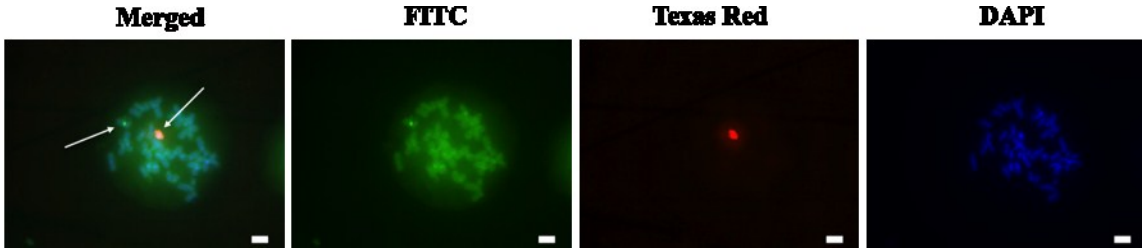

Figure 4:24 FISH on metaphases showing the presence of one X chromosome (FITC labelled probe) and one Y chromosome (Texas Red labelled probe) and confirming the male sex cell. Scale bars represent 5μm. Arrows highlight X and Y chromosomes.

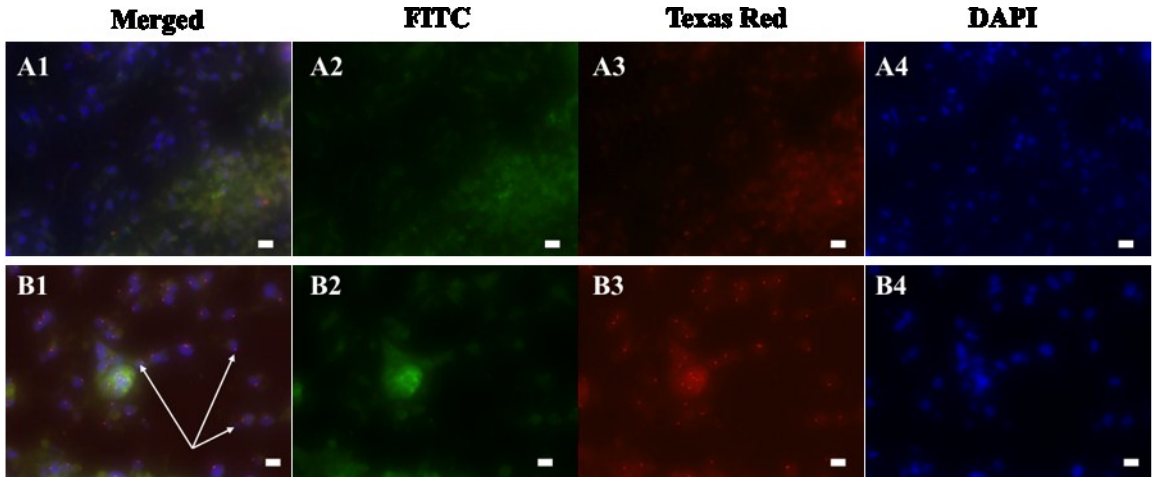

Figure 4:25 Optimisation of FISH protocol using human embryonic stem cell populations alone. A1-A4, protocol without addition of a citrate step, B1-B4 protocol with addition of citrate step. A/B1) FITC, Texas Red and DAPI merged images, A/B2) FITC image (to show presence of X chromosome), A/B3) Texas Red image (to show presence of Y chromosome) and A/B4) DAPI nuclear marker image. The overall red/green staining seen is background with positive staining indicated by the bright spots of colour and is highlighted by the arrows in images A1 and B1. Scale bars represent 10μm.

4.3.7.2 Pellet Characterisation

A total of three different pellet combinations were run with two conditions each. Mixed pellets consisting of equal numbers ($1.5x10^5$) of foetal and embryonic stem cells were compared to foetal only pellets with a total cell number of either $1.5x10^5$ or $3x10^5$ cells per pellet. By running these foetal only pellets along side, the effect of the embryonic cell population can be determined as well as the affect of the starting foetal cell number.

In the foetal cell only pellets, similar results were seen in the Alcian Blue/Sirius Red and alkaline phosphatase staining for both pellet sizes (Figure 4:26 and 4:27). The day 0 pellets predominantly stained for collagen, and no alkaline phosphatase staining was observed for both sized pellets. At day 7 of culture under osteogenic conditions predominantly Sirius Red staining was observed, with the strongest staining seen at the edges of the pellet. Similarly under chondrogenic conditions, predominate collagen staining was observed with negligible proteoglycan seen in the centre of the pellet. The same phenotype was observed in the day 28 pellets, however with stronger staining for collagen seen in the osteogenic pellet, with little proteoglycan observed in the centre of the pellet and at the outer edges.

No alkaline phosphatase staining was observed in the day 0 cultures for both $1.5x10^5$ and $3x10^5$ pellet sizes. At day 7 no alkaline phosphatase staining was seen in the osteogenic cultures with minimal staining seen in the chondrogenic pellets for the $1.5x10^5$ cell pellets with a loss of staining at day 28. In the osteogenic pellets, minimal alkaline phosphatase staining was observed at the edges of the pellet only. For the $3x10^5$ cell pellets, little alkaline phosphatase staining was seen in the osteogenic and chondrogenic pellets at day 7 with a complete loss of staining at day 28 (Figure 4:26 and 4:27).

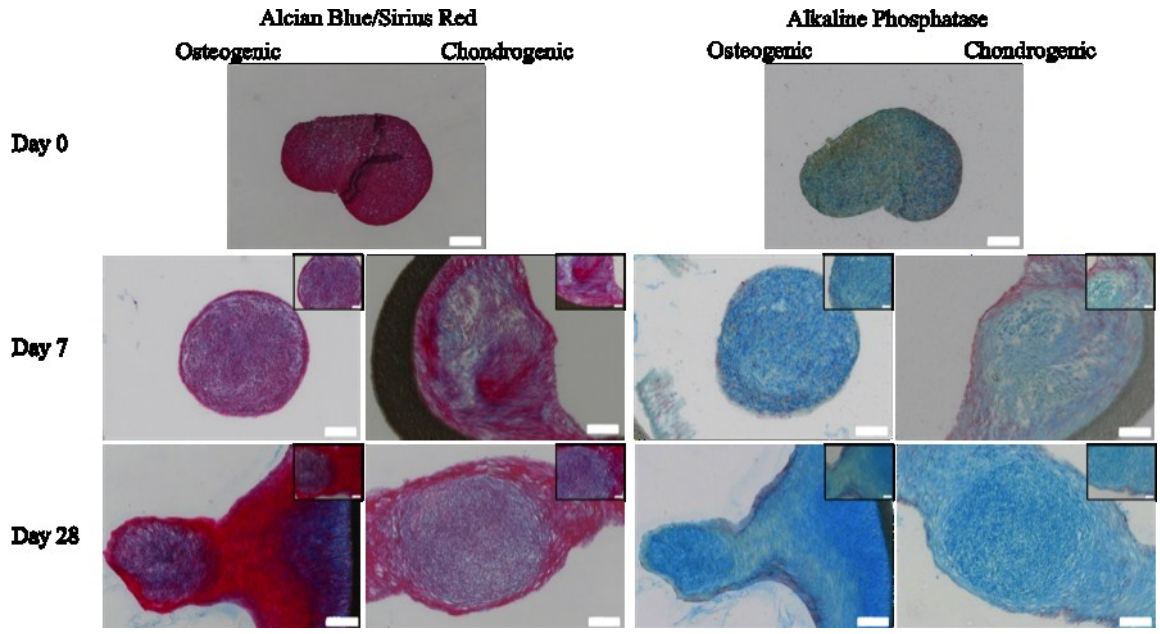

Figure 4:26 Foetal cell only pellets ($1.5x10^5$ cells/pellet). Alcian blue/Sirius Red and alkaline phosphatase staining for day 0, 7 and 28 days in osteogenic and chondrogenic conditions. Scale bars represent 100μm and inserts represent 50μm.

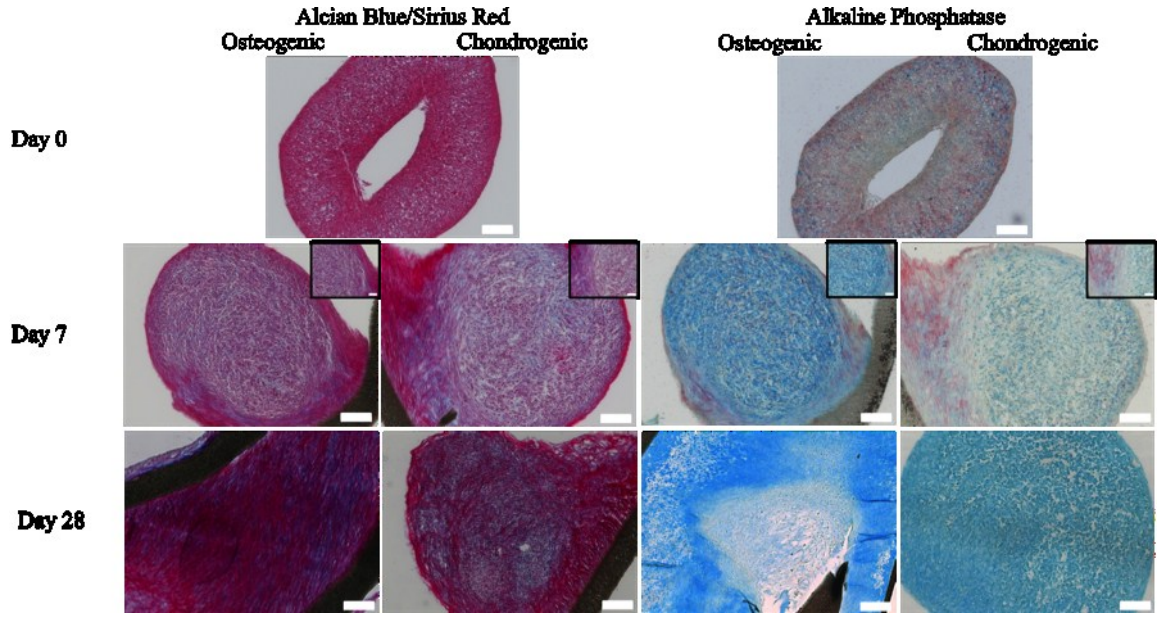

Figure 4:27 Foetal cell only pellets ($3x10^5$ cells/pellet). Alcian blue/Sirius Red and alkaline phosphatase staining for day 0, 7 and 28 days in osteogenic and chondrogenic conditions. Scale bars represent 100μm and inserts represent 50μm.

Alcian Blue/Sirius Red staining on the co-culture pellets at day 0 revealed predominantly collagen and minimal alkaline phosphatase. FISH was performed in order to identify the two cell types within the pellet. At day 0, the mix of the pellets is clearly visible. By day 7, FISH revealed the beginning of separation of the cell populations, which was more pronounced by day 28 of culture. Day 7 mixed pellets showed small clumps of embryonic cells that grew in ring like structures; this region of cells also displayed a different morphology (long and flat) to the surrounding foetal cells (rounded) (Figure 4:28). By day 28 of culture there was a more pronounced special organization of the cells into distinct areas and these cells had different morphologies. Distinct separation of regions was observed in the mixed pellets only (particularly in the day 28 cultures) and therefore is not thought to be a processing artefact. Under osteogenic conditions, distinct clumps of highly dense cells were seen and determined to be the embryonic cell population. Predominantly in these cultures throughout the pellet the majority of the cells were from the embryonic cell population with foetal cells located more sparsely in the spaces between the embryonic clumps, throughout the pellet. There was also a distinct separation of regions of the pellet, which was not seen in the chondrogenic pellet cultures suggesting that this was not a processing artefact. In contrast to this in the chondrogenic pellets, a majority foetal cell population and an alternative cellular structure was observed. There was a distinct foetal cell core, where the cells were packed much closer together. Cells with different morphologies defined the edge of the core. Although there was the presence of some lone embryonic cells, the majority was found at the edges of the pellet and this was consistent throughout the sections (Figure 4:28).

Similarly to the foetal only pellets, at day 0 of culture, Alcian Blue/Sirius Red staining revealed collagen staining alone. At day 7 in both the mixed osteogenic and chondrogenic pellets, mixed staining is observed with the strongest Sirius Red staining observed at the edges of the pellet. At day 28 of culture, in the osteogenic pellets, due to the separation of the cell regions it is difficult to determine the location of the staining with respect to the inner or outer region of the pellet. The embryonic cell clump showed Alcian Blue staining only, indicating strong proteoglycan. However, pellets cultured in each conditioned revealed extreme proteoglycan staining. In the chondrogenic pellets, strong Sirius Red staining was observed, with staining also observed in the ring structures determined by FISH to be the embryonic stem cells (Figure 4:28). Minimal

alkaline phosphatase staining was observed in the day 0 pellets. Strong alkaline phosphatase staining was seen at the edges of both the chondrogenic and osteogenic cultured pellets at day 7 of culture, with the strongest staining observed in the osteogenic pellets. Staining was observed in the centre of each of the pellets also, and where the ring structures of embryonic cells are located. By day 28, the alkaline phosphatase expression was lost with no staining observed in the osteogenic pellets and only minimal staining in the chondrogenic pellets.

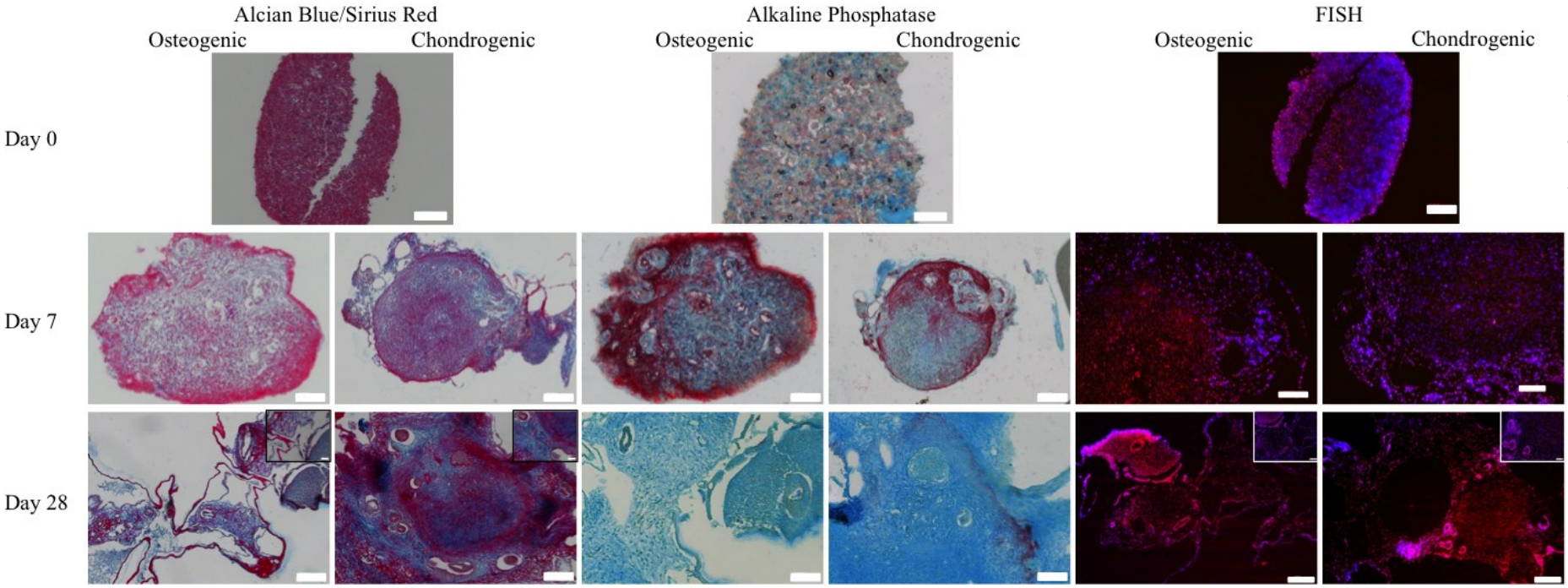

populations. Alcian blue/Sirius Red and alkaline phosphatase staining for day 0, 7 and 28 days in osteogenic and chondrogenic conditions. FISH staining also shown for localisation of foetal and human ES cells, defined red spots of stain show location of human ES cells. Scale bars represent 100μm and inserts represent 50μm.

Type I and II collagen staining was also performed. Looking at foetal cell only pellets, in both sized day 0 pellets, there was minimal type I collagen staining observed, and greater type II collagen staining. In the $1.5x10^5$ cell pellets at day 7, strong type I and II collagen staining was observed, and this was also seen in the chondrogenic pellets. By day 28 of culture, in osteogenic conditions strong type I collagen staining was observed and less type II collagen staining (Figure 4:29). Similar expression was seen in the $3x10^5$ pellets, however stronger type I staining was observed in the osteogenic pellets at day 28, and weaker expression of type II staining was observed in the day 7 chondrogenic pellets (Figure 4:30).

The co-culture pellets revealed little type I collagen at day 0, with greater type II collagen staining observed. Expression of type I and II collagen was observed in the mixed pellets, however, staining was weaker than that observed for the foetal only pellets. Additionally staining observed was limited to the regions around the foetal cells, none from the embryonic cell regions (Figure 4:31).

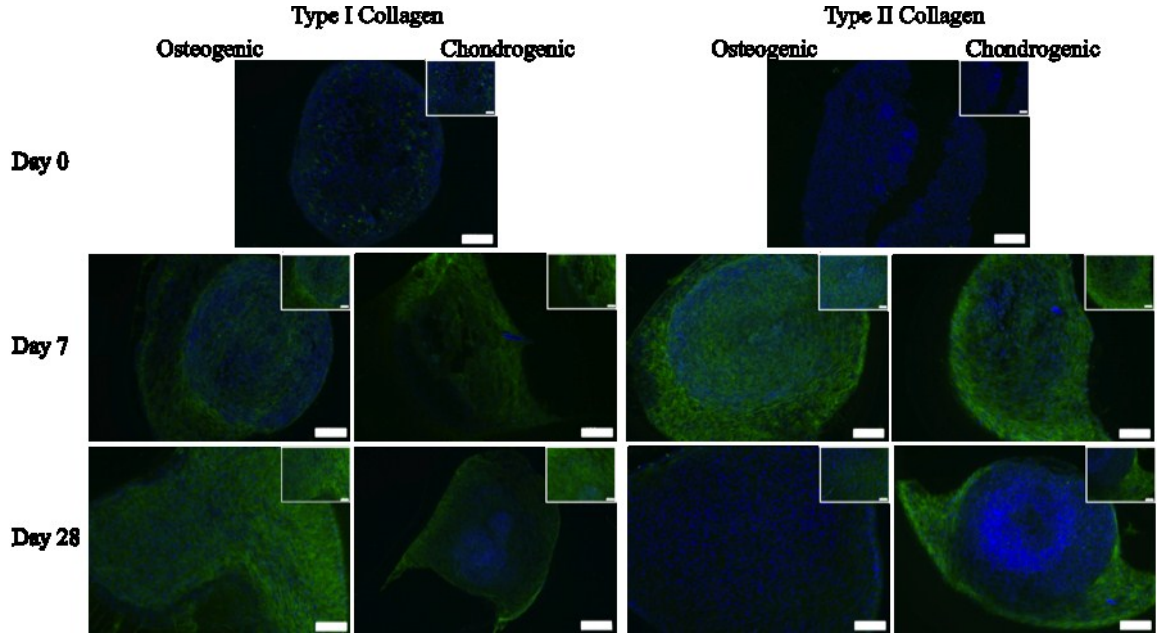

Figure 4:29 Foetal cell only pellets ($1.5x10^5$ cells/pellet). Type I and II collagen staining (FITC with DAPI nuclear counterstain) for day 0, 7 and 28 days in osteogenic and chondrogenic conditions. Scale bars represent 100μm and inserts represent 50μm.

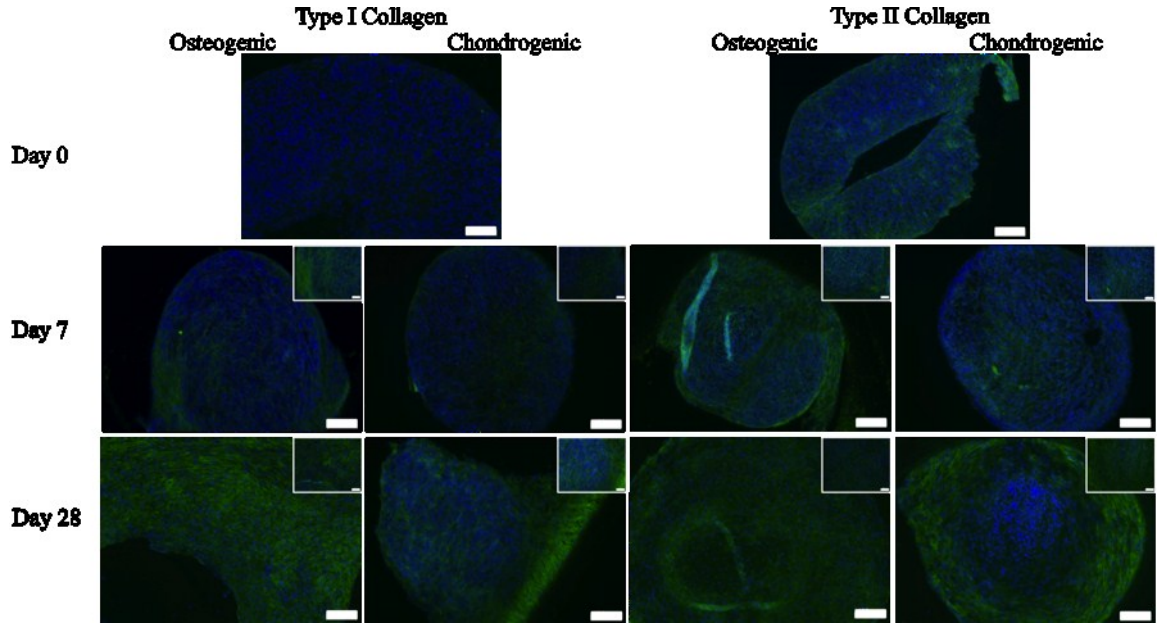

Figure 4:30 Foetal cell only pellets ($3x10^5$ cells/pellet). Type I and II collagen staining (FITC with DAPI nuclear counterstain) for day 0, 7 and 28 days in osteogenic and chondrogenic conditions. Scale bars represent 100μm and inserts represent 50μm.

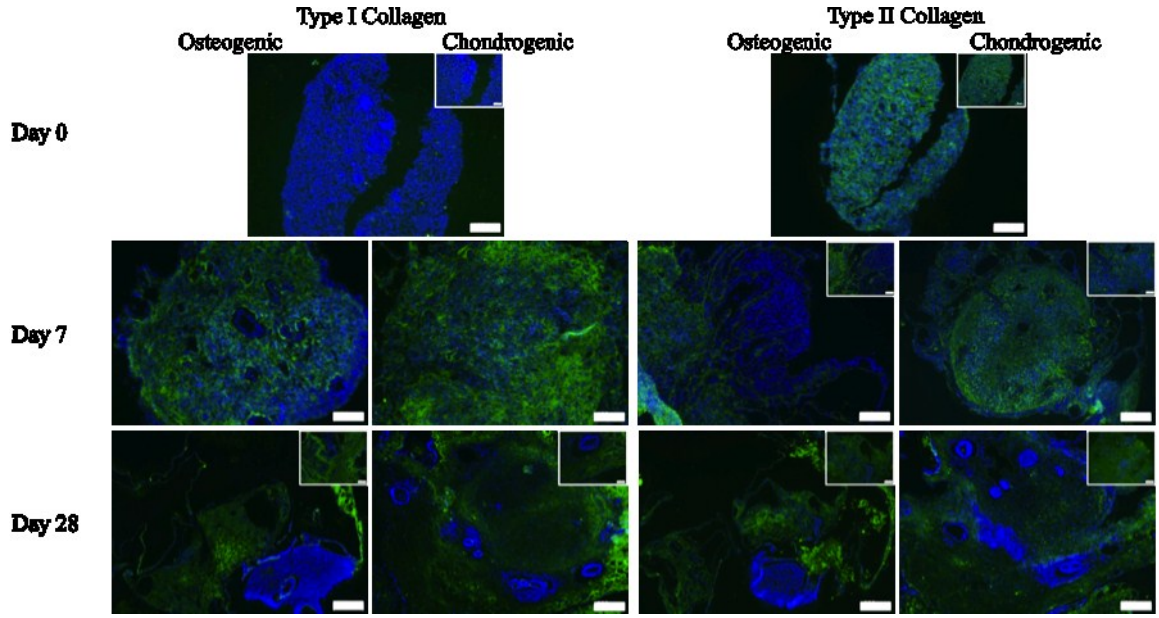

Figure 4:31 Co-culture pellets for HUES- 7 and foetal mixed cell populations. Type I and II collagen staining (FITC with DAPI nuclear counterstain) for day 0, 7 and 28 days in osteogenic and chondrogenic conditions. Scale bars represent 100μm and inserts represent 50μm.

4.4 Discussion

These studies focussed on devising strategies for the differentiation of human ES cells (toward the mesoderm lineage) and foetal femur-derived cells, followed by their characterisation. The initial differentiation strategy taken was the formation of EBs. The formation of EBs from ES cells that had been cultured on matrigel was detrimental to EB formation. However, EB formation using ES cells that were cultured on MEF feeder layer was successful. This occurrence was also observed by Denning et al (2006), who also used the HUES-7 cell line as well as the BG01 cell line and using both cell lines was unable to successfully form EBs from feeder free cultures. Similarly, Denning and colleagues opted to generate EBs directly from MEF feeder layer cultures in a suspension culture system.

The culture conditions and media composition for the maintenance of the pluripotent state of ES cells is better characterised than methods for the formation of EBs, which is likely to contribute greatly to the lineage differentiation of the cells. As several methods can be adopted for the formation of EBs, there is significant heterogeneity of EBs in morphology and differentiation status (Bratt-Leal et al., 2009). In the majority of reports, the resulting spherical aggregate is considered an EB irrespective of the differentiation status (Koike et al., 2007). The formation and early differentiation of EBs occurs in two phases: within the first 2–4 days of suspension culture, endoderm forms on the surface of EBs, giving rise to structures termed ‘‘simple embryoid bodies’’; subsequently, around day 4, ‘‘cystic’’ EBs develop with the formation of a central cavity and differentiation of a columnar epithelium with a basal lamina (Khoo et al., 2005). In these studies, the formation of cystic EBs was observed by day 5 of culture (data shown in section 3.4.2). In vitro culturing of EBs commences with the development of cells indicative of the ectoderm, mesoderm, and endoderm germ lineages, with continued culturing resulting in more differentiated cell types, including insulin-producing cells, neuronal cells, and hematopoietic cells (reviewed by Khoo et al (2005)).

Alkaline phosphatases are found in a variety of species, comprising a multi-gene family and are generally located at the cell surface (MacGregor et al., 1995). Alkaline phosphatase staining was performed on EBs grown in osteogenic and chondrogenic

conditions with no loss in expression observed over 15 days. In human ES cells, alkaline phosphatase positive colony formation has been used as a specific endpoint for quantifying pluripotent ES cells. In mouse ES cells the loss of this ability is one of the earliest indicators of differentiation induction (O'Connor et al., 2008). The expression of alkaline phosphatase as a marker of both bone differentiation and the pluripotent ES cell make the use of alkaline phosphatase as a histological marker difficult and inconclusive.

EBs were generated in standard EB media supplemented with osteogenic and chondrogenic factors in order to direct the cells toward the osteogenic and chondrogenic lineages. Typically following formation and over time in culture, we would expect to see markers for all three germ layer lineages in those EBs cultured under standard conditions as shown by Itskovitz-Eldor and colleagues (2000). Although it has been suggested that some cell lines show a greater affinity for differentiation along a particular lineage (Karner et al., 2007).

The addition of growth factors immediately following the dissociation of the ES cells to form EBs ensures the exposure of the majority of the cells to the factors. Growth factor addition following EB formation risks the exposure of only the outer most cells, as they are unable to diffuse to the cells in the centre of the EB. However, investigations into EB oxygenation by Gassmann et al (1996) revealed a shallow oxygen tension gradient across day 13 and 14 EBs, attributing this finding to the loose packing of cells within EBs. The authors went on to show that most cells, regardless of position within the EB, were viable and concluded that it was therefore likely that most cells within an EB are appropriately supplied with nutrients and should not suffer from an accumulation of toxic metabolic waste products. Dang et al (2002) suggested that at later stages of embryoid body development, agglomeration of the EBs may have negative effects on cell proliferation and differentiation, as was shown in the mouse system. When formed in static cultures, agglomerated large EBs revealed extensive cell death and eventually large necrotic centres due to mass transport limitations. Gothard and colleagues (2009) suggested that significant core necrosis was only observed in EBs cultured for more than 5 days. In relation to the studies performed here this suggests that the EBs formed were unlikely to have problems relating to nutrient supply and due to a culture time of 5 days were unlikely to have many necrotic cells.

Molecular characterisation of EBs cultured for 5 days, were inconsistent across experiments, although the results suggested a loss in pluripotency, with expression of pluripotency markers OCT-4 and NANOG lost in all three media conditions examined. Similarly, differentiation marker expression was inconsistent across the studies. Noaksson et al (2005) developed a quantitative-PCR method in which by measuring the relative mRNA levels of Oct-4, Cripto, Nanog and AFP and combining these values to form an expression index, they were able to distinguish between undifferentiated ES cells and their early derivatives. The authors observed a difference between the expression indexes for undifferentiated ES cells cultured on MEFs and on matrigel. Similar to the profiles observed here the kinetics of disappearance of the various antigens tested were different. Although it was unclear if this difference was a true reflection of expression levels or a difference in the antigen turnover. As observed in this work, Noaksson and colleagues observed that none of the pluripotency marker antigens disappeared completely in the ES cell populations.

It would be anticipated that the EBs grown in standard EB conditions would reveal expression of various embryonic lineage markers, corresponding to all three embryonic germ lineages, as shown by Itskovitz-Eldor and colleagues (2000). The authors used different embryonic lineages markers to those used in these studies, namely zeta-globin (mesoderm), neurofilament 68Kd (ectoderm), and alpha-fetoprotein (endoderm). The authors also presented a synchronously pulsing embryoid body expressing the myocardium marker alpha-cardiac actin. In this current study, when cultured in standard EB media, a 4-fold increase in BMP-4 expression was observed in all 3 experiments, as well as an increase in SOX-1 expression in 2 studies, suggesting a differentiation of the cells toward the mesoderm and ectoderm lineages. For the EBs formed and cultured in the presence of chondrogenic conditions, a significant increase in the relative expression of BMP-4 was observed in 2 of the 3 repeats suggesting a possible push in the differentiation of the cells toward the mesoderm lineage. There was also an increase in BMP-4 expression in osteogenic conditions in 2 of the 3 repeats. These results suggest a potential for the ES cells to be directed toward mesoderm differentiation, although from the results obtained it is unclear which factors in the media are the most critical to induce and direct the cells differentiation, however it would be anticipated that members of the TGFβ or BMP signalling pathways could play a role. zur Neiden et al (2007),

suggested that the timing of factor addition was crucial in optimisation of ES cell differentiation protocols, specifically the addition of BMP-2 later than 6 days from EB formation enhanced osteoinduction. Similarly, Jackson et al (2010) showed that ES cells pass through a series of 'windows' in which the ES cells gain and lose competence to respond to three inducers of primitive streak transcription factors, BMP4, Wnt3a and Activin A. The group also showed that a portion of the differentiating cells were committed to mesoderm formation by day 3 (of 5) of culture and did not require further signalling from inducing molecules in the final 2 days of the differentiation. In order to expand on this study a greater number time points in would be needed in order to identify possible 'windows' of marker expression, which may not have been identified here. This would provide a more reliable determination of the differentiation pathway taken by the cells.

In contrast to 2-D planar culture formats, only the cells on the exterior of 3-D EBs (and similarly, it must be assumed for the 3-D pellet organotypic culture described later) are in direct contact with soluble factors present in the culture medium. Soluble factors must diffuse through the multilayered cell environment and transport barriers, which are likely to vary as a function of stages of EB differentiation (Bratt-Leal et al., 2009). Bratt-Leal and colleagues, performed high-power SEM microscopy analysis of EBs, and showed that the surface layer of epithelial-like cells exhibit tight cell-cell junctions. Cross-sectional analysis revealed that the EBs tended to form a dense layer of ECM at the EB periphery compared to the centre. The authors concluded that steric barriers to diffusion posed by the EB structure made it unlikely that homogenous concentrations of molecules could be attained uniformly throughout the EB, and would therefore limit the efficacy of differentiation strategies that rely solely on the addition of soluble factors to the culture medium. However, as discussed previously, studies by Gassmann et al (1996), Dang et al (2002) and Gothard et al (2009) suggest that cells in the centre of EBs are provided with nutrients and that necrosis of the core does not occur in day 5 EBs and therefore that this would be in the case for the EBs formed in these studies. Additionally, combined with published data, since growth factor application was begun at day 0 of study, it would not be anticipated that the exposure of the cells to the growth factors would be a limiting factor in these studies.

In these current studies, a series of co-culture studies in monolayer were performed, the first, the passage of HUES-7 cells onto a foetal cell layer. HUES-7 cells successfully adhered to the cells and remained as a colony in culture. Cells were cultured in basal and osteogenic conditions with similar staining profile for both. Alkaline phosphatase staining was stronger in osteogenic conditions than basal conditions, although as discussed previously the expression profile of alkaline phosphatase cannot be used as a reliable marker of differentiation of the ES cells. A loss of pluripotency marker expression was observed in the ES cell colonies in both basal and osteogenic conditions, although there was no type I or II collagen expression from the colonies, limiting the determination of the level of differentiation. The type I and II collagen staining observed in the foetal cells, may be a result of matrix secretion prior to ES cell addition (as the foetal layer was confluent). In order to expand on this study the use of mitotically inactivated foetal femur-derived cells could be used which would allow for longer time course studies, whilst still enabling the secretion of any soluble factors from the foetal cells and the maintenance of cell-cell contact.

In comparison to the culture of single ES cells alone, a greater proportion of the ES cells were observed to adhere in the presence of foetal cells (although this was not quantified) and equally greater cell adherence was observed when the ES cells were cultured with foetal cell conditioned media. Koyanagi-Katsuta et al (2000) observed that the apoptosis of mouse ES cells was induced when the cells were dispersed as single cells as opposed to dispersion as aggregates, similarly this was observed in the HUES-7 cells which had been trypsin treated to produce single cells and cultured in both osteogenic and chondrogenic medium as well as MEF conditioned media. The findings of Koyanagi-Katsuta and colleagues support the idea that ES cells easily commit to apoptosis and it is cell-cell interaction between the ES cells which blocks this process. This may explain the lack of adhesion of the HUES-7 cells when cultured as single cells. It was also observed that single cell cultures in foetal cell conditioned osteogenic media were able to adhere and proliferate where those cultured in osteogenic media alone did not thrive in culture. This suggests that a factor secreted from the foetal cells was responsible for either protecting the cells from apoptosis or aiding the adherence and thus proliferation of the cells. The observations of this study also suggest that the stress of placing the cells into single cell suspensions can influence the differentiation pathway. This could explain the inconsistencies seen in the molecular

data for all cells that have been exposed to trypsin treatment. Although unlike the conditions, where the ES cells were cultured as single cells and not exposed to foetal cell conditioned media, the stress already exposed to the cells begun their differentiation along a particular lineage. Alternatively, differences in osteogenic conditioned media composition could be responsible for the differences in the molecular data obtained.
A loss of the alkaline phosphatase specific activity of the co-cultured cells, compared to foetal only cell activity was observed and confirmed by histological staining. These results suggest a possible inhibition of differentiation of the foetal cells by the presence of the embryonic cell population. Portnoy et al (2006), observed an inhibition of fibroblast proliferation in a co-culture with ATII cells, due to the transcription factors secreted by the cells. Specifically the secretion of interleukin-1α (IL-1α) by ATII cells stimulates prostaglandin E2 (PGE2) production and inhibits fibroblast differentiation.

Single ES cells cultured in the presence of foetal cell osteogenic conditioned media displayed a loss of pluripotency marker expression in all studies, suggesting differentiation of the cells. Differentiation marker expression was variable with no clear trend observed for Brachyury or alkaline phosphatase expression. For both SOX-1 and SOX-17 expression, increase in expression levels was observed in 3 of the 4 populations, although this was observed at different time points in each population. In the case of BMP-4, an increase of up to 50 fold was observed, although the peak expression levels varied over time. Overall, the results here indicate early differentiation of the cells. This finding is supported by the findings of Akiyama et al (2000), who using ATDC5 cells (murine chondrocytic cell line), which expressed transcripts of BMP-4 in the undifferentiated (day 3) and condensation (day 5) stages, observed a decline in the BMP-4 mRNA levels when the growth of cartilage nodules ceased after 2 weeks. Previous studies have also shown that short-term treatment of ES cells with BMP-4 initiates mesoderm formation, whereas long-term treatment results in the formation of extra-embryonic endoderm and trophoblast (Zhang et al., 2008). Additionally, this increase in BMP-4 expression may be the result of the conditioned media application. BMP-2 was supplemented to the foetal cells for conditioned media. The effects of BMP-2 on expression of other BMPs has been investigated, using recombinant BMP-2, this resulted in enhanced BMP-3 and -4 mRNA expression associated with increased expression of bone cell differentiation marker genes, alkaline

phosphatase, type I collagen, osteocalcin, osteopontin, and bone sialoprotein (Chen et al., 1997). In the studies performed here, BMP-2 was not added to EBs in osteogenic conditions. No increase in BMP-4 mRNA expression was observed. A time dependent effect of BMP-2 to increase chondrogenic differentiation in EBs has also been observed, limited to a time window between day 2 and 5 of EB development. This early stage of ES differentiation is a period of early mesoderm development characterised by Brachyury and BMP-4 expression, with BMP-2 playing a pivotal role in inducing precursor cells to the chondrogenic fate (Kramer et al., 2000). Previous studies have also shown that at the early stage of mesoderm differentiation, other differentiation factors such as retinoic acid can act to influence the differentiation pathway (Wobus et al., 1994).

The human ES cell microenvironment has been shown to contain soluble factors capable of inhibiting the growth of cancer cells (Giuffrida et al., 2009). Similarly to the studies performed here, human ES cell conditioned media was used from cells cultured on MEFs. Experiments were performed using different concentrations of conditioned medium as well as conditioned media obtained from day 3 cultures. It was found that 25%, 50% and 70% dilution of conditioned media caused a decrease in cell proliferation when compared to MEF CM alone, confirming that the effect of inhibiting cancer cell growth was not the result of depleting culture medium of crucial growth factors. Giuffrida et al (2009), suggested that the mechanism by which the human ES cell conditioned medium was able to inhibit the growth of cancer cells was through the production of soluble factors capable of blocking cancer cell proliferation by slowing progression of cancer cells through the cell cycle without affecting cell death. However, the authors did not identify the specific factor responsible. This data complements the data obtained here with the application of 50% and 100% ES cell conditioned media to foetal femur derived cells, where the relative expression levels of typical bone and cartilage markers were observed to be decreased after three days of culture, demonstrating a possible inhibition or dedifferentiation mechanism by soluble factors within the conditioned media. The morphology of these cells was not observed to be significantly different from the standard fibroblastic morphology seen under typical culture conditions.

A loss of type II collagen expression was observed in 3 of 4 of the repeats in the treated samples compared to the original untreated cells, with a significant loss in expression seen in all 3 samples treated with 50% ES conditioned media. For both 100% and 50% ES cell conditioned media conditions in all studies, alkaline phosphatase showed a significant two fold decrease or greater in expression. Significant increase in RUNX-2 expression was observed in 2 of the 4 samples, whilst a significant 2 fold loss or greater in expression of SOX-9 and SOX-1 was observed in 3 samples. In the case of the fourth sample set an increase in the expression levels of SOX-9 and SOX-1 was observed, supporting the hypothesis that differences in the cell starting population are responsible for the differentiation path. Finally, osteonectin and BSP expression levels were also quantified and found to be variable across all repeats. The loss of type II collagen, alkaline phosphatase and SOX-9 expression indicating the foetal cells had stopped differentiating. RUNX-2 is an important transcription factor necessary for osteoblast differentiation and bone formation, so it is unclear why an increase in expression would be seen in the two populations. However, these studies were only performed for a limited time frame (3 days), so it is possible that this increase in expression would be followed by a decrease in expression levels, supporting the idea that the differentiation of the cells has been halted. To expand on these studies and determine any de-differentiation of the cells, a longer time course would be needed, looking at expression levels at various time points of culture as well as any effects on cell proliferation.

Both 2- and 3- dimensional culture systems were investigated in order to establish the differences in differentiation potential and path of the cells. Osteogenic and chondrogenic cells have been extensively investigated using the traditional 2-D culture systems. For studies of chondrogenic differentiation, the 3-D culture model, (pellet culture) has successfully been utilised for maintenance of the chondrogenic phenotype (Tare et al., 2005). Three dimensional culture conditions may mimic the *in vivo* environment more closely, with some reports indicating distinct cellular behaviour within 3-D culture systems that are not observed in monolayer culture (Levenberg et al., 2003, Baharvand et al., 2006). Jarrahy et al (2005) investigated the osteogenic and angiogenic differentiation of murine preosteoblastic cells (MC3T3-E1) cultured in 2-D and 3-D culture conditions. Their results indicated that the MC3T3-E1 cells commit to osteogenic differentiation at a slower rate when cultured on 3-D scaffolds. In contrast, these cells when cultured in three dimensions preferentially express markers for

angiogenic expression. The organotypic model as well as providing a 3-D model also provides a liquid-air interface to further mimic the *in vivo* environment. Co-culture pellets of HUES-7 ES cells and foetal femur derived cells were utilised to ultimately direct the differentiation of the ES cells toward bone and cartilage. Foetal only pellets displayed an abundance of type I and II collagen at days 7 and 28. Type I collagen was predominantly located on the edges of the pellet with proteoglycan located in the centre. Alkaline phosphatase expression was lost in the day 28 pellets. Alkaline phosphatase seen at day 0 and 7 is likely to be carry-over from the original foetal culture. As the phenotype observed in the two foetal sized pellets were similar, pellet size was not thought to be a determining factor in the differentiation pathway in these studies. The loss of alkaline phosphatase staining in the day 28 mixed cell pellets compliments the biochemical data obtained in the 2-D co-culture study, which demonstrated a fall in alkaline phosphatase specific activity of the co-cultured cells, compared to foetal only cell activity. This was also observed in the histological analysis. These results support a possible inhibition of differentiation of the foetal cells by the presence of the embryonic cell population. However, total loss of expression was also observed in the foetal only pellets.

At day 28 of culture, in the mixed cell pellets, type I and II collagen staining was not as prominent as that observed in the foetal only pellets. Clear regions of embryonic stem cells, particularly the dense cell clumps and any substantial matrix did not surround epithelial structures. This observation similarly suggests a possible inhibition of differentiation or a loss of differentiation potential by the foetal cell population, due to the presence of the embryonic cell population.

Spatial organisation of the two cell types in the mixed pellets was observed in the day 28 pellets, with some separation of the ES and foetal cells seen at day 7 of culture. The separation could be observed in culture by the spreading of the pellet across the membrane. In contrast to the foetal only pellets which remained uniform in shape. The absence of any spaces in the foetal pellets suggests that the gaps between cell groups observed in the mixed pellets are not a processing artefact. Spatial organisation of three-dimensional co-cultures has been observed in human breast cancer cells that were drug resistant or drug sensitive (Starzec et al., 2003). Immunostaining showed that in the mixed cell cultures (termed nodules), the drug sensitive cells arranged themselves at the

periphery, whereas the drug resistant cells were located in the central part of the nodule (Starzec et al., 2003).

Day 28 mixed pellets cultured in chondrogenic media, displayed a striking morphology with foetal cells located in a central cluster, whilst surrounded by a majority of ES cells. Within the ES cell arrangement, cells of distinct morphologies were apparent, particularly cells which displayed an epithelial-like morphology. Similarly, these structures were also observed in the osteogenic pellets, however fewer foetal cells were observed which were found amongst the sparse embryonic cell population, although the reason for this remains unclear.

In these studies, the starting cell population and differences in their pluripotent state may also act as a critical factor in the potential of the cells to be directed toward a particular lineage regardless of differentiation strategy. However, since the foetal femur-derived cells are a primary cell line, the level of heterogeneity in the sample cannot be controlled.

As yet, the biological significance of the cell arrangement observed in the mixed organotypic culture pellets remains unclear. It may represent a protection mechanism, by which cells could maintain their viability under unfavourable culture conditions, i.e., the presence of a second cell type or the result of a hypoxic or nutritional gradient within the pellet (Jarrahy et al., 2005). The differentiation pathway and indeed rate of differentiation may also be influenced by the presence of the second cell type, for example by inhibition of differentiation by soluble factors secreted by the cells, which has been discussed previously. The ECM can be a potent mitigator of cell fate decision as it provides a complex assembly of morphogenic cues to cells (Bratt-Leal et al., 2009). The findings here suggest that the cell-cell contacts and cell-matrix contacts may play a significant role in the differentiation and organisation of the cells within the pellet.

In order to develop these studies, characterisation of the ES cell differentiation would be performed. In the organotypic culture studies, within the mixed cell pellets, an epithelial-like cell structure was observed in the embryonic stem cells, forming circular regions of cells. Further characterisation of these pellets would require the testing of the

presence of tight junctions. Tight-junctions are the closely associated areas of two cells whose membranes join together forming a virtually impermeable barrier to fluid. The presence of tight junctions would indicate structural specialisation typical for epithelial-like polarization (Chung et al., 2008). The tight junction-specific peripheral membrane protein, ZO-1, has been used previously to determine tight junction development in the mouse preimplantation embryo (Fleming et al., 1989). Additionally, since the co-culture organotypic model was unsuccessful in completely driving the cells toward osteogenic and chondrogenic differentiation, an investigation into the most suitable growth factors would allow for the optimisation of the model as a tissue engineering strategy.

In summary, the data presented in this chapter suggest a potential for the differentiation of human ES cells along the bone and cartilage lineages through a combination of foetal cell interactions and growth factor supplementation. The use of growth factors such as ascorbate and dexamethasone typically used in bone and cartilage differentiation media, were able to successfully induce an increase in BMP-4 expression in both EBs and in monolayer culture. Although the organotypic culture system was unsuccessful in completely driving the cells toward osteogenic and chondrogenic differentiation, the model confirms the potential for tissue engineering strategies. This would require an investigation into the most suitable growth factors to direct the differentiation of the cells, as well as investigation into the timing of their application.

Chapter 5 Use of dielectrophoresis for progenitor cell selection and characterisation

(work in collaboration with Dr Fatima Labeed and Professor Mike Hughes at the University of Surrey and Dr Lisa Flanagan at University of California, Irvine).

5.1 Introduction

The term dielectrophoresis (DEP) is applied to particles that have been subjected to a non-uniform electric field. The phenomenon was first described by Herbert Pohl (Pohl, 1978). This force does not require the particle to be charged but instead affects all particles that experience an electric field. DEP is an example of an AC electro kinetic technique, which measures the movement of particles subjected to a non-uniform electric field and can be used to manipulate, separate and analyse cellular scale particles, utilising the differences in the electric polarisability of particles and the surrounding liquid (Hughes, 2002a). These properties can then be used to infer biological properties, as well as offering a novel method by which cells can be separated based on their unique dielectrophoretic profile.

The development of devices that utilise DEP for the characterisation and later separation of cells has a broad range of applications in biomedical sciences. The development of a DEP based separation technique removes the need for biochemical labels and tags, which is particularly relevant when in some cases these have not been identified. Typically, for a heterogeneous cell population, FACS or MACS is used to separate cell subsets, which is reliant on the identification and availability of unique cell surface antigens and their specific antibodies. It is for this reason that the dielectric properties of stem or progenitor cells are of particular interest. Once identified and separated from heterogeneous cell populations this would allow the investigation of the stem cell biology of these cells as well as their potential for use in regenerative medicine therapies.

There are a number of examples utilising DEP for cell enrichment. CD34+ cells have been enriched from peripheral blood stem cell harvests using DEP (Stephens et al., 1996). CD34+ cells were placed in a separation chamber and using selective trapping of the cells by either positive or negative DEP, a five-fold enrichment of the CD34+ cell population was achieved. A further finding of this work was that the colony-forming capability of these cells was not affected by the application of the electric field (which ranged from 5kHz–500kHz). The dielectric properties of breast carcinoma and the surrounding tissues have also been characterised and significant differences in the dielectric properties of the samples derived from different locations observed (Surowiec

et al., 1988). These differences were associated with cellular heterogeneity and structural differences within the samples. This work suggests that dielectrophoresis can be used as a diagnostic model for breast carcinoma. Following on from this Becker and colleagues (1995), were able to show that the dielectric properties of the human breast cancer cell line MDA231 were significantly different from those of erythrocytes and T lymphocytes, and were able to exploit these properties to separate cancer cells from normal blood cells.

It has also been suggested that DEP can be used for cell patterning in tissue engineering strategies (Lin et al., 2006). This can be achieved by using either positive or negative DEP. In positive DEP, the cells are attracted and concentrated to a local electric field, as opposed to negative DEP where the cells are pushed away from the electrodes and toward an electric field minimum.

To date, there have been few studies looking at the effects of DEP on osteoblasts and osteoblasts-like cells and their dielectrophoretic characterisation. A study by Zou et al (2006), used DEP to manipulate and position osteoblasts using micro-electro-mechanical systems (MEMS) technology. The experiments showed that the osteoblasts experienced negative DEP at 0.1MHz, and positive DEP when suspended in iso-osmotic culture medium and exposed to AC fields at 5MHz frequency. The viability of the osteoblasts exposed to dielectrophoresis was also assessed and found to be three times higher than control values, from which the authors concluded that DEP "may have an anabolic effect on osteoblasts".

In the current studies, two distinct systems have been used to characterise skeletal cells. The first approach uses a well chip device, this is a novel 3-D dielectrophoretic device fabricated from laminate and copper tape alternating layers with insulating polyimide layers of adhesive. This is an extension of the original concept of alternating conductor-insulator laminates described for flow separation systems (Fatoyinbo et al., 2005), and described further by Hubner et al (2005a) with images of device set-up shown in section 2.11.2. The design of the three-dimensional electrode is relevant to the 'lab-on-a-chip' systems that are currently being developed for use in research and diagnostics in biological sciences. The capability of this system has previously been shown in determining the effects of different drugs on red blood cells (Hubner et al., 2005a), and

antibiotic resistance in *E.Coli* (Hoettges et al., 2007). It has also been used as a quantitative tool in revealing dielectric differences in the cytoplasm and membrane of oral cancer cells (Broche et al., 2007), as well as to study apoptotic cells (Labeed et al., 2006).

The second device used, employed a microfluidics system and the induction of a frequency-dependent dipole in cells as a characterisation technique. The device was fabricated as described by Wang et al (2007). Using either a silicon wafer or glass slide, a series of SU-8 (epoxy based photoresist) patterning techniques were used to make the walls of the channel with the microelectrodes embedded using an electroplating technique, in total there were 3 groups of electrodes in each channel with each group containing 16 electrodes. In contrast to the 3-D dielectric device, this device used a fluid flow and used cell trapping data at 8 voltages and various frequencies between 25kHz-10MHz. Using this device, the unique dielectric properties of undifferentiated mouse neural stem/precursor cell populations were determined and found to be different to the differentiated neurons and astrocytes. Flanagan et al (2008b), showed a shift in the dielectric properties of cells isolated at different developmental stages and suggested that this shift was reflective of a fate bias of the cells which preceded detectable marker expression in these cells and thereby identifying specific progenitor cell populations. These findings support the use of DEP as a cell characterisation and sorting tool.

This work was conducted in collaboration with University of Surrey and UCI through a series of extensive collaborative visits. The two sites provided all necessary facilities while cells were provided by University of Southampton (Bone and Joint group). All data capture and analysis was led by Ayshe Ismail and reviewed with the collaborators.

5.2 Aims

The current study set sought to examine, using these two devices the following;

- A dielectric fingerprint for homogenous osteogenic cell populations.
- The potential for separation of osteoprogenitor cells from heterogeneous populations.

5.3 Materials and Methods

Tissue culture plastics were obtained from Elkay, Basingstoke, UK and Greiner Bio-one, Gloucester, UK and reagents from Sigma-Aldrich, Dorset, UK unless otherwise stated. Equipment utilised for DEP studies were from University of Surrey (Faculty of Engineering and Physical Sciences) and University of California, Irvine (School of Medicine, Pathology & Laboratory Medicine).

5.3.1 Data Analysis

The camera, signal generator and oscilloscope used were controlled by MatLab (release 2006b Mathworks, Natick, USA) script. Image capture, signal processing, and data analysis (including graphs and model plotting) were performed using specifically designed MatLab scripts by Dr Kai Hoettges. Cell radius was measured using Image J (downloaded from http://rsbweb.nih.gov/ij/).

5.3.2 Dielectrophoretic Well Chip – Microwell System

The microwell system used was a 3-D dielectrophoretic device made up of insulating layers of metal and insulator. This is briefly described in section 5.1 and further by Fatoyinbo et al (2005) and Hubner et al (2005a).

5.3.3 Cell Culture

MG-63 (human osteoblast like) and SAOS-2 (sarcoma osteogenic) cell lines were maintained in basal medium (DMEM containing 10% FCS) at 37^{o}C, supplemented with 5% CO_2. STRO-1 positive cells were maintained in standard media and culture conditions. The cells were maintained by routine passage at 70-80% confluence.

5.3.3.1 Cell Preparation

Cells were prepared by repeated washing to remove as much of the standard culture media as possible. The cells were detached from the plastic using trypsin-EDTA for 5 minutes, and then spun at 1100rpm for 4 minutes at 4^{o}C. The pellet was then resuspended in conductivity medium and washed twice before being finally resuspended in 1ml of 100µS conductivity medium as described in section 2.12.1.1.

5.3.4 Dielectrophoretic Procedure

Cells were prepared as described in section 5.3.3.1. For each experiment, approximately 1µl of cell solution was injected into the well. Using a signal generator, electrodes were energised with $10V_{pk-pk}$ using a sinusoidal signal at a range of frequencies from 1kHz-20MHz at 5 points per decade. Light transmitted through the wells was viewed at 4x magnification under a Nikon Eclipse E400, with a Photonic Science Coolview camera connected to a PC running Photolite to capture the images. One image was taken every 3 seconds for a total of 1 minute, with the first image being taken before the application of the electric field. The analysis was carried out using the MatLab script to determine the change in light intensity in relation to the initial picture frame. The entire diameter of the well was analysed (the highest electric field is found at the perimeter of the well, and does not reach the centre of the well) as well as being split into 10 different bands that were analysed separately or in various combinations to show the overall movement of the cells. The light intensity across the well was normalised with respect to the initial conditions in the well, due to any potential changes in starting cell concentrations. An example of the movement of the cells is given in Figure 5:1 with the initial image shown in Figure 5:1 A and following the application of the electric field the movement of the cells toward the electrode shown in Figure 5:1 B. Figure 5:2 shows an example colour intensity plot, showing the levels of DEP across the entire well. The greatest radius represents the closer distance to the high electric field/electrodes. The bands of interest (7-9) analysed, fall between 250-350 radius. The arbitrary colour scale depicts whether positive or negative DEP occurred across the well, with values less than 0 indicating negative DEP.

For all cell types, the experiments were run a minimum of three times and the data plotted on an intensity-frequency plot for each individual data set. The ‘best-fit’ model was used to fit the model to the experimental points and determine cellular characteristics (Broche et al., 2005). It is the shape of the curve and the values that determine its shape as opposed the individual data points, which is the important factor in the determining the cell characteristics. Each log phase of the graph is controlled by a cellular characteristic, shifting the curve left or right depending upon its value.

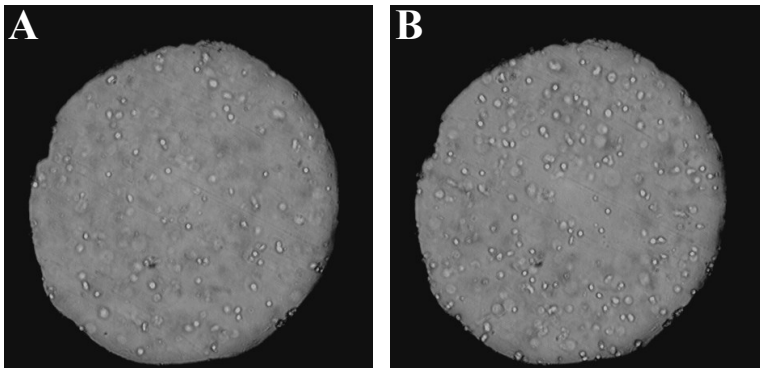

Figure 5:1 Difference observed in the well following application of high frequency. At the start of the experiment A) the cells are evenly distributed. B) Following one-minute of 16kHz frequency the cells have experienced positive DEP and moved toward the electrodes based at the edge of the well. Some dipole-dipole interactions can be observed, with the cells forming a 'pearl-chain'. The movement of the cells to the outside edge of the well increases the light intensity measured by the camera and this value is then plotted on the graph.

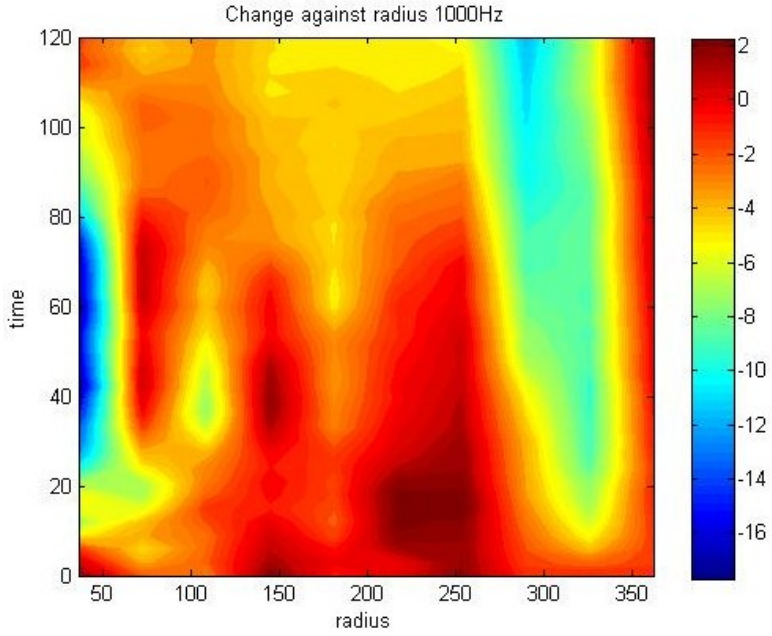

Figure 5:2 Example of light intensity change spectra produced. Plot of radius against time span. The greater radius represents the closer distance to the high electric field/electrodes. In this example at 1kHz we see overall negative DEP in bands of interest (7-9) which fall between radius 250-350, with the colour scale indicating values less than 0.

Apart from the cellular properties, the cross over frequency (the point at which the cells begin to exhibit positive DEP, zero on the intensity axis, an again negative DEP at higher frequencies) was also determined. Although this is a more simplistic means of sorting, there is potential for the separation of a mixed population of cells by the simultaneous attraction of the target population and repulsion of the unwanted cells.

5.3.5 DEP Channel Device

A channel device was developed by Professor Abraham Lee's group at the University of California, Irvine (Flanagan et al., 2007; Wang et al., 2007), which utilised flow of the cells through the conductivity medium and the DEP force as a means for cell trapping. The fabrication of the device is briefly discussed in section 5.1 and in detail in Flanagan et al (2008a) and Wang et al (2007).

5.3.6 DEP Channel Device – Dielectric Procedure

The cell preparation for the channel device was the same as that for the well chip as described in section 2.10.1, with a cell count taken and a desired concentration of $8x10^5$-$1x10^6$/ml cells utilised. Of this, less than a 200µl volume of cells was needed to run an experiment. The DEP channel device was placed on the stage of an upright microscope and the channel region of the device visualised using a 10x objective, as shown in section 2.11.4. The microchannel outlet of the DEP device was connected to a syringe pump (Pico Plus, Harvard Apparatus, MA) using Teflon tubing. Prior to the addition of cells, fluid flow was initiated and the channel cleaned with trypsin-EDTA followed by washing with DEP buffer. A high flow rate (40µl/min) was used to fill the channel and tubing with fluid before stabilizing the rate at 2µl/min for the experimental runs. A function generator was used to produce an AC signal (8V with the frequency ranging between 25kHz–10MHz) to provide the DEP force in the channel. A colour digital camera was attached to the microscope and the CamStudio screen recorder used to capture movies (100 frames/second) of the cells trapped at each frequency. The cells were recorded for 5 seconds before applying the DEP force with recording continuing for a further 5 seconds. Three video segments per frequency were captured. To calculate the percentage of trapped cells at each frequency, a 5 second frame of the videos were viewed (PFV, Photoron, Ltd.) and the cells flowing through the channel manually counted. The cells trapped by the electrodes in the last frame of the videos were also counted and the figure expressed as a percentage of the total cells.

5.3.7 Statistics

Statistical analysis was performed using the non-parametric Kruskal-Wallis test and a Dunns post-hoc test. All experiments were repeated at least 3 times (unless otherwise stated), values were expressed as mean ± standard deviation (SD).

5.4 Results

5.4.1 Cell Culture

Cells were observed to display typical morphological features prior to application to the DEP well system. MG-63 cells showed a characteristic polygonal shape. In contrast SAOS-2 cells also grown in monoculture showed an epithelial-like morphology while, STRO-1 positive cells showed a fibroblastic morphology as well as the human bone marrow cells from which the STRO-1 cells were derived (Figure 5:3).

Following preparation for DEP studies, viability of the cells at the start and end of the experiment were determined using trypan blue staining and counting of the dead cell population. Typically, viability at 75% or above was observed in cells maintained for up to 2 hours in DEP medium at room temperature.

5.4.2 Experimental Validation

Initially experiments were run based on experimental conditions established used in the original DEP experiments reported by Labeed et al (2003), using needles with manual recording of positive DEP observed by the attraction of cells to a defined needle region. These conditions included recording the amount of positive DEP occurring for 2 minutes in total and placing the cells in 25μS conductivity medium. However, the parameters were not optimal in the case of the DEP well chip device. The 2-minute time frame resulted in cells exposed to the current for a long period of time, as well as exposure in conductivity medium for longer periods. This resulted in large variation between the data points and difficulty in fitting the data to the model (an example of this is given in Figure 5:4).

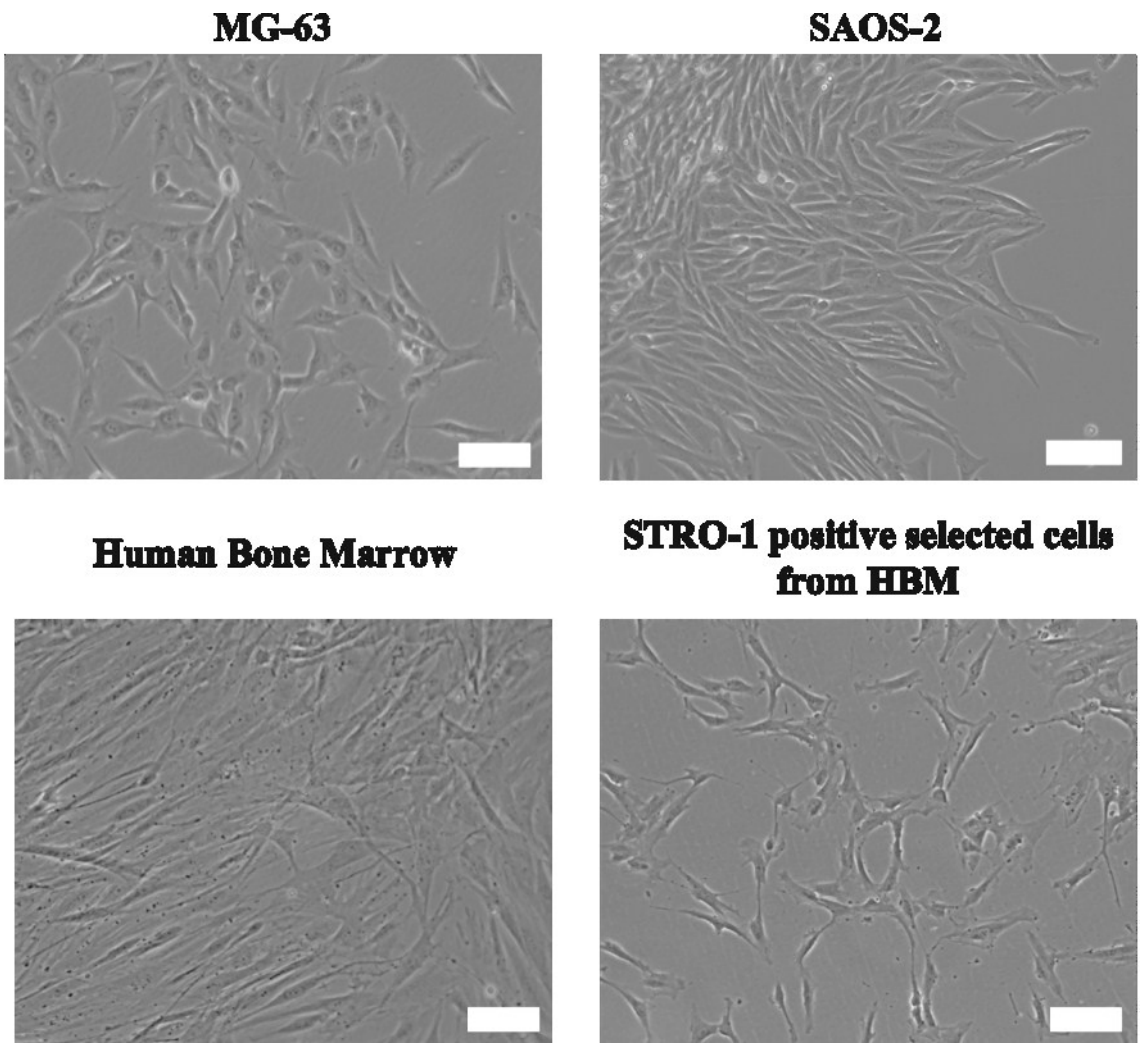

Figure 5:3 Cells in culture. MG-63 cells show a typical polygonal morphology whilst SAOS-2 cells are epithelial-like. Both human bone marrow cells and STRO-1 positive isolated cells display a fibroblastic morphology. Scale bars represent 100μm.

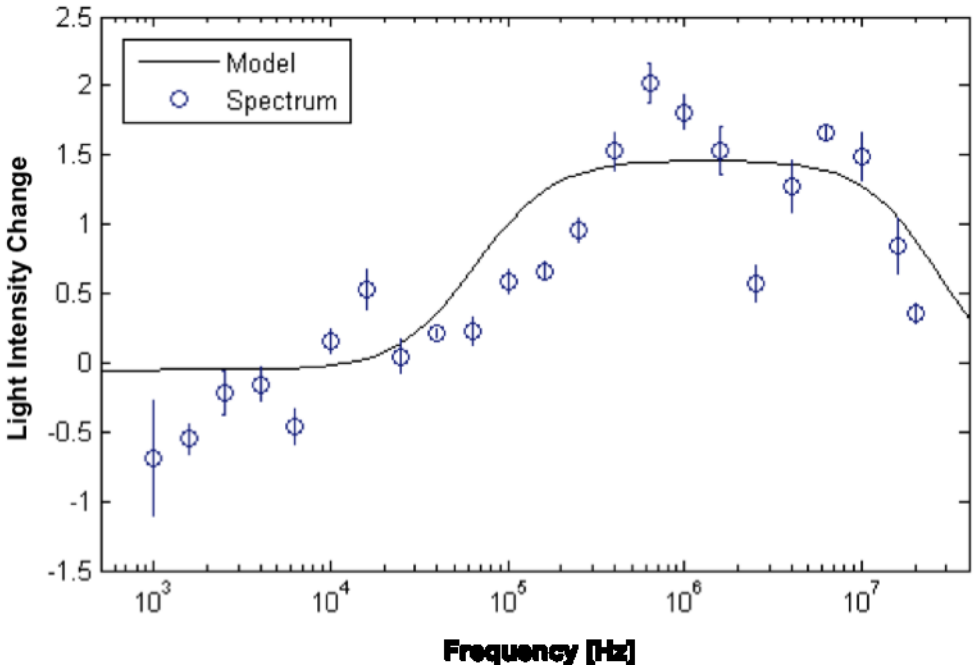

Figure 5:4 Light intensity (arbitrary units) DEP spectra for MG-63 cells in 25µS conductivity medium, together with a 'best-fit' model from which the dielectric properties were determined. The data was obtained by measuring the change in light intensity across the well after 60s of exposure to frequencies between 1.6kHz-20MHz. Error bars shown depict the error across the well as analysed by the MatLab script. Data drawn from one population.

5.4.3 Derivation of Cellular Characteristics

With the demonstration of variable success in running experiments using 25μS conductivity media, 100μS was used in order to obtain a more representative characteristic of the cell lines. At 100μS, positive DEP would not be observed in the absence of higher frequencies although a data set with improved 'best-fit' to the curve would be anticipated. The use of 25μS conductivity media proved the most suitable for running the DEP experiments using a needle device, which looked at positive DEP only. Negative DEP could not be measured in a needle device (Labeed et al., 2003). The timing of each run was reduced from 2 minutes to 1 minute to limit the amount of exposure of the cells to conductivity medium and the effects of the electric field on the cells. Upon a decrease in the total exposure time from 2 to 1 minute, a reduction in the variation of the data points was observed. The increase of the conductivity of the medium in turn increased the frequency at which positive DEP was observed in.

Representative graphs are given for each of the cell types shown, MG-63, SAOS-2 and STRO-1 positive cells in Figures 5:5-5:7 respectively. The model/curve exhibited during the experimental runs show the cells experienced both positive and negative DEP depending on the applied frequency. Generally, cells exhibited a negative response at the lower frequencies and a positive response at the higher frequencies. In all three cell populations, cell collections (positive DEP) was observed at frequencies of more than 10kHz and declined at more than 1MHz. It should be noted that this effect is a result of the conductivity of the medium. For those cells in 25μS conductivity medium the frequency at which positive DEP was observed was lower than those cells in 100μS conductivity medium.

The models were determined by the application of values corresponding to the membrane and cytoplasmic properties of the cells as well as the medium properties and cell size. The Y-axis shows arbitrary values corresponding to the level of DEP (the light intensity change). Values less than one correspond to frequencies at which cells experience negative DEP while values greater than one correspond to positive DEP. The crossover value can be determined by reading off the frequency value when the DEP level is 0 (this will occur twice in the DEP spectrum, at the lower frequencies and

again at the highest frequencies). However, the second DEP crossover frequency cannot be determined due to limitations of the signal generator.

Table 5:1 shows a summary of the cellular characteristics as determined by the modelling of the data. A 1μm difference in cell radii was measured between the MG-63 and SAOS-2 cells. However, differences were observed in the Cspec and cytoplasmic conductivities although these were not significant. Cytoplasmic conductivity was observed to be 126% higher in SAOS-2 cells than the STRO-1 positive cell population and 48% higher than the MG-63 cells. The MG-63 cells exhibited a cytoplasmic conductivity (σ_{cyto}, reflecting the ionic concentration) of 0.23S/m (the lowest of the three cell types), and the highest specific membrane capacitance (Cspec, reflecting membrane morphology) at 16.0 mF m^{-2}. Cspec was 60% higher in the MG-63 cell population than the STRO-1 positive population, and 30% higher than the SAOS-2 cell population. The SAOS-2 cells exhibited the highest cytoplasmic conductivity of 0.52 S/m and a specific membrane capacitance of 13.6 mF m^{-2}. Finally, the STRO-1 positive fraction of human bone marrow cells exhibited the lowest cytoplasmic conductivity of 0.34 S/m and a specific membrane capacitance of 10.7 mF m^{-2}. The smallest cells were measured to be the SAOS-2 cells, which were also determined to have the highest cytoplasmic conductivity. No significant difference was seen in the Gspec values across the cell types. However, the differences observed in the Gspec of the cells could potentially be used as a means of separation should the cells be placed in a heterogeneous mixture, particularly in the case of MG-63 versus SAOS-2 cells and MG-63 versus STRO-1 positive cells.

	MG-63	SAOS-2	STRO-1
Cell Radius μm	7.4	6.4	7.7
Cytoplasm Conductivity (σ) S/m	0.23 (0.05)	0.52 (0.11)	0.34 (0.28)
Cspec (mF m^{-2})	16.0 (7)	13.6 (3.3)	10.7 (3.2)
Gspec	408.9 (74.2)	358.0 (70.4)	391.6 (162.5)

Table 5:1 Cellular characteristics as determined by the DEP well chip and the model applied to the data. Values shown averaged over 3-4 repeats of separate populations, with SD given in brackets.

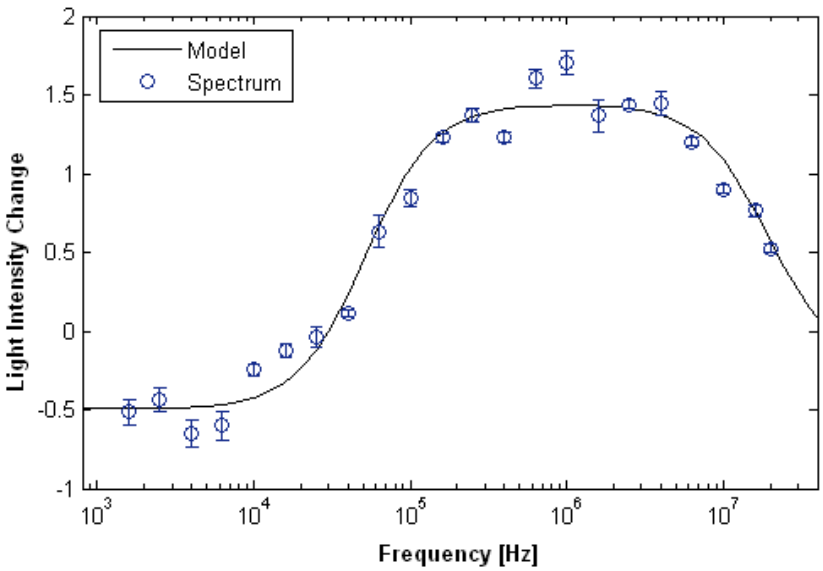

Figure 5:5 Light intensity (arbitrary units) DEP spectra for MG-63 cells, together with a 'best-fit' model from which the dielectric properties were determined. The data was obtained by measuring the change in light intensity across the well after 60s of exposure to frequencies between 1.6kHz-20MHz. Error bars shown depict the error across the well as analysed by the MatLab script. Data drawn from one population.

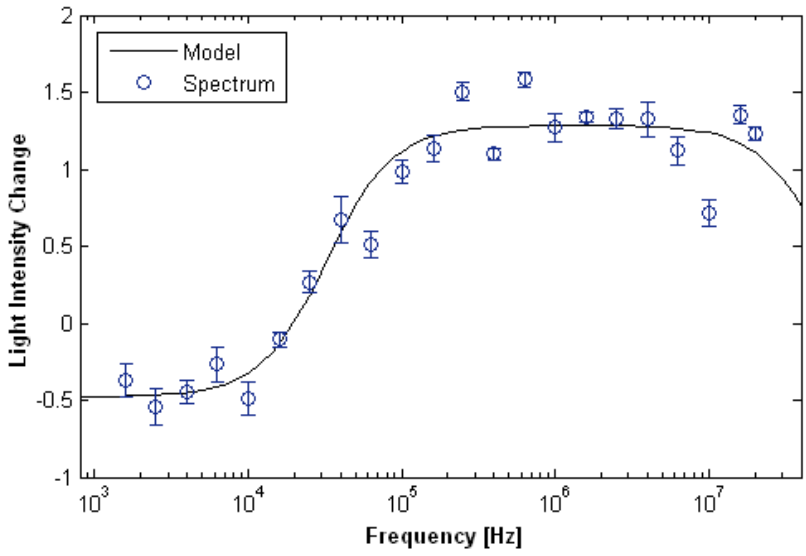

Figure 5:6 Light intensity (arbitrary units) DEP spectra for SAOS-2 cells, together with a 'best-fit' model from which the dielectric properties were determined. The data was obtained by measuring the change in light intensity across the well after 60s of exposure to frequencies between 1.6kHz-20MHz. Error bars shown depict the error across the well as analysed by the MatLab script. Data drawn from one population.

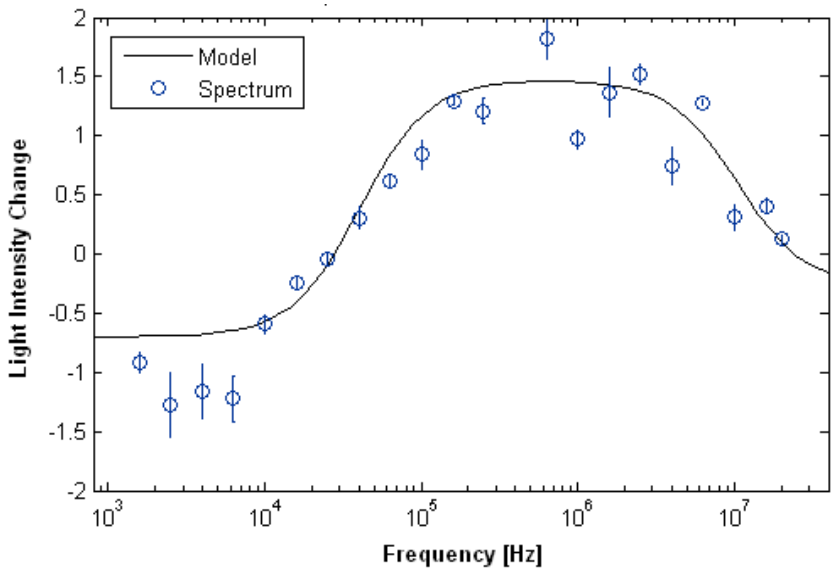

Figure 5:7 Light intensity (arbitrary units) DEP spectra for STRO-1 cells, together with a 'best-fit' model from which the dielectric properties were determined. The data was obtained by measuring the change in light intensity across the well after 60s of exposure to frequencies between 1.6kHz-20MHz. Error bars shown depict the error across the well as analysed by the MatLab script. Data drawn from one population.

5.4.4 DEP Channel Device

Using a microfluidics based device, the trapping efficiency of the osteosarcoma cell lines was examined, and to supplement the previous data obtained using the well chip device.

To test the DEP responses of MG-63 and SAOS-2 cells in the channel device, the number of cells that were trapped by positive DEP at frequencies ranging from 25kHz to 10 MHz was measured. The percentage of trapped cells as a function of frequency, was plotted to generate trapping efficiency curves which reflect the positive DEP force felt by the cell population. At high frequencies (5 and 10 MHz), the vast majority of cells (for both MG-63 and SAOS-2 populations) experienced positive DEP and was trapped at the electrodes (Figure 5:9). However, at lower frequencies (from 25 kHz to 1 MHz) the amount of positive DEP was significantly different among the two cell types. At the lowest frequency run (25 kHz), no trapping of the SAOS-2 cells was observed, however a trapping efficiency of close to 20% was achieved for the MG-63 cells. As 25 kHz was the lowest frequency applied it is not known whether additional cell trapping at a lower frequency, for example 10 kHz, would occur, or if the percentage of cell trapping would be less followed by a sharper increase in the percentage trapping as observed for the SAOS-2 cells. After application of 100 kHz frequencies and greater there was no distinguishable difference in the percentage of cells being trapped, with modest increases and negligible variation in the trapping efficiencies and a plateau was subsequently reached.

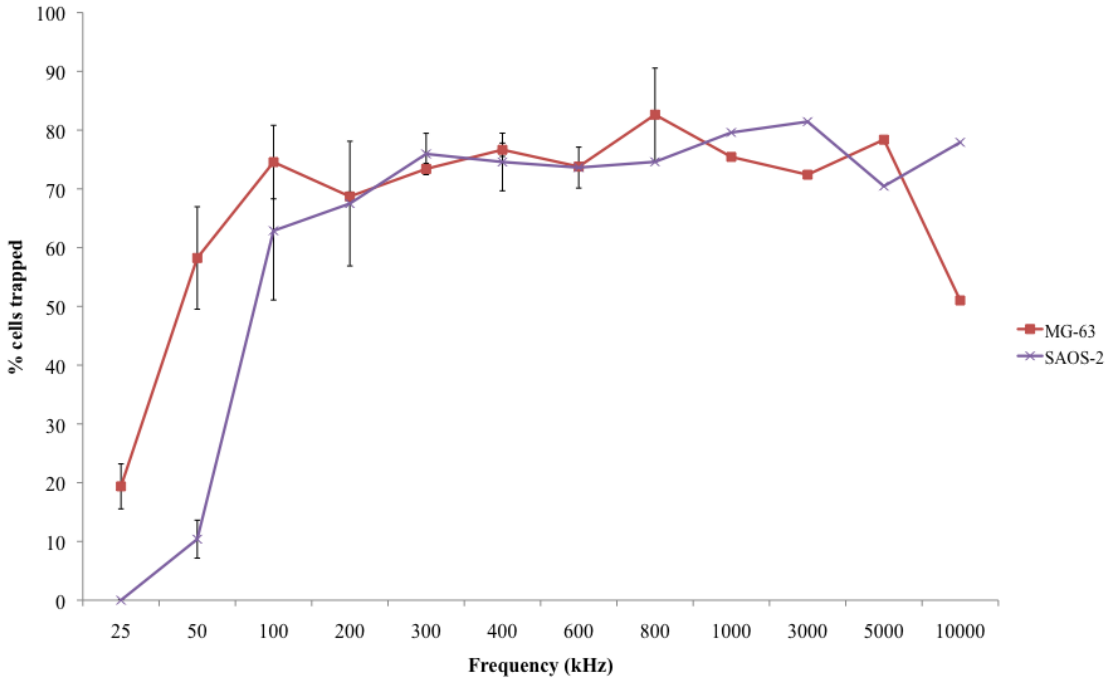

Figure 5:8 DEP trapping efficiency curves. 5 second video frames were analysed, with the number of cells trapped by the device expressed as a percentage of total cells flowing through the device. Each data point was repeated 3 times with the average trapping efficiencies shown for 3 populations, values were expressed as mean ± standard deviation (SD).

Following determination of the cell trapping efficiencies, in order to aid the separation of the MG63 and SAOS-2 cells, fluorescent tags were linked with the cells. MG-63 cells were tagged with cell tracker orange (CTO) and SAOS-2 cells with cell tracker green (CTG). Since cell tracker binds to the cytoplasm of the cell, it would be anticipated that this would change the cell properties. It was observed that for both cell types there was a right shift in the cell trapping efficiency shown in Figure 5:10. This indicated there was an increase in the frequency at which positive DEP occurs and an increase in which the DEP force is great enough to trap the cells. Similarly, to the unlabelled cell populations at high frequencies, the vast majority the cells were trapped in the channel device, and negligible variation was observed between the MG-63 and SAOS-2 cells. MG-63 cells labeled with cell tracker green had no collection of cells at 25kHz where, the unlabelled cell population had 20% trapping. In the SAOS-2 population where trapping was previously around 10% at 50kHz, the labelling of the cells with cell tracker orange reduced this. The greatest difference in trapping was observed at 100kHz, where 15% of SAOS-2 cell tracker orange labelled cells were trapped compared to over 60% of the unlabelled cells.

Potentially the channel device can be fabricated to enable populations to be separated using 2 of the 3 electrode regions of the device and a dual output function generator. Future studies would be aimed at examining whether cell separation could be achieved in this system using unlabelled MG-63 cells and SAOS-2 cells labelled with cell tracker orange, since this combination of cells shows the greatest differences in trapping efficiency at the lowest frequencies.

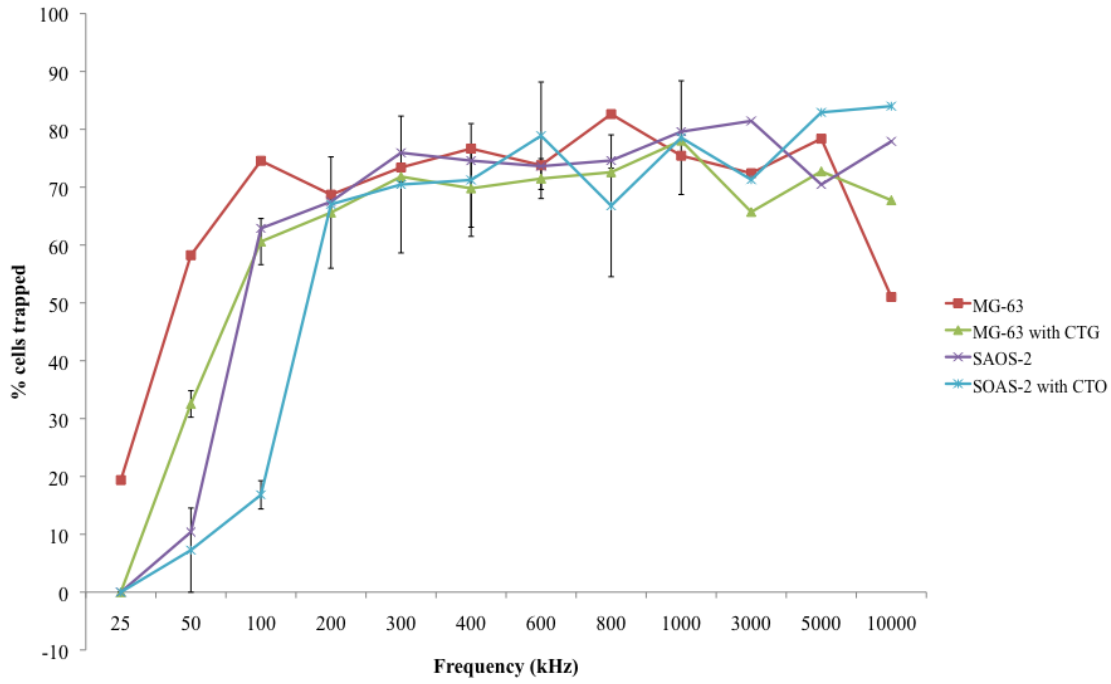

Figure 5:9 DEP trapping efficiency curves, including cell tracker labelled cells. Each data point was repeated 3 times with the average trapping efficiencies shown for 3 populations, values were expressed as mean ± standard deviation (SD).

5.5 Discussion

5.5.1 DEP Well Device

These studies have examined the potential of dielectrophoresis to differentiate between skeletal cell types to enable the separation of cells in a mixed population, for example human bone marrow cultures. For this, two separate DEP devices were used in order to characterise the skeletal cell lines MG-63 and SAOS-2 to determine their potential for separation. The DEP well chip was used to determine cell properties that could subsequently be used as a means of separation, whereas the DEP channel device was used to determine the trapping efficiency of the cells when exposed to DEP forces as well as flow. The well chip device could measure both positive and negative DEP whilst the channel device provides only an approximate estimate of the point of positive DEP.

In these studies, the MG-63 and SAOS-2 osteosarcoma cell lines were cultured under standard conditions prior to preparation for DEP analysis. MG-63 cells showed a characteristic polygonal shape and were well separated from one another in culture. In contrast, SAOS-2 cells which were also grown in monoculture showed an epithelial-like morphology. Both cells were allowed to grow to 80% confluence before being utilised. Since, it would be expected that the differentiated cell phenotype would result in a different DEP profile to the undifferentiated cell type. STRO-1 positive cells in culture showed a similar fibroblastic morphology to the human bone marrow population from which they were isolated.

The dielectric parameters and the model were determined by the application of values corresponding to the membrane and cytoplasmic properties of the cell as well as the medium properties and cell radius, using a single-shell dielectric mathematical model (Irimajiri et al., 1979). The relative permittivity of the medium was given the same value as water (78) (Huang et al., 1995). In order to determine cell size for DEP calculations, cell diameters were measured using Image J software to analyze microscope images of cells. The best-fit model was determined by matching the curve to the measured data, and then altering the dielectric parameters of the membrane and the cytoplasm until a best match was found (Broche et al., 2005, Hubner et al., 2005a).

In optimising the experimental conditions, a problem that was encountered was the inconsistency in profile determination and model fit. It is possible that any dead cells in the solution or cells which were exposed to the electric field multiple times, and therefore dying were giving the scattered data points at the highest plateaux in the curve. Previous studies have also looked at the changes in the membrane properties between apoptotic and healthy cells that clearly differentiate viable cells verses cells undergoing apoptosis (Huang et al., 1992, Labeed et al., 2006, Wang et al., 2002). Excluded in the analysis and modelling was the data for 1kHz frequency. Dielectrophoretic and electrohydrodynamic (EHD) forces have been demonstrated to cause movement of particles across the surface of planar electrodes when exposed to low-frequency (≈1 kHz) electric fields (Hoettges et al., 2003), suggesting that EHD effects are more likely to influence the movement of the cells rather than the electric field.

One of the variables changed in order to determine a clearer DEP profile for each of the cells was the conductivity of the medium. The medium used to perform DEP experiments has an important influence on their outcome and must be tightly controlled since all properties are measured in relation to the medium. Positive DEP can only be achieved when the particle is more polarisable than the medium. Media with a very high conductivity (such as culture media) are highly polarisable and therefore show only negative DEP. Therefore most experiments are performed in media with a conductivity between 1 mS/m and 10 mS/m (100μS and 1000μS), in order to achieve spectra with high information content, ideally with several strong transitions between positive and negative DEP (Hoettges, 2010). Very low conductivity media (less than 1 mS/m) is not practical in most cases since the conductivity often changes over time, by absorbing CO_2 from the atmosphere as well as dissolving ions from surfaces or even the cells losing ions to the medium. Lower conductivity media also have a lower current flowing through the liquid and thereby cause less joule heating. While the currents in high conductivity media can cause local ‘‘hot-spots’’ that can cause convention currents and electro-thermal flow (Hoettges, 2010). The osmotic pressure of the solution is another factor to consider. To overcome this problem, non-charged molecules such as sugars are added to the solution until a solution that is iso-osmotic to culture medium is attained. In general a concentration of 280 mMol/L is considered adequate (Hoettges, 2010).

The studies performed here have determined that the parameter used in order to separate a mixed MG-63 and SAOS-2 population, (or equally a mixed population with the STRO-1 cells) would use the specific membrane conductance (Gspec). Exploiting the differences in the Gspec values and altering the conductivity of the media used could enable separation of the mixed cell populations, since the conductivity of the surrounding media defects the membrane conductance under the influence of the electric field. Membrane conductance reflects the transposition of charge carriers across the membrane through membrane channels and pores (Gascoyne et al., 1997a). If the suspension conductivity is high enough, it can effectively suppress the influence of membrane conductance on cell electrokinetic responses (Gascoyne et al., 1997b). As yet there are no examples in the literature that have used differences in the specific membrane conductance of the cells as a cell sorting strategy although the idea was suggested by Gascoyne and Vykoukal (2002).

Parameters such as membrane thickness, incorporated into the modelling of the data, cannot be measured, therefore, in order to account for this Gspec and Cspec values are used which are membrane thickness independent. Membrane capacitance (Gspec) is the measure of the membrane that acts as a barrier toward, and can accumulate, ionic charges in the suspending medium in response to the applied electric field. Alternatively, membrane conductance (Cspec) reflects the net transport of ionic species across the membrane and through pores and ion channels (Wang et al., 2002). No significant difference was observed in the Cspec of the cell types, however the cytoplasmic conductivity and Gspec showed differences that could potentially be exploited for the purposes of cell separation. Three possible explanations might account for the differences observed in the specific membrane capacitance values for the different cell types, namely, differences in the thickness, composition, and folding of the membrane (Gascoyne et al., 1997b). Since an increase in the Cspec equals an increase in the membrane morphology, which could be the result of more folding taking place in the membranes of these cells (Labeed, 2004). Cspec is calculated by taking into account the surface area; hence, the more folding there is of the membrane the greater the surface area.

Membrane capacitance is proportional to cell surface area (Holevinsky and Nelson, 1998), as no significant changes have been observed in the membrane capacitance of

the cells it can be implied that the cell surface areas of the cells are comparable. The measurement of membrane capacitance has become an important technique for studying exocytosis, endocytosis, and stimulus secretion coupling mechanisms in a variety of cells. Changes in the membrane capacitance provide a direct and quantitative record of the time course of cytoplasmic granule insertion into the plasma membrane during exocytosis (Holevinsky and Nelson, 1998).

Conductivity is a measure of the ability to conduct an electric field whilst the permittivity is a measure of the cytoplasm or membranes ability to transmit an electric field. The MG-63 cells exhibited a cytoplasmic conductivity (σ_{cyto}, reflecting the ionic concentration) of 0.23S/m (the lowest of the three cell types), and the highest specific membrane capacitance (Cspec, reflecting membrane morphology) at 16.0 mF m^{-2}. The SAOS-2 cells exhibited the highest cytoplasmic conductivity of 0.52 S/m and a specific membrane capacitance of 13.6 mF m^{-2}. Finally, the STRO-1 positive fraction of human bone marrow cells exhibited the lowest cytoplasmic conductivity of 0.34 S/m and a specific membrane capacitance of 10.7 mF m^{-2}. The smallest cells were measured to be the SAOS-2 cells, which were also determined to have the highest cytoplasmic conductivity. This could be explained by the cytoplasm of the SAOS-2 cells being more concentrated than that of the other two cell types. Although the difference in radius of the SAOS-2 cells compared to the MG-63 cells is small, the 30% reduction in volume may have a significant influence on the conductivity of the cytoplasm. A similar reduction in cell size was observed in K562 (human myelogenous leukaemia) cells following treatment with drugs that induce apoptosis. DEP was used to detect early apoptosis in these cells, with a low σ_{cyto} measured in the apoptotic cell population. A possible mechanism proposed for this was that throughout the apoptotic process, cells become smaller, causing the cytoplasm to become concentrated with the remaining ions as the water is effluxed in an attempt to restore the osmotic balance, increasing the conductivity of the interior (Chin et al., 2006). Typically a very low σ_{cyto} value (approaching that of the suspending medium) is indicative of necrosis, as the membrane permeabilizes and cell interior equilibrates with the medium (Chin et al., 2006). Due to limitations on the higher voltages that could be reached by the signal generator available at University of Surrey, a more accurate representation of the cytoplasmic properties of the cells could not be obtained.

Preliminary studies looking at determining the DEP profile of the total human bone marrow cell populations were also performed, and confirmed a heterogeneous population (data shown in appendix 3). A dielectrophoretic profile was unable to be determined for the HBM cells. In a study by Thomas et al (2010) the isolation and recovery of specific cells was demonstrated using dielectrophoretic ring traps. Of particular relevance to the studies performed here, the target cell population was the osteoblast-like cell line MG-63 cells. Using the ring traps, the authors were able to recover low numbers of cells. Although these studies illustrated the potential of such a dielectrophoretic device for cell isolation from heterogeneous populations this technique still relied on the determination of sufficient surface antigens to enable identification of stem cells with fluorescent markers. However, it is possible that the STRO-1 positive cell population, whose DEP profile has been characterised here, could be sorted using these ring traps and fluorescent tagging of the cells for identification within the homogenous bone marrow cell population.

The studies presented here suggest the potential of positive DEP as a cell sorting strategy. Previously this has used positive DEP to trap and hold the cells of interest, while the rest of the cell population was removed. Finally the cells of interest are released for further handling (Yang et al., 2006, Perch-Nielsen et al., 2003). A similar approach has also been used to capture DNA on microelectrodes (Bakewell and Morgan, 2006). However, having both capturing and releasing of cells as discrete steps in the sample handling can make the fluidic control of the microsystem difficult. Therefore, a great deal of effort has been placed into addressing the development of continuous cell sorting techniques (Christensen et al., 2007). The use of negative DEP has been proposed as a continuous cell sorting technique. One negative DEP method uses electrodes microfabricated in the bottom of a channel bottom with a conducing lid as counter electrode for guiding cells from one part of the channel to another. This conducting and transparent lid eliminates difficult top/bottom electrode alignment and gives visual access to the microchannel (Christensen et al., 2007). Negative DEP traps have also been designed which allow the trapping of cells in high conductivity physiological media, which aids in ensuring the long term viability of the cells (Thomas et al., 2009).

5.5.2 DEP Channel Device

Using the same device as in these studies, Flanagan et al. (2008a) applied DEP to neural stem cell populations and concluded the ultimate fate of cells after differentiation can be predicted by distinct changes in their dielectrophoretic properties before the presence of specific cell-surface proteins (antigens) can be detected. As in the studies presented here, DEP signatures for the neural stem cells were obtained by monitoring the rate at which they collected at the electrodes. This was also deduced by extrapolating values of the DEP crossover frequency for the cell types. DEP profiling showed that neural stem cells efficiently trapped at mid-range frequencies, 100% trapped at 1,000 kHz. This distinguished them from their differentiated progeny; neurons trapped at higher frequencies, with 100% trapped at 5000 kHz, and astrocytes trapped at lower frequencies with 100% trapping at 300 kHz.

Unlike the DEP well device, the channel device does not allow for a definitive cross over frequency to be determined. At 25 kHz frequency, no trapping of the SAOS-2 cells was observed, however a trapping efficiency of close to 20% was achieved for the MG-63 cells. As 25 kHz was the lowest frequency applied it is not known whether additional cell trapping at a lower frequency, for example 10 kHz, would occur, or if the percentage of cell trapping would be less followed by a sharper increase in the percentage trapping as observed for the SAOS-2 cells. Similarly, although cell trapping was not observed at 25kHz, the cross over frequency is likely to fall in the 25-50kHz frequency range for the SAOS-2 cells.

In the channel system it would be expected that at the highest frequencies, (5 and 10 MHz), 100% trapping would be achieved. However, it is likely that cells that could not be trapped were non-viable. Normalisation of the data is possible to correct for the non-viable cell population. Video analysis suggests that at the lowest frequencies, those closest to the crossover frequencies, cell death was occurring whilst travelling through the channel. Cell death observed was possibly due to a combination of the weak DEP force and the shear strength imposed by the fluid flow. Although the studies by Flanagan et al (2008) did not show cell viability to be affected by the system, and equally, other studies have not shown cell viability to be seriously affected by cell sorting (Becker et al., 1995). Although of interest in an unrelated study, Kapur et al

(2003) showed that the signal transduction mechanism of shear stress in osteoblasts involves multiple pathways for the differentiation of normal human osteoblasts.

In order to aid the separation of the MG-63 and SAOS-2 cells, fluorescent tags were linked with the cells. As cell tracker binds to the cytoplasm of the cell, it would be anticipated that this would change the cell properties. It was observed that for both cell types there was a shift in the cell trapping efficiency. These results indicate an increase in the frequency at which positive DEP is observed and an increase in which the DEP force is sufficient to trap the cells. In the channel device, the highest frequencies could not be used as a means of separating the cells as the percentage trapping is at similar levels. Ideally a frequency would be used that would allow simultaneous attraction of the target population of cells and repulsion of the unwanted cells. However, in the DEP channel system the cells can also be separated by the strength of the DEP force being experienced by the cells.

Potentially the channel device can be fabricated to enable populations to be separated using 2 of the 3 electrode regions of the device and a dual output function generator. Future studies would be aimed at examining whether cell separation could be achieved in this system using unlabelled MG-63 cells and SAOS-2 cells labelled with cell tracker orange. This would allow evaluation of trapped cells using a fluorescence camera to record the images.

DEP has been successfully applied on microchip scales to manipulate and separate a variety of biological cells including bacteria, yeast and mammalian cells is well reviewed by Andersson and van den Berg (2003). For example, DEP enrichment in a flow cell of microliter volumes has been shown for concentrating *E. coli* (20 times) from a diluted sample and peripheral blood mononuclear cells (28-fold enrichment) from diluted whole blood. A 30-fold enrichment of white blood cells from diluted whole blood has also been achieved.

In summary, these studies have provided proof of concept for the potential of a DEP-based cell characterisation and sorting device for use in the detection and isolation of skeletal cell populations from a heterogeneous sample such as human bone marrow. In these studies, differences in the specific membrane conductance of a mixed population

of MG-63 and SAOS-2 cells could be exploited in order to develop the sorting strategy. The development of the DEP well device to perform characterisation and sorting in a sterile environment would provide a 'lab-on-a-chip' tool that would provide a cheap and quick way of identifying cells of interest in a heterogeneous cell population.

At present a disadvantage of the DEP well system is that the cells cannot be recovered and placed back into culture. Additionally to perform the experiment the cells are removed from sterile culture conditions. However, for the sake of characterisation of the cells alone this is not an issue, although an enhanced sterile environment would potentially reduce any errors/outliers in the data as a consequence of debris. Collectively these studies show that DEP can be used as a technique to determine the differences in cellular characteristics of distinct cell lines. Thus demonstrating the potential application of this technique as a means to separate heterogeneous populations of cells, based on a unique characterised DEP profile.

Further studies could look at optimisation of the culture media conditions for separation of MG-63 and SAOS-2 cells from a mixed cell culture. Additionally, characterisation of the human bone marrow population and the identification of the STRO-1 positive cells would enable the potential for sorting without the need of the STRO-1 antigen and MACS.

Chapter 6 General Discussion

6.1 General Discussion

The present studies have characterised the phenotype of human foetal femur-derived cells and sub-populations therein, as well as an examination of their differentiation potential to skeletal lineages. In addition the phenotype of human embryonic stem cells, HUES-7 cell line has been characterised, with their differentiation potential toward the skeletal lineage also assessed. As an alternative tissue engineering strategy, the interaction of the two cell types has been assessed by co-culture and conditioned media studies to direct the cells toward the osteogenic and chondrogenic lineages.

In an evaluation of tissue engineering strategies, isolation and expansion of human foetal femur-derived cells was successful following explant culture and collagenase digest. Culture of human foetal femur-derived populations in the presence of dexamethasone and ascorbate favoured osteogenesis, as evidenced by expression of alkaline phosphatase and type I collagen. Additionally, populations cultured in basal conditions displayed STRO-1 and 7D4 expression. The addition of 100μM ascorbate and 10nM dexamethasone to basal media conditions was found to enhance osteogenic differentiation of adult mesenchymal stem cells by Jaiswal and co-workers (1997). Differentiation factors such as bone morphogenetic protein-2 (BMP-2), vitamin D_3, simvastatin and pleiotrophin could selectively target populations within a heterogeneous source. The foetal cells in this study were derived from human femurs containing predominantly epiphyseal chondrocytes surrounded by a periosteum consisting of an outer fibroblastic layer and an inner layer of non-committed mesenchymal stem cells. Additionally, relatively small numbers of differentiated osteoblasts were present along the central diaphysis, as indicated by the presence of a bone collar.

Orthopaedic approaches already use autologous bone marrow stromal cells isolated from the patient and either re-implanted in theatre or expanded *ex-vivo* for re-implantation at a later date. However, the harvest of adult bone marrow is a painful and invasive procedure for the patient and can lead to complications such as donor site morbidity. This has led to the need for alternative stem cell sources. Human foetal stem cells are a promising candidate for clinical use, reducing the need for autologous cells, as tissue from abortive human foetal femurs could provide an allogeneic source. Validation of the immunopriveledged status of the cells would be necessary. Practical

application of the cells for clinical use would require the collection, isolation and expansion of the foetal femur-derived cells in clinical grade laboratories prior to banking for long term storage and use in future tissue engineering applications. Additionally, there are also implications of the human foetal femur cell culture for stem and progenitor cell research, for example acting as an important model system for wound healing and tissue regeneration, as well as screening of drugs.

The application of human foetal femur-derived cells to tissue engineering strategies would seem ideal, however, the feasibility of human foetal cell use relies upon three key criteria, i) population characterisation, ii) immunogenicity and iii) ethical approval. Human foetal cells were isolated from cartilaginous femurs at 8–12 weeks post conception (WPC). Two antibodies, STRO-1 and 7D4 were identified to select for subpopulations of cells within the foetal femur, which showed no loss of expression over 21 days in culture. Upon selection of these fractions using FACS, STRO-1 expression was recorded at 0.6–12.6% of the foetal cell populations, 7D4 expression was recorded at 0.1-5.1% of the foetal cell population. The differences observed in the percentage of 7D4 and STRO-1 may be due to the starting cell population and the level of differentiation/the number of progenitor cells within (Yang et al., 2007). Typical stem cell enrichment methods such as MACS, FACS, and adherence to plastic are generally laboratory-based and require tissue harvesting and purification to be carried out days or weeks before administration of cell therapy. Furthermore, label or cell culture dependent enrichment methods yield tissue preparations that contain modified, activated or otherwise altered cells; for clinical applications, it is preferable that isolated cells be unlabeled, and minimally manipulated (Vykoukal et al., 2008).

Expression of both STRO-1 and 7D4 was observed for 21 days. Expression of STRO-1 (and 7D4) was not examined following differentiation, therefore this test would be required for the foetal femur-derived populations to determine commitment to the osteogenic lineage since loss of STRO-1 expression has been demonstrated following osteogenic differentiation (Stewart et al., 1999).

Cell proliferation studies of the unselected human foetal-derived cells demonstrated negligible variation in population doubling time (21.4±3.0 hours), compared to the STRO-1 positive (19.86±6.0 hours), and STRO-1 negative fractions (22.4±3.0 hours).

The doubling time of the foetal cells is greater than that of ES cells and of HBM cells, therefore suggesting the foetal cells offer a halfway model for the study of skeletal differentiation. Molecular characterisation of the foetal femur cells has been performed previously by Mirmalek-Sani et al (2005) who indicated that the foetal femur–derived cells displayed an undifferentiated skeletal phenotype rather than cartilaginous phenotype with alkaline phosphatase expression, type I collagen, and osteopontin expression in basal conditions, whereas culture in osteogenic conditions resulted in expression of osteocalcin. This data was complemented and extended here, with the positive staining of alkaline phosphatase, type I collagen and STRO-1 in cultures as well as expression of alkaline phosphatase, and early markers SOX-9 and RUNX-2 in basal conditions upon molecular analysis. Molecular characterisation of the STRO-1 positive sorted cell fraction, revealed expression of early bone markers, SOX-9 and RUNX-2 and lack markers of more mature osteogenic cells. STRO-1 positive cells demonstrated a significant increase in alkaline phosphatase expression in osteogenic conditions at both days 7 and 21 of culture compared to the unsorted cell population, confirming the presence of osteogenic precursors in the STRO-1 positive cell population. Increased type II collagen levels were recorded in the STRO-1 positive fractions in both osteogenic and chondrogenic conditions at day 7 of culture, the upregulation of type II collagen suggests that the cells are reaching the stage of prehypertrophic chondrocytes, that is a marker of late chondrogenic differentiation status (Rada et al., 2010). The expression of type II collagen in the STRO-1 positive fraction is consistent with the data presented by Simmons (1991b). In the Simmons study (1991b), particularly high SOX-9 expression levels were observed in the chondrogenic media conditions. SOX-9 expressing cells are said to mark osteochondroprogenitor cells (Kawakami et al., 2006), the increase in SOX-9 expression observed in the STRO-1 positive fraction would support this observation. For the expression patterns of some markers (alkaline phosphatase, RUNX-2, osteocalcin and type II collagen), similar results were seen in both the STRO-1 positive and negative fractions at various time points. This may be due to the presence of a progenitor cell population in the negative fraction, expressing STRO-1 following the cell sorting process upon re-culture. This would suggest a temporal expression of STRO-1, which has previously been proposed by Walsh and colleagues (2000). However, FACS purification is not sufficiently efficient to ensure a total depletion of the undesired cell population. In a clinical setup, the transfer of as few as one single cell

should theoretically be avoided. In model studies, bone marrow with 10% tumour cell contamination could be purged by a factor of 2–4 logs using FACS, meaning that 0.1% of malignant cells could still be returned to the patient (reviewed by Geens et al (2007)).

The data obtained here indicate a propensity of the STRO-1 positive cell population to differentiate along the osteogenic pathway. The osteogenic propensity of the STRO-1 positive stem cell fraction has been demonstrated in a study by Rada et al (2010) originally aimed at isolating selected adipose derived stem cells (ASCs) subpopulations. Rada and co-workers set to analyse the behavior of the heterogeneous adipose cell population regarding the expression of stem cell markers and also regarding their osteogenic and chondrogenic differentiation potential. Human ASCs subpopulations were isolated using immunomagnetic beads coated with several different antibodies (CD29, CD44, CD49d, CD73, CD90, CD 105, STRO-1 and p75) and real time PCR performed looking for the presence of osteogenic and chondrogenic markers. The results obtained from this study allowed for the conclusion that among all the ASCs subpopulations isolated, the cells isolated with immunomagnetic beads coated with anti STRO-1 antibody showed the highest osteogenic potential while the ones isolated using immunomagnetic beads coated with anti CD29 antibody and anti CD105 antibody had the highest chondrogenic differentiation potential. Moreover, the data described demonstrated that the cells subpopulations have different in vitro chondrogenic or osteogenic differentiation profiles (Rada et al., 2010). This is particularly relevant for the studies performed here, where the use of additional markers, such as CD146 could be used to further select the most suitable cell population from the human foetal femur-derived cells that have higher potential application in bone and/or cartilage regenerative medicine approaches. CD146 is a cell surface adhesion molecule currently used as a marker for endothelial cell lineage. However, CD146 has been identified as a marker for skeletal progenitors (Sacchetti et al., 2007). STRO-1/CD146 positive sorted human bone marrow stromal stem cells have been shown to express smooth muscle actin, but not the endothelial specific marker von Willebrand factor, providing direct evidence that this primitive precursor population displays a characteristic perivascular phenotype (Shi and Gronthos, 2003).

An as yet unexplored opportunity is the application of dielectrophoresis (DEP) to pluripotent stem cells, derived from embryos or at varying stages of development. To

date the isolation and renewal of pluripotent stem cell populations is significantly challenged by the absence of non-invasive methods to discriminate and specifically promote the growth of the stem cells (Pethig et al., 2010). The tendency of pluripotent stem cells to spontaneously differentiate and their unpredictability to commit to specific lineages underlines the need for sensitive and non-invasive methods to monitor and separate cell populations. This is particularly true when co-culturing these cells with other cell types (e.g. feeders) supportive of self-renewal and/or differentiation (Pethig et al., 2010). Equally there is a need for homogenous bone marrow cell populations, which remain to be isolated in the literature. Thus, in a therapeutic context, DEP may provide a simple and non-invasive technique for the positive or negative selection of target or contaminating cell types prior to transplantation (Pethig et al., 2010).

The studies in this thesis demonstrated the potential for the use of DEP as a technique to determine the differences in cellular characteristics of progenitor skeletal stem cells, potentially acting as a reliable technique for the identification and separation of the STRO-1 and 7D4 cell fractions. The approach may offer advantages over the use of surface antigens and FACS. Thus, it would be anticipated that each of the STRO-1 and 7D4 cell fractions would have a unique dielectric profile, as was observed in the MG-63 and SAOS-2 cell lines and the STRO-1 positive fraction of human bone marrow cells. The data presented here suggests a possible separation strategy using the Cspec or cytoplasmic conductivity of the cells, following observation that Cspec was observed to be 60% higher in the MG-63 cell population than the STRO-1 positive population, and 30% higher than the SAOS-2 cell population. Cytoplasmic conductivity was observed to be 126% higher in SAOS-2 cells than the STRO-1 positive population and 48% higher than the MG-63 cells. Additionally, using the same channel system used in these studies, Flanagan et al. (2008a) applied DEP to neural stem cell populations and concluded that the ultimate fate of cells following differentiation can be predicted by distinct changes in the cells' dielectrophoretic properties before the presence of specific cell-surface proteins (antigens) can be detected. This study indicates the potential of DEP to selectively isolate target subpopulations of cells from other cells in suspension, without damage to the cells or the need for biochemical labels/tags (Pethig et al., 2010).

Maintenance of a pluripotent undifferentiated state in human embryonic stem (ES) cells was demonstrated following culture on a mouse embryonic fibroblast (MEF) feeder

layer with the expression of nuclear markers, Oct-3/4, Sox-2 and Nanog as well as surface markers, SSEA3, TRA-1-60 and alkaline phosphatase. In the case of most markers the precise control of their levels of expression are necessary for maintenance of the pluripotent state. It has been found that the precise level of Oct-3/4 governs three distinct fates of ES cells. A less than twofold increase in expression results in differentiation into primitive endoderm and mesoderm. In contrast, repression of Oct-3/4 induces loss of pluripotency and dedifferentiation to trophectoderm (Niwa et al., 2000).

Upon culture of the ES cells on a foetal feeder cell layer, although the morphology of the cells was comparable to that on MEF feeder layer, expression of all pluripotency markers was lost. ES cells cultured on the foetal cell layer failed to express type I or II collagen, which was seen in the foetal cells. From the staining performed, the extent of differentiation of the cells, as well as the pathway could not be determined.

A typical differentiation strategy taken for the differentiation of ES cells is the formation of EBs. EBs were generated in standard EB media supplemented with osteogenic and chondrogenic factors in order to direct the cells down toward the osteogenic and chondrogenic lineages at the start of the differentiation process. EBs were cultured for 5 days before molecular characterisation. It would be expected that those cells cultured in standard EB media would display markers for all three germ layer lineages as shown by Itskovitz-Eldor and colleagues (2000), whilst those cultured with osteogenic and chondrogenic factors would display typical markers of mesoderm differentiation. However, expression of differentiation markers was inconsistent and irreproducible, although loss in the pluripotency marker expression of OCT-4 and NANOG was observed.

Culture of foetal femur-derived cells with embryonic cells cultured in monolayer showed a significantly reduced alkaline phosphatase specific activity in comparison to culture of foetal cells alone. Alkaline phosphatase activity in the ES cells alone was minimal. This suggests an inhibition of differentiation as observed in other co-culture studies (Portnoy et al., 2006, Pan et al., 2001).

The idea that the ES cells may inhibit differentiation of the foetal cells, either by direct

contact or by factors secreted by the ES cells was investigated. ES cell conditioned media (50% and 100%) was applied to the foetal cells. The relative expression levels of typical bone and cartilage markers were observed to be decreased following three days culture. Furthermore, these studies support the plasticity of the foetal femur-derived cells. The switch of cell types between lineages is referred to as 'plasticity'. In a study by Park and co-workers (1999), single adipocytes were subjected to osteogenic growth conditions and were found to dedifferentiate to an earlier fibroblast-like state, then redifferentiate to the osteoblast phenotype. Human bone marrow cell populations have been found to have the potential to differentiate into multiple stromal lineages under controlled conditions, including bone, cartilage, fat, and possibly muscle, neural cells, and, beta-pancreatic islets cells (Bianco and Robey, 2001b, Heng et al., 2004, Pittenger et al., 1999). The plasticity of MSC may be attributed to de-differentiation, transdifferentiation or cell-cell fusion (Grove et al., 2004).

Pellets formed from foetal cells and placed in organotypic culture conditions displayed a predominantly collagen phenotype in both osteogenic and chondrogenic culture conditions. In mixed ES and foetal cell pellets, although a mixed proteoglycan/collagen phenotype was observed at day 7 of culture, by day 28 proteoglycan only expression (with minimal collagen staining) was observed. Any expression of type I and II collagen was limited to the regions where foetal cell populations were present. As observed in monolayer culture, minimal alkaline phosphatase staining was seen in day 28 organotypic pellets, however this was also observed in the foetal only pellets and may therefore be a result of the 3-D culture system. Optimisation of culture conditions will thus be required to elicit an osteogenic and chondrogenic response, since neither was observed in the foetal-embryonic cell co-cultures. Epithelial-like cells were observed to form from the ES cell populations, which demonstrated spatial organisation with distinct cell clumps/regions within the pellets. The cadherins are a superfamily of transmembrane calcium-dependent cell–cell adhesion molecules. The importance of cadherins in morphogenetic processes was first suggested by the observation that cell rearrangements during development are often associated with changes in cadherin subtype (reviewed by Takeichi et al (1988)). The sorting-out of embryonic cells from a cell mixture and the selective spreading of one cell population over the surface of another have been attributed to various causes. These include differences in chemotaxis, cellular adhesiveness, cell surface contractility, speed of cell movement, and in the

timing of postulated changes in cellular adhesive and motile properties (Steinberg and Takeichi, 1994). Based on a mathematical model it was predicted that two motile cell types differing only in the level of expression of a single cell adhesion system should not only segregate from one another but also arrange themselves with the less cohesive cells enveloping a core of the more cohesive ones (Steinberg and Takeichi, 1994). In the osteogenic cultured pellets, there was no distinct outer or inner core of cells, since the pellet spread across the confetti membrane, however for the pellets cultured in chondrogenic conditions, a foetal cell core was observed. There has been no equivalent converse demonstration of the ability of differences in cadherin subtype to produce these behaviors in the absence of differences in cadherin expression levels (Duguay et al., 2003). The difference in expression levels of cadherins may be the case of the cell segregation observed in the mixed co-culture pellets in these studies, it has been shown that purely quantitative differences in expression levels of a single cadherin suffice to produce these rearrangements in the absence of any difference in cadherin subtypes (Duguay et al., 2003). The importance of cell-cell interactions has also be demonstrated by Koyanagi-Katsuta et al (2000), who observed that the apoptosis of mouse ES cells was induced when the cells were dispersed as single cells as opposed to dispersion as aggregates, similarly this was observed in the HUES-7 cells when cultured as single cells. Successful adhesion and culture of the ES cells as single cell populations was only observed with the use of foetal-cell conditioned medium, which implies the secretion of a factor by the foetal cell population which encourages the adherence and proliferation of the cells. Examples of such factors are cell adhesion molecules (CAMs), typically proteins located on the cell surface involved with the binding with other cells or with the ECM (Aplin et al., 1999). Possible CAMS responsible include the cadherins (the types of which are cell type specific) for example, E-cadherin which is present on epithelial cells. Cells expressing E-cadherin tend to cluster together, with the exclusion of other cell types. Equally components of the mitogen-activated protein kinase (MAPK) pathway play a role in adhesion-mediated signaling (Aplin et al., 1999). Engagement of integrins with the ECM allows permissive growth factor (GF) signaling to the MAPK cascade. Regulation of this cascade can occur at the level of the receptor, Raf or MAPK Kinase (MEK). Integrin engagement also leads to tyrosine phosphorylation of focal adhesion kinase (FAK) and the formation of complexes capable of adhesion-dependent binding (Aplin et al., 1999).

In summary, the data presented in this thesis has demonstrated the potential of human foetal femur derived cells as a unique intermediate model and system to address bone stem cell differentiation as a pre-natal source in comparison to embryonic stem cells, umbilical cord blood (earliest post-natal) and adult-derived (aged) sources. Furthermore, the multipotentiality of the cells has also been demonstrated with the use of growth factors known to promote osteogenic and chondrogenic differentiation. The application of human ES cells to foetal cell culture led to the loss of markers of a more differentiated cells, indicating a plasticity of the foetal cells. Additionally, the presence of a subfraction of cells in the human foetal femur with osteogenic potential has been demonstrated using the STRO-1 antigen. HUES-7 human ES cells were also characterised and differentiated using both 2-D and 3-D culture systems. The culture of EBs in osteogenic and chondrogenic promoting factors, was successful in initiating the differentiation of the cells making up the EB toward the mesoderm phenotype as demonstrated by increased BMP-4 expression. BMP-4 expression was also increased in single cell cultures in monoculture, supplemented by foetal cell conditioned media, highlighting the need for secreted factors in the cells to be identified which promote the differentiation of the cells toward mesoderm. A novel organotypic model was utilised to co-culture populations of foetal femur cells and ES cells as pellets and determine their differentiation potential. The culture of foetal cells alone resulted in high levels of collagens and proteoglycan, which was not observed in the mixed cell pellets. This inferred an inhibition of the foetal cell population differentiation by the presence of the ES cells. This idea is supported by the observations made in monolayer layer culture where a significant reduction in alkaline phosphatase specific activity was observed in mixed foetal/ES cell populations, compared to foetal populations alone. Another observation made in the mixed pellet cultures was the spatial organisation of the cells as early as day 7 of culture, suggesting the importance of cell-cell interactions in cell growth and differentiation.

Clearly, harnessing the differentiation potentials of human ES and foetal cell populations into the required human tissues for regeneration remains a significant challenge. Determination of the stem and progenitor cell sub-populations within foetal femur cell source will increase our understanding of foetal cell biology, however, may not be necessary for effective clinical outcome of cell therapies which are reliant on heterogeneous cell populations (Quesenberry et al., 2005). The studies reported here

indicate that the interaction of human foetal femur-derived cell populations and human embryonic stem cell populations warrant further examination for fundamental research and for determination of their suitability for clinical use which, ultimately, may improve the quality of life for many as a result of derived strategies to augment skeletal regeneration.

6.2 Future Directions

The current studies have indicated a potential for the differentiation of HUES-7 cells toward bone and cartilage by the co-culture of ES and foetal cell populations as well as the application of osteogenic stimulatory growth factors and foetal conditioned medium. The investigation of these approaches further, offers a number of novel tissue engineering strategies.

Further investigation and application of the interaction of human ES cells and human foetal femur-derived populations in order to successfully differentiate the cells could include:

- **Foetal age:** Isolation, expansion and differentiation of cells at 8 to 12 weeks post conception with comparative studies to determine phenotypic differences related to age of collection.

- **Osteogenic conditioned medium (OCM):** Optimisation of OCM culture to determine a protocol to elicit an osteogenic and chondrogenic response in ES cells. Determination of the factors responsible for cell adhesion and differentiation.

- **Stimulatory factors:** Application of osteogenic factors in combination and in sequence, and the timing of these factors therein, to examine differentiation potential and preferred conditions for differentiation of ES cells in both monolayer culture and 3-D/organotypic culture conditions. Examples of factors that would be utilised include ascorbate, dexamethasone, BMP-2, TGF-β3 and retinoic acid.

- **Mechanism of ES/foetal cell segregation;** in organotypic mixed cell pellets. Determine the presence of tight junctions in ES cell populations as well as factors responsible for cell adhesion and differentiation.

- ***In vivo*** **culture;** Osteogenic/chondrogenic pre-treated cells (STRO-1/7D4 cell fractions) seeded on appropriate scaffolds and implanted subcutaneously in immunodeficient mice. Following culture, analysis of matrix formed and new tissue formation to be performed.

- **Dielectrophoretic characterisation;** of differentiated cell types. Use of dielectrophoretic separation device to sort heterogeneous cell populations.

6.3 Appendix 1

WST-1 formula derivation:

Estimation of the population doubling time uses a 2 parameter exponential growth function, displayed below:

$$y = ae^{bx}$$

Where 'a' is the initial cell number, 'e' is the exponential function, 'b' is the rate of change and 'x' is the doubling time (in days). Therefore, if we wish to know the time taken for the cell population to double, i.e. twice the initial cell number (2 X a), we enter this into the equation:

$$2a = ae^{bx}$$

Divide by 'a':

$$\frac{2a}{a} = e^{bx}$$

Simplified equation:

$$2 = e^{bx}$$

Apply logarithmic function:

$$\ln(2) = bx$$

Divide by 'b' to give 'x':

$$\frac{\ln(2)}{b} = x$$

Derivation of the equation gives a simplified version needing only the 'b' value, (obtained when datasets are plotted) to give the doubling time.

6.4 Appendix 2

7D4 sorted and unsorted cell populations, molecular data.

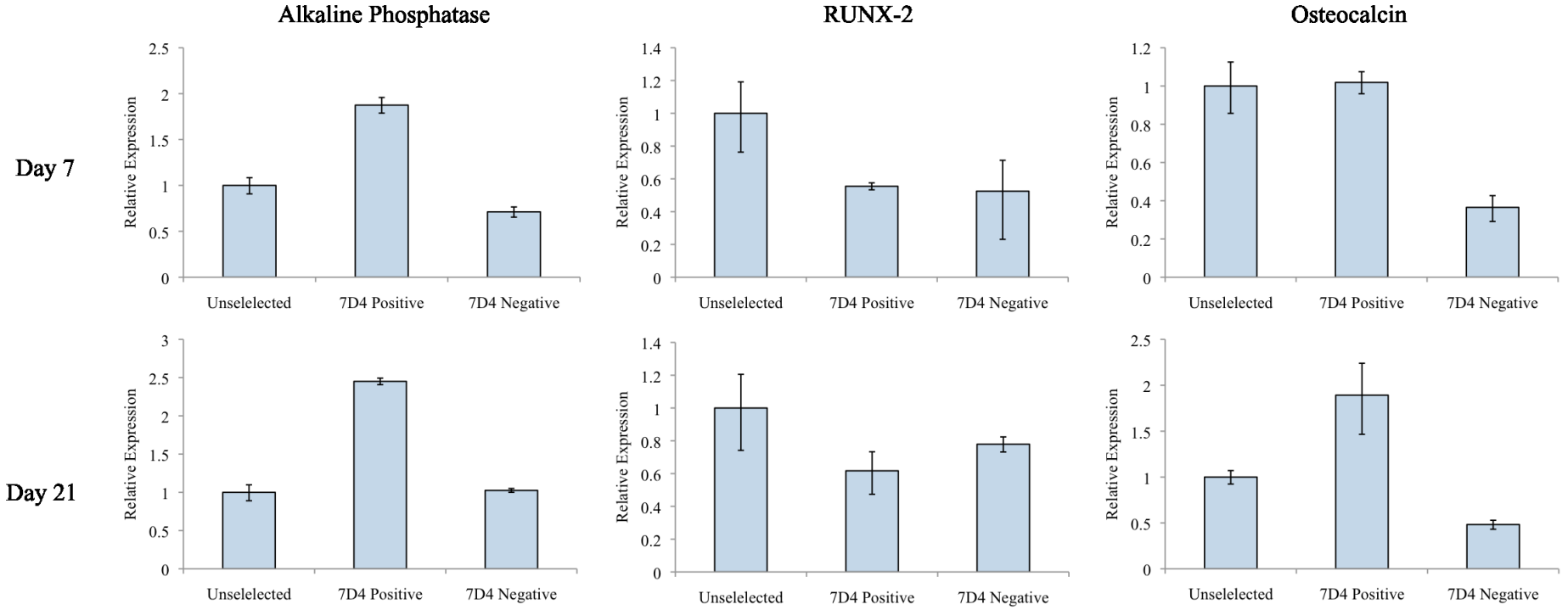

Figure 6:1 Unselected, 7D4 positive and 7D4 negative cell groups cultured in basal media. Expression of osteogenic markers alkaline phosphatase, RUNX-2 and osteocalcin relative to β-actin. Expression levels were observed following 7 and 21 days in culture relative to β-actin. Relative expression of the sorted cell populations was calculated against unselected cells set at 1. * Indicates significance $p<0.05$ relative to the unselected cell population, as well as between 7D4 positive and negative cell populations.

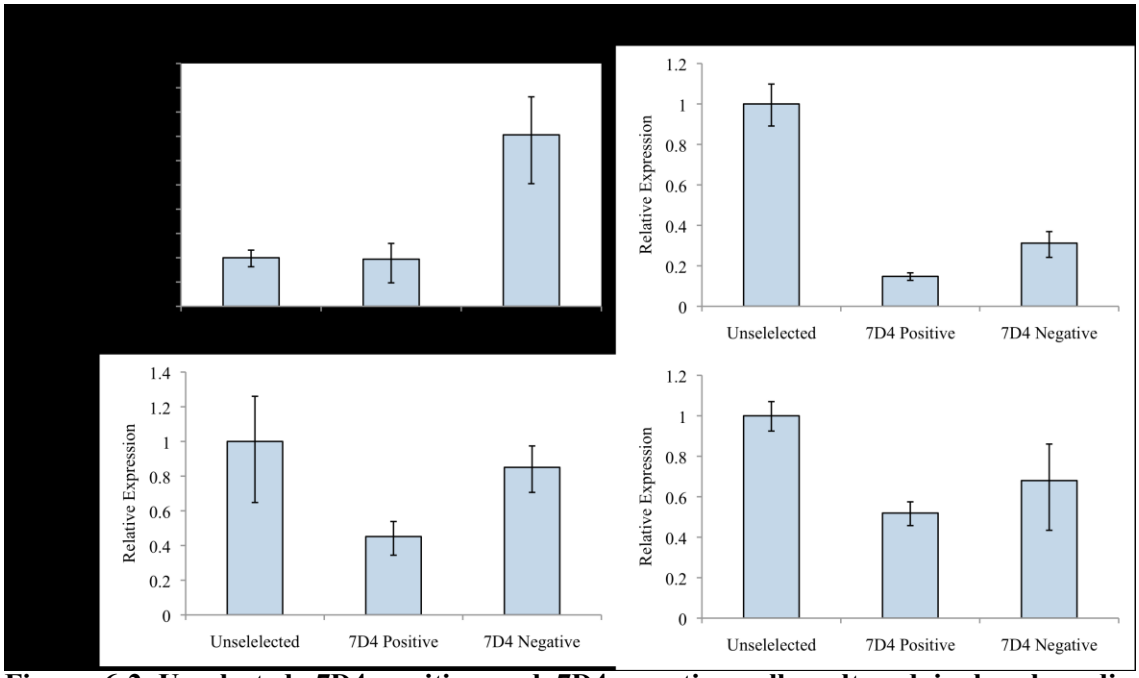

Figure 6:2 Unselected, 7D4 positive and 7D4 negative cells cultured in basal media. Chondrogenic markers, Type II collagen and SOX-9 expression relative to β-actin. Expression levels were observed following 7 and 21 days in culture. Relative expression of the sorted cell populations was calculated against unselected cells set at 1. * Indicates significance $p<0.05$ relative to the unselected cell population, as well as between 7D4 positive and negative cells.

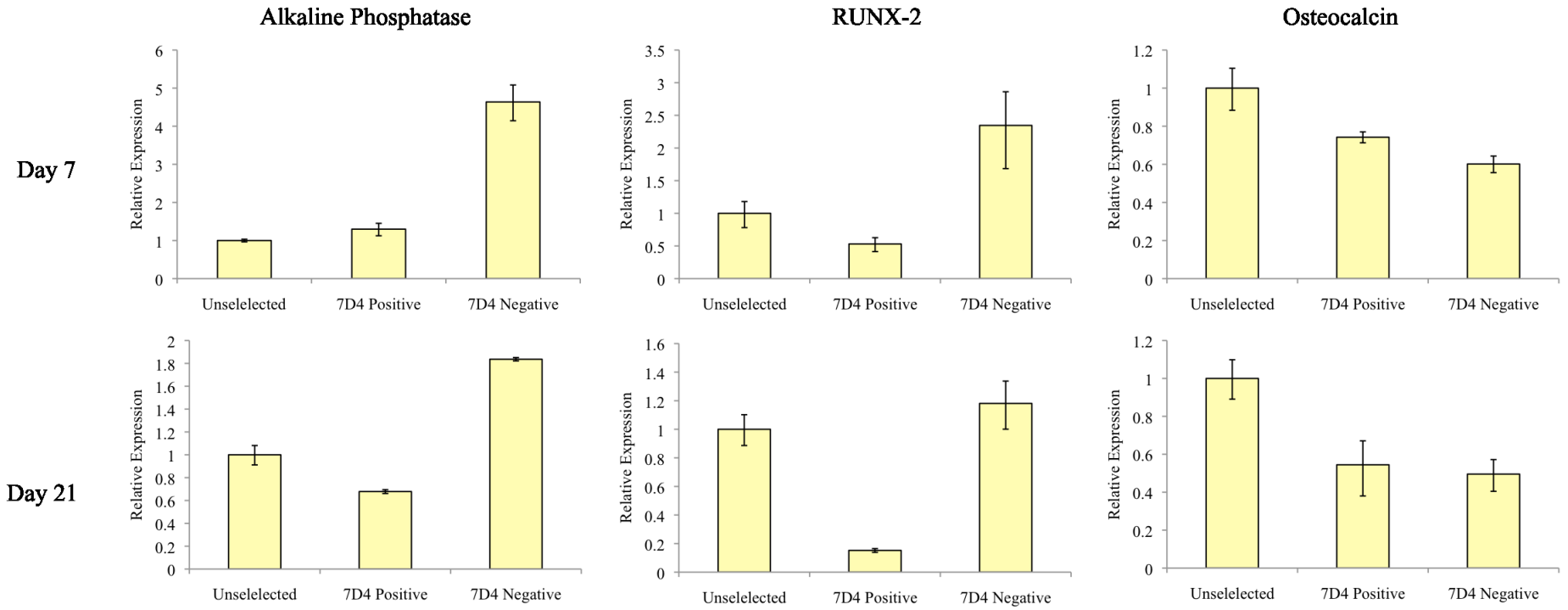

Figure 6:3 Unselected, 7D4 positive and 7D4 negative cell groups cultured in osteogenic media. Expression of osteogenic markers alkaline phosphatase, RUNX-2 and osteocalcin relative to β-actin. Expression levels were observed following 7 and 21 days in culture relative to β-actin. Relative expression of the sorted cell populations was calculated against unselected cells set at 1. * Indicates significance $p<0.05$ relative to the unselected cell population, as well as between 7D4 positive and negative cell populations.

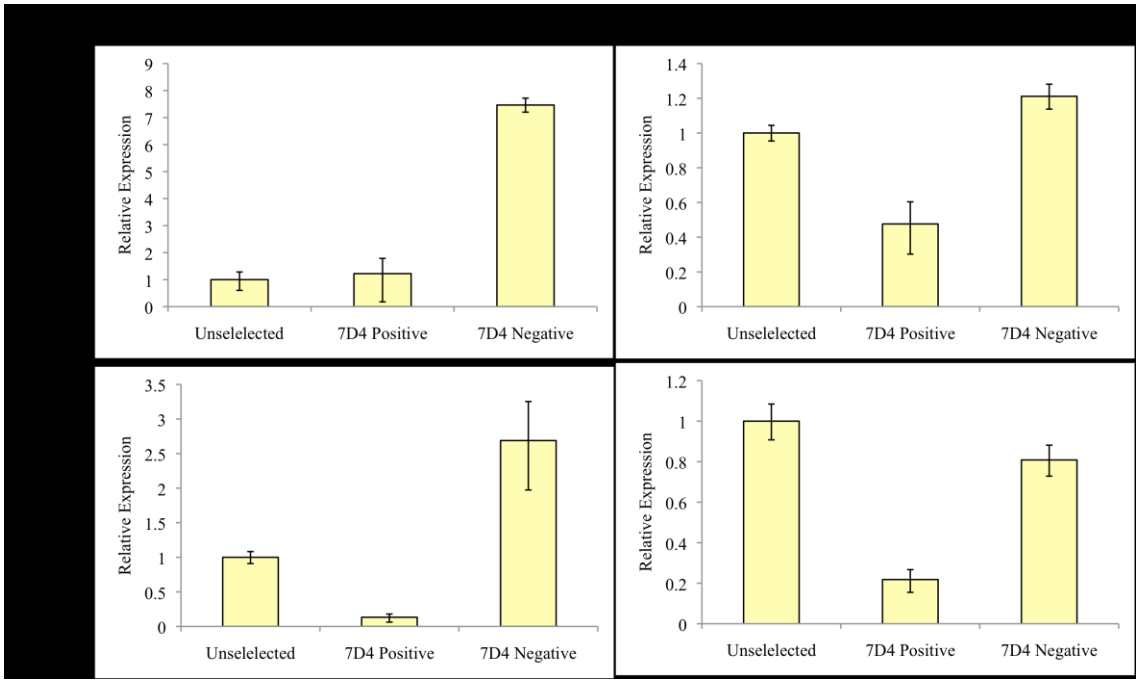

Figure 6:4 Unselected, 7D4 positive and 7D4 negative cells cultured in osteogenic media. Chondrogenic markers, Type II collagen and SOX-9 expression relative to β-actin. Expression levels were observed following 7 and 21 days in culture. Relative expression of the sorted cell populations was calculated against unselected cells set at 1. * Indicates significance $p<0.05$ relative to the unselected cell population, as well as between 7D4 positive and negative cells.

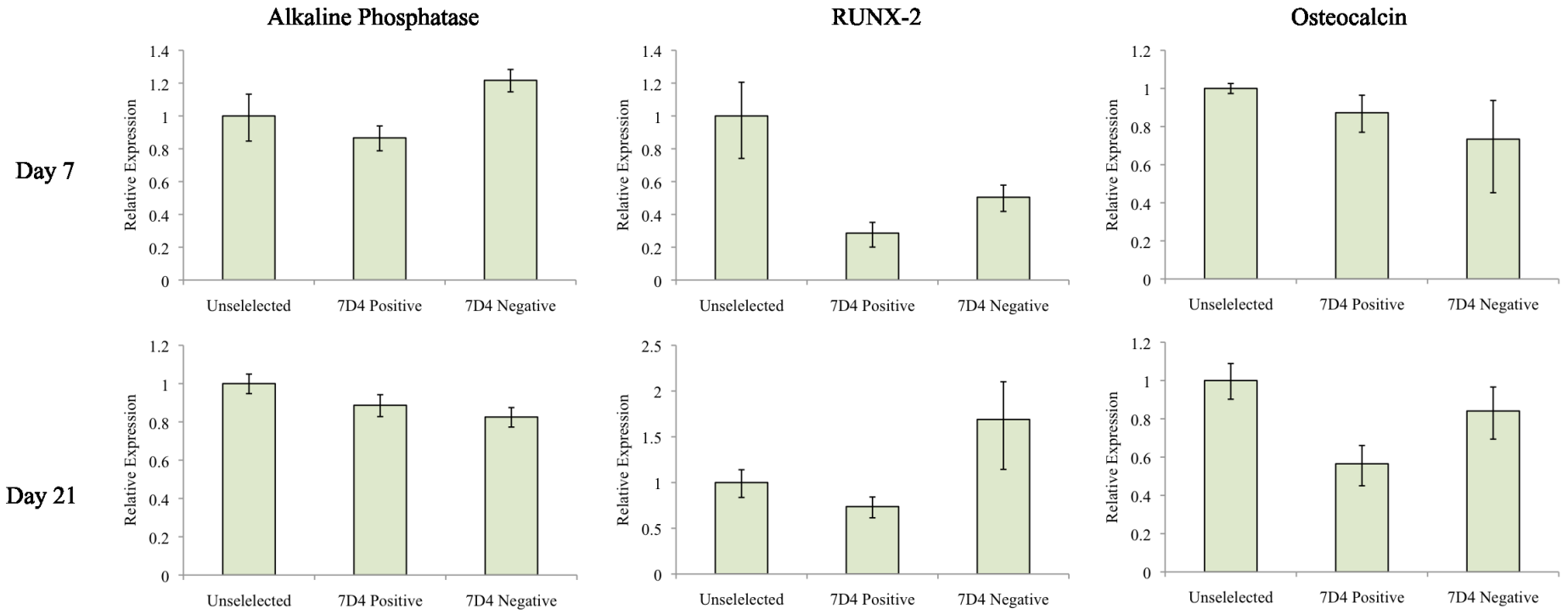

Figure 6:5 Unselected, 7D4 positive and 7D4 negative cell groups cultured in chondrogenic media. Expression of osteogenic markers alkaline phosphatase, RUNX-2 and osteocalcin relative to β-actin. Expression levels were observed following 7 and 21 days in culture relative to β-actin. Relative expression of the sorted cell populations was calculated against unselected cells set at 1. * Indicates significance $p<0.05$ relative to the unselected cell population, as well as between 7D4 positive and negative cell populations.

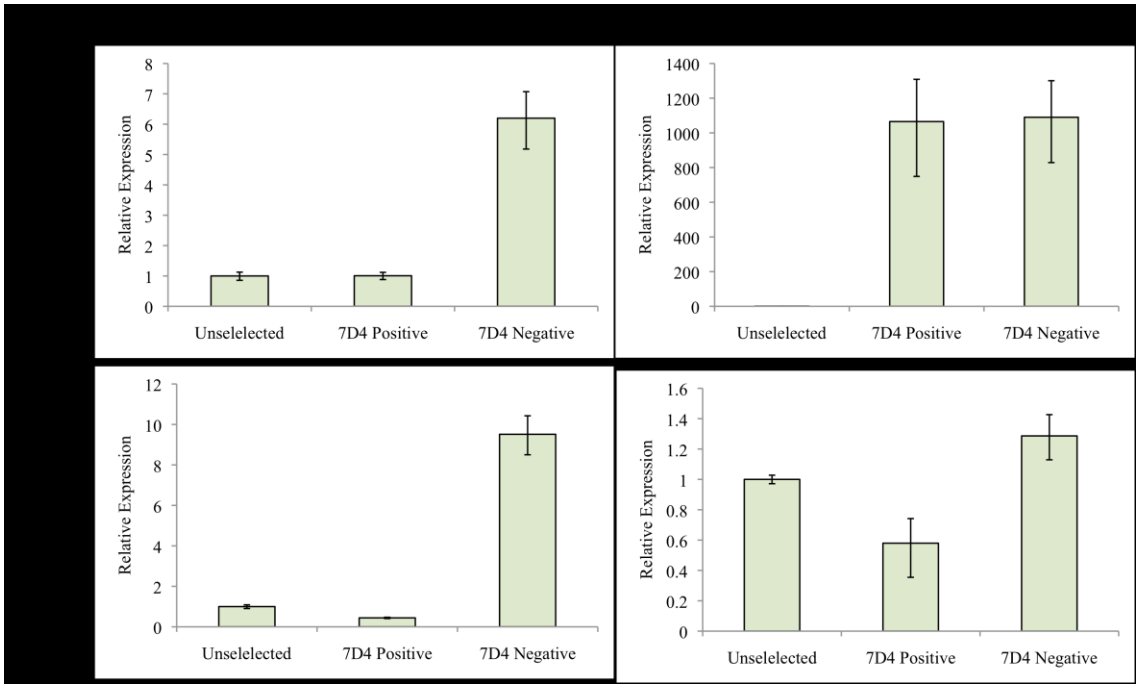

Figure 6:6 Unselected, 7D4 positive and 7D4 negative cells cultured in chondrogenic media. Chondrogenic markers, Type II collagen and SOX-9 expression relative to β-actin. Expression levels were observed following 7 and 21 days in culture. Relative expression of the sorted cell populations was calculated against unselected cells set at 1. * Indicates significance $p<0.05$ relative to the unselected cell population, as well as between 7D4 positive and negative cells.

6.5 Appendix 3

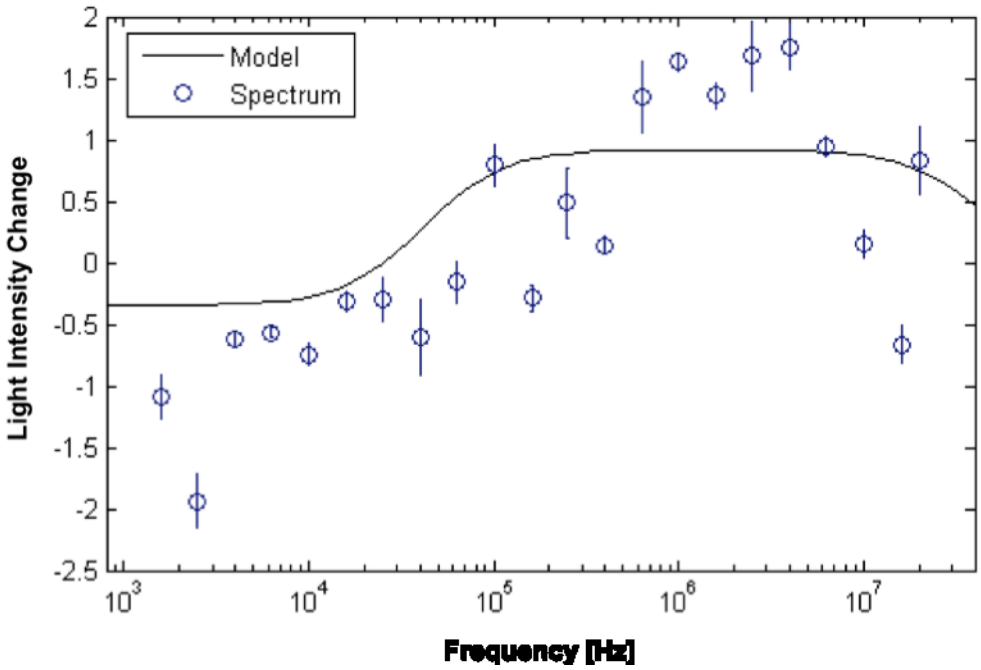

Figure 6:7 Light intensity (arbitrary units) DEP spectra for HBM cells. The data was obtained by measuring the change in light intensity across the well after 60s of exposure to frequencies between 1.6kHz-20MHz. Error bars shown depict the error across the well. A 'best fit' model was not successfully applied due to the variability of the data points at each frequency. Error bars shown depict the error across the well as analysed by the MatLab script. Data drawn from one population.

6.6 Glossary

Adipocyte	Fat cell
Adipo-	Fat
Adipogenesis	Formation of fat cells
Centrifugation	Spinning of cells to produce a pellet
Chondro-	Cartilage
Chondrocyte	Cartilage cell
Chondrogenesis	Formation of cartilage cells
Erythrocyte	Red blood cell
Ex vivo	Outside of body
Genotype	Genetic arrangement
In situ	Within its place
In utero	Within the womb
In vitro	Within the laboratory
In vivo	In patient/animal
Karyotype	Standard arrangement of chromosomes
Lacunae	Cell pits
Osteo-	Bone
Osteoblast	Mature bone cell – responsible for bone formation
Osteoclast	Bone remodelling cell (resorption)
Osteocyte	Mature bone cell encased in matrix
Osteogenesis	Formation of bone cells
Passage	Splitting of cell populations
Phenotype	Physical appearance/expression of distinct markers
Plasticity	Differentiation from one cell type to another

6.7 References

ADEWUMI, O., AFLATOONIAN, B., AHRLUND-RICHTER, L., AMIT, M., ANDREWS, P., BEIGHTON, G., BELLO, P., BENVENISTY, N., BERRY, L. BEVAN, S. et al 2007. Characterization of human embryonic stem cell lines by the International Stem Cell Initiative. *Nature Biotechnology,* 25**,** 803-816.

AKINO, K., MINETA, T., FUKUI, M., FUJII, T. & AKITA, S. 2003. Bone morphogenetic protein-2 regulates proliferation of human mesenchymal stem cells. *Wound Repair and Regeneration,* 11**,** 354-360.

AKIYAMA, H., CHABOISSIER, M., MARTIN, J., SCHEDL, A. & DE CROMBRUGGHE, B. 2002. The transcription factor Sox9 has essential roles in successive steps of the chondrocyte differentiation pathway and is required for expression of Sox5 and Sox6. *Genes & development,* 16**,** 2813-2828.

AKIYAMA, H., SHUKUNAMI, C., NAKAMURA, T. & HIRAKI, Y. 2000. Differential expressions of BMP family genes during chondrogenic differentiation of mouse ATDC5 cells. *Cell Structure and Function,* 25**,** 195-204.

ALFORD, A. & HANKENSON, K. 2006. Matricellular proteins: extracellular modulators of bone development, remodeling, and regeneration. *Bone,* 38**,** 749-757.

AMABILE, G. & MEISSNER, A. 2009. Induced pluripotent stem cells: current progress and potential for regenerative medicine. *Trends in molecular medicine,* 15**,** 59-68.

ANDERSON, D., SELF, T., MELLOR, I., GOH, G., HILL, S. & DENNING, C. 2007. Transgenic enrichment of cardiomyocytes from human embryonic stem cells. *Molecular Therapy,* 15**,** 2027-2036.

ANDERSSON, H. & VAN DEN BERG, A. 2003. Microfluidic devices for cellomics: a review. *Sensors & Actuators: B. Chemical,* 92**,** 315-325.

ANDREWS, P., BANTING, G., DAMJANOV, I., ARNAUD, D. & AVNER, P. 1984. Three monoclonal antibodies defining distinct differentiation antigens associated with different high molecular weight polypeptides on the surface of human embryonal carcinoma cells. *Hybridoma,* 3**,** 347-361.

ANDREWS, P., MATIN, M., BAHRAMI, A., DAMJANOV, I., GOKHALE, P. & DRAPER, J. 2005. Embryonic stem (ES) cells and embryonal carcinoma (EC) cells: opposite sides of the same coin. *Biochemical Society Transactions,* 33**,** 1526-1530.

APLIN, A., HOWE, A. & JULIANO, R. 1999. Cell adhesion molecules, signal transduction and cell growth. *Current Opinion in Cell Biology,* 11**,** 737-744.

AUBIN, J. E. 1998. Bone stem cells. *J.Cell Biochem.Suppl,* 30-31**,** 73-82.

AVERY, S., INNISS, K. & MOORE, H. 2006. The regulation of self-renewal in human embryonic stem cells. *Stem Cells and Development,* 15**,** 729-740.

BAHARVAND, H., HASHEMI, S., ASHTIANI, S. & FARROKHI, A. 2006. Differentiation of human embryonic stem cells into hepatocytes in 2D and 3D culture systems in vitro. *International Journal of Developmental Biology,* 50**,** 645-652.

BAKEWELL, D. & MORGAN, H. 2006. Dielectrophoresis of DNA: time-and frequency-dependent collections on microelectrodes. *IEEE transactions on nanobioscience,* 5**,** 139-146.

BANDYOPADHYAY, A., TSUJI, K., COX, K., HARFE, B., ROSEN, V. & TABIN, C. 2006. Genetic analysis of the roles of BMP2, 4, and 7 in limb patterning and skeletogenesis. 2**,** e216.

BARBERI, T., WILLIS, L. M., SOCCI, N. D. & STUDER, L. 2005. Derivation of multipotent mesenchymal precursors from human embryonic stem cells. *PLoS.Med.,* 2**,** e161.

BARON, R. 2003. *Chapter 1: General Principals of Bone Biology*, American Society of Bone and Mineral Research.

BAUWENS, C. L., PEERANI, R., NIEBRUEGGE, S., WOODHOUSE, K. A., KUMACHEVA, E., HUSAIN, M. & ZANDSTRA, P. W. 2008. Control of Human Embryonic Stem Cell Colony and Aggregate Size Heterogeneity Influences Differentiation Trajectories. *Stem Cells,* 26**,** 2300-2310.

BECKER, F., WANG, X., HUANG, Y., PETHIG, R., VYKOUKAL, J. & GASCOYNE, P. 1995. Separation of human breast cancer cells from blood by differential dielectric affinity. *Proceedings of the National Academy of Sciences,* 92**,** 860-864.

BENBROOK, D. 2006. Organotypic cultures represent tumor microenvironment for drug testing. *Drug Discovery Today: Disease Models,* 3**,** 143-148.

BERESFORD, J., GALLAGHER, J., POSER, J. & RUSSELL, R. 1984. Production of osteocalcin by human bone cells in vitro. Effects of 1, 25 (OH) 2D3, 24, 25 (OH) 2D3, parathyroid hormone, and glucocorticoids. *Metabolic bone disease & related research,* 5**,** 229-234.

BERESFORD, J., GALLAGHER, J. & RUSSELL, R. 1986. 1, 25-Dihydroxyvitamin D3 and human bone-derived cells in vitro: effects on alkaline phosphatase, type I collagen and proliferation. *Endocrinology,* 119**,** 1776-1785.

BESSA, P., CASAL, M. & REIS, R. 2008. Bone morphogenetic proteins in tissue engineering: the road from laboratory to clinic, part II (BMP delivery). *Journal of Tissue Engineering and Regenerative Medicine,* 2**,** 81-96.

BHOSALE, A. M. & RICHARDSON, J. B. 2008. Articular cartilage: structure, injuries and review of management. *Br Med Bull,* 87**,** 77-95.

BI, W., DENG, J., ZHANG, Z., BEHRINGER, R. & DE CROMBRUGGHE, B. 1999. Sox9 is required for cartilage formation. *Nature Genetics,* 22**,** 85-89.

BIANCO, P., KUZNETSOV, S., RIMINUCCI, M. & GEHRON, R. 2006. Postnatal skeletal stem cells. *Methods in Enzymology,* 419**,** 117-148.

BIANCO, P., RIMINUCCI, M., GRONTHOS, S. & ROBEY, P. G. 2001a. Bone Marrow Stromal Stem Cells: Nature, Biology, and Potential Applications. *Stem Cells,* 19**,** 180-192.

BIANCO, P. & ROBEY, P. 2001b. Stem cells in tissue engineering. *Nature,* 414**,** 118-121.

BIELBY, R. C., BOCCACCINI, A. R., POLAK, J. M., BUTTERY, L. D., BIELBY, R. C., BOCCACCINI, A. R., POLAK, J. M. & BUTTERY, L. D. K. 2004. In vitro differentiation and in vivo mineralization of osteogenic cells derived from human embryonic stem cells. *Tissue Engineering,* 10**,** 1518-1525.

BIGDELI, N., KARLSSON, C., STREHL, R., CONCARO, S., HYLLNER, J. & LINDAHL, A. 2009. Coculture of Human Embryonic Stem Cells and Human Articular Chondrocytes Results in Significantly Altered Phenotype and Improved Chondrogenic Differentiation. *Stem Cells,* 27**,** 1812-1821.

BLAUER, M., HEINONEN, P., MARTIKAINEN, P., TOMAS, E. & YLIKOMI, T. 2005. A novel organotypic culture model for normal human endometrium: regulation of epithelial cell proliferation by estradiol and medroxyprogesterone acetate. *Human Reproduction,* 20**,** 864-871.

BRATT-LEAL, A., CARPENEDO, R. & MCDEVITT, T. 2009. Engineering the embryoid body microenvironment to direct embryonic stem cell differentiation. *Biotechnology progress,* 25**,** 43-51.

BROCHE, L., BHADAL, N., LEWIS, M., PORTER, S., HUGHES, M. & LABEED, F. 2007. Early detection of oral cancer–Is dielectrophoresis the answer? *Oral oncology,* 43**,** 199-203.

BROCHE, L., LABEED, F. & HUGHES, M. 2005. Extraction of dielectric properties of multiple populations from dielectrophoretic collection spectrum data. *Physics in Medicine and Biology,* 50**,** 2267-2274.

BRONCKERS, A., GAY, S., FINKELMAN, R. & BUTLER, W. 1987. Developmental appearance of Gla proteins (osteocalcin) and alkaline phosphatase in tooth germs and bones of the rat. *Bone and mineral,* 2**,** 361-373.

BULLEN, P. & WILSON, D. 1997. *The Carnegie staging of human embryos: a practical guide. In: Strachan, T., Lindsay, S., Wilson, D.I., (Eds.),.*

BUMA, P., SCHREURS, W. & VERDONSCHOT, N. 2004. Skeletal tissue engineering--from in vitro studies to large animal models. *Biomaterials,* 25**,** 1487-1495.

BURRIDGE, P., ANDERSON, D., PRIDDLE, H., BARBADILLO MUNOZ, M., CHAMBERLAIN, S., ALLEGRUCCI, C., YOUNG, L. & DENNING, C. 2007. Improved human embryonic stem cell embryoid body homogeneity and cardiomyocyte differentiation from a novel V-96 plate aggregation system highlights interline variability. *Stem Cells,* 25**,** 929-938.

BURT, J. P. H., PETHIG, R., GASCOYNE, P. R. C. & BECKER, F. F. 1990. Dielectrophoretic characterisation of Friend murine erythroleukaemic cells as a measure of induced differentiation. *Biochimica et Biophysica Acta (BBA) - General Subjects,* 1034**,** 93-101.

BUTLER, D., . GOLDSTEIN, SA,. GUILAK, F,. 2000. Functional Tissue Engineering: The Role of Biomechanics. *J. Biomech. Eng,* 122**,** 570-576.

BUTTERY, L., BOURNE, S., XYNOS, J., WOOD, H., HUGHES, F., HUGHES, S., EPISKOPOU, V. & POLAK, J. 2001. Differentiation of osteoblasts and in vitro bone formation from murine embryonic stem cells. *Tissue Engineering,* 7**,** 89-99.

CAMPAGNOLI, C., ROBERTS, I., KUMAR, S., BENNETT, P., BELLANTUONO, I. & FISK, N. 2001. Identification of mesenchymal stem/progenitor cells in human first-trimester fetal blood, liver, and bone marrow. *Blood,* 98**,** 2396-2402.

CANCEDDA, R., DOZIN, B., GIANNONI, P. & QUARTO, R. 2003. Tissue engineering and cell therapy of cartilage and bone. *Matrix biology,* 22**,** 81-91.

CAO, T., HENG, B. C., YE, C. P., LIU, H., TOH, W. S., ROBSON, P., LI, P., HONG, Y. H. & STANTON, L. W. 2005. Osteogenic differentiation within intact human embryoid bodies result in a marked increase in osteocalcin secretion after 12 days of in vitro culture, and formation of morphologically distinct nodule-like structures. *Tissue and Cell,* 37**,** 325-334.

CARPENTER, M. K., ROSLER, E. & RAO, M. S. 2003. Characterization and differentiation of human embryonic stem cells. *Cloning Stem Cells,* 5**,** 79-88.

CHAMBERS, I. 2004. The molecular basis of pluripotency in mouse embryonic stem cells. *Cloning Stem Cells,* 6**,** 386-391.

CHAMBERS, I., COLBY, D., ROBERTSON, M., NICHOLS, J., LEE, S., TWEEDIE, S. & SMITH, A. 2003. Functional Expression Cloning of Nanog, a Pluripotency Sustaining Factor in Embryonic Stem Cells. *Cell,* 113**,** 643-655.

CHEN, D., HARRIS, M. A., ROSSINI, G., DUNSTAN, C. R., DALLAS, S. L., FENG, J. Q., MUNDY, G. R. & HARRIS, S. E. 1997. Bone Morphogenetic Protein 2 (BMP-2) Enhances BMP-3, BMP-4, and Bone Cell Differentiation Marker Gene Expression During the Induction of Mineralized Bone Matrix Formation in Culturesof Fetal Rat Calvarial Osteoblasts. *Calcified Tissue International,* 60**,** 283-290.

CHENG, H., JIANG, W., PHILLIPS, F., HAYDON, R., PENG, Y., ZHOU, L., LUU, H., AN, N., BREYER, B. & VANICHAKARN, P. 2003. Osteogenic activity of the fourteen types of human bone morphogenetic proteins (BMPs). *The Journal of Bone and Joint Surgery,* 85**,** 1544-1552.

CHENG, S., YANG, J., RIFAS, L., ZHANG, S. & AVIOLI, L. 1994. Differentiation of human bone marrow osteogenic stromal cells in vitro: induction of the osteoblast phenotype by dexamethasone. *Endocrinology,* 134**,** 277-286.

CHIN, S., HUGHES, M., COLEY, H. & LABEED, F. 2006. Rapid assessment of early biophysical changes in K562 cells during apoptosis determined using dielectrophoresis. *International Journal of Nanomedicine,* 1**,** 333-337.

CHRISTENSEN, T., PEDERSEN, C., BANG, D. & WOLFF, A. 2007. Sample preparation by cell guiding using negative dielectrophoresis. *Microelectronic Engineering,* 84**,** 1690-1693.

CHUNG, Y., KLIMANSKAYA, I., BECKER, S., LI, T., MASERATI, M., LU, S., ZDRAVKOVIC, T., ILIC, D., GENBACEV, O. & FISHER, S. 2008. Human

embryonic stem cell lines generated without embryo destruction. *Cell Stem Cell,* 2**,** 113-117.

COELHO, M. & FERNANDES, M. 2000. Human bone cell cultures in biocompatibility testing. Part II: effect of ascorbic acid,[beta]-glycerophosphate and dexamethasone on osteoblastic differentiation. *Biomaterials,* 21**,** 1095-1102.

COWAN, C., KLIMANSKAYA, I., MCMAHON, J., ATIENZA, J., WITMYER, J., ZUCKER, J., WANG, S., MORTON, C., MCMAHON, A. & POWERS, D. 2004. Derivation of embryonic stem-cell lines from human blastocysts. *The New England Journal of Medicine,* 350**,** 1353-1356.

CUI, Y., WANG, H., YU, M., XU, T., LI, X. & LI, L. 2006. Differentiation plasticity of human fetal articular chondrocytes. *Otolaryngology-Head and Neck Surgery,* 135**,** 61-67.

CYRANOSKI, D. 2008. Stem cells: 5 things to know before jumping on the iPS bandwagon. *Nature,* 452**,** 406-408.

D'AMOUR, K., AGULNICK, A., ELIAZER, S., KELLY, O., KROON, E. & BAETGE, E. 2005. Efficient differentiation of human embryonic stem cells to definitive endoderm. *Nature Biotechnology,* 23**,** 1534-1541.

DANG, S., KYBA, M., PERLINGEIRO, R., DALEY, G. & ZANDSTRA, P. 2002. Efficiency of embryoid body formation and hematopoietic development from embryonic stem cells in different culture systems. *Biotechnology and bioengineering,* 78**,** 442-453.

DEB, S., MANDEGARAN, R. & DI SILVIO, L. 2010. A porous scaffold for bone tissue engineering/45S5 BioglassÆ derived porous scaffolds for co-culturing osteoblasts and endothelial cells. *Journal of Materials Science: Materials in Medicine,* 21**,** 893-905.

DEMARTEAU, O., JAKOB, M., SCH‰FER, D., HEBERER, M. & MARTIN, I. 2003. Development and validation of a bioreactor for physical stimulation of engineered cartilage. *Biorheology,* 40**,** 331-336.

DENNING, C., ALLEGRUCCI, C., PRIDDLE, H., BARBADILLO-MUNOZ, M., ANDERSON, D., SELF, T., SMITH, N., PARKIN, C. & YOUNG, L. 2006. Common culture conditions for maintenance and cardiomyocyte differentiation of the human embryonic stem cell lines, BG01 and HUES-7. *International Journal of Developmental Biology,* 50**,** 27-37.

DIJKGRAAF, L. C., DE BONT, L. G. M., BOERING, G. & LIEM, R. S. B. 1995. The structure, biochemistry, and metabolism of osteoarthritic cartilage: A review of the literature. *Journal of Oral and Maxillofacial Surgery,* 53**,** 1182-1192.

DRAPER, J., SMITH, K., GOKHALE, P., MOORE, H., MALTBY, E., JOHNSON, J., MEISNER, L., ZWAKA, T., THOMSON, J. & ANDREWS, P. 2003. Recurrent gain of chromosomes 17q and 12 in cultured human embryonic stem cells. *nature biotechnology,* 22**,** 53-54.

DRAPER, J. S., MOORE, H. D., RUBAN, L. N., GOKHALE, P. J. & ANDREWS, P. W. 2004. Culture and characterization of human embryonic stem cells. *Stem Cells Dev.,* 13**,** 325-336.

DUGUAY, D., FOTY, R. A. & STEINBERG, M. S. 2003. Cadherin-mediated cell adhesion and tissue segregation: qualitative and quantitative determinants. *Developmental Biology,* 253**,** 309-323.

DUPLOMB, L., DAGOUASSAT, M., JOURDON, P. & HEYMANN, D. 2006. Embryonic stem cells: new tool to study osteoblast and osteoclast differentiation. *Stem Cells***,** 2006-0395.

EAMES, B., SHARPE, P. & HELMS, J. 2004. Hierarchy revealed in the specification of three skeletal fates by Sox9 and Runx2. *Developmental Biology,* 274**,** 188-200.

EFFENHAUSER, C. & MANZ, A. 1994. Miniaturizing a whole analytical laboratory down to chip size. *American laboratory(Fairfield),* 26**,** 15-15.

ERICKSON, D. & LI, D. 2004. Integrated microfluidic devices. *Analytica Chimica Acta,* 507**,** 11-26.

ETHERIDGE, S. L., SPENCER, G. J., HEATH, D. J. & GENEVER, P. G. 2004. Expression profiling and functional analysis of wnt signaling mechanisms in mesenchymal stem cells. *Stem Cells,* 22**,** 849-860.

EVANS, M. J. & KAUFMAN, M. H. 1981. Establishment in culture of pluripotential cells from mouse embryos. *Nature,* 292**,** 154-156.

EZEKIEL, U., MUTHUCHAMY, M., RYERSE, J. & HEUERTZ, R. 2007. Single embryoid body formation in a multi-well plate. *Electronic Journal of Biotechnology,* 10**,** 328-335.

FATOYINBO, H., KAMCHIS, D., WHATTINGHAM, R., OGIN, S. & HUGHES, M. 2005. A high-throughput 3-D composite dielectrophoretic separator. *IEEE Transactions on Biomedical Engineering,* 52**,** 1347-1349.

FLANAGAN, L., LU, J., WANG, L., MARCHENKO, S., JEON, N., LEE, A. & MONUKI, E. 2008a. Unique dielectric properties distinguish stem cells and their differentiated progeny. *Stem Cells,* 26**,** 656-665.

FLANAGAN, L. A., LU, J., WANG, L., MARCHENKO, S. A., JEON, N. L., LEE, A. P. & MONUKI, E. S. 2008b. Unique Dielectric Properties Distinguish Stem Cells and Their Differentiated Progeny. *Stem Cells,* 26**,** 656-665.

FLEMING, T. P., MCCONNELL, J., JOHNSON, M. H. & STEVENSON, B. R. 1989. Development of tight junctions de novo in the mouse early embryo: control of assembly of the tight junction-specific protein, ZO-1. *The Journal of Cell Biology,* 108**,** 1407-1418.

FRANCESCHI, R. & YOUNG, J. 1990. Regulation of alkaline phosphatase by 1, 25-dihydroxyvitamin D3 and ascorbic acid in bone-derived cells. *Journal of bone and mineral research: the official journal of the American Society for Bone and Mineral Research,* 5**,** 1157-1167.

FREED, L., VUNJAK-NOVAKOVIC, G., BIRON, R., EAGLES, D., LESNOY, D., BARLOW, S. & LANGER, R. 1994. Biodegradable polymer scaffolds for tissue engineering. *nature biotechnology,* 12**,** 689-693.

GADUE, P., HUBER, T. L., NOSTRO, M. C., KATTMAN, S. & KELLER, G. M. 2005. Germ layer induction from embryonic stem cells. *Experimental Hematology,* 33**,** 955-964.

GAHWILER, B. 1981. Organotypic monolayer cultures of nervous tissue. *Journal of neuroscience methods,* 4**,** 329-342.

GANG, E. J., BOSNAKOVSKI, D., FIGUEIREDO, C. A., VISSER, J. W. & PERLINGEIRO, R. C. 2007. SSEA-4 identifies mesenchymal stem cells from bone marrow. *Blood,* 109**,** 1743-1751.

GASCOYNE, P., PETHIG, R., SATAYAVIVAD, J., BECKER, F. F. & RUCHIRAWAT, M. 1997a. Dielectrophoretic detection of changes in erythrocyte membranes following malarial infection. *Biochimica et Biophysica Acta (BBA) - Biomembranes,* 1323**,** 240-252.

GASCOYNE, P., WANG, X., HUANG, Y. & BECKER, F. 1997b. Dielectrophoretic separation of cancer cells from blood. *IEEE transactions on industry applications,* 33**,** 670-678.

GASCOYNE, P. R. C. & VYKOUKAL, J. 2002. Particle separation by dielectrophoresis. *Electrophoresis,* 23**,** 1973-1983.

GASSMANN, M., FANDREY, J., BICHET, S., WARTENBERG, M., MARTI, H., BAUER, C., WENGER, R. & ACKER, H. 1996. Oxygen supply and oxygen-dependent gene expression in differentiating embryonic stem cells. *Proceedings of the National Academy of Sciences of the United States of America,* 93**,** 2867-2872.

GEENS, M., VAN DE VELDE, H., DE BLOCK, G., GOOSSENS, E., VAN STEIRTEGHEM, A. & TOURNAYE, H. 2007. The efficiency of magnetic-activated cell sorting and fluorescence-activated cell sorting in the decontamination of testicular cell suspensions in cancer patients. *Human Reproduction,* 22**,** 733-742.

GIUFFRIDA, D., ROGERS, I. M., NAGY, A., CALOGERO, A. E., BROWN, T. J. & CASPER, R. F. 2009. Human embryonic stem cells secrete soluble factors that inhibit cancer cell growth. *Cell Proliferation,* 42**,** 788-798.

GO, M., TAKENAKA, C. & OHGUSHI, H. 2007. Forced expression of Sox2 or Nanog in human bone marrow derived mesenchymal stem cells maintains their expansion and differentiation capabilities. *Experimental Cell Research*.

GOSHIMA, J., GOLDBERG, V. & CAPLAN, A. 1991. The osteogenic potential of culture-expanded rat marrow mesenchymal cells assayed in vivo in calcium phosphate ceramic blocks. *Clin Orthop Relat Res.,* 262**,** 298-311.

GOTHARD, D., ROBERTS, S., SHAKESHEFF, K. & BUTTERY, L. 2009. Controlled embryoid body formation via surface modification and avidinñbiotin cross-linking. *Cytotechnology,* 61**,** 135-144.

GREEN, D., HOWARD, D., YANG, X., KELLY, M. & OREFFO, R. 2003. Natural marine sponge fiber skeleton: a biomimetic scaffold for human osteoprogenitor cell attachment, growth, and differentiation. *Tissue Engineering,* 9**,** 1159-1166.

GRONTHOS, S., BRAHIM, J., LI, W., FISHER, L., CHERMAN, N., BOYDE, A., DENBESTEN, P., ROBEY, P. & SHI, S. 2002. Stem cell properties of human dental pulp stem cells. *Journal of Dental Research,* 81**,** 531-535.

GRONTHOS, S., GRAVES, S. E., OHTA, S. & SIMMONS, P. J. 1994. The STRO-1+ fraction of adult human bone marrow contains the osteogenic precursors. *Blood,* 84**,** 4164-4173.

GRONTHOS, S. & SIMMONS, P. J. 1995. The growth factor requirements of STRO-1-positive human bone marrow stromal precursors under serum-deprived conditions in vitro. *Blood,* 85**,** 929-940.

GRONTHOS, S., ZANNETTINO, A. C., GRAVES, S. E., OHTA, S., HAY, S. J. & SIMMONS, P. J. 1999. Differential cell surface expression of the STRO-1 and

alkaline phosphatase antigens on discrete developmental stages in primary cultures of human bone cells. *J.Bone Miner.Res,* 14**,** 47-56.

GROVE, J., BRUSCIA, E. & KRAUSE, D. 2004. Plasticity of bone marrow-derived stem cells. *Stem Cells,* 22**,** 487-500.

HANNA, J., WERNIG, M., MARKOULAKI, S., SUN, C., MEISSNER, A., CASSADY, J., BEARD, C., BRAMBRINK, T., WU, L. & TOWNES, T. 2007. Treatment of sickle cell anemia mouse model with iPS cells generated from autologous skin. *Science,* 318**,** 1879-1880.

HAO, J., VARSHNEY, R. R. & WANG, D.-A. 2008. TGF-β3: A promising growth factor in engineered organogenesis. *Expert Opinion on Biological Therapy,* 8**,** 1485-1493.

HARRIS, S., ENGER, R., RIGGS, L. & SPELSBERG, T. 1995. Development and characterization of a conditionally immortalized human fetal osteoblastic cell line. *Journal of Bone and Mineral Research,* 10**,** 178-186.

HAYES, A. J., HUGHES, C. E. & CATERSON, B. 2008a. Antibodies and immunohistochemistry in extracellular matrix research. *Methods,* 45**,** 10-21.

HAYES, A. J., TUDOR, D., NOWELL, M. A., CATERSON, B. & HUGHES, C. E. 2008b. Chondroitin sulfate sulfation motifs as putative biomarkers for isolation of articular cartilage progenitor cells. *J.Histochem.Cytochem.,* 56**,** 125-138.

HEALY, C., UWANOGHO, D. & SHARPE, P. 1999. Regulation and role of Sox9 in cartilage formation. *Developmental Dynamics,* 215**,** 69-78.

HENG, B. C., CAO, T., STANTON, L. W., ROBSON, P. & OLSEN, B. 2004. Strategies for Directing the Differentiation of Stem Cells Into the Osteogenic Lineage In Vitro. *Journal of Bone and Mineral Research,* 19**,** 1379-1394.

HING, K. 2004. Bone repair in the twenty-first century: biology, chemistry or engineering? *Philos Transact A Math Phys Eng Sci.,* 362**,** 2821-2850.

HOETTGES, K. 2010. Dielectrophoresis as a cell characterisation tool. *Methods Mol Biol.,* 583**,** 183-189.

HOETTGES, K., DALE, J. & HUGHES, M. 2007. Rapid determination of antibiotic resistance in E. coli using dielectrophoresis. *Physics in Medicine and Biology,* 52**,** 6001-6010.

HOETTGES, K., MCDONNELL, M. & HUGHES, M. 2003. Use of combined dielectrophoretic/electrohydrodynamic forces for biosensor enhancement. *Journal of Physics D: Applied Physics,* 36**,** L101.

HOFFMAN, L. M. & CARPENTER, M. K. 2005. Characterization and culture of human embryonic stem cells. *Nat.Biotechnol.,* 23**,** 699-708.

HOLEVINSKY, K. & NELSON, D. 1998. Membrane capacitance changes associated with particle uptake during phagocytosis in macrophages. *Biophysical journal,* 75**,** 2577-2586.

HUANG, Y. & HOLZEL, R. 1992. Differences in the AC electrodynamics of viable and non-viable yeast cells determined through combined dielectrophoresis and electrorotation studies. *Phys. Med,* 37**,** 1499-1517.

HUANG, Y., HOLZEL, R., PETHIG, R. & WANG, X. 1992. Differences in the AC electrodynamics of viable and non-viable yeast cells determined through combined dielectrophoresis and electrorotation studies. *Physics in Medicine and Biology,* 37**,** 1499-1517.

HUANG, Y., WANG, X., BECKER, F. & GASCOYNE, P. 1996. Membrane changes associated with the temperature-sensitive P85gag-mos-dependent transformation of rat kidney cells as determined by dielectrophoresis and electrorotation. *BBA-Biomembranes,* 1282**,** 76-84.

HUANG, Y., WANG, X., HOLZEL, R., BECKER, F. & GASCOYNE, P. 1995. Electrorotational studies of the cytoplasmic dielectric properties of Friend murine erythroleukaemia cells. *Physics in Medicine and Biology,* 40**,** 1789-1806.

HUBNER, Y., HOETTGES, K., KASS, G., OGIN, S. & HUGHES, M. 2005a. Parallel measurements of drug actions on erythrocytes by dielectrophoresis, using a three-dimensional electrode design. *Nanobiotechnology, IEE Proceedings,* 152**,** 150-154.

HUBNER, Y., HOETTGES, K., KASS, G., OGIN, S. & HUGHES, M. Year. Parallel measurements of drug actions on erythrocytes by dielectrophoresis, using a three-dimensional electrode design. *In*, 2005b. 150-154.

HÜBNER, Y., MULHALL, H., HOETTGES, K., KASS, G., OGIN, S. & HUGHES, M. 2007. Dielectrophoresis: A new in vitro approach to measure drug-induced cytotoxicity. *Toxicology,* 240**,** 183-184.

HUGHES, M. 2002a. Strategies for dielectrophoretic separation in laboratory-on-a-chip systems. *Electrophoresis,* 23.

HUGHES, M. 2002b. Strategies for dielectrophoretic separation in laboratory-on-a-chip systems. *Electrophoresis,* 23**,** 2569-2582.

HUGHES, M. P. 2002c. Strategies for dielectrophoretic separation in laboratory-on-a-chip systems. *Electrophoresis,* 23**,** 2569-82.

HUH, D., GU, W., KAMOTANI, Y., GROTBERG, J. & TAKAYAMA, S. 2005. Review: Microfluidics for flow cytometric analysis of cells and particles. *Physiological measurement,* 26**,** R73-R98.

HUTMACHER, D. 2000. Scaffolds in tissue engineering bone and cartilage. *Biomaterials,* 21**,** 2529-2543.

HYSLOP, L., ARMSTRONG, L., STOJKOVIC, M. & LAKO, M. 2005a. Human embryonic stem cells: biology and clinical implications. *Expert reviews in molecular medicine,* 7**,** 1-21.

HYSLOP, L., STOJKOVIC, M., ARMSTRONG, L., WALTER, T., STOJKOVIC, P., PRZYBORSKI, S., HERBERT, M., MURDOCH, A., STRACHAN, T. & LAKO, M. 2005b. Downregulation of NANOG induces differentiation of human embryonic stem cells to extraembryonic lineages. AlphaMed Press.

IRIMAJIRI, A., HANAI, T. & INOUYE, A. 1979. A dielectric theory of "multi-stratified shell" model with its application to a lymphoma cell. *Journal of Theoretical Biology,* 78**,** 251-269.

ITSKOVITZ-ELDOR, J., SCHULDINER, M., KARSENTI, D., EDEN, A., YANUKA, O., AMIT, M., SOREQ, H. & BENVENISTY, N. 2000. Differentiation of human embryonic stem cells into embryoid bodies compromising the three embryonic germ layers. *Molecular Medicine,* 6**,** 88-95.

JACKSON, S. A., SCHIESSER, J., STANLEY, E. G. & ELEFANTY, A. G. 2010. Differentiating Embryonic Stem Cells Pass through 'Temporal Windows' That Mark Responsiveness to Exogenous and Paracrine Mesendoderm Inducing Signals. *PLoS One,* 5**,** e10706.

JAISWAL, N., HAYNESWORTH, S., CAPLAN, A. & BRUDER, S. 1997. Osteogenic differentiation of purified, culture-expanded human mesenchymal stem cells in vitro. *Journal of Cellular Biochemistry,* 64**,** 295-312.

JARRAHY, R., HUANG, W., RUDKIN, G. H., LEE, J. M., ISHIDA, K., BERRY, M. D., SUKKARIEH, M., WU, B. M., YAMAGUCHI, D. T. & MILLER, T. A. 2005. Osteogenic differentiation is inhibited and angiogenic expression is enhanced in MC3T3-E1 cells cultured on three-dimensional scaffolds. *Am J Physiol Cell Physiol,* 289**,** C408-414.

JOHARI, J., HUBNER, Y., HULL, J., DALE, J. & HUGHES, M. 2003. Dielectrophoretic assay of bacterial resistance to antibiotics. *Physics in Medicine and Biology,* 48**,** N193-N198.

JOHNSON, M. 2002. *Human biology: concepts and current issues,* San Francisco, Benjamin Cummings.

JONES, T. 1995. *Electromechanics of particles*, Cambridge Univ Pr.

JONES, T. 2003. Basic theory of dielectrophoresis and electrorotation. *IEEE Engineering in Medicine and Biology Magazine,* 22**,** 33-42.

JUKES, J., VAN BLITTERSWIJK, C. & DE BOER, J. 2009. Skeletal tissue engineering using embryonic stem cells. *Journal of Tissue Engineering and Regenerative Medicine,* 4**,** 165 - 180.

KAPUR, S., BAYLINK, D. J. & WILLIAM LAU, K. H. 2003. Fluid flow shear stress stimulates human osteoblast proliferation and differentiation through multiple interacting and competing signal transduction pathways. *Bone,* 32**,** 241-251.

KARNER, E., UNGER, C., SLOAN, A. J., HRLUND-RICHTER, L., SUGARS, R. V. & WENDEL, M. 2007. Bone matrix formation in osteogenic cultures derived from human embryonic stem cells in vitro. *Stem Cells Dev.,* 16**,** 39-52.

KARP, J. M., FERREIRA, L. S., KHADEMHOSSEINI, A., KWON, A. H., YEH, J. & LANGER, R. S. 2006. Cultivation of human embryonic stem cells without the embryoid body step enhances osteogenesis in vitro. *Stem Cells,* 24**,** 835-843.

KAWAGUCHI, J. 2006. Generation of osteoblasts and chondrocytes from embryonic stem cells. *Methods Mol.Biol.,* 330**,** 135-148.

KAWAGUCHI, J., MEE, P. J. & SMITH, A. G. 2005. Osteogenic and chondrogenic differentiation of embryonic stem cells in response to specific growth factors. *Bone,* 36**,** 758-769.

KAWAKAMI, Y., RODRIGUEZ-LEÛN, J. & BELMONTE, J. C. I. A. 2006. The role of TGF[beta]s and Sox9 during limb chondrogenesis. *Current Opinion in Cell Biology,* 18**,** 723-729.

KELLER, G., KENNEDY, M., PAPAYANNOPOULOU, T. & WILES, M. 1993. Hematopoietic commitment during embryonic stem cell differentiation in culture. *Molecular and Cellular Biology,* 13**,** 473-486.

KENNEDY, M., FIRPO, M., CHOI, K., WALL, C., ROBERTSON, S., KABRUN, N. & KELLER, G. 1997. A common precursor for primitive erythropoiesis and definitive haematopoiesis. *Nature* 386**,** 488-493.

KHOO, M. L. M., MCQUADE, L. R., SMITH, M. S. R., LEES, J. G., SIDHU, K. S. & TUCH, B. E. 2005. Growth and Differentiation of Embryoid Bodies Derived from

Human Embryonic Stem Cells: Effect of Glucose and Basic Fibroblast Growth Factor. *Biology of Reproduction,* 73**,** 1147-1156.

KLEIN-NULEND, J., BACABAC, R. & MULLENDER, M. 2005. Mechanobiology of bone tissue. *Pathologie Biologie,* 53**,** 576-580.

KLEINMAN, H. & MARTIN, G. 2005. Matrigel: basement membrane matrix with biological activity. *Seminars in Cancer Biology,* 15**,** 378-386.

KOIKE, M., SAKAKI, S., AMANO, Y. & KUROSAWA, H. 2007. Characterization of embryoid bodies of mouse embryonic stem cells formed under various culture conditions and estimation of differentiation status of such bodies. *Journal of bioscience and bioengineering,* 104**,** 294-299.

KOROSSIS, S., BOLLAND, F., KEARNEY, J., FISHER, J. & INGHAM, E. 2005. *Bioreactors in tissue engineering*.

KOYANAGI-KATSUTA, R., AKIMITSU, N., ARIMITSU, N. & HATANO, T. 2000. Apoptosis of mouse embryonic stem cells induced by single cell suspension. *Tissue and Cell,* 32**,** 66-70.

KRAMER, J., HEGERT, C., GUAN, K., WOBUS, A., M¸LLER, P. & ROHWEDEL, J. 2000. Embryonic stem cell-derived chondrogenic differentiation in vitro: activation by BMP-2 and BMP-4. *Mechanisms of Development,* 92**,** 193-205.

KRUMLAUF, R. 1994. Hox genes in vertebrate development. *Cell(Cambridge),* 78**,** 191-201.

KUROSAWA, H. 2007. Methods for inducing embryoid body formation: in vitro differentiation system of embryonic stem cells. *Journal of bioscience and bioengineering,* 103**,** 389-398.

LABEED, F. 2004. *Applications of Dielectrophoresis in Oncology.*

LABEED, F., COLEY, H. & HUGHES, M. 2006. Differences in the biophysical properties of membrane and cytoplasm of apoptotic cells revealed using dielectrophoresis. *BBA-General Subjects,* 1760**,** 922-929.

LABEED, F., COLEY, H., THOMAS, H. & HUGHES, M. 2003. Assessment of multidrug resistance reversal using dielectrophoresis and flow cytometry. *Biophysical journal,* 85**,** 2028-2034.

LAFLAMME, M., CHEN, K., NAUMOVA, A., MUSKHELI, V., FUGATE, J., DUPRAS, S., REINECKE, H., XU, C., HASSANIPOUR, M. & POLICE, S. 2007. Cardiomyocytes derived from human embryonic stem cells in pro-survival factors enhance function of infarcted rat hearts. *nature biotechnology,* 25**,** 1015-1024.

LASLETT, A. L., FILIPCZYK, A. A. & PERA, M. F. 2003. Characterization and culture of human embryonic stem cells. *Trends Cardiovasc.Med.,* 13**,** 295-301.

LEVENBERG, S., HUANG, N. F., LAVIK, E., ROGERS, A. B., ITSKOVITZ-ELDOR, J. & LANGER, R. 2003. Differentiation of human embryonic stem cells on three-dimensional polymer scaffolds. *Proceedings of the National Academy of Sciences,* 100**,** 12741-12746.

LI, R. & WOZNEY, J. 2001. Delivering on the promise of bone morphogenetic proteins. *TRENDS in Biotechnology,* 19**,** 255-265.

LIEBERMAN, J., DALUISKI, A. & EINHORN, T. 2002. The role of growth factors in the repair of bone: biology and clinical applications. *The Journal of Bone and Joint Surgery,* 84**,** 1032-1044.

LIN, R.-Z., HO, C.-T., LIU, C.-H. & CHANG, H.-Y. 2006. Dielectrophoresis based-cell patterning for tissue engineering. *Biotechnology Journal,* 1**,** 949-957.

MACGREGOR, G., ZAMBROWICZ, B. & SORIANO, P. 1995. Tissue non-specific alkaline phosphatase is expressed in both embryonic and extraembryonic lineages during mouse embryogenesis but is not required for migration of primordial germ cells. *Development,* 121**,** 1487-1496.

MALLON, B., PARK, K., CHEN, K., HAMILTON, R. & MCKAY, R. 2006. Toward xeno-free culture of human embryonic stem cells. *The international journal of biochemistry & cell biology,* 38**,** 1063-1075.

MARKS, G., HUANG, Y., ZHOU, X. & PETHIG, R. 1994. Dielectrophoretic characterization and separation of micro-organisms. *Microbiology,* 140**,** 585.

MARKS, S. & HERMEY, D. 1996. *The structure and development of bone*.

MARTIN, I., WENDT, D. & HEBERER, M. 2004. The role of bioreactors in tissue engineering. *TRENDS in Biotechnology,* 22**,** 80-86.

MASON, C. & DUNNILL, P. 2008. A brief definition of regenerative medicine. *Regen. Med.,* 3**,** 1-5.

MESSANA, J., HWANG, N., COBURN, J., ELISSEEFF, J. & ZHANG, Z. 2008. Size of the embryoid body influences chondrogenesis of mouse embryonic stem cells. *Journal of Tissue Engineering and Regenerative Medicine,* 2**,** 499-506.

METALLO, C., AZARIN, S., JI, L., DE PABLO, J. & PALECEK, S. 2008. Engineering tissue from human embryonic stem cells. *Journal of cellular and molecular medicine,* 12**,** 709-729.

MIRMALEK-SANI, S., TARE, R., MORGAN, S., ROACH, H., WILSON, D., HANLEY, N. & OREFFO, R. 2005. Characterization and multipotentiality of human fetal femur-derived cells: implications for skeletal tissue regeneration. *Stem Cells,* 24**,** 1042-1053.

MONTJOVENT, M., BURRI, N., MARK, S., FEDERICI, E., SCALETTA, C., ZAMBELLI, P., HOHLFELD, P., LEYVRAZ, P., APPLEGATE, L. & PIOLETTI, D. 2004. Fetal bone cells for tissue engineering. *Bone,* 35**,** 1323-1333.

MURRY, C. & KELLER, G. 2008. Differentiation of embryonic stem cells to clinically relevant populations: lessons from embryonic development. *Cell,* 132**,** 661-680.

NAKAGAWA, T., LEE, S. & REDDI, A. 2009. Induction of chondrogenesis from human embryonic stem cells without embryoid body formation by bone morphogenetic protein 7 and transforming growth factor 1. *Arthritis & Rheumatism,* 60**,** 3686-3692.

NG, E., DAVIS, R., AZZOLA, L., STANLEY, E. & ELEFANTY, A. 2005. Forced aggregation of defined numbers of human embryonic stem cells into embryoid bodies fosters robust, reproducible hematopoietic differentiation. *Blood,* 106**,** 1601-1603.

NIWA, H. 2001. Molecular mechanism to maintain stem cell renewal of ES cells. *Cell Struct.Funct.,* 26**,** 137-148.

NIWA, H., MIYAZAKI, J. & SMITH, A. 2000. Quantitative expression of Oct-3/4 defines differentiation, dedifferentiation or self-renewal of ES cells. *Nature Genetics,* 24**,** 372-376.

NOAKSSON, K., ZORIC, N., ZENG, X., RAO, M., HYLLNER, J., SEMB, H., KUBISTA, M. & SARTIPY, P. 2005. Monitoring differentiation of human embryonic stem cells using real-time PCR. *Stem Cells,* 23**,** 1460-1467.

O'CONNOR, M., KARDEL, M., IOSFINA, I., YOUSSEF, D., LU, M., LI, M., VERCAUTEREN, S., NAGY, A. & EAVES, C. 2008. Alkaline phosphatase-positive colony formation is a sensitive, specific, and quantitative indicator of undifferentiated human embryonic stem cells. *Stem Cells,* 26**,** 1109-1116.

O'RAHILLY, R. & MULLER, F. 1987. *Developmental stages in human embryos: including a revision of Streeter's" Horizons" and a survey of the Carnegie collection*, Carnegie Institution of Washington.

ODORICO, J. S., KAUFMAN, D. S. & THOMSON, J. A. 2001. Multilineage differentiation from human embryonic stem cell lines. [Review]. *Stem Cells,* 19**,** 193-204.

OLIVIER, E. N., RYBICKI, A. C. & BOUHASSIRA, E. E. 2006. Differentiation of human embryonic stem cells into bipotent mesenchymal stem cells. *Stem Cells,* 24**,** 1914-1922.

OWEN, M. & FRIEDENSTEIN, A. 1988. Stromal stem cells: marrow-derived osteogenic precursors. *Ciba Found Symp. ,* 136**,** 42-60.

PAN, T., MASON, R. J., WESTCOTT, J. Y. & SHANNON, J. M. 2001. Rat Alveolar Type II Cells Inhibit Lung Fibroblast Proliferation In Vitro. *Am. J. Respir. Cell Mol. Biol.,* 25**,** 353-361.

PARK, S., OREFFO, R. & TRIFFITT, J. 1999. Interconversion potential of cloned human marrow adipocytes in vitro. *Bone,* 24**,** 549-554.

PARTRIDGE, K., YANG, X., CLARKE, N., OKUBO, Y., BESSHO, K., SEBALD, W., HOWDLE, S., SHAKESHEFF, K. & OREFFO, R. 2002. Adenoviral BMP-2 gene transfer in mesenchymal stem cells: in vitro and in vivo bone formation on biodegradable polymer scaffolds. *Biochemical and Biophysical Research Communications,* 292**,** 144-152.

PATEL, A., PARK, E., KUZMAN, M., BENETTI, F., SILVA, F. & ALLICKSON, J. 2008. Multipotent menstrual blood stromal stem cells: isolation, characterization, and differentiation. *Cell Transplantation,* 17**,** 303-311.

PATEL, M. & YANG, S. 2010. Advances in Reprogramming Somatic Cells to Induced Pluripotent Stem Cells. *Stem Cell Reviews and Reports***,** E-publication.

PERCH-NIELSEN, I., BANG, D., POULSEN, C., EL-ALI, J. & WOLFF, A. 2003. Removal of PCR inhibitors using dielectrophoresis as a selective filter in a microsystem. *Lab on a Chip,* 3**,** 212-216.

PETHIG, R. 1996. Dielectrophoresis: using inhomogeneous AC electrical fields to separate and manipulate cells. *Critical reviews in biotechnology,* 16**,** 331-348.

PETHIG, R., LEE, R. & TALARY, M. 2004. Cell physiometry tools based on dielectrophoresis. *Journal of the Association for Laboratory Automation,* 9**,** 324-330.

PETHIG, R., MENACHERY, A., PELLS, S. & DE SOUSA, P. 2010. Dielectrophoresis: A Review of Applications for Stem Cell Research. *J Biomed Biotechnol.* [Online].

PHINNEY, D. & PROCKOP, D. 2007. Concise review: mesenchymal stem/multipotent stromal cells: the state of transdifferentiation and modes of tissue repair current views. *Stem Cells,* 25**,** 2896-2902.

PITTENGER, M. F., MACKAY, A. M., BECK, S. C., JAISWAL, R. K., DOUGLAS, R., MOSCA, J. D., MOORMAN, M. A., SIMONETTI, D. W., CRAIG, S. & MARSHAK, D. R. 1999. Multilineage Potential of Adult Human Mesenchymal Stem Cells. *Science,* 284**,** 143-147.

POCHAMPALLY, R. R., SMITH, J. R., YLOSTALO, J. & PROCKOP, D. J. 2004. Serum deprivation of human marrow stromal cells (hMSCs) selects for a subpopulation of early progenitor cells with enhanced expression of OCT-4 and other embryonic genes. *Blood,* 103**,** 1647-1652.

POHL, H. 1978. *Dielectrophoresis*, Cambridge University Press, Cambridge.

POHL, H. & HAWK, I. 1966. Separation of Living and Dead Cells by Dielectrophoresis. *Science,* 152**,** 647-649.

PORTNOY, J., PAN, T., DINARELLO, C. A., SHANNON, J. M., WESTCOTT, J. Y., ZHANG, L. & MASON, R. J. 2006. Alveolar type II cells inhibit fibroblast proliferation: role of IL-1{alpha}. *Am J Physiol Lung Cell Mol Physiol,* 290**,** L307-316.

POUNTOS, I., JONES, E., TZIOUPIS, C., MCGONAGLE, D. & GIANNOUDIS, P. V. 2006. Growing bone and cartilage: The role of mesenchymal stem cells. *Journal of Bone & Joint Surgery - British Volume,* 88-B**,** 421-426.

PRINGLE, A., MORRISON, B., BRADLEY, M., IANNOTTI, F. & SUNDSTROM, L. 2003. Characterisation of a novel class of polyamine-based neuroprotective compounds. *Naunyn-Schmiedeberg's archives of pharmacology,* 368**,** 216-224.

PROVOT, S. & SCHIPANI, E. 2005. Molecular mechanisms of endochondral bone development. *Biochemical and Biophysical Research Communications,* 328**,** 658-665.

PRUSA, A., MARTON, E., ROSNER, M., BERNASCHEK, G. & HENGSTSCHLAGER, M. 2003. Oct-4-expressing cells in human amniotic fluid: a new source for stem cell research? *Human Reproduction,* 18**,** 1489-1493.

QUESENBERRY, P., DOONER, G., COLVIN, G. & ABEDI, M. 2005. Stem cell biology and the plasticity polemic. *Experimental Hematology,* 33**,** 389-394.

RADA, T., REIS, R. & GOMES, M. 2010. Distinct Stem Cells Subpopulations Isolated from Human Adipose Tissue Exhibit Different Chondrogenic and Osteogenic Differentiation Potential. *Stem Cell Reviews and Reports***,** 1-13.

RATANACHOO, K., GASCOYNE, P. & RUCHIRAWAT, M. 2002. Detection of cellular responses to toxicants by dielectrophoresis. *BBA-Biomembranes,* 1564**,** 449-458.

REUBINOFF, B., PERA, M., FONG, C., TROUNSON, A. & BONGSO, A. 2000. Embryonic stem cell lines from human blastocysts: somatic differentiation in vitro. *nature biotechnology,* 18**,** 399-404.

RICHARDS, M. & BONGSO, A. 2006. Propagation of human embryonic stem cells on human feeder cells. *Methods Mol.Biol.,* 331**,** 23-41.

RODOLFA, K. & EGGAN, K. 2006. A transcriptional logic for nuclear reprogramming. *Cell,* 126**,** 652-655.

ROSE, F., HOU, Q. & OREFFO, R. 2004. Delivery systems for bone growth factors-the new players in skeletal regeneration. *Journal of Pharmacy and Pharmacology,* 56**,** 415-427.

SACCHETTI, B., FUNARI, A., MICHIENZI, S., DI CESARE, S., PIERSANTI, S., SAGGIO, I., TAGLIAFICO, E., FERRARI, S., ROBEY, P. & RIMINUCCI, M. 2007. Self-renewing osteoprogenitors in bone marrow sinusoids can organize a hematopoietic microenvironment. *Cell,* 131**,** 324-336.

SADLER, T. W. 2003. *Langman's medical embryology. Part 1*.

SCHULDINER, M., YANUKA, O., ITSKOVITZ-ELDOR, J., MELTON, D. A. & BENVENISTY, N. 2000. From the Cover: Effects of eight growth factors on the differentiation of cells derived from human embryonic stem cells. *Proceedings of the National Academy of Sciences,* 97**,** 11307-11312.

SCHULZ, R. & BADER, A. 2007. Cartilage tissue engineering and bioreactor systems for the cultivation and stimulation of chondrocytes. *European Biophysics Journal,* 36**,** 539-568.

SELLAYAH, D., SEK, K., ANTHONY, F., HANSON, M. & CAGAMPANG, F. 2008. Sensitivity of housekeeping genes in the hypothalamus to mismatch in diets between pre-and postnatal periods in mice. *Neuroscience Letters,* 447**,** 54-57.

SENGER, P. L. 2003. *Pathways to Pregnancy and Parturition. 2nd Edition*.

SHI, S. & GRONTHOS, S. 2003. Perivascular Niche of Postnatal Mesenchymal Stem Cells in Human Bone Marrow and Dental Pulp. *Journal of Bone and Mineral Research,* 18**,** 696-704.

SHI, S., GRONTHOS, S., CHEN, S., REDDI, A., COUNTER, C., ROBEY, P. & WANG, C. 2002. Bone formation by human postnatal bone marrow stromal stem cells is enhanced by telomerase expression. *Nature Biotechnology,* 20**,** 587-591.

SHIN, H., JO, S. & MIKOS, A. 2003. Biomimetic materials for tissue engineering. *Biomaterials,* 24**,** 4353-4364.

SHORE, E., XU, M., FELDMAN, G., FENSTERMACHER, D., BROWN, M. & KAPLAN, F. 2006. A recurrent mutation in the BMP type I receptor ACVR1 causes inherited and sporadic fibrodysplasia ossificans progressiva. *Nature Genetics,* 38**,** 525-527.

SIMMONS, P. & TOROK-STORB, B. 1991a. CD34 expression by stromal precursors in normal human adult bone marrow. *Blood,* 78**,** 2848.

SIMMONS, P. J. & TOROK-STORB, B. 1991b. Identification of stromal cell precursors in human bone marrow by a novel monoclonal antibody, STRO-1. *Blood,* 78**,** 55-62.

SONG, L. & TUAN, R. S. 2004. Transdifferentiation potential of human mesenchymal stem cells derived from bone marrow. *The FASEB Journal,* 18**,** 980-982.

SOTTILE, V., THOMSON, A. & MCWHIR, J. 2003. In vitro osteogenic differentiation of human ES cells. *Cloning & Stem Cells,* 5**,** 149-155.

SPAGNOLI, F. M. & HEMMATI-BRIVANLOU, A. 2006. Guiding embryonic stem cells towards differentiation: lessons from molecular embryology. *Current Opinion in Genetics & Development,* 16**,** 469-475.

STADTFELD, M., NAGAYA, M., UTIKAL, J., WEIR, G. & HOCHEDLINGER, K. 2008. Induced pluripotent stem cells generated without viral integration. *Science,* 322**,** 945-949.

STARK, H., BAUR, M., BREITKREUTZ, D., MIRANCEA, N. & FUSENIG, N. 1999. Organotypic keratinocyte cocultures in defined medium with regular epidermal morphogenesis and differentiation. *Journal of Investigative Dermatology,* 112**,** 681-691.

STARZEC, A., BRIANE, D., KRAEMER, M., KOUYOUMDJIAN, J. C., MORETTI, J. L., BEAUPAIN, R. & OUDAR, O. 2003. Spatial organization of three-

dimensional cocultures of adriamycin-sensitive and -resistant human breast cancer MCF-7 cells. *Biology of the Cell,* 95**,** 257-264.

STEINBERG, M. & TAKEICHI, M. 1994. Experimental specification of cell sorting, tissue spreading, and specific spatial patterning by quantitative differences in cadherin expression. *Proceedings of the National Academy of Sciences of the United States of America,* 91**,** 206-209.

STEPHENS, M., TALARY, M., PETHIG, R., BURNETT, A. & MILLS, K. 1996. The dielectrophoresis enrichment of CD 34 + cells from peripheral blood stem cells harvests. *Bone marrow transplantation(Basingstoke),* 18**,** 777-782.

STEWART, K., WALSH, S., SCREEN, J., JEFFERISS, C., CHAINEY, J., JORDAN, G. & BERESFORD, J. 1999. Further characterization of cells expressing STRO-1 in cultures of adult human bone marrow stromal cells. *Journal of Bone and Mineral Research,* 14**,** 1345-1356.

STOJKOVIC, P., LAKO, M., PRZYBORSKI, S., STEWART, R., ARMSTRONG, L., EVANS, J., ZHANG, X. & STOJKOVIC, M. 2005. Human-Serum Matrix Supports Undifferentiated Growth of Human Embryonic Stem Cells. *Stem Cells,* 23**,** 895-902.

STOPPINI, L., BUCHS, P. & MULLER, D. 1991. A simple method for organotypic cultures of nervous tissue. *Journal of neuroscience methods,* 37**,** 173-182.

SUROWIEC, A., STUCHLY, S., BARR, J. & SWARUP, A. 1988. Dielectric properties of breast carcinoma and the surrounding tissues. *IEEE Transactions on Biomedical Engineering,* 35**,** 257-263.

SUVA, D., GARAVAGLIA, G., MENETREY, J., CHAPUIS, B., HOFFMEYER, P., BERNHEIM, L. & KINDLER, V. 2004. Non-hematopoietic human bone marrow contains long-lasting, pluripotential mesenchymal stem cells. *Journal of cellular physiology,* 198**,** 110-118.

TAKAHASHI, K. & YAMANAKA, S. 2006. Induction of Pluripotent Stem Cells from Mouse Embryonic and Adult Fibroblast Cultures by Defined Factors. *Cell,* 126**,** 663-676.

TAKAMIZAWA, S., MAEHATA, Y., IMAI, K., SENOO, H., SATO, S. & HATA, R. 2004. Effects of ascorbic acid and ascorbic acid 2-phosphate, a long-acting vitamin C derivative, on the proliferation and differentiation of human osteoblast-like cells. *Cell Biology International,* 28**,** 255-265.

TAKEICHI, M. 1988. The cadherins: cell-cell adhesion molecules controlling animal morphogenesis. *Development,* 102**,** 639-655.

TALARY, M., BURT, J., TAME, J. & PETHIG, R. 1996. Electromanipulation and separation of cells using travelling electric fields. *Journal of Physics- London- D Applied Physics,* 29**,** 2198-2203.

TARE, R., HOWARD, D., POUND, J., ROACH, H. & OREFFO, R. 2005. Tissue engineering strategies for cartilage generation of micromass and three dimensional cultures using human chondrocytes and a continuous cell line. *Biochemical and Biophysical Research Communications,* 333**,** 609-621.

TARE, R. S., BABISTER, J. C., KANCZLER, J. & OREFFO, R. O. 2008. Skeletal stem cells: phenotype, biology and environmental niches informing tissue regeneration. *Mol Cell Endocrinol,* 288**,** 11-21.

THOMAS, R., MITCHELL, P., OREFFO, R. & MORGAN, H. 2010. Trapping single human osteoblast-like cells from a heterogeneous population using a dielectrophoretic microfluidic device. *Biomicrofluidics,* 4**,** 022806-9.

THOMAS, R., MORGAN, H. & GREEN, N. 2009. Negative DEP traps for single cell immobilisation. *Lab on a Chip,* 9**,** 1534-1540.

THOMAS, R. J., CHANDRA, A., HOURD, P.C., WILLIAMS, D.J. 2008. Cell Culture Automation and Quality Engineering: A Necessary Partnership to Develop Optimized Manufacturing Processes for Cell-Based Therapies. *JALA,* 13**,** 152-158.

THOMSON, J. A., ITSKOVITZ-ELDOR, J., SHAPIRO, S. S., WAKNITZ, M. A., SWIERGIEL, J. J., MARSHALL, V. S. & JONES, J. M. 1998. Embryonic Stem Cell Lines Derived from Human Blastocysts. *Science,* 282**,** 1145-1147.

TORTELLI, F. & CANCEDDA, R. 2009. Three-dimensional cultures of osteogenic and chondrogenic cells: A tissue engineering approach to mimic bone and cartilage in vitro. *European Cells and Materials,* 17**,** 1-14.

TRIFFITT, J. 2002. Stem cells and the philosopher's stone. *Journal of Cellular Biochemistry,* 85**,** 13-19.

TURNPENNY, L., BRICKWOOD, S., SPALLUTO, C. M., PIPER, K., CAMERON, I. T., WILSON, D. I. & HANLEY, N. A. 2003. Derivation of human embryonic germ cells: an alternative source of pluripotent stem cells. *Stem Cells,* 21**,** 598-609.

TURNPENNY, L., SPALLUTO, C. M., PERRETT, R. M., O'SHEA, M., HANLEY, K. P., CAMERON, I. T., WILSON, D. I. & HANLEY, N. A. 2006. Evaluating Human Embryonic Germ Cells: Concord and Conflict as Pluripotent Stem Cells. *Stem Cells,* 24**,** 212-220.

UNGRIN, M., JOSHI, C., NICA, A., BAUWENS, C. & ZANDSTRA, P. 2008. Reproducible, ultra high-throughput formation of multicellular organization from single cell suspension-derived human embryonic stem cell aggregates. *PLoS One,* 3**,** e1565.

VOLDMAN, J. 2006. Electrical forces for microscale cell manipulation. *Annu Rev Biomed Eng.,* 8**,** 425-452.

VYKOUKAL, J., VYKOUKAL, D., FREYBERG, S., ALT, E. & GASCOYNE, P. 2008. Enrichment of putative stem cells from adipose tissue using dielectrophoretic field-flow fractionation. *Lab on a Chip,* 8**,** 1386.

WALSH, S., JEFFERISS, C., STEWART, K., JORDAN, G. R., SCREEN, J. & BERESFORD, J. N. 2000. Expression of the developmental markers STRO-1 and alkaline phosphatase in cultures of human marrow stromal cells: regulation by fibroblast growth factor (FGF)-2 and relationship to the expression of FGF receptors 1-4. *Bone,* 27**,** 185-195.

WALSH, S., JORDAN, G., JEFFERISS, C., STEWART, K. & BERESFORD, J. 2001. High concentrations of dexamethasone suppress the proliferation but not the differentiation or further maturation of human osteoblast precursors in vitro: relevance to glucocorticoid-induced osteoporosis. *Rheumatology,* 40**,** 74-83.

WANG, L., FLANAGAN, L. & LEE, A. 2007. Side-wall vertical electrodes for lateral field microfluidic applications. *Microelectromechanical Systems, Journal of,* 16**,** 454-461.

WANG, X., BECKER, F. & GASCOYNE, P. 2002. Membrane dielectric changes indicate induced apoptosis in HL-60 cells more sensitively than surface phosphatidylserine expression or DNA fragmentation. *BBA-Biomembranes,* 1564**,** 412-420.

WARE, C. B., NELSON, A. M. & BLAU, C. A. 2006. A Comparison of NIH-Approved Human ESC Lines. *Stem Cells,* 24**,** 2677-2684.

WARTENBERG, M., GUNTHER, J., HESCHELER, J. & SAUER, H. 1998. The embryoid body as a novel in vitro assay system for antiangiogenic agents. *Laboratory investigation; a journal of technical methods and pathology,* 78**,** 1301-1314.

WILES, M. & KELLER, G. 1991. Multiple hematopoietic lineages develop from embryonic stem (ES) cells in culture. *Development,* 111**,** 259-267.

WILLIAMS JR, D., PRESAR, A., RICHMOND, A., MJAATVEDT, C., HOFFMAN, S. & CAPEHART, A. 2005. Limb chondrogenesis is compromised in the versican deficient hdf mouse. *Biochemical and Biophysical Research Communications,* 334**,** 960-966.

WOBUS, A., ROHWEDEL, J., MALTSEV, V. & HESCHELER, J. 1994. In vitro differentiation of embryonic stem cells into cardiomyocytes or skeletal muscle cells is specifically modulated by retinoic acid. *Development Genes and Evolution,* 204**,** 36-45.

WOZNEY, J. 1992. The bone morphogenetic protein family and osteogenesis. *Molecular reproduction and development,* 32**,** 160-167.

XU, C., INOKUMA, M. S., DENHAM, J., GOLDS, K., KUNDU, P., GOLD, J. D. & CARPENTER, M. K. 2001. Feeder-free growth of undifferentiated human embryonic stem cells. *Nat.Biotechnol.,* 19**,** 971-974.

XU, C., ROSLER, E., JIANG, J., LEBKOWSKI, J. S., GOLD, J. D., O'SULLIVAN, C., AVAN-BOORSMA, K., MOK, M., BRONSTEIN, A. & CARPENTER, M. K. 2005. Basic Fibroblast Growth Factor Supports Undifferentiated Human Embryonic Stem Cell Growth Without Conditioned Medium. *Stem Cells,* 23**,** 315-323.

YANG, L., BANADA, P., CHATNI, M., LIM, K., BHUNIA, A., LADISCH, M. & BASHIR, R. 2006. A multifunctional micro-fluidic system for dielectrophoretic concentration coupled with immuno-capture of low numbers of Listeria monocytogenes. *Lab on a Chip,* 6**,** 896-905.

YANG, X., VAN DEN DOLDER, J., WALBOOMERS, X., ZHANG, W., BIAN, Z., FAN, M. & JANSEN, J. 2007. The odontogenic potential of STRO-1 sorted rat dental pulp stem cells in vitro. *Journal of Tissue Engineering and Regenerative Medicine,* 1**,** 66-73.

YING, Q. L., NICHOLS, J., CHAMBERS, I. & SMITH, A. 2003. BMP Induction of Id Proteins Suppresses Differentiation and Sustains Embryonic Stem Cell Self-Renewal in Collaboration with STAT3. *Cell,* 115**,** 281-292.

YOON, B. & LYONS, K. 2004. Multiple functions of BMPs in chondrogenesis. *Journal of Cellular Biochemistry,* 93**,** 93-103.

YOON, B., YOO, S., LEE, J., YOU, S., LEE, H. & YOON, H. 2006. Enhanced differentiation of human embryonic stem cells into cardiomyocytes by combining hanging drop culture and 5-azacytidine treatment. *Differentiation,* 74**,** 149-159.

YU, J., HE, H., TANG, C., ZHANG, G., LI, Y., WANG, R., SHI, J. & JIN, Y. 2010. Differentiation potential of STRO-1+ dental pulp stem cells changes during cell passaging. *BMC Cell Biology,* 11**,** 1-7.

YU, J., VODYANIK, M., SMUGA-OTTO, K., ANTOSIEWICZ-BOURGET, J., FRANE, J., TIAN, S., NIE, J., JONSDOTTIR, G., RUOTTI, V. & STEWART, R. 2007. Induced pluripotent stem cell lines derived from human somatic cells. *Science,* 318**,** 1917-1920.

ZHANG, P., LI, J., TAN, Z., WANG, C., LIU, T., CHEN, L., YONG, J., JIANG, W., SUN, X., DU, L., DING, M. & DENG, H. 2008. Short-term BMP-4 treatment initiates mesoderm induction in human embryonic stem cells. *Blood,* 111**,** 1933-1941.

ZHANG, Z., TEOH, S., CHONG, M., SCHANTZ, J., FISK, N., CHOOLANI, M. & CHAN, J. 2009. Superior Osteogenic Capacity for Bone Tissue Engineering of Fetal Compared with Perinatal and Adult Mesenchymal Stem Cells. *Stem Cells,* 27**,** 126-137.

ZOU, H., MELLON, S., SYMS, R. & TANNER, K. 2006. 2-dimensional MEMS dielectrophoresis device for osteoblast cell stimulation. *Biomedical Microdevices,* 8**,** 353-359.

ZUR NIEDEN, N., PRICE, F., DAVIS, L., EVERITT, R. & RANCOURT, D. 2007. Gene Profiling on Mixed Embryonic Stem Cell Populations Reveals a Biphasic Role for {beta}-Catenin in Osteogenic Differentiation. *Molecular Endocrinology,* 21**,** 674-685.

ZUR NIEDEN, N. I., KEMPKA, G. & AHR, H. J. 2003. In vitro differentiation of embryonic stem cells into mineralized osteoblasts. *Differentiation,* 71**,** 18-27.

ZWEIGERDT, R., BURG, M., WILLBOLD, E., ABTS, H. & RUEDIGER, M. 2003. Generation of confluent cardiomyocyte monolayers derived from embryonic stem cells in suspension: a cell source for new therapies and screening strategies. *Cytotherapy,* 5**,** 399-413.